ANALYTICA CHIMICA ACTA

International monthly devoted to all branches of analytical chemistry
Revue mensuelle internationale consacrée à tous les domaines de la chimie analytique
Internationale Monatsschrift fur alle Gebiete der analytischen Chemie

ELSEVIER SCIENTIFIC PUBLISHING COMPANY

AMSTERDAM

✓ *Anal. Chim. Acta*, Vol. 74, No. 1, 1–224, January 1975

Published monthly

Vol. 74, No. 1, 1–224, January 1975

Publication Schedule for 1975

Vol. **74**, No. **1**	January 1975	
Vol. **74**, No. **2**	February 1975	**(completing Vol. 74)**
Vol. **75**, No. **1**	March 1975	
Vol. **75**, No. **2**	April 1975	**(completing Vol. 75)**
Vol. **76**, No. **1**	May 1975	
Vol. **76**, No. **2**	June 1975	**(completing Vol. 76)**
Vol. **77**, No. **1**	July 1975	
Vol. **77**, No. **2**	August 1975	**(completing Vol. 77)**
Vol. **78**, No. **1**	September 1975	
Vol. **78**, No. **2**	October 1975	**(completing Vol. 78)**
Vol. **79**, No. **1**	November 1975	
Vol. **79**, No. **2**	December 1975	**(completing Vol. 79)**

Subscription price: Dfl. 570.00 plus Dfl. 54.00 postage, US$ 249.60 inclusive of postage. Subscribers in the U.S.A. and Canada receive their copies by airmail. Additional charges for airmail to other countries are available on request. For advertising rates apply to the publishers.

Subscriptions should be sent to:
Elsevier Scientific Publishing Company, P.O. Box 211, Amsterdam, The Netherlands.

GENERAL INFORMATION

Languages

Papers will be published in English, French or German.

Submission of papers

Papers should be sent to:

PROF. PHILIP W. WEST,
Coates Chemical Laboratories,
College of Chemistry and Physics,
Louisiana State University,
Baton Rouge 3,
La. 70803 (U.S.A.)

or to:

DR. A. M. G. MACDONALD,
Department of Chemistry,
The University,
P.O. Box 363
Birmingham B15 2TT (Great Britain)

Reprints

Fifty reprints will be supplied free of charge. Additional reprints (minimum 100) can be ordered at quoted prices. They must be ordered on order forms which are sent together with the proofs.

PRINTED IN THE NETHERLANDS

ANALYTICA CHIMICA ACTA
Vol. 74 (1975)

ANALYTICA CHIMICA ACTA

International monthly devoted to all branches of analytical chemistry
Revue mensuelle internationale consacrée à tous les domaines de la chimie analytique
Internationale Monatsschrift für alle Gebiete der analytischen Chemie

ELSEVIER SCIENTIFIC PUBLISHING COMPANY
AMSTERDAM

Anal. Chim. Acta, Vol. 74 (1975)

PRINTED IN THE NETHERLANDS

Analytica Chimica Acta, 74 (1975) 1–9

DETERMINATION OF CHROMIUM IN IRON AND STEELS BY U.H.F. PLASMA-TORCH SPECTROMETRY

IKUO ATSUYA
Kitami Institute of Technology, Kitami (Japan)
(Received 12th April 1974)

The plasma torch based on a high-frequency plasma generator, and the plasma-jet flame based on an arc-jet plasma generator, have been suggested in recent years as new light sources for emission spectrometry, because a high-temperature, stable flame can be obtained. Several studies of plasma-jet spectrometry based on an arc-jet plasma generator as a light source have been reported by Margoshes and Scribner[1], Greenfield *et al.*[2] and Gotō and Atsuya[3–4]. Studies on high-frequency plasma-torch spectrometry have been described by various authors[5–10]

In the present work, the determination of chromium in iron and steels was examined by means of u.h.f. plasma-torch spectrometry; some interesting results were obtained. A method for the rapid determination of chromium in iron and steels was established.

EXPERIMENTAL

Reagents

Standard chromium stock solution. Chromium metal (99.99%) was dissolved in hydrochloric acid (1+1); the solution was evaporated in order to eliminate excess of hydrochloric acid, and diluted with water to make a solution containing 10 mg Cr ml^{-1}. This solution was diluted to the desired concentration at the time of use.

All acids and other metals and salts used were of analytical grade.

Apparatus

The high-frequency plasma-torch spectrometer used was a Hitachi UHF plasma-torch spectrometer 300, which is similar in principle to the discharge generator described by Gotō *et al.*[7]. A schematic diagram of the plasma-torch spectrometer is shown in Fig. 1. Argon was used as a plasma-forming gas and a plasma-sheath gas.

Working conditions for plasma-torch spectrometry

Factors affecting the intensity of spectral lines in u.h.f. plasma-torch spectrometry are the field and anode current, the flow-rate of the plasma-forming gas and sheath gas. Therefore, in order to determine the optimal working con-

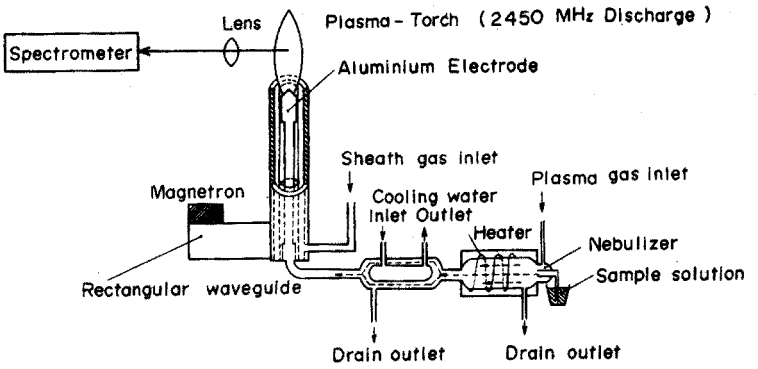

Fig. 1. Schematic diagram of the u.h.f. plasma-torch spectrometer.

ditions, the relationships between these factors and the spectral line intensity were examined.

Selection of spectral lines for chromium. As shown in Table I, several spectral lines of chromium may be used. The line intensity of CrI 357.848 nm was the strongest, but there was some spectral interference at this wavelength. The CrI 359.348-nm line was therefore adopted.

Spatial distribution of spectral line intensity in the plasma torch. The spatial distributions of the line intensity at 359.348 nm were investigated in the presence of iron in 3 *M* hydrochloric acid and in the absence of iron. As shown in Fig. 2, the intensity was strongest at a position 3 mm from the center of the plasma torch in the absence of iron, and background intensity decreased. However, the peak of the intensity distribution shifted to the center of the plasma torch in the presence of iron in 3 *M* hydrochloric acid, and the line intensity was strongest at a position 1.5 mm from the center of the plasma torch. In this case, the observations were made at a height of 0–15 mm from the top of the electrode.

These results indicate that the spatial distributions of line intensity must be examined for each sample solution.

TABLE I

COMPARISON OF LINE INTENSITIES FOR CHROMIUM

(Cr, 0.25 μg ml^{-1})

Wavelength (nm)	*Intensity*[11]	*eV*	*Intensity, plasma torch*[a]
205.559	M1900	6.03	24
360.532	M1600	3.43	95
357.868	M2400	3.44	180
359.348	M2100	3.46	132
425.433	M1700	2.91	74
427.481	M1300	2.90	60
428.973	M850	2.89	43
520.843	M900	3.32	7

[a] Arbitrary units.

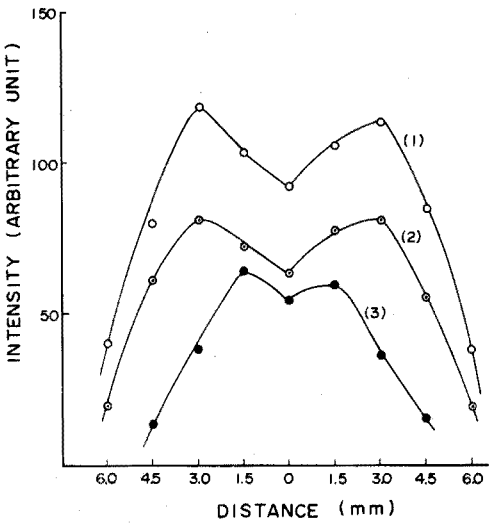

Fig. 2. Projected intensity distribution for the line CrI 359.348 nm. Cr: (1) 0.25 μg ml^{-1} (distilled water); (2) 0.50 μg ml^{-1} (3 *M* HCl); (3) 0.50 μg ml^{-1} (3 *M* HCl, 2 mg Fe ml^{-1}).

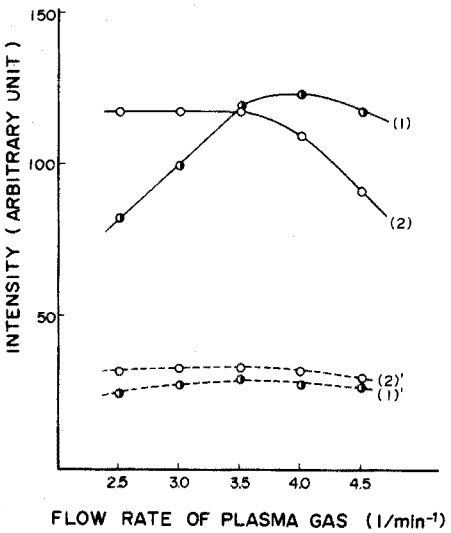

Fig. 3. Relation between line intensity and the flow rate of plasma gas. Cr: (1) 0.25 μg ml^{-1} (distilled water), corrected for background intensity; (2) 0.50 μg ml^{-1} (3 *M* HCl, 2 mg Fe ml^{-1}); (1)′ and (2)′, background intensity of (1) and (2) at 359.348 nm.

Relation between the spectral line intensity and gas flow-rate. Argon was used as the plasma-forming gas and plasma-sheath gas; sample solutions were carried by the plasma-forming gas. The relationship between the intensity of the CrI 359.348-nm line and the gas flow-rates was examined. As shown in Fig. 3, the intensity showed a maximum in the range 3.5–4.5 l min^{-1} for the plasma-forming gas when a sample solution containing 0.25 p.p.m. of chromium was used. But the intensity decreased above 3.5 l min^{-1} when a sample solution

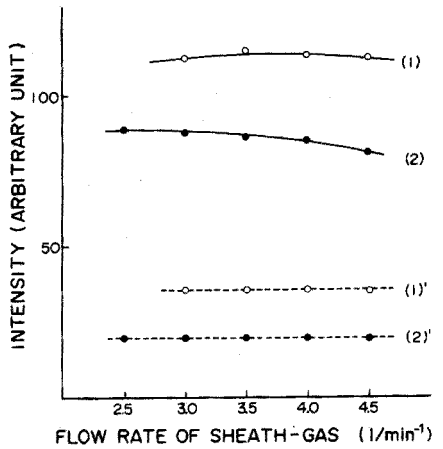

Fig. 4. Relation between the line intensity and the flow-rate of sheath gas. Curves are numbered as in Fig. 3.

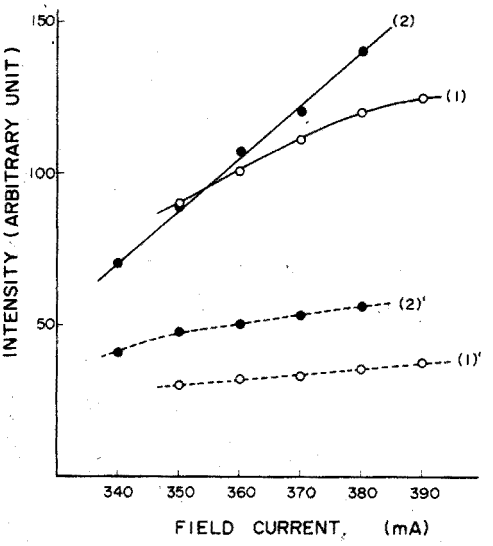

Fig. 5. Relation between the line intensity and the field current for the magnetron. Curves are numbered as in Fig. 3.

containing 0.5 p.p.m. of chromium and 2 mg Fe ml^{-1} in 3 *M* hydrochloric acid was measured. The effects of the flow-rate of plasma-forming gas on the line intensity depended not only on the composition of the sample solution, but also on the characteristics of the nebulizer.

The effects of the plasma-sheath gas flow-rate were also examined. As shown in Fig. 4, this flow-rate scarcely affected the line intensity, and the sample solution composition made little difference.

Effect of the field current and anode current on the line intensity. The effects of the field current for the magnetron on line intensity and background intensity were first examined. As shown in Fig. 5, an approximately linear relationship existed between the line intensity and field current, but the slope for the sample

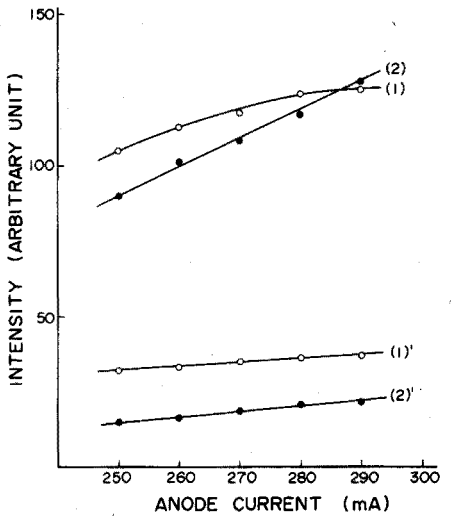

Fig. 6. Relation between the line intensity and the anode current for the magnetron. Curves are numbered as in Fig. 3.

TABLE II

WORKING CONDITIONS

Frequency	2450 MHz
Flow-rate of plasma-forming gas	3.0 l min^{-1}
Flow-rate of plasma-sheath gas	3.0 l min^{-1}
Field current	360 mA
Anode current	280 mA
Entrance slit width	30 μm
Exit slit width	50 μm

solution containing 2 mg Fe ml^{-1} in 3 *M* hydrochloric acid was sharper than for the sample solution without iron.

As shown in Fig. 6, the effect of anode current on the line intensity showed the same tendency as that of field current.

Based on these examinations, conditions for the measurement were established as shown in Table II, and all subsequent experiments were carried out under these conditions.

RESULTS AND DISCUSSION

Effects of acids

The effects of common acids used for dissolving the sample, such as hydrochloric, nitric and sulfuric acids, were examined for solutions containing 0.25 μg Cr ml^{-1}. As shown in Fig. 7, the line intensity decreased significantly with increasing concentration of acid, but it remained approximately constant in the concentration range 2.0–3.5 *M* for hydrochloric and nitric acids; sulfuric acid was found to give a large effect and was considered to be unsuitable for use.

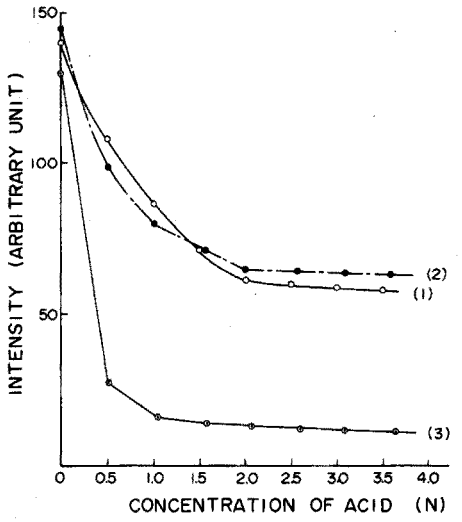

Fig. 7. Effect of various acids on chromium spectral line intensity. 0.25 μg Cr ml^{-1}. Corrected for background intensity (1) HCl, (2) HNO_3, (3) H_2SO_4.

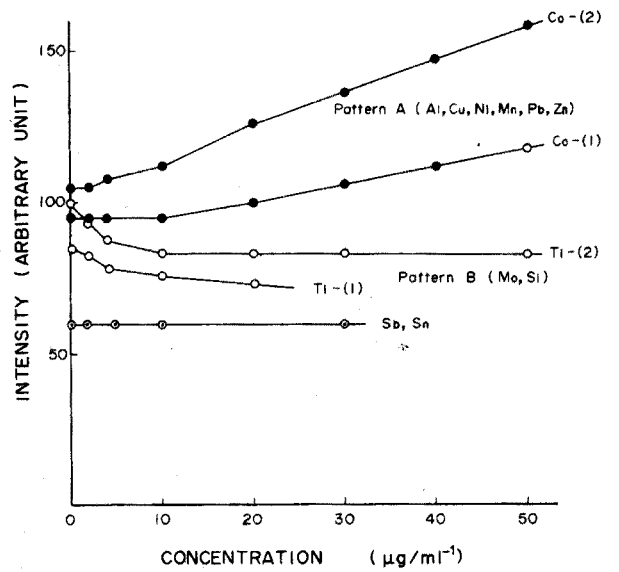

Fig. 8. Effect of other elements on chromium spectral line intensity. (1) 0.25 μg Cr ml^{-1} (distilled water), (2) 0.50 μg Cr ml^{-1} (3 *M* HCl).

Effects of diverse elements

The effects of the usual elements found in iron and steels were examined by adding manganese, copper, cobalt, *etc.* As shown in Fig. 8, there were three kinds of patterns. Elements showing pattern A, such as Al, Co, Cu, Mn, Ni, Pb and Zn, increased the line intensity with increasing concentration of the element. Elements showing pattern B, such as Ti and Mo, slightly decreased the line intensity.

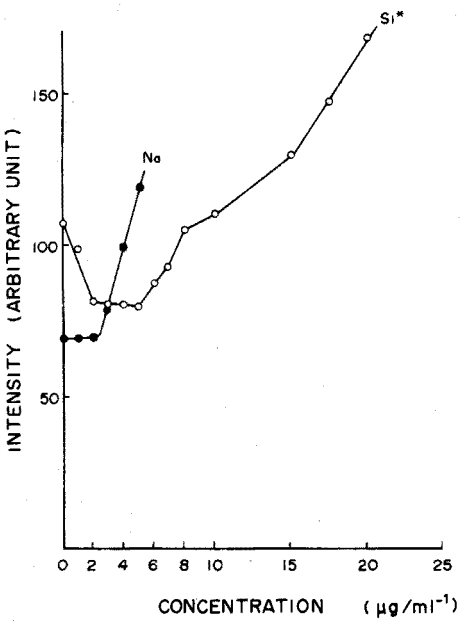

Fig. 9. Effect of sodium and silicon on the chromium spectral line intensity. 0.25 μg Cr ml^{-1} (distilled water). Si*, sodium silicate was dissolved in distilled water.

Elements showing pattern C, such as Sn and Sb, did not affect the line intensity as their concentration increased.

The effect of these elements on the line intensity increased in the presence of hydrochloric acid.

It is necessary to explain the effect of silicon (as sodium silicate) on the line intensity for CrI 359.348 nm. As shown in Fig. 9, a small amount of silicon decreased the line intensity whereas a small amount of sodium did not affect it. More than *ca.* 10 μg Si ml^{-1} apparently increased the line intensity, but this was largely due to sodium; above 4 μg Na ml^{-1} rapidly increased the line intensity. Above a definite quantity of sodium, the line intensity of chromium mainly depended on the concentration of sodium.

These tests showed that it is necessary to exclude the influence of other elements for determinations of chromium in iron and steels.

There are two possible methods: (a) separation of chromium, and (b) addition of a large amount of another element, to provide a levelling effect. Since application to the determination of chromium in iron and steel was mainly intended, the levelling effect of a large amount of iron was examined. As shown in Fig. 10, the chromium line intensity remained essentially constant in the concentration range 0.2–0.4 g of iron per 100 ml in 3 *M* hydrochloric acid; the presence of a large amount of iron increased the line intensity. These results indicated that the determination of chromium in iron and steels should be possible by means of a calibration curve prepared from solutions containing 2.0–4.0 mg Fe ml^{-1} in 3 *M* hydrochloric acid, provided that this amount of iron prevented interference from other elements. Studies of the effects of other elements on the intensity of 0.5 μg

Cr ml^{-1} in the presence of 2.0 mg Fe ml^{-1} in 3 *M* hydrochloric acid showed that concentrations of 50 μg ml^{-1} of Al, As, Co, Cu, Mn, Mo, Ni, Pb, Sb, Sn and Zn did not interfere. As silicon was added as sodium silicate, above 4 μg Si ml^{-1},

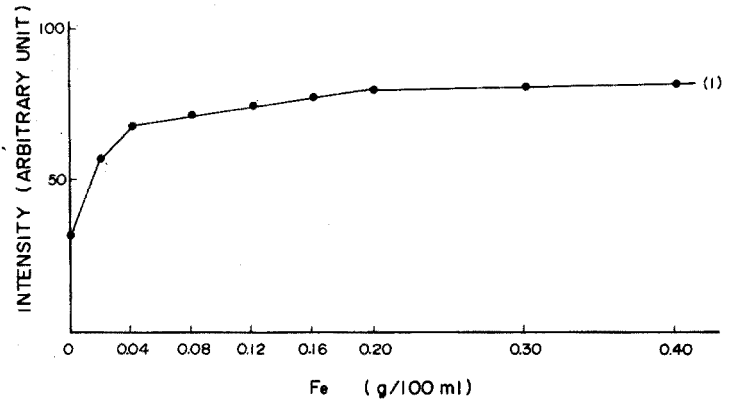

Fig. 10. Effect of iron on chromium spectral line intensity. 0.5 μg Cr ml^{-1}, 3 *M* HCl.

i.e. above 6 μg Na ml^{-1}, increased the line intensity in spite of the presence of a large amount of iron. Titanium(IV) caused a negative error of 5% at a concentration of 50 μg ml^{-1}, but did not interfere at 10 μg ml^{-1}.

Calibration curves

Calibration curves for chromium were prepared in the presence of iron in 3 *M* hydrochloric acid under the working conditions shown in Table II. Linear relationships were obtained between the concentration of chromium and the line intensity in the ranges 0.125–1.0 μg Cr ml^{-1}, 0.5–2.0 μg Cr ml^{-1}, 1.0–7.0 μg Cr ml^{-1} and 5–30 μg Cr ml^{-1}. A wide range of chromium concentrations can thus be determined. A blank test was examined, but a correction was not necessary.

Analytical procedure

Based on these results, the following analytical procedure for chromium in iron and steels was established. An exactly weighed sample (0.2–0.4 g) was dissolved in 10–20 ml of 6 *M* hydrochloric acid and a small amount of nitric acid by heating. The solution was evaporated to dryness, the residue was dissolved in 20 ml of 3 *M* hydrochloric acid, and the solution was transferred to a 100-ml volumetric flask, and diluted with 3 *M* hydrochloric acid to the mark. When the content of chromium in iron and steels was large, it was necessary to add a constant volume of pure iron solution in order to keep the concentration of iron in the sample solution in the range 2–4 mg ml^{-1}.

When the sample contained a large amount of silicon, silicon was removed by treatment with hydrofluoric acid in a platinum crucible, after filtration of the sample solution in 3 *M* hydrochloric acid. The residue in the platinum crucible was also dissolved in 3 *M* hydrochloric acid and then added to the main solution. Then, the intensity of the chromium line was measured as before.

Analytical results and precision

Analytical results for the determination of chromium in iron and steels are listed in Table III. The results obtained are in satisfactory agreement with the certificate values. A relative standard deviation of 2.4% for 0.10% of chromium in iron and steels was obtained.

TABLE III

ANALYTICAL RESULTS AND PRECISION FOR CHROMIUM IN IRON AND STEELS BY PLASMA-TORCH SPECTROMETRY

Sample	*Cr (%) found*	*Certificate value*	*s_r (%)*
J.S.I.S.156-2[a]	0.310, 0.313	0.30	—
J.S.I.S.157-2	0.103[b]	0.10[b]	2.4
J.S.I.S.158-2	0.013, 0.013	0.014	—

[a] J.S.I.S.: Japanese Standard of Iron and Steel.
[b] Average of 11 determinations (range 0.100–0.107%).

SUMMARY

Factors affecting the intensity of the chromium 359.348-nm line in u.h.f. plasma-torch spectrometry were examined, and optimal working conditions were determined for the determination of chromium in iron and steels. The effects of acids were examined; the influence of small amounts of diverse elements was depressed by the presence of a large amount of iron. An analytical procedure for chromium in iron and steels was established; a relative standard deviation of 2.4% for 0.1% of chromium in iron and steels was obtained.

REFERENCES

1 M. Margoshes and B. F. Scribner, *Spectrochim. Acta*, 15 (1962) 138.
2 S. Greenfield, I. L. Jones and C. T. Berry, *Analyst*, 89 (1964) 713.
3 H. Gotō and I. Atsuya, *Z. Anal. Chem.*, 225 (1967) 121.
4 H. Gotō and I. Atsuya, *Z. Anal. Chem.*, 240 (1968) 102.
5 W. Teppe and J. van Calker, *Z. Anal. Chem.*, 198 (1963) 13.
6 R. H. Wendt and V. A. Fassel, *Anal. Chem.*, 37 (1965) 920.
7 H. Gotō, K. Hirokawa and M. Suzuki, *Z. Anal. Chem.*, 225 (1967) 130.
8 C. D. West and D. N. Hume, *Anal. Chem.*, 36 (1964) 412.
9 K. M. Aldons, R. M. Dagnall, B. L. Sharp and T. W. West, *Anal. Chim. Acta*, 54 (1971) 233.
10 S. Murayama, H. Matsuno and M. Yamamoto, *Spectrochim. Acta*, 23B (1968) 513.
11 A. N. Zaidel, V. K. Prokofev and S. M. Raiski, *Tables of Spectral Lines*, VEB, Verlag Technik, Berlin, 1955.

Analytica Chimica Acta, 74 (1975) 11–16

A SPECIAL HOLDER FOR THE JARRELL-ASH SPECTROMETER 750 V FOR THE ANALYSIS OF STEEL ROD SAMPLES

R. K. DHUMWAD

Fuel Reprocessing Division, Bhabha Atomic Research Centre, Trombay, Bombay 400 085 (India)

S. RAMACHANDRAN

Steel Melt Shop, Mukand Iron and Steel Works Ltd., Kalwe, Thana (India)

(Received 2nd May 1974)

For quick and accurate analyses of melts and other products in steel and other metal industries, spectrometric direct readers are very successful. The Atom-Counter 750 V (Jarrell-Ash Company, USA) has been in regular use in these laboratories for the analysis of steel melts which are normally cast as cups with a diameter of 16 mm or more. Samples of smaller diameter could not be analysed by this spectrometer, mainly because of the geometry of the spark chamber which was intended for the analysis of flat samples with minimum circular areas of 200 mm^2. Since speedy reliable analyses of wire rod samples drawn from billets on a daily production basis were needed, attempts were made to use the spectrometer by designing a special holder.

The present paper describes the details of a wire rod holder and control ring which have made it possible to analyse wire rod samples in a few minutes. The wire rod sample is fixed in the holder and placed (after the bottom face of the holder and the wire rod have been polished) on the top plate of the spark chamber. With this arrangement, either flat or wire rod samples can be analyzed easily without loss of time or fine adjustments. Emphasis was laid on simple quick manipulations for fixing the wire rod into the holder so that large numbers of samples can be handled.

DESIGN OF THE WIRE ROD SAMPLE HOLDER*

Description of the spark chamber

As shown in Fig. 1, the controlled atmosphere spark chamber (Part No. 66–718) consists essentially of a block of electrically insulating material with a central hollow cup where the spark can take place in an argon atmosphere between the thoriated tungsten counter electrode and the flat sample to be analysed, on applying a potential of 16000 V a.c. The top plate of the spark chamber has a hole of 16-mm diameter, which is sealed by placing the polished flat sample over it, thus avoiding leakage of argon gas. The radiation emitted during sparking is directed into the spectrometer for diffraction and subsequent analysis.

The major problems to be overcome in adapting the spectrometer for the

* An application for patenting "the wire rod holder in spectrometric analysis" is being processed.

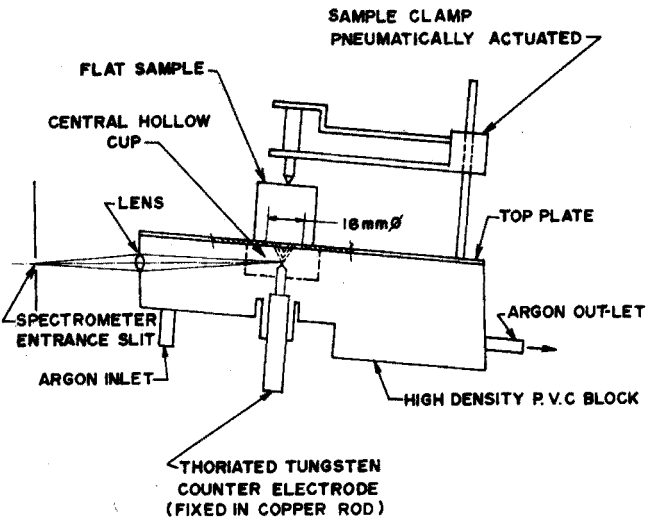

Fig. 1. Controlled atmosphere spark chamber.

analysis of wire rods of 6-mm diameter were as follows:

(i) the device had to hold firmly wire rods of diameter 6 mm $\pm$ 0.25 mm;

(ii) rapid positioning of the holder on the hole of the top plate, so that the centre of the wire rod, the centre of the hole on the top plate and the tip of the counter electrode were aligned, was essential;

(iii) Some procedure was necessary to ensure that the gap between the surface of the wire rod and the counter electrode was 3 mm as in the case of analysis of flats;

(iv) the device had to be leak proof so that there would be no leakage of argon gas during sparking;

(v) sparking had to take place between the counter electrode and the wire rod only.

Description of the wire rod holder

Figure 2 shows the details of the wire rod holder, which was made by Messrs Nyloplast, Bombay. The wire rod (of length 35 mm $\pm$ 3 mm) is inserted into the central bore and is held rigidly by nine balls spaced uniformly around the circumference as well as along the length of the bore. The balls are spring-loaded to exert uniform pressures and hold the wire rod firmly at the centre of the bore (point (i)). The cap on the top of the holder is screwed and held firmly in position by tightening the checknut. This ensures that there is no displacement of the wire rod when the bottom face of the holder with the wire rod is polished on the belt grinder before sparking. The holder can then be positioned and aligned on the counter electrode by the control ring (point (ii)). To carry out the analysis in duplicate or more, the wire rod may be advanced by screwing the cap further down, retightening the cap by the check nut and repolishing the surface of the wire rod together with the bottom face of the holder.

With regard to point (ii), a number of other methods such as external

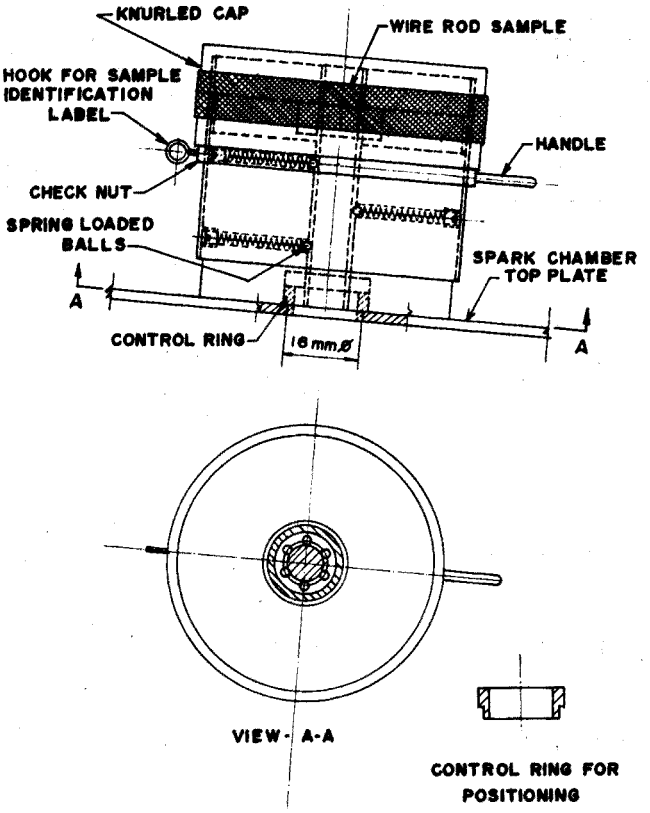

Fig. 2. Holder for wire rod.

stops on the top plate were tested originally for centrally positioning the wire rod holder on the top plate. These were found to be unsuitable since they imposed restrictions on the size of the flat samples. It was therefore necessary to adopt a method which would keep the plane of the top plate free from any stops, so that odd sizes and large flat samples also could be analysed by simply removing the control ring from the top plate.

Polishing the bottom face of the holder along with the wire rod sample (held in position) gave a perfectly plane surface as in the case of flats (point (iii)).

Tightening the top cap not only avoided any significant leakage of argon gas but also helped to hold the wire rod in position while polishing the bottom face of the holder (point (iv)).

A cavity (about 5 mm in depth and 16 mm in diameter) at the bottom face of the holder and around the central bore for inserting the wire rod sample ensured that sparking took place correctly (point (v)).

Details of the area of burns from sparking

A study of the burns on the flat samples indicated that the average diameter of the circular burns was about 6 mm. Thus one would expect that the number of counts for a given element obtained by sparking either a flat (having larger

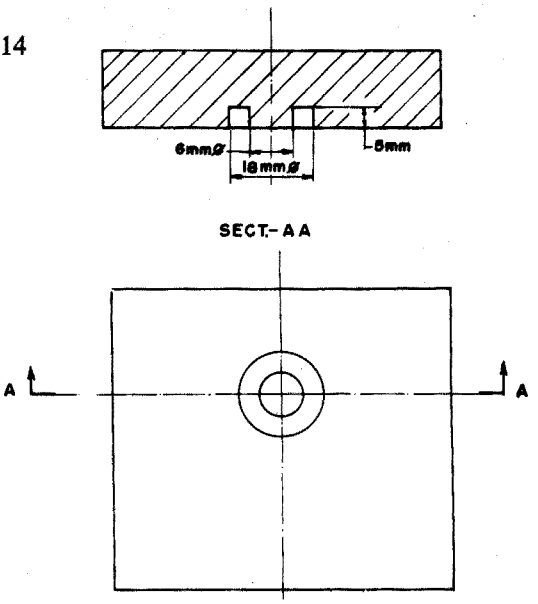

Fig. 3. Standard (B.S.S. 434) with built-in wire rod.

TABLE I

COMPARISON OF ANALYTICAL RESULTS FOR FIVE WIRE ROD SAMPLES

(All values are expressed in percentages)

Sample no.	*Element*	*Chemical analysis*	*Spectrometric analysis as described*
2053	C	0.64	0.66
	Mn	0.66	0.69
	Si	0.61	0.64
	P	0.053	0.054
	S	0.022	0.025
2203	C	0.69	0.70
	Mn	0.55	0.56
	Si	0.34	0.37
	P	0.069	0.072
	S	0.030	0.033
A 101	C	0.60	0.63
	Mn	0.35	0.35
	Si	0.11	0.11
	S	0.040	0.044
	P	0.028	0.030
B 304	C	0.59	0.60
	Mn	0.61	0.61
	Si	0.20	0.19
	S	0.015	0.013
	P	0.024	0.024
Y 23108[a]	C	0.49[a]	0.49
	Mn	0.70	0.71
	Si	0.25	0.26
	S	0.009	0.010
	P	0.016	0.020

[a] Sample Y 23108 was obtained from Sumi-to-mo, Japan, with the chemical analysis.

surface) or a wire rod sample of 6 mm diameter would be identical. This was confirmed as follows.

A cavity of about 5 mm in depth and 16 mm in diameter was cut in a large sized flat standard B.S.S. 434 (plain carbon steel; Bureau of Analysed Samples Ltd., England) around a central pedestal of 6-mm diameter as shown in Fig. 3. Several experiments were carried out first by sparking the central flat polished pedestal (equivalent to a wire rod) and then by sparking the remaining flat. There was no significant difference between the two sets of counts thus obtained for any given element.

RESULTS

Comparison of chemical and spectrometric values

Various wire rods were analysed in duplicate by the proposed method. The working curves for the various elements drawn by sparking the flat standards of the B.S.S. series 431–435 (plain carbon steels) were used to obtain the percentage concentrations of the elements in the wire rods. The spectrometric results for five selected elements were compared with their corresponding values obtained by standard chemical methods. Table I shows a comparison of the analytical results of five samples; there is a good agreement between the two sets of values. Clearly working curves obtained from large flat standards can be used for the analysis of wire rods also.

Comparison of precision

In order to determine the standard deviation of the method proposed, spectrometric data were obtained by analysing the same wire rod 25 times. Standard deviations and relative standard deviations were calculated by using standard formulae. The percentage concentrations of the various elements under study were obtained by standard chemical methods. Table II includes the results for carbon and phosphorus. In addition, it includes for comparison the corresponding data furnished by Jarrell-Ash with N.B.S. flat standards when the spectrometer was

TABLE II

COMPARISON OF PRECISION AND COEFFICIENT OF VARIATION

Evaluation parameter	*Carbon*		*Phosphorus*	
	Jarrell-Ash data[1] for flats	*Present method for wire rods*	*Jarrell-Ash data[1] for flats*	*Present method for wire rods*
Average counts	214	196	204.3	371
s^2	8.6	6.83	21.61	18.66
s (for counts)	±2.93	±2.61	±4.64	±4.35
s_r	1.37	1.34	2.27	2.16
% Concn. in sample	0.32	0.19	0.013	0.012
s_r (in concn.)	2.028	2.63	7.44	8.33
Absolute precision	±0.0065	±0.005	±0.001	±0.001

supplied[1]. The results show that the precision and standard deviations of the proposed method of analysis for wire rods are comparable with the corresponding data for flats.

CONCLUSIONS

With the use of the special holder, it is possible to analyse wire rods with the Jarrell-Ash spectrometer 750 V as quickly as one would analyse flat samples. The technique involved in using the wire rod holder is quite simple. There is no delay in changing over from wire rod to flat sample analysis, as there are no fixtures on the top plate. Separate sets of holders with appropriate bore diameters were fabricated and used for the analysis of wire rods having diameters of 8, 10 and 12 mm. The working curves drawn by sparking the flat standards hold good for reading out concentrations in wire rod analysis.

The authors wish to thank the authorities of Bhabha Atomic Research Centre, Trombay, and Messrs Mukand Iron and Steel Works, for giving permission and extending facilities for this development work.

SUMMARY

For quick and accurate analysis of small diameter steel wire rods, a special holder has been designed for use with the Atom-Counter 750 V spectrometer (JARRELL-ASH). The spectrometer is normally used for analysis of large flat samples. Wire rod samples with diameters of 6–16 mm were rapidly analysed (with the same precision and accuracy as flat samples) by using the holder. The procedure for wire rod analysis is simple and versatile; no time is wasted in changing from wire rod to flat sample analysis.

REFERENCE

1 Jarrell-Ash Engineering publication No. 66750 Rev. No. 2, *Master calibration for Mukand Iron and Steel*, No. 1201 66785, 7 (1971).

Analytica Chimica Acta, 74 (1975) 17–21

DETERMINATION OF MERCURY IN TOTAL DIET SAMPLES BY NEUTRON ACTIVATION

JAMES T. TANNER

Division of Chemistry and Physics, Food and Drug Administration, Washington, D.C. 20204 (U.S.A.)

WILLIAM S. FORBES

University of South Florida, Tampa, Florida 33620 (U.S.A.)

(Received 10th June 1974)

A study was initiated by the Food and Drug Administration to determine if foods other than fish contain significant amounts of mercury. The first part of this study involved analysis of 10 common foods that have a high nationwide consumption. The results of this first part were published[1] and demonstrated that the mercury concentrations in all of these foods were below 50 p.p.b.

The second part of the study is reported in this paper. This part involved a much more complex sampling of food. Samples comprising 117 food items were collected. These were separated into 12 commodity groups to represent the two-week diet ("total diet") of a 15- to 20-year-old male for the region of the country in which the samples were collected. This was based on a survey of household food consumption conducted by the U.S. Department of Agriculture in 1955.

The purpose of this paper is to tabulate the information acquired on mercury concentrations in total diet composites and to detail the chemical procedure used for analysis of these samples.

EXPERIMENTAL

Samples

Total diet samples were collected within each geographical region according to instructions set forth in the FDA's "Inspector's Shopping Guide"[2]. The "market basket" samples were then forwarded (perishables were packed in dry ice) to the Kansas City Laboratory of FDA for preparation. There the samples were separated into two parts: (a) items which required processing by the dietician, and (b) items to be added directly to a composite. The items requiring processing were weighed and prepared in edible portions in the dietary kitchen. All items were then composited into 12 commodity groups. To insure homogeneity, where necessary, items were chopped, ground, etc., and then the composites of each group were slurried. The slurried composites were divided into 100-g portions (the fluid slurries were frozen), packaged and reserved for analysis. A 100-g portion of each commodity group was forwarded to the FDA Headquarters laboratory for the determination of mercury by neutron activation analysis.

To avoid contamination, the food samples were shipped in plastic-coated containers and handled in a clean-room until they were sealed into quartz sample vials. The contents were thoroughly mixed before shipment and before any sampling was done. A food sample which had a water content of more than 15% was freeze-dried in order to lessen any pressure increase when the sample, enclosed in a sealed quartz vial, was irradiated in the reactor. In practice, a sample of 1–10 g of food commodity was withdrawn, transferred to a 25-ml Erlenmeyer flask, frozen in liquid nitrogen, and freeze-dried. After the sample had reached ambient temperature it was kept under vacuum for a further 2 h. The freeze-dried sample was finely pulverized, transferred to a small polyethylene vial, and placed in a desiccator.

Standards

The mercury standard consisted of 13.8 μg of mercury (in the form of mercury(II) acetate in 1 *M* acetic acid) which was adsorbed onto about 30 mg of powdered silicon dioxide and sealed in quartz vials.

Irradiation

The standards and samples were irradiated in the 10 MW research reactor at the National Bureau of Standards, Washington, D.C., and processed approximately 1 week later. The importance of minimizing any contamination cannot be overemphasized for mercury measurements at the p.p.b. level.

Instrumentation

The instrumentation used in this work consisted of a Nuclear Data 4410 multichannel analyzer connected to either a Harshaw 3 × 3 in. NaI(Tl) well detector or an Ortec Low Energy Photon Ge(Li) detector (l.e.p.d.). The l.e.p.d. is particularly sensitive to photons in the region of the ^{197}Hg x-rays[6].

Chemical separation

Because the mercury content of these samples was quite low, a chemical separation was needed to enhance the γ-ray peaks of mercury with respect to the background. Mercury was separated by a procedure developed by Jervis *et al.*[3], which involved anion-exchange chromatography and sulfide precipitation. Other methods of analysis such as the electrolytic procedure developed by Sjöstrand[4] and a volatilization procedure developed by Rook *et al.*[5] were also tried and found to give satisfactory results. For the data reported here, the procedure of Jervis was used because it was readily adaptable to processing a large number of samples and did not require any special equipment. Carrier mercury was used to determine the chemical yield, which averaged about 90%. Complete equilibrium was achieved by allowing the sample and carrier to digest together overnight in fuming nitric acid.

Radioactive selenium interferes with the determination of mercury, since ^{75}Se has a γ-ray close to the same energy as the γ-ray from ^{203}Hg (279 keV). A small quantity of selenium nitrate solution (*ca.* 1 mg Se) was added at the digestion step to ensure the elution of selenium during the 0.01 *M* hydrochloric acid wash step.

Procedure

Accurately weigh *ca.* 200 mg of dry food sample into a clean quartz vial. Seal the quartz vial by heating the tip in an oxygen–methane flame and crimping the end with forceps.

Irradiate samples and standards in the reactor (neutron flux of *ca.* $6 \cdot 10^{13}$ $ncm^{-2}\ s^{-1}$) for 4 h ($8.6 \cdot 10^{17}$ nvt).

After a decay of one week or less, open the irradiation container, clean the quartz vials in aqua regia, rinse with distilled water, and place the sample vials in liquid nitrogen until cool; then place the quartz sample vial in a moistened 1-ounce gelatin capsule (the gelatin capsule is used to confine the sample within the beaker) and break the vial with a pair of needle-nose pliers into a 150-ml beaker.

To the sample add 15 ml of fuming nitric acid, about 50 mg of mercury carrier in solution as mercury(II) acetate and about 1 mg of selenium (1 ml of selenium nitrate solution). Place the beaker, covered with a watch glass, in an ice bath and leave to digest overnight.

Add concentrated hydrochloric acid to 100 ml and heat to boil off excess of nitric acid, reducing the volume to 40 ml. Then add concentrated hydrochloric acid to 80 ml, reduce to 30 ml, and dilute with water to 100 ml.

Add the sample solution to an anion-exchange column (Baker CGA-540, 100–200 mesh: column bed 1×10 cm) and wash with 140 ml of 0.01 *M* hydrochloric acid. Elute the mercury with 80 ml of 0.1 *M* thiourea in 0.01 *M* hydrochloric acid.

Add 1 ml of ammonia liquor to the solution to precipitate mercury(II) sulfide, and let it stand until it has coagulated.

Centrifuge the mercury(II) sulfide and discard the excess of solution. Dissolve the mercury(II) sulfide in 10 drops of aqua regia in a water bath, heat to dryness, add 10 drops of concentrated hydrochloric acid, evaporate to dryness, and add water to 20 ml. Bubble in hydrogen sulfide to precipitate mercury(II) sulfide.

Filter the precipitate onto a tarred Whatman No. 42 paper, dry overnight at 100°C, and weigh as mercury(II) sulfide. Compute the yield, correcting for water loss from the filter paper.

Place the precipitate onto Saran wrap, fold it up and insert into a 2/5-dram polyethylene vial for counting.

Determine the mercury, using the 279-keV γ-ray from the decay of ^{203}Hg, or the x-rays from the decay of ^{197}Hg. Compute the amount of mercury by using the following equation:

$$\text{p.p.m. Hg} = \frac{(\mu\text{g Hg in standard})(\text{activity of Hg in sample})(\%\text{ wet weight})}{(\text{g sample})(\text{activity of Hg in standard})(\text{chemical yield})}$$

DISCUSSION

In the first part of this study the samples of separated mercury were counted by using a 3×3 in. NaI(Tl) well detector, connected to a multichannel analyzer[1]. A Ge(Li) detector was used routinely to check for interferences, none

of which were noted in the mercury x-ray and γ-ray region of the spectrum. For the work reported here a low-energy photon Ge(Li) detector was used for the determination of the ^{197}Hg x-rays[6].

Validation of this procedure has been reported by Tanner *et al.*[1]. At regular intervals National Bureau of Standards standard reference materials (orchard leaves and bovine liver) were analyzed as a continuing check on the validity of the procedure. Methods of integration of photopeaks and the sensitivity of the method have already been discussed[1]. The upper limits of the mercury concentrations given in Table I were defined as 2.33 times the standard deviation of the background as defined by Currie[7].

The results shown in Table I indicate that all commodity groups, with the exception of meat, fish and poultry, contain mercury concentrations of generally less than 10 p.p.b. Up to 41 p.p.b. of mercury was found in the meat, fish and poultry group (group II). When similar meat, fish and poultry composites were analyzed in the FDA District Laboratories, component by component, only the fish component demonstrated elevated levels of mercury greater than 0.1 p.p.m.[8].

TABLE I

MARKET BASKET SURVEY—TOTAL DIET ANALYSIS FOR MERCURY

Collecting districts	*Commodity groups[a] (p.p.b. Hg)*								
	I	*II*	*III*	*IV*	*V*	*VI*	*VII*	*VIII*	*IX*
Baltimore									
20-BAL-5	<1	—	< 3	3	1	< 2	2	<1	<2
25-BAL-6	—	30	—	<2	9	< 2	2	4	<2
30-BAL-7[b]	6	—	<13	14	< 3	8	—	—	—
Boston									
16-BOS-4	<1	13	< 2	<1	1	< 1	<1	—	<1
21-BOS-5	<1	26	11	1	3	< 1	<1	2	4
26-BOS-6	<1	41	4	<2	2	< 1	<1	<1	1
36-BOS-8	<1	—	13	13	6	2	2	<1	1
31-BOS-7[b]	—	—	—	<8	<12	<14	<8	<8	<8
Kansas City									
14-KAN-4	<1	6	9	<2	4	< 2	<1	<1	3
19-KAN-5	<1	4	< 3	<1	1	< 1	<1	<1	<1
24-KAN-6	<1	13	< 2	<2	1	< 1	<1	<1	<1
39-KAN-9	<1	4	< 3	<2	< 1	1	<1	<1	<2
Los Angeles									
17-LOS-4	2	27	< 2	<1	1	< 1	<1	<1	—
Minneapolis									
18-MIN-4	3	9	< 2	3	1	< 1	<1	<1	<1

[a] The different commodity group composites are: I, dairy products; II, meat, fish, and poultry; III, grain and cereal products; IV, potatoes; V, leafy vegetables; VI, legume vegetables; VII, root vegetables; VIII, garden fruits; IX, fruits; X, oils, fats, and shortening; XI, sugars and adjuncts; XII, beverages. Groups X, XI, and XII were not analyzed.

[b] Samples analyzed by modified method[9].

During the course of this work a modified procedure was tried. This procedure was used by Rottschafer *et al.*[9] and appears to offer some savings in time by stopping the separation after the sample solution has been added to the ion exchange column and counting the ion exchange bed directly. For these low concentrations of mercury only upper limits could be obtained. The sensitivity was less with this procedure[9] because of the additional contribution to the background from radionuclides retained on the resin bed in addition to mercury. This procedure offers some advantages for higher concentrations of mercury (>0.1 p.p.m.) but seems to have only limited use for very low concentrations of mercury.

In conclusion, mercury has been determined in samples of total diet and found to be present only in concentrations of less than 0.05 p.p.m.

We thank the personnel of the District Laboratories of the Food and Drug Administration for collecting the samples, and also Mr. R. E. Simpson and Dr. M. H. Friedman, Food and Drug Administration, Washington, D.C. and the personnel of the N.B.S. Reactor Radiation Division for their contributions to various phases of this work.

SUMMARY

The mercury contents of food samples representative of the total diet have been determined by neutron activation analysis. The mercury was separated by anion-exchange chromatography and precipitated as the sulfide. The mercury concentrations for the different fractions of total diet samples were well below 50 p.p.b. Only in the meat, fish, and poultry fraction were measurable amounts of mercury encountered regularly.

REFERENCES

1 J. T. Tanner, M. H. Friedman, D. N. Lincoln, L. Ford and M. Jaffee, *Science*, 177 (1972) 1102.
2 R. E. Duggan and F. J. McFarland, *Pestic. Monit. J.*, 1 (1967) 1.
3 R. E. Jervis, D. Debrun, W. LePage and B. Tiefenbach, *Summary of Progress*, National Health Grant Project No. 605-7-510, University of Toronto, Canada, July 1970.
4 B. Sjöstrand, *Anal. Chem.*, 36 (1964) 814.
5 H. L. Rook, T. E. Gills and P. D. LaFleur, *Anal. Chem.*, 44 (1972) 1114.
6 M. H. Friedman, E. Miller and J. T. Tanner, *Anal. Chem.*, 46 (1974) 236.
7 L. A. Currie, *Anal. Chem.*, 40 (1968) 586.
8 D. Manske and P. Corneliussen, *Pestic. Monit. J.*, 8 (1) (1974) in press.
9 J. M. Rottschafer, J. D. Jones and H. B. Mark, Jr., *Environ. Sci. Technol.*, 5 (1971) 336.

Analytica Chimica Acta, 74 (1975) 23–28

AN EVALUATION OF SOLID-STATE LUMINESCENCE OF CHELATES IN TRACE METAL ANALYSIS

THE ALUMINIUM–OXINE SYSTEM

H. ROLLIER and D. E. RYAN*

Trace Analysis Research Centre, Chemistry Department, Dalhousie University, Halifax, Nova Scotia, B3H 4J1 (Canada)

(Received 29th May 1974)

The fluorescence of metal chelates has been widely used in solution for the detection and determination of trace metals. The limits of detection are generally much lower than by absorption spectrophotometry but the sensitivity may be limited, if extraction steps are necessary, because of high solution volumes and low partition coefficients. The preconcentration obtained by the use of coprecipitation techniques to introduce microgram amounts of activators in milligram amounts of phosphors led recently to the determination of p.p.b. bismuth and lead by solid-state luminescence[1–3]. It is of interest to determine whether preconcentration of a microconstituent by using a carrier precipitate of organic reagent (with which the microconstituent reacts to form a fluorescent product) would improve the sensitivity of the fluorescence determination of metal chelates. The aluminium–oxine system was used in the present study. Although it is not the best, in terms of sensitivity and selectivity, for the determination of aluminium, it is well known in solution analysis and has been applied to a wide range of practical samples[4–12].

EXPERIMENTAL

Apparatus, reagents, solutions

A Multi-Dosimat Metrohm E 415 fitted with 5- and 10-ml burets was used to measure precisely small volumes of reagents. All fluorimetric measurements were made with a Farrand Vis–u.v. Chromatogram Analyzer and with a Turner Model 111 Fluorimeter fitted with CAMAG t.l.c. Scanner. The sample cell was a blackened aluminium sheet with drilled holes (5 mm diam.) covered with a thin glass plate. The holes were packed with a sample powder which was held in place by masking tape.

A stock solution (1000 μg ml^{-1}) of aluminium was prepared from $AlK(SO_4)_2 \cdot 12\ H_2O$ (Fisher). Solutions of desired concentrations were prepared by dilution of this stock solution. The fluorescence of solid oxine was measured before use, to detect possible contamination by aluminium. The oxine, supplied by G. Frederick Smith Co., was selected and used to prepare solutions (8% in

* To whom reprint requests should be addressed.

ethanol). All other chemicals were analytical or reagent grade. Fresh double-distilled water was used to prepare solutions and aluminium contamination by glassware was prevented by using Nalgene labware.

Development of procedure

pH of precipitation. The optimal pH of precipitation is that giving the maximum weight of precipitate since it ensures the best gravimetric reproducibility. This pH was determined to be 6.8–6.9, with a standard Soerensen buffer (KH_2PO_4/Na_2HPO_4).

Amount of reagent. The different factors that need to be considered when establishing the amount of reagent to be used include: volume of the sample cell, weight reproducibility of the precipitate, solubility of the reagent in the analytical solution, and the partition coefficient of the analyzed element between precipitated and dissolved reagent.

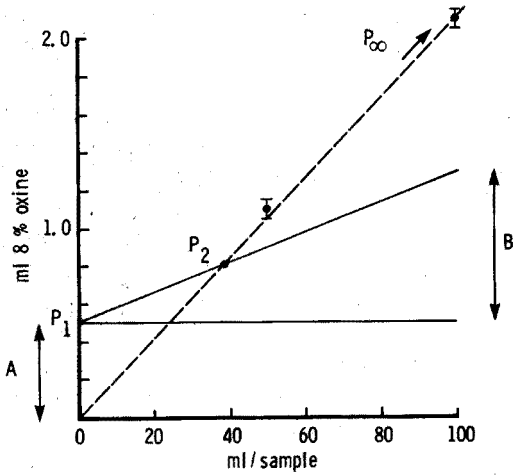

Fig. 1. Determination of the optimal amount of reagent *versus* sample volume; (——) amount of reagent giving *A* g of precipitate, (– – –) optimal reagent amount/sample volume ratio giving maximum fluorescence reading for 10 μg Al.

The weight of precipitate necessary to fill the sample cell is about 30 mg. This weight can be obtained reproducibly. Figure 1 shows how the optimal amount of reagent is determined for different sample volumes (curve $P_1P_2P_\infty$); *A* is the amount of precipitate required to fill the sample cell (32 mg=0.5 ml of 8% oxine) and *B* is the solubility of oxine in the solution (50 mg/100 ml=0.8 ml of 8% oxine). Under 35 ml, the solubility of oxine is the determining factor (P_1P_2). Over 35 ml, the partition coefficient of aluminium between solution and precipitate governs the optimal amount of reagent (P_2P_∞). The amounts of reagent to be used are thus 0.7, 1.1 and 2.1 ml of 8% oxine for 25-, 50- and 100-ml samples. These two factors (solubility and partition coefficient) show the first prerequisites for further application of the solid-state process: unless the reagent is practically insoluble and the element being determined is quantitatively collected by the precipitate, both samples and standards have to be adjusted to the same volume.

Procedure

To 100 ml of solution containing 0.1–1000 μg of aluminium, add 5 ml of buffer (60 ml of 0.07 *M* KH_2PO_4+40 ml of 0.07 *M* Na_2HPO_4). Adjust the pH to 6.8–6.9 with hydrochloric acid or sodium hydroxide. Precipitate by slow addition of 2.1 ml of 8% (w/v) oxine solution; stir rapidly with a magnetic stirrer during precipitation. (For other sample and standard volumes, simply change the amount of oxine solution added (Fig. 1).) Let stand for 1 h and filter through a filter crucible. Do not wash the precipitate. Dry for 2 h in a vacuum desiccator. Grind and mix the precipitate in an agate mortar, pack the cell and measure the luminescence. Settings on the Farrand instrument were λ_{ex}, 385 nm; λ_{em}, 524 nm; source slit removed; excitation filter 7-54; emission filter 8; aperture 0.75, PM RCA 1P21 with the slit removed. For the Turner fluorimeter, use excitation filter 7-54 (or 7-60) and emission filter 8.

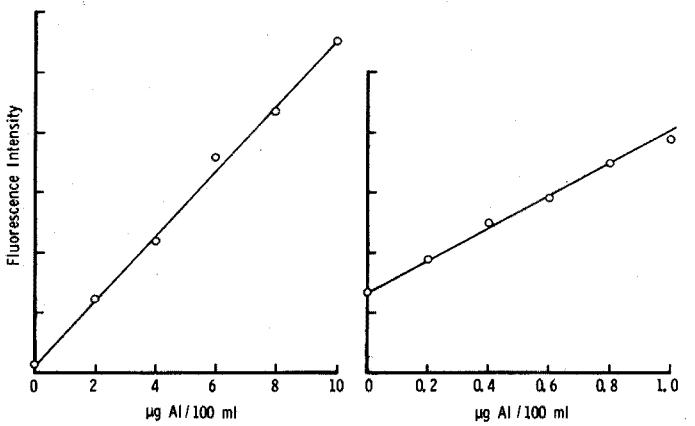

Fig. 2. Calibration curves for aluminium.

RESULTS AND DISCUSSION

The fluorescence intensity is a linear function of aluminium concentration from 0.1 to 10 μg (Fig. 2). From 10 to 1000 μg, the calibration curve is no longer a straight line, but satisfactory and reproducible results are readily obtained. For higher aluminium concentrations there is no substantial increase in fluorescence intensity because the precipitate is essentially aluminium oxinate, *i.e.* no longer oxine with coprecipitated complex. The described procedure may be used over a concentration range of four orders of magnitude, by using the appropriate set of standards for each concentration range. The detection limit is 0.1 μg (or 1 p.p.b. if 100-ml samples are available) with the Farrand instrument. With the Turner fluorimeter the detection limit is 1 μg. The relative standard deviation of six determinations of 10 μg of aluminium was 2.2% for 10-ml samples and 4.8% for 100-ml samples.

Interferences

Oxine is not a specific reagent, since it reacts with a considerable number

of metals[13,14]; many of the chelates formed are fluorescent[11]. Consequently, severe interferences are encountered when analyzing aluminium fluorimetrically or spectrophotometrically with this reagent[6–12,15–18]. Usually, these interferences are either removed by extraction, or masked while extracting aluminium.

In order to evaluate the dependence of the solid-state determination of aluminium upon interferences, five typical interferents were selected (Cu, Zn, Fe, Mn and Ca) and their interferences were established in the determination of 10 μg Al in 100-ml volumes. All observed interferences were severe. For equivalent amounts of copper, the fluorescence reading was reduced by half and a 20-fold (weight) excess reduced the fluorescence by 90%. For zinc, equivalent amounts did not change the fluorescence, but a 5-fold excess increased the reading by a factor of seven, owing to the fluorescence of zinc oxinate. Both iron and manganese induced a strong reduction of fluorescence even at equivalent amounts, and completely quenched the fluorescence in 10- and 50-fold amounts, respectively. Since these interferences are similar in order of magnitude to those observed in the liquid-state procedure, the coprecipitation technique does not improve the selectivity of the determination.

Masking and extraction procedures were studied as a possible means of eliminating interferences. Experiments with cyanide as masking agent showed that even 0.5 g of potassium cyanide did not interfere with the determination of 10 μg Al in 100-ml samples. The interferences of Cu^{2+}, Zn^{2+}, Fe^{3+} and Mn^{2+} were therefore determined in the presence of 0.5 g of potassium cyanide, by the standard procedure. The interference of copper was completely suppressed up to a 20-fold (weight) amount of this element. However, interference of zinc, iron and manganese was still severe, although slightly reduced. Tartrate[19], sodium diethyldithiocarbamate and 1-pyrrolidinedithiocarbamate were also unsuccessful as masking agents. There appear to be two reasons for the failure to mask interfering metals: (1) the pH used (optimal for the precipitation of oxine) is not optimal for a strong complexation of interferents by masking reagents; (2) the excess of oxine used is very high and is thus favorable to the formation of interferent–oxine compounds.

Since copper, zinc, iron and manganese ions can be extracted by 8-hydroxyquinaldine in chloroform[15], 100 ml of aqueous solutions containing 10 μg Al^{3+}, 5 μg Cu^{2+}, 30 μg Zn^{2+}, 30 μg Fe^{3+} and 100 μg Mn^{2+} (typical amounts of elements found in 0.5 g of dried leaves of a crop grown in acidic soil) were vigorously shaken with 2 ml of a 5% solution of 8-hydroxyquinaldine in chloroform. The extraction was then done with two 20-ml aliquots of chloroform at the standard pH of 6.8–6.9 and was followed by the precipitation procedure. As shown by the color of the precipitates obtained, the extraction was not complete and a strong quenching was observed in precipitates. The extraction was also done[15] at pH 9.2, followed by precipitation at pH 6.8–6.9. Interferents were removed from the precipitate, but the collection of aluminium was almost completely prevented.

CONCLUSIONS

A good reagent for solid-state luminescence analysis should be non-

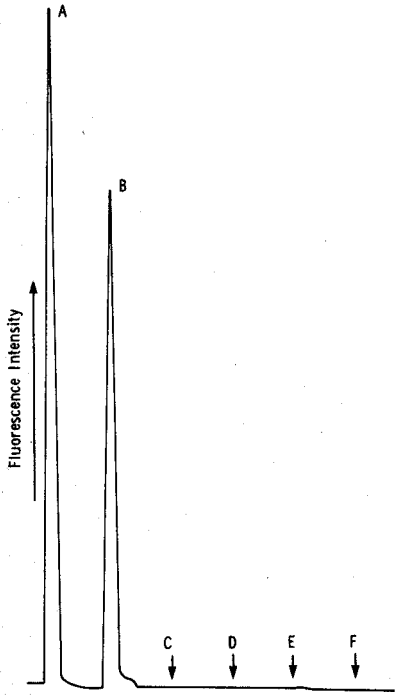

Fig. 3. Determination of the purity of six commercially available oxine reagents (A–F).

fluorescent (because the high excess of reagent used as collector amplifies the effect of its own fluorescence), insoluble (so that the determination is independent of sample volume), and selective (either in its own action or in that interferents may be easily masked under the precipitation conditions). A reagent with these qualities (1,3-di(2-naphthyl)-1,3-propanedione) has been successfully applied to the determination of trace amounts of beryllium[20].

Solid-state luminescence measurements are very useful in the determination of reagent purity. For example, two of six commercially available oxine reagents were found to be contaminated with aluminium by simply measuring their solid-state fluorescence at the standard excitation and emission wavelengths (Fig. 3). Rapid evaluation of metal contamination of most reagents used in fluorescence analysis should be possible by this technique.

For aluminium oxinate, the detection limit is 0.1 μg per sample. For small sample volumes, this limit is comparable to that obtained in solution (0.02–0.1 μg ml^{-1}) but, for higher sample volumes, the solid-state collection procedure is more sensitive (1 ng ml^{-1} if 100-ml samples are available). The detection limit may be affected by the sensitivity of detection and by the reproducibility of measurements. Reproducibility is not the limiting factor here and improvements in instrumental detection would result in a lower detection limit. The solubility of oxine necessitates working with standards and samples of the same volume; much more insoluble reagents render the measurements essentially independent of solution volume.

The selectivity of the method is, of course, dependent on the selectivity of the reagent. For oxine, which is highly unselective, interferences in the determination of aluminium are numerous, and the optimal pH for masking is incompatible with the optimal pH for the precipitation. Masking of interferent metals would be expected to be more difficult in the solid-state method because of the high excess of reagent used.

This work was supported by a grant from the National Research Council of Canada.

SUMMARY

The potential of solid-state fluorescence analysis applied to metal–chelate systems is evaluated, with aluminium oxinate as a model. The coprecipitation of aluminium oxinate in excess of oxine, and measurement of the luminescence of the separated solid (λ_{ex}, 385 nm; λ_{em}, 524 nm) allows the determination of 0.1 μg Al/sample (1 ng ml^{-1} if 100-ml volumes available). Factors influencing the detection limit are discussed, and the interferences of several metals are determined. The requirements of a good reagent for general use are outlined.

REFERENCES

1 D. E. Ryan, R. J. Prime, J. Holzbecher and R. E. Young, *Anal. Lett.*, 6 (1973) 721.
2 D. E. Ryan, H. Rollier and J. Holzbecher, *Can. J. Chem.*, 52 (1974) 1942.
3 D. E. Ryan, J. Holzbecher and H. Rollier, *Anal. Chim. Acta*, in press.
4 H. Goto, *J. Chem. Soc. Jap.*, 60 (1939) 937.
5 C. Gentry and L. Sherrington, *Analyst (London)*, 71 (1946) 432.
6 E. Goon, J. E. Rethy, W. H. McMullen and S. E. Wiberley, *Anal. Chem.*, 25 (1953) 608.
7 F. S. Grimaldi and H. Levine, *U.S. Geol. Surv.*, 992 (1953) 39.
8 J. W. Collat and L. B. Rogers, *Anal. Chem.*, 27 (1955) 961.
9 W. T. Rees, *Analyst (London)*, 87 (1962) 202.
10 Ch. A. Noll and L. J. Stefanelli, *Anal. Chem.*, 35 (1963) 1914.
11 D. C. Bhatnagar and L. S. Forster, *Spectrochim. Acta*, 21 (1965) 1803.
12 T. Kambara and H. Hashitaui, *Anal. Chem.*, 31 (1959) 567.
13 T. S. West, *Anal. Chim. Acta*, 25 (1961) 404.
14 G. H. Morrison and H. Freiser, *Solvent Extraction in Analytical Chemistry*, Wiley, New York, 1957.
15 R. J. Hynek and L. J. Wrangell, *Anal. Chem.*, 28 (1956) 1521.
16 C. R. Frink and D. E. Peaslee, *Analyst (London)*, 93 (1968) 469.
17 R. Villarreal, J. R. Krsul and S. A. Barker, *Anal. Chem.*, 41 (1969) 1420.
18 R. Oberhauser, *Materialpruefung*, 15 (1973) 85.
19 J. L. Kassner and M. A. Ozier, *Anal. Chem.*, 23 (1951) 1453.
20 D. E. Ryan, M. Granda and M. Janmohammed, *Anal. Chim. Acta*, submitted for publication.

Analytica Chimica Acta, 74 (1975) 29–33

SIMPLIFIED FLUORIMETRIC DETERMINATION OF DIGITALIS ALKALOIDS

DATTA V. NAIK, J. STEPHEN GROOVER and STEPHEN G. SCHULMAN*
College of Pharmacy, University of Florida, Gainesville, Florida 32610 (U.S.A.)
(Received 30th May 1974)

The digitalis alkaloids are currently widely employed in the treatment of cardiovascular disease. It has recently been shown that the bioavailability of the digitalis alkaloids in commercial preparations is quite variable and is directly related to the dissolution rates of the tablets[1]. Because the usual dosages of digitalis alkaloids are in the fraction of a milligram region, the constancy of composition of the tablets, in both the chemical and mechanical senses, should be controlled as carefully as possible. The USP has recently proposed a new lower limit of rate of dissolution of 40% per hour, for digoxin tablets. The USP also recommends a fluorimetric method for the determination of digitalis alkaloids and for the rate of tablet dissolution[2]. This method employs methanol, ascorbic acid, hydrogen peroxide and concentrated hydrochloric acid to generate an analytically useful fluorophore from digoxin. An alternative fluorimetric method[3] employing acetic anhydride, acetyl chloride and trifluoroacetic acid to generate fluorophores from digoxin and digitoxin has also been reported. However, both methods entail rather elaborate derivatizing procedures and are time-consuming. Moreover, neither method is very sensitive. Herein a simple procedure is reported for generating a fluorophore, from the digitalis alkaloids, whose fluorescence is stable, intense and developed considerably more rapidly than those of the fluorophores in the previously reported fluorimetric methods for digitalis.

EXPERIMENTAL

Materials and reagents

Pure digoxin, digitoxin, digoxigenin, and digitoxigenin were obtained from K & K Laboratories, Inc., Plainview, New York. Analytical grade (95–98%) sulfuric acid and spectro-grade dichloromethane (Mallinckrodt Chemical Works), digoxin (lanoxin)and digitoxin (lanatoxin) tablets, and digoxin elixir (Burroughs–Wellcome) were also used.

Apparatus

Fluorescence spectra and intensity measurements were taken on a Perkin-Elmer MPF-2A fluorescence spectrophotometer whose monochromators were calibrated against the xenon line emission spectrum and whose output was corrected for instrumental response by means of a rhodamine-B quantum counter.

* To whom correspondence should be addressed.

Standard curves

Stock solutions of the digitalis compounds were prepared in 95% ethanol. Appropriate dilutions to give a range of concentrations were also made with 95% ethanol. In the case of digoxin, 0.1 ml of the appropriate ethanolic stock solution (concentration = 100 times that desired) was delivered to a 25-ml beaker by means of a 100-μl pipet. The ethanol was evaporated on an oil bath (70°C) and 10.0 ml of concentrated sulfuric acid was added to the residue. The mixture then was heated for 15 min in an oil bath maintained at 70°C. The spectrum of the solution was recorded after cooling to room temperature. For the digitoxin determination, the acid solutions were prepared as above but were not heated.

Tablet extraction

For individual tablet analysis, a tablet was ground to a fine powder and the powder transferred to a 10-ml Erlenmeyer flask containing about 8 ml of dichloromethane. The suspension formed was shaken in an ultrasonic bath for 10 min to effect dissolution of the digitalis drug. The dichloromethane solution was then filtered through a sintered-glass funnel. The residue in the funnel was washed three times with 5 ml of dichloromethane, and the washings and filtrate were then transferred to a 25-ml volumetric flask and diluted to volume with dichloromethane. With this procedure the final concentration of the solution of a tablet, whose labeled contents are 0.25 mg of a drug, would be 10 μg ml^{-1}.

Tablet analysis

An aliquot of dichloromethane extract, enough to give 40 μg of the drug, was evaporated to dryness in a 25-ml beaker on an oil bath kept at 70°C. This dry residue was then treated with 10 ml of concentrated (96.0%) sulfuric acid. For digoxin tablets, the acid solution was heated at 70°C in an oil bath for 15 min, and cooled to room temperature before the fluorescence intensity was measured at 420 nm ($\lambda_{ex} = 390$ nm). For digitoxin tablets, the fluorescence intensity of the acid solution, at 435 nm ($\lambda_{ex} = 418$ nm), was measured without heating. The background intensity from sulfuric acid alone was also measured and subtracted from the intensity obtained for the drug solution. The concentration of each digitalis drug can be determined by referring to its fluorescence intensity *vs.* drug concentration calibration curve, or alternatively by the ratio method.

Ratio method

In this method, an appropriate amount of ethanolic solution of pure drug, containing 40.0 μg of the drug, is evaporated to dryness. The residue is treated with concentrated sulfuric acid in the same way as the residue obtained from the dichloromethane extract of the tablet. The two treatments are carried out simultaneously, and fluorescent intensities of pure drug, F_0, and of tablet extract, F_x, are measured and corrected for background intensity. The percent purity of the tablet can then be obtained by using the simple relationship, % purity = $(F_x/F_0) \times 100$.

It was found that individual tablets from the same batch, varied in their contents over an appreciable range (*ca.* 12%). That this variation was not due to experimental error was verified as follows. Ten tablets of each drug, digoxin and

digitoxin, were weighed and then ground to a fine powder. This powder in the amount exactly equal to the average tablet weight was used to check on the reproducibility of the proposed technique. The average mean deviation obtained, for the same number of samples as above, was only 4%.

Analysis of digoxin elixir

Digoxin elixir (2 ml; 0.05 mg ml^{-1}) was extracted with 25 ml of dichloromethane. An aliquot (10 ml) of this extract was evaporated to dryness, and the residue was treated in the same way as the residue obtained from tablet analysis.

DISCUSSION

When digoxin or digitoxin is added to concentrated sulfuric acid, a light yellow solution is produced instantly. The absorption spectra of the acidic solutions of these compounds are shown in Fig. 1. These compounds in concentrated sulfuric acid exhibit two fluorescence bands, probably as a result of more than one product derived from reaction with the acid. The characteristics of these emissions are given in Table I. Of the two fluorescence emissions, the one in the violet region is more intense than that in the green region. Consequently, the violet fluorescence was employed for the determinations. After digoxin had been added to the acid, the fluorescence intensity increased with time. Heating the acidic solution of digoxin for 15 min at 70°C produced maximal fluorescence intensity which was constant for at least 15 min after cooling to room temperature. Hence heating was incorporated into the procedure. The acidic solution of digitoxin, however, did not show appreciable change in the fluorescence intensity with time. Heating the acid solution of digitoxin resulted in decrease of its fluorescence intensity. Thus

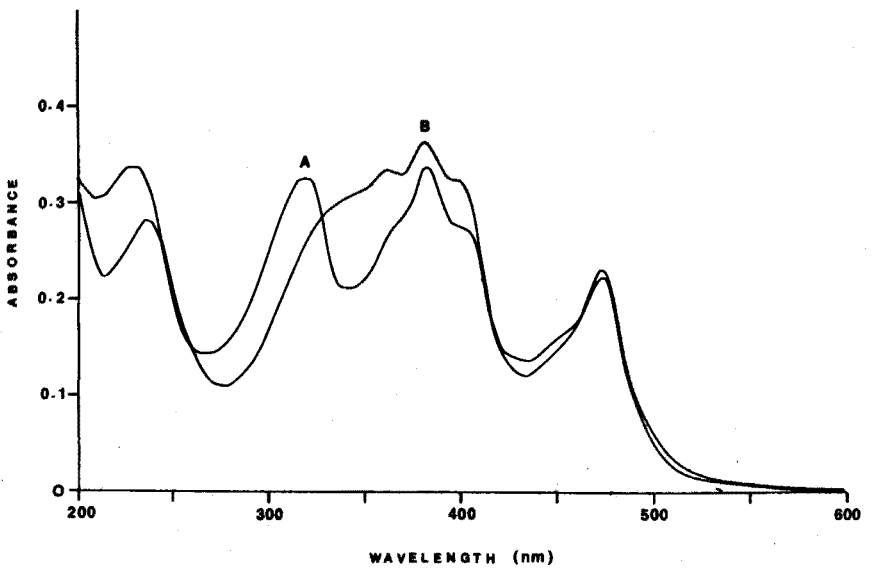

Fig. 1. U.V.–visible spectra of (A) digoxin and (B) digitoxin in concentrated sulfuric acid. Concentration of both the compounds was 10 μg ml^{-1}.

TABLE I

FLUORESCENCE CHARACTERISTICS OF DIGITALIS COMPOUNDS IN CONCENTRATED SULFURIC ACID

Compound	λ_{ex} *(nm)*	λ_{em} *(nm)*	λ'_{ex} *(nm)*	λ'_{em} *(nm)*
Digoxin	390	420	490	510
Digitoxin	418	435	485	518
Digoxigenin	390	420	488	518
Digitoxigenin	418	435	485	510

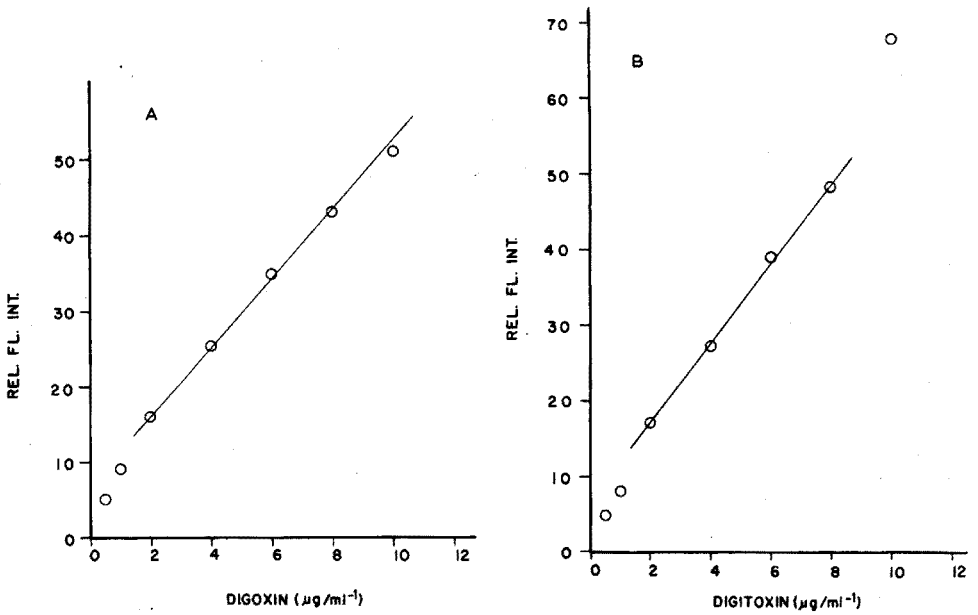

Fig. 2. Standard curves for (a) digoxin ($\lambda_{ex}=390$, $\lambda_{em}=420$ nm), and (b) digitoxin ($\lambda_{ex}=418$, $\lambda_{em}=435$ nm).

digitoxin–acid solutions were not heated for analytical purposes. Because the fluorescence intensities of the products of the reactions of digoxin and digitoxin with sulfuric acid are extremely temperature-sensitive, reasonable control of temperature in the cell compartment should be maintained. Moreover, because of the tendency of sulfuric acid solutions to adsorb atmospheric moisture and become warm, fluorescence measurements should be made in stoppered cells.

Figure 2 shows the standard curves obtained for digoxin and digitoxin, in the concentration range 0.5–10 μg ml^{-1}. The linear region was 2–8 μg ml^{-1}. The limit of detection, based on the amount of compound required to yield a fluorescence intensity greater than twice that of the background, was 0.05 μg ml^{-1} for both drugs. Table II shows the results of the analysis of lanoxin (digoxin) and lanatoxin (digitoxin) tablets, and lanoxin elixir.

The variation in water content of concentrated sulfuric acid can seriously

TABLE II

RESULTS OF ANALYSES OF COMMERCIAL DIGITALIS PREPARATIONS

	Labeled contents (mg)	*Average found (mg)*	*Percent*
Lanoxin (digoxin) tablet[a]	0.25	0.21 + 0.01	84 ± 4
Lanatoxin (digitoxin) tablet[a]	0.25	0.22 + 0.01	88 ± 4
Lanoxin (digoxin) elixir (2 ml of elixir analyzed)	0.05 per ml	0.041 + 0.002 per ml	82 ± 4

[a] Based on five determinations on samples from ten-tablet batch.

affect the production of fluorophores from digitalis drugs. For example, 90% sulfuric acid will not produce any detectable fluorophore. Therefore, care should be taken to use at least 95.0% sulfuric acid.

Since sulfuric acid absorbs moisture rapidly, the standard curve technique can be used only when the same sulfuric acid is used for both standard and sample measurement, and that too within a short time period. The error caused by small changes in the moisture content of sulfuric acid can be avoided by using the ratio method, provided that the approximate concentration of the sample is known.

Digoxigenin and digitoxigenin also react with sulfuric acid to give fluorophores similar to digoxin and digitoxin respectively. Table I lists the fluorescence characteristics of digoxigenin and digitoxigenin. Thus the present technique cannot distinguish between digoxin and digoxigenin or digitoxin and digitoxigenin. Also the fluorescence from digoxin occurs within a few nm of that from digitoxin and therefore the method cannot be used to analyze a mixture of the digitalis drugs.

The fact that digoxigenin and digitoxigenin react with sulfuric acid to give fluorophores, indicates that the fluorescent product must be a result of reaction between sulfuric acid and the aglycone part of the digitalis drugs.

SUMMARY

A new fluorimetric procedure for the determination of digoxin and digitoxin is described. The method is based upon the development of a fluorophore when the digitalis drugs are treated with concentrated sulfuric acid. Applications to tablet and elixir forms of the drugs are described.

REFERENCES

1 J. Lindenbaum, V. P. Butler, Jr., J. E. Murphy and R. M. Cresswell, *Lancet*, June 2, 1973, p. 1215.
2 D. Wells, B. Katzung and F. H. Myers, *J. Pharm. Pharmacol.*, 13 (1961) 389.
3 I. M. Jokovljevic, *Anal. Chem.*, 35 (1963) 1513.

Analytica Chimica Acta, 74 (1975) 35–42

TRENDS IN ATOMIC ABSORPTION SPECTROMETRY

R. R. BROOKS* and L. E. SMYTHE
School of Chemistry, University of New South Wales, Sydney (Australia)
(Received 10th June 1974)

The progress of atomic absorption spectrometry, since its inception in 1955[1], has been extremely rapid and has resulted in many books and nearly 100 reviews on the subject. Because of this large number of publications, any further reviews should of necessity be designed to cover ground not previously considered. Here, an attempt is made to achieve this aim by studying long-term trends for the period 1955–1971 and by concentrating on such questions as: the volume of the literature, the countries in which the work was done, the language in which it was reported and the journals in which it was published. Development trends in atomic absorption spectrometry are also considered, and the benefits of the technique to the world economy are assessed.

THE VOLUME OF LITERATURE ON ATOMIC ABSORPTION SPECTROMETRY

Sources for a survey on the literature of atomic absorption spectrometry were: *Atomic Absorption and Flame Emission Abstracts* (AAFESA) and the annual bibliographies which have appeared regularly in *Atomic Absorption Newsletter*[2–4] (AAN). The former publication is more detailed and has had a wider coverage in recent years, whereas *Atomic Absorption Newsletter* bibliographies extend further back in time, and are more complete for the earlier years. Counting of all entries in the two sources up to the end of 1971, showed that AAFESA has had consistently 1.75 times the number of entries of AAN for the period 1970–1971. The year 1971 was chosen as a final cut-off point for this survey because this was the latest date for which a complete bibliography was available (*i.e.* 1972 papers are still appearing in current numbers of AAFESA).

The total number of atomic absorption papers was calculated in the following way. Entries in AAN were counted and multiplied by 1.75 for 1960 and later, in order to obtain the maximum possible number of papers. These figures were then reduced by 15% to remove papers dealing with flame emission spectrometry. The figure of 15% was a mean value obtained from the 11% and 18% of flame emission papers found in AAN and AAFESA, respectively. The final total of purely atomic absorption papers was obtained by deleting all entries dealing with atomic fluorescence.

* Present address: Department of Chemistry, Biochemistry and Biophysics, Massey University, Palmerston North, New Zealand.

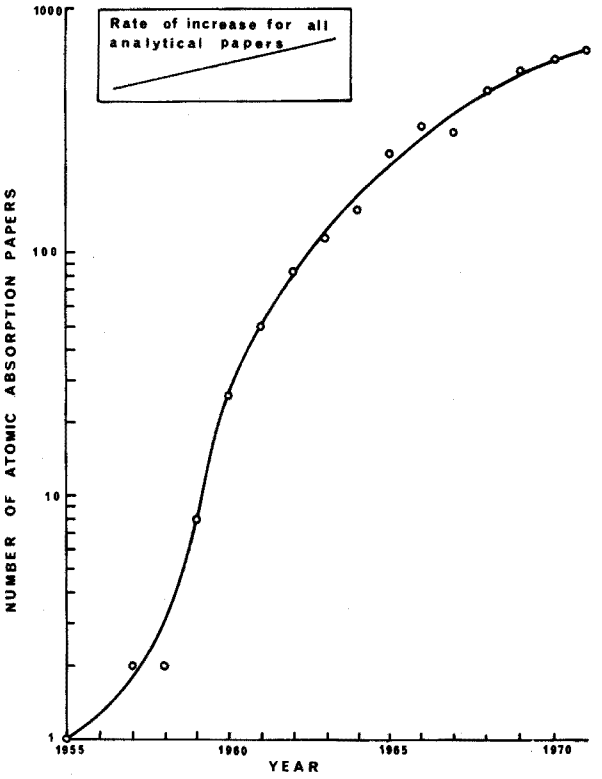

Fig. 1. Annual publication rate of atomic absorption papers.

Data and discussion

In Fig. 1, the number of atomic absorption papers has been plotted as a function of the year of publication. The curve (logarithmic) is sigmoidal and is typical of the "surge pattern" reported previously by Brooks and Smythe[5]. When a new technique is developed, there is a rush to work in this new field, and thus an upsurge in the number of papers published ("bandwaggon effect"). After a certain period, the method becomes well established and the rate of increase of papers levels off to a constant exponential increase. It will be observed from Fig. 1, that atomic absorption has now reached the top of the "surge", the rate of increase is beginning to level off and will shortly approach the rate for all analytical papers[5] (see inset).

In 1970, atomic absorption papers (662) represented 3.4% of the world total of all analytical papers, compared with 0.25% (26) in 1960. Judged by the trends shown in Fig. 1, the proportion is likely to stabilize at about 4.0% of the world total by the mid-1970's.

COUNTRIES IN WHICH ATOMIC ABSORPTION RESEARCH WAS CARRIED OUT AND THE LANGUAGE IN WHICH IT WAS PUBLISHED

Entries in AAFESA for 1970 were classified according to the countries of

origin. These were compared with AAN entries for 1962 (AAFESA not being available for this year). The data were expressed as a percentage of all entries for the year.

Data and discussion

The data are given in Table I which shows the pre-eminence of Australasia and South Africa in the earlier years, because of the pioneering work of A. Walsh and his associates in Australia, J. E. Allan in New Zealand, and A. Strasheim and L. R. P. Butler in South Africa. The momentum of some of this earlier work was not maintained, and by 1970 South Africa had ceased to be important in volume of publications, although Australia still had eminence in the field.

The Soviet Union has been a world leader in general analytical chemistry ever since 1935, and in 1970 accounted for 28% of the world total of analytical papers[5]. In spite of this, however, Russia has been relatively slow in developing atomic absorption spectrometry, and in 1970 accounted for only 5.6% of all atomic absorption publications.

Nearly half of all atomic absorption papers were published in the United States in 1970, with the United Kingdom in second place. Czechoslovakia, which accounted for 5.6% of the world total of analytical papers in 1970[5], also accounted for an almost identical percentage (5.5) of atomic absorption papers in the same year.

In the period 1962–1970, English has maintained itself as the chief medium of publication of atomic absorption papers. The constant value of about 70% compares with 30% for the world total of all analytical papers in the same

TABLE I

COUNTRIES IN WHICH ATOMIC ABSORPTION RESEARCH WAS CARRIED OUT AND THE LANGUAGE IN WHICH IT WAS PUBLISHED

Country	*Language*	*Percentage of atomic absorption papers*	
		1962	*1970*
United States		35.5	43.8
United Kingdom		3.4	14.0
Soviet Union		7.0	5.6
Czechoslovakia		1.7	5.5
Canada		1.7	5.1
Australia		15.8	4.9
Japan		7.0	4.5
France		1.7	4.3
Germany (East and West)		10.5	3.0
South Africa		14.0	0.3
Other countries		1.7	9.0
	English	70.4	69.1
	Russian	7.0	5.6
	Czech	1.7	5.5
	Japanese	7.0	4.5
	French	1.7	4.3
	German	10.5	3.0
	Other	1.7	8.0

TABLE II

PRINCIPAL JOURNALS WHICH PUBLISH ATOMIC ABSORPTION PAPERS

Journal	*Period*							*Total*	*% of all papers*
	1955–59	*1960–61*	*1962–63*	*1964–65*	*1966–67*	*1968–69*	*1970–71*		
Atomic Absorption Newsletter (U.S.)	—	—	16	69	110	92	94	381	15.22
Analytica Chimica Acta (Holl.)	—	4	11	10	30	67	72	194	7.75
Analytical Chemistry (U.S.)	1	5	11	17	31	45	44	154	6.15
Spectrochimica Acta (U.K.)	5	12	5	8	17	37	31	115	4.59
The Analyst (U.K.)	4	7	3	2	10	35	33	94	3.75
Applied Spectroscopy (U.S.)	—	—	2	2	15	25	21	63	2.52
Bunseki Kagaku (Japan)	—	—	—	3	2	9	37	51	2.04
J. Association Official Anal. Chemists (U.S.)	—	—	—	2	10	16	22	50	2.00
Talanta (U.K.)	—	—	1	6	6	23	13	49	1.96
Zhurnal Prikladnoi Spektroskopii (U.S.S.R.)	—	—	—	2	10	18	17	47	1.88
Zhurnal po Analiticheskoi Khimii (U.S.S.R.)	—	1	4	8	4	10	18	45	1.80
Zeitschrift für Analytische Chemie (Ger.)	—	1	2	5	6	12	11	37	1.48
Clinical Chemistry (U.S.)	—	—	—	—	6	11	18	35	1.40
Zavodskaya Laboratoriya (U.S.S.R.)	—	1	4	6	3	7	10	31	1.24
Nature (U.K.)	1	7	3	4	6	2	5	30	1.20
Clinica Chimica Acta (Holl.)	—	—	—	—	—	12	6	18	0.72
Analytical Biochemistry (U.S.)	—	—	1	1	6	4	4	16	0.64
Mikrochimica Acta (Austria)	—	2	2	2	1	—	6	13	0.52
Chimie Analytique (France)	—	—	—	1	—	5	6	12	0.48
Japan Analyst (Japan)	—	—	—	3	1	4	2	10	0.40
Chemicke Listy (Czech.)	—	—	—	1	2	1	2	6	0.24
Total	11	40	65	152	276	435	472	1451	57.98

period[5]. In 1962, the second most frequent language of communication in this field was German (10.5%) which has now been superseded by Russian (5.6%) and Czech (5.5%) in second and third places, respectively.

PRINCIPAL JOURNALS WHICH PUBLISH ATOMIC ABSORPTION PAPERS

The number of atomic absorption papers appearing in various journals was obtained from AAN for the period 1955–1971. Data were also expressed as a percentage of the total numbers of papers published in each period. This total (2504) was based on the number appearing in AAN. The wider coverage of AAFESA would have given a total of 3731 papers, but could not be used to calculate the percentage because only AAN had been used as source material for this part of the survey.

Data and discussion

The data are shown in Table II from which it can be seen that 21 journals have carried nearly 60% of the world total of atomic absorption papers since 1955. As might have been expected from its specialist nature, *Atomic Absorption Newsletter* has carried the greatest proportion of papers. Of the non-specialist journals, *Analytica Chimica Acta* and *Analytical Chemistry* carried the greatest number of atomic absorption papers. Table II also shows that *Spectrochimica Acta* and *The Analyst* were the first journals to publish atomic absorption papers to any extent before 1962.

Russian journals appear to be under-represented in the atomic absorption field. For example, *Zhurnal Analiticheskoi Khimii* had accounted for only 1.80% of the world total of atomic absorption papers by 1971, whereas in 1970 it accounted for 3.36% of the total for all papers on analytical chemistry[5]. *Zavodskaya laboratoriya* shows the same pattern to an even greater extent with values of 1.24% and 4.38%, respectively.

English language journals carried a greater percentage of the atomic absorption papers compared with analytical publications in general. In 1970, the major English language journals carried 29.8% of the world total of all analytical papers[5], whereas they accounted for 47.9% of all atomic absorption papers for the period 1955–1971. In the year 1970, the predominance of English language journals was even greater in the field of atomic absorption with a figure of 81.4% compared with the above figure of 47.9% for the entire period of study.

CATEGORIES OF ATOMIC ABSORPTION RESEARCH

The information for this survey was taken from summaries in AAN. Each paper was classified into one of nine categories. The ninth category (development of methods without specific applications) is not included in the appropriate Table, but its total was used for expressing each of the other groups as a percentage of the total number of papers. The "Instrumental" category was subdivided into 11 components.

Data and discussion

Table III shows broad categories of research in atomic absorption spectro-

TABLE III

PERCENTAGE OF ATOMIC ABSORPTION PAPERS IN VARIOUS GENERAL CATEGORIES

Category	*Year*					
	1961	*1963*	*1965*	*1967*	*1969*	*1971*
Agricultural	3.6	1.8	3.3	4.9	4.9	5.4
Biological	17.9	10.9	19.8	17.9	17.9	12.9
Food	—	—	1.1	4.6	2.0	3.2
Geochemical	3.6	3.6	10.9	9.8	10.4	10.2
Industrial	3.6	5.5	9.9	8.4	9.3	9.7
Instrumental	25.1	49.1	39.6	44.2	44.6	47.9
Metallurgical	14.2	20.0	7.7	7.7	9.2	9.8
Reviews	32.0	9.1	7.7	2.5	1.7	0.9

TABLE IV

ATOMIC ABSORPTION PAPERS IN VARIOUS INSTRUMENTAL CATEGORIES EXPRESSED AS A PERCENTAGE OF THE INSTRUMENTAL SECTION IN TABLE III

Instrumental category	*Year*					
	1961	*1963*	*1965*	*1967*	*1969*	*1971*
Automation	—	—	3.6	4.0	5.2	3.0
Burners and flames	—	29.1	7.1	15.9	9.7	10.1
Electrodeless discharge tubes	—	—	—	—	7.8	3.0
Flameless atomic absorption (Hg)	—	—	—	4.7	0.6	9.3
Hollow cathodes	—	16.7	17.8	8.7	4.5	3.0
Instruments	50.0	29.2	21.4	15.8	7.1	2.6
Nebulization	—	8.3	3.6	5.5	3.2	1.1
Non-flame excitation (carbon rod etc.)	—	—	—	2.4	5.2	9.7
Sources (other than above)	—	—	17.8	4.0	1.9	0.7
Techniques and theory	17.0	12.5	10.9	29.5	15.9	7.5
Other techniques	33.0	4.2	17.8	9.5	38.8	50.0

metry. It can be seen that in recent years, nearly half of the research effort has been devoted to instrumental developments. All other categories except "Geochemical" and "Reviews" have maintained a relatively constant proportion during the period 1965–1971. The sharp increase in the "Geochemical" category after 1963 is almost certainly due to the world-wide mineral boom, when atomic absorption spectrometry afforded a ready, speedy, accurate and inexpensive method for analysing very large numbers of geochemical samples such as soils, stream sediments, rocks, vegetation and waters.

It is noteworthy that the number of reviews has fallen sharply and consistently since the euphoria of the early days. Altogether, a total of nearly 100 reviews has appeared in the period 1960–1971, half of which appeared during the first four years.

When the "Instrumental" section is subdivided into 11 categories of research, certain trends become clear (Table IV). The proportion of research into hollow-cathode lamps has dropped steadily from 17.8% of the "Instrumental" category in

1965 to 3.0% in 1971. This is probably because of diversion of effort to other sources such as electrodeless discharge tubes, and because hollow cathodes have now reached a degree of refinement which does not warrant such extensive work upon them. Work on other "Sources" has also dropped from 17.8% in 1965 to 0.7% in 1971, perhaps because most other possible sources have now been investigated and found to be less suitable than hollow cathodes or electrodeless discharge tubes.

Developments in nebulization seem to have slackened, as the proportion of work in this field has dropped steadily since 1963. Further improvement in nebulization efficiency remains the main goal.

Perhaps the most interesting finding to emerge from the survey is the enormous decrease in work on new instruments: from 50.0% in 1961 to 2.6% in 1971. This trend confirms the "coming of age" of atomic absorption spectrometry, when basic instrument design has become more or less standardized and where further work is devoted to refinement rather than innovation. The great contribution of the Division of Chemical Physics, C.S.I.R.O., Victoria, Australia, where the whole field began about 20 years ago with the pioneering work of Walsh[1] should not be forgotten. World patents for the basic instrument were also held by C.S.I.R.O.[6] and these have now expired.

Table IV also shows the increasing interest in non-flame excitation (carbon rod atomizer, etc.) and in flameless atomic absorption of mercury. The large increase in "Other" techniques is almost entirely due to atomic fluorescence research (11.0% in 1969 and 13.2% in 1971) which has been included in Table IV for comparison, although in general it lies outside the scope of this review.

ECONOMIC BENEFITS OF ATOMIC ABSORPTION SPECTROMETRY

There can be no doubt that atomic absorption spectrometry has been of immense benefit to national economies. It is possible to assess this benefit with some degree of confidence because precise details of sales of instruments are available[7]; all units are manufactured under licence to C.S.I.R.O., Australia[6]. Brown[8] has carried out an excellent assessment of the economic benefits to Australia of atomic absorption spectrometry. A survey of the 400 instruments in use in 1968 showed that 7% were employed by geochemical assaying laboratories, 15% by the mining and smelting industry, 20% by Government departments, 7% by C.S.I.R.O., 16% by universities, 8% by hospitals and 27% by industrial and other users. The greatest gains in productivity were for the geochemical assayers whose instruments had the highest loadings with up to 150,000 determinations per instrument per year. Overall the instruments had had a cumulative total of $A6,000,000 in direct benefit to users by the end of 1968. This figure was projected to reach $A8,800,000 in 1970 and $A10,785,000 by 1978.

The above data relate only to direct benefit to users on the basis of increased output of analytical data at a lower unit cost compared with older classical techniques, and takes no account of hidden benefits which are more difficult to assess. As an example of a hidden benefit, we can cite the increased mineral finds which have resulted throughout the world as a direct result of a much greater volume of geochemical exploration (*cf.* Table III). Even if a very conservative view is adopted, and direct and indirect benefits to Australia are

assessed as having reached a cumulative total of $A10,000,000 by the end of 1970, a value of $A200,000,000 or $US300,000,000 is reached for the world as a whole because Australia contained about 5% of the world total of instruments in 1970. This figure does, however, make the assumption that world usage pattern is the same as that of Australia with its high proportion of instruments carrying very heavy loadings of geochemical analyses. With due allowance for this, it seems that the most conservative estimate must assess the cumulative direct and indirect benefits of atomic absorption spectrometry to the world economy as at least $US250,000,000 in the years following the experiments of A. Walsh in the early 1950's, which led to the development of this outstanding analytical technique.

We would like to acknowledge with gratitude our source material: *Atomic Absorption and Flame Emission Abstracts* and the annual bibliographies by W. and S. Slavin of the Perkin-Elmer Corp. which have appeared in *Atomic Absorption Newsletter.*

SUMMARY

The progress of atomic absorption spectrometry has been reviewed for the period 1955–1971. Topics discussed are: the volume of literature, countries in which research was carried out and the language in which the work was published, the identity of the principal journals which publish atomic absorption papers, broad categories of research, and the economic benefit of the technique.

REFERENCES

1 A. Walsh, *Spectrochim. Acta*, 7 (1955) 108.
2 Anon., *At. Absorption Newslett.*, 1 (1962) 4; 2 (1963) 59; 4 (1965) 201.
3 W. Slavin, *At. Absorption Newslett.*, 5 (1966) 50; 6 (1967) 41; 7 (1968) 11.
4 S. Slavin, *At. Absorption Newslett.*, 8 (1969) 8; 9 (1970) 13; 10 (1971) 17; 11 (1972) 7; 11 (1973) 75; 12 (1973) 9.
5 R. R. Brooks and L. E. Smythe, *Talanta*, in press.
6 Anon., *Patents Specifications*, Australia 23041/53, Great Britain 33068/54, U.S.A. 469,221, France 679,886, Germany C10276 IXb/421, Holland 192460, Italy 82/322, Sweden 10436/54.
7 Anon., *C.S.I.R.O. Ann. Rep. Div. Chem. Physics*, (1970–71) 2.
8 A. W. Brown, *Econ. Record*, 45 (1969) 158.

Analytica Chimica Acta, 74 (1975) 43–52

A HOLLOW-T CARBON ATOMIZER FOR ATOMIC ABSORPTION SPECTROMETRY

J. W. ROBINSON and D. K. WOLCOTT

Department of Chemistry, Louisiana State University, Baton Rouge, Louisiana 70803 (U.S.A.)

(Received 17th June 1974)

Many papers in the past few years have reported on the greatly increased sensitivity that can be attained in atomic absorption spectrometry through the use of electrically heated atomizers. The first analytical use of such a device was reported by L'Vov[1]. In his system the sample was atomized by an arc discharge and then expanded into a resistance heated cell for absorbance measurement. Later modifications by Massman[2] and West and Williams[3] produced devices in which the sample was atomized merely by the high temperature of a carbon rod heated electrically. Robinson *et al.*[4] reported on an r.f.-heated carbon atomizer for continuous monitoring of lead in air. More recently, electrothermal atomizers have become commercially available and have gained great popularity for various analyses.

The commercially available resistance heated atomizers all have several factors in common: (1) they depend on rapid resistance heating to reduce the sample to free atoms and (2) they utilize a three-step atomization step to eliminate broad-band absorption[5]. Unfortunately, the utilization of a three-step atomization process can introduce errors into the analysis through losses of the compounds of interest by volatilization before atomization can occur[6]. With more volatile elements, losses can occur even during the low-temperature drying step for solvent removal[7] and more extensive losses occur during the hotter ashing steps. Moreover, even a three-step atomization process cannot completely eliminate background absorption if the matrix contains relatively non-volatile components[8].

A single-step atomization process (with little or no molecular background) would eliminate the above-mentioned sources of error. The r.f. carbon bed atomizer has shown these capabilities[9–11]. With this atomizer, atomic vapor can be generated remote from the light path, and the atomic absorption can be subsequently measured. Separating the two processes of atomization and absorption measurement resulted in the reduction of molecular background and hence removed the necessity for a separate dry, ash and atomize sequence. Unfortunately, because the original atomizer was constructed with quartz tubing, the maximum useable temperature was 1500°C. Such a temperature was sufficient to atomize the more volatile elements such as Cd, Pb and Hg, but proved inadequate for the atomization of less volatile elements such as Be and Cr.

This paper describes the design, construction and operation of a simple, resistance heated atomizer with the same operational advantages as the r.f. carbon bed atomizer; it consisted of a hollow graphite T-piece (Fig. 1).

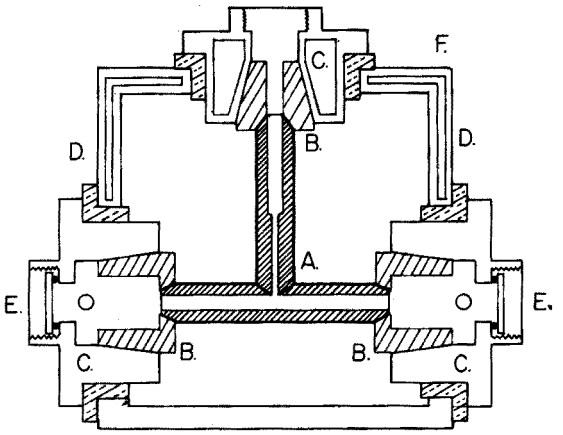

Fig. 1. A, graphite T cell; B, graphite contacts; C, water-cooled electrodes; D, insulators; E, quartz windows; F, water-cooled housing.

Nebulization and atomization take place in one section of the system. The free atoms are swept into a second section where the absorption measurement is made. In addition to reducing molecular absorption, the physical separation of the atomization and measurement step greatly decreases chemical interference.

EXPERIMENTAL

Equipment

A Barnes demountable hollow-cathode lamp, with a Barnes power supply (GPS-1), and gas flow control, was used. Other equipment included a Jarrell-Ash 0.5-m Ebert monochromator, a Heathkit EU-703-1 photometric readout module, a Beckman potentiometric recorder, a Beckman deuterium lamp and power supply, a Signal Transformer Co. stepdown transformer rated 9 V at 500 A, two 20-A Variacs, Drummond Micropipettes, a vacuum flow pump, and rotameters.

Atomizer

A schematic diagram of the atomizer is shown in Fig. 1. Essentially the atomizer consisted of a T-piece made of graphite with the end of the stem connected to one electrode and each end of the cross piece connected to a second electrode. Current flowed through the stem across the T-piece and the whole system was heated up to the desired temperature. The T-piece was hollow and permitted nebulization and atomization to take place in the stem, and absorption measurements to be made in the cross piece. The entire system was maintained in an inert atmosphere by enclosing in a metal case. The electrodes and the metal case were all water-cooled.

Construction of atomizer housing. The atomizer housing was constructed of 1/8-in. aluminum sheet, welded at the seams. It was a double wall construction to permit water cooling. The housing contained three welded flanges to hold the electrodes; water inlet ports and inert gas inlet port were also incorporated. One side of the atomizer was a single 1/8-in. aluminum plate, held in place by four

no. 6 screws and sealed by a Teflon gasket, the plate allowing easy access to the interior of the atomizer.

Construction of electrodes. The electrodes were constructed of stainless steel and were water-cooled. The electrodes at the ends of the cross piece were equipped with O-ring grooves and threaded rings to contain silica windows. This permitted radiation from the hollow cathode to pass through the absorption cell into the monochromator. The same two electrodes contained exhaust ports to allow gas flow.

The upper electrode was made with a threaded lip, to allow attachment of different sample injectors. All electrodes were insulated from the aluminum atomizer housing by large bakelite flanges. In addition, the electrodes were held in place by springs, to assure positive contact with the atomizer carbon.

Graphite atomizer. The graphite T-tube was machined from 1.75-cm (0.5-in.) spectroscopic rods, with a 42.5° taper at each end. The atomizer vertical was 2.5 in. long, drilled through 0.25-in. diameter for 1.5 in., through 1/16-in. for 1 in. The atomizer horizontal was drilled out 3/16 in. the entire length.

The T-piece was supported and connected to the electrodes by graphite interface contacts. These electrodes greatly reduced any cold zone created by the connection to the metal electrodes. Such cold zones cause free metal atoms to deposit resulting in loss of sensitivity and possible memory effects when the instrument is used. During studies so far no memory effects have been observed.

Maintenance of atomizer. When air was used as the carrier gas in this system some combustion of the atomizer took place. This led to a decrease in the thickness of the atomizer itself and would normally lead to the demise of the system within a relatively short period of time. However, if benzene was introduced into the atomizer under reducing conditions the benzene broke down and liberated free carbon. The carbon thus produced re-coated the inside wall of the atomizer thus producing a new surface and prolonging the life of the system.

Power supply. Power for the atomizer was provided by a large step-down transformer, which was rated at 9 V, 500 A. Variation of output was obtained by ganging two 20-A Autotransformers in series across the step-down transformer primary (Fig. 2). Input power was 208 V. Plans are underway to replace the two Variacs with a solid-state power controller. Cables to the atomizer were No 0000 braided copper welding cable, tipped at the ends by brass plugs.

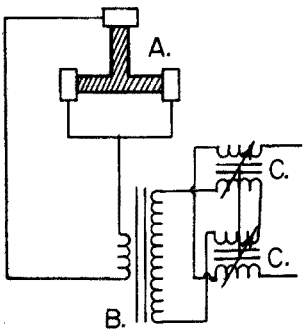

Fig. 2. A, carbon tube; B, step-down transformer; C, 20 A autotransformers ganged in series.

When the 9-V transformer was used, the maximum temperature attainable was 2600°C. Higher temperatures could be attained through the use of a 12-V transformer, and a higher resistance graphite T-piece.

Sample introduction

Liquid samples. Liquid samples were injected directly into the vertical stem of the atomizer by means of a modified Drummond Micropipette. The sample size was usually about 2 μl. It was found that under normal conditions the precision of introduction of such a small volume of sample was poor when a microliter syringe was used. It was felt that this limitation was due to the large dead volume of the needle, and that the precision could be improved if the dead volume could be eliminated. It was decided to obtain a pipetting device with a plunger which travelled the entire length of the needle. Such a device was the Drummond Scientific Corporation's Microdispenser, which employed a disposable glass barrel. The plunger of the microdispenser traversed the entire length of the barrel. As delivered, the syringe was unsatisfactory, owing to excessive drop hangup. The original microdispenser is shown in Fig. 3a. By drawing a fine capillary tip on the end of the glass barrel, and transferring the travel limiting sleeve from inside the pipette body to the plunger, as shown in Fig. 3b, the microdispenser was converted to an air-displacement device. In the modified device, an excess volume of air was retained between the plunger and the sample. Upon pressing the plunger, the excess of air assured that the entire volume of liquid was ejected from the barrel.

During the period of introduction of the sample, gas was flowing continuously through the atomizer. The gas used was either clean air or argon, and

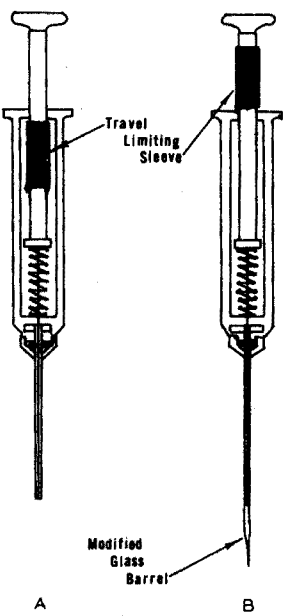

Fig. 3. A, unmodified micropipette; B, modified pipette.

was carefully controlled to a flow rate between 50 and 150 $cm^3\ min^{-1}$, depending on the type of solvent being used. A gas flow was necessary in order to prevent atoms formed during the injection period from escaping out of the top of the atomizer. The gas flow parameters were studied for different types of solvent. The data are described below.

No sample pretreatment was necessary except for dilution with suitable solvent if the samples were too concentrated.

Solid samples. Solid samples were introduced into the atomizer in a similar fashion to that used for liquid samples. The samples were weighed out and dropped directly into the vertical arm of the atomizer. Organic samples such as polymers or filter paper discs burned rapidly, and the products of combustion were drawn into the cross-piece by a steady stream of gas. No systematic study was carried out on an inorganic sample.

RESULTS

The most important analytical parameters were studied, *i.e.* analytical sensitivity, the effect of chemical interferences and the degree of molecular absorption encountered when different solvents were introduced into the atomizer.

Sensitivity

Sensitivity (for 1% absorption) measurements were obtained by injecting aqueous 2-μl samples of standard solutions directly into the atomizer. The sensitivities obtained are listed in Table I. It can be seen that the sensitivities were in most cases significantly better than those hitherto recorded in the literature, particularly for the more volatile elements.

TABLE I

SENSITIVITY OF MEASUREMENT

Element	*Sensitivity (g/0.004 A)*	*Element*	*Sensitivity (g/0.004 A)*
As	$1 \cdot 10^{-10}$	Mn	$2 \cdot 10^{-11}$
Be	$1 \cdot 10^{-10}$	Ni	$4 \cdot 10^{-10}$
Cd	$8 \cdot 10^{-14}$	Pb	$2 \cdot 10^{-13}$
Cr	$8 \cdot 10^{-10}$	Se	$4 \cdot 10^{-10}$
Cu	$1 \cdot 10^{-10}$	Zn	—[a]
Hg	$6 \cdot 10^{-10}$		

[a] The sensitivity for zinc could not be determined because all samples of "pure" water obtainable gave 100% absorption, and standard solutions could not be prepared.

Interferences

Extensive chemical interferences studies were done only for manganese, which was chosen because a comprehensive study of the chemical interferences of this metal has already been carried out by West *et al.*[12], who reported that numerous chemical interferences were encountered when the carbon filament atomizer was used.

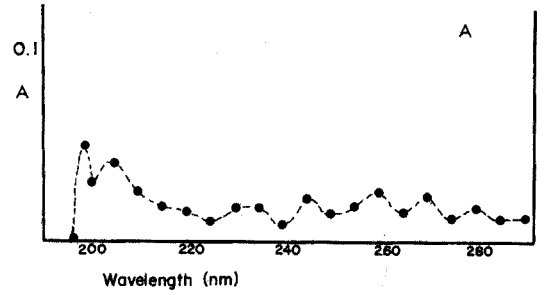
A
0.1
A
200
220
240
260
280
Wavelength (nm)

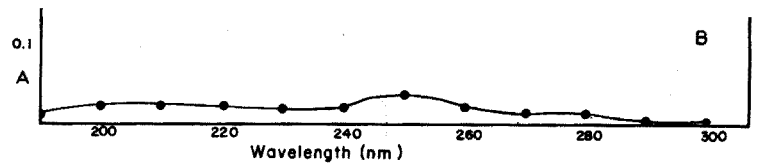
B
0.1
A
200
220
240
260
280
300
Wavelength (nm)

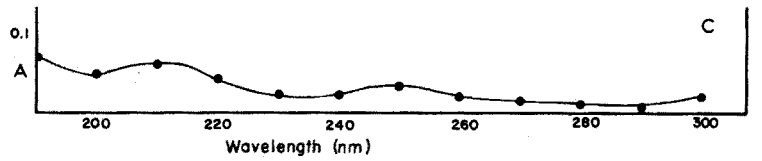
C
0.1
A
200
220
240
260
280
300
Wavelength (nm)

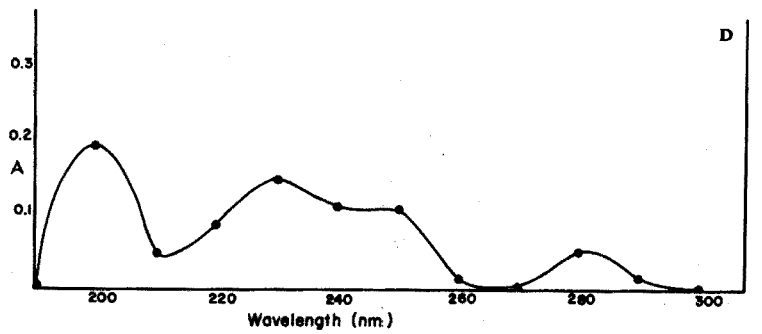
D
0.3
0.2
A
0.1
200
220
240
260
280
300
Wavelength (nm)

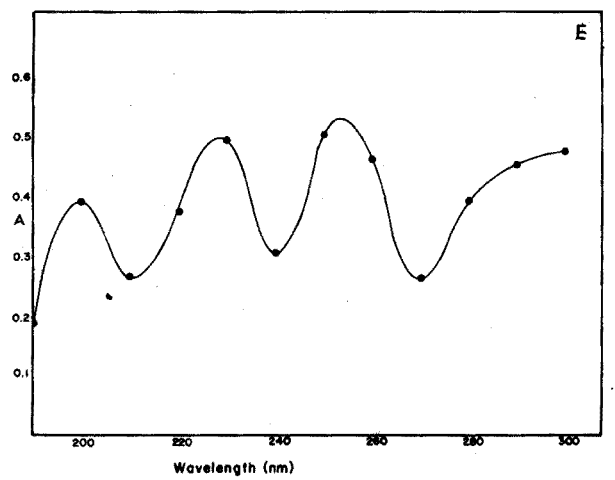
E
0.6
0.5
0.4
A
0.3
0.2
0.1
200
220
240
260
280
300
Wavelength (nm)

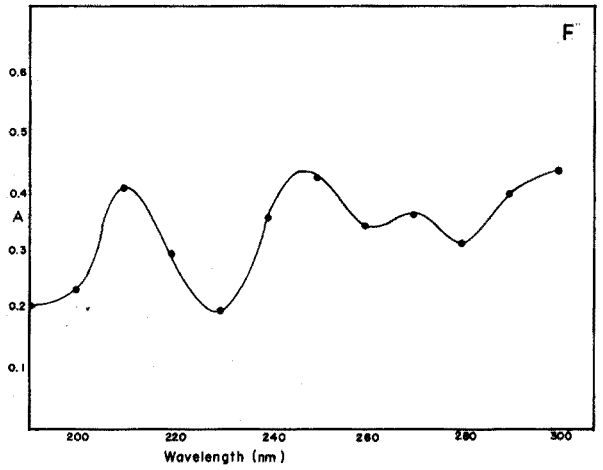

Fig. 4. Molecular absorbance *vs.* wavelength. Ar flow rate 100 cm^3 min^{-1}. A, water, 2 μl; B, methanol, 1 μl; C, formic acid, 1 μl; D, 0.2 *M* EDTA (di-Na salt), 10 μl; E, ethyl propionate, 1 μl; F, heptane, 1 μl.

Chemical interferences arise primarily because of the different rates of atomization when different chemical forms are introduced into the atomizer. When the carbon filament was used, small changes in the rate of production of free atoms gave rise to significant changes in absorption measurements at any instant in time. However, in the present system, the atomization took place in one part of the atomizer and measurement in another; because of the delay between atomization and measurement, the major source of chemical interference was removed; the atomization can take place at any variable but reasonably fast rate without interfering with the total population of atoms ultimately formed and pulled into the cross-piece for measurement.

No interference was found from 1000-fold amounts of borate, perchlorate, molybdate, sulfate, tellurite, vanadate, tungstate, fluoride, chloride, bromide or iodide. A 1000-fold amount of silicate caused a 50% reduction in signal. It is interesting to note that this anion is the major source of chemical interference with manganese when flame atomizers are used.

Molecular absorption

When other carbon atomizers are used, direct interference from molecular absorption caused by the incomplete breakdown of solvents in the light path has been reported. In order to eliminate this interference, a three-stage atomization process has been adhered to in most commercial equipment; thus, evaporation of the solvent and decomposition of the residue occurs before atomization. For many elements, this process is satisfactory although rigid control of temperature and timing is vital for reproducibility. However, direct interference can still be encountered, particularly for volatile elements such as cadmium, lead, mercury, arsenic, selenium, zinc, etc. There has been definite evidence that such metals are lost during the evaporation and pre-heat step, causing inaccuracies.

In the device described herein, the sample was introduced into the stem of

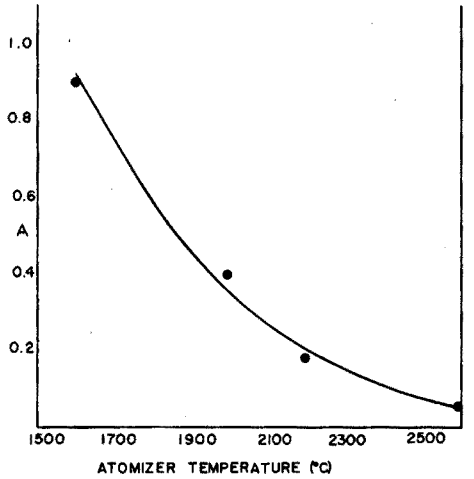

Fig. 5. Molecular absorbance *vs.* temperature. Heptane, 1 μl sample, measured over lead 283.3-nm spectral bandpass. Ar flow rate 100 cm^3 min^{-1}.

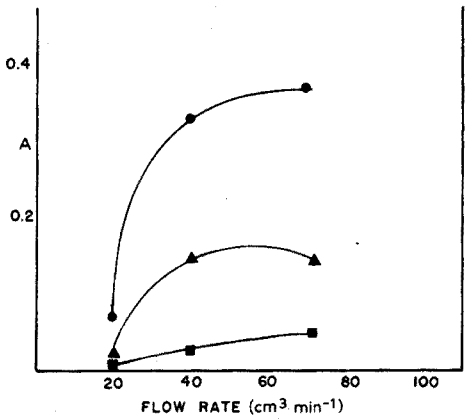

Fig. 6. Molecular absorbance *vs.* argon flow rate. Spectral bandpass, Be 234.9 nm. Sample size 1 μl. (■), water; (▲), acetone; (●), heptane.

the T-piece. At this point, the organic solvent was broken down and nebulization and atomization took place. The entire process was carried out remote from the light path. Hence it was not likely that molecular absorption would be a major source of interference since the molecular fragments were mostly destroyed before the free atoms were drawn into the cross-piece of the atomizer.

Some typical absorption spectra for different solvents are shown in Fig. 4. It was noted that whenever the solvent molecule contained oxygen (*e.g.* H_2O, CH_3OH, HCOOH), the molecular absorption was low. It should also be noted that when oxygen was included in the gas streams, solvent combustion was facilitated and molecular absorption decreased. For example, the molecular absorbance of benzene at 200 nm was 0.295 units when argon was used as flow gas, but only 0.116 units when oxygen was used. With paraffinic compounds,

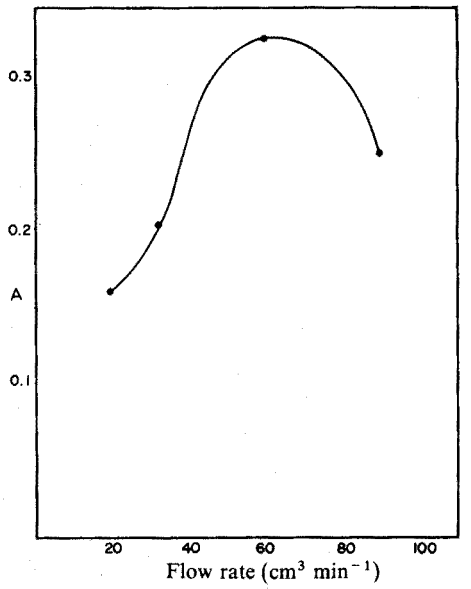

Fig. 7. Atomic absorbance *vs.* flow rate. Lead at 283.3 nm, 1 μg ml^{-1}, 1 μl sample.

absorption was greater and varied with wavelength. The greatest absorption was encountered with aromatic solvents such as benzene. When oxygen-containing solvents were used, the molecular absorption was so low that a correction could be made with a hydrogen lamp or other background corrector. Correction was more difficult with other solvents and impossible with aromatic solvents. It is important to note, however, that aqueous samples can be analysed directly.

A study of the effect of temperature (Fig. 5) clearly indicated that molecular absorbance decreased as temperatures increased. A study of the effect of gas flow rate on atomic and molecular absorption was carried out (Figs. 6 and 7). The results indicated that an optimal flow rate was encountered. Presumably when the flow rate was too low, transport of the sample from the atomizer to the measuring arm was too slow. When flow rate was too high, combustion of the solvent was incomplete.

These studies also showed that the degree of molecular absorption was dependent on the length of the side-arm of the T-piece. However, in the particular instrument described, it was not easy to change this length; perhaps if a longer side piece were used, molecular absorption could be eliminated altogether.

This investigation was supported by grant R 800771, Air Pollution Control Office, Environmental Protection Agency.

SUMMARY

A hollow T-piece atomizer for atomic absorption spectrometry has been developed and tested. No heating program is necessary for ashing or solvent removal. Chemical interferences are very low, and molecular interferences from aqueous solvents are virtually removed. Sensitivities are at least as good as, and in many cases better than, those hitherto reported in the literature.

REFERENCES

1 B. V. L'vov, *Spectrochim. Acta*, 17 (1961) 761.
2 H. Massman, *Spectrochim. Acta, Part B*, 23 (1968) 215.
3 T. S. West and X. K. Williams, *Anal. Chim. Acta*, 45 (1969) 27.
4 H. P. Loftin, C. M. Christian and J. W. Robinson, *Spectrosc. Lett.*, 3 (1970) 161.
5 P. A. Ulucci, C. J. Mokeler and J. Y. Hwang, *Amer. Lab.*, August, 1972, p. 65.
6 D. A. Segar and J. G. Gonzalez, *Anal. Chim. Acta*, 58 (1972) 11.
7 J. W. Robinson and D. K. Wolcott, *Anal. Chim. Acta*, 66 (1973) 333.
8 H. L. Rahn and D. C. Manning, *Amer. Lab.*, August, 1972, p. 51.
9 J. W. Robinson, P. J. Slevin, G. D. Hindman and D. K. Wolcott, *Anal. Chim. Acta*, 61 (1972) 431.
10 J. W. Robinson, D. K. Wolcott, P. J. Slevin and G. D. Hindman, *Anal. Chim. Acta*, 66 (1973) 13.
11 J. W. Robinson, P. J. Slevin and G. D. Hindman, *Anal. Chim. Acta*, 66 (1973) 165.
12 L. Ebdon, G. F. Kirkbright and T. S. West, *Anal. Chim. Acta*, 58 (1972) 39.

Analytica Chimica Acta, 74 (1975) 53–60

SPECTROPHOTOMETRIC DETERMINATION OF COPPER WITH α, β, γ, δ-TETRAPHENYLPORPHINE TRISULFONATE

JUN-ICHI ITOH, TAKAO YOTSUYANAGI and KAZUO AOMURA

Laboratory of Analytical Chemistry, Faculty of Engineering, Hokkaido University, Sapporo, 060 (Japan)

(Received 19th June 1974)

Extensive studies have been made on the physicochemical properties of the simpler porphyrins and their metal derivatives in the last 45 years, with the special reference to their relationship to the more complex porphyrins found in hemoglobin, chlorophyll and petroleum. The porphyrins and their metal derivatives have intense and characteristic absorption bands in the visible region of the spectrum[1,2]. However, only one paper has been published on their application to analytical methods for the determination of metal ions; this deals with the spectrophotometric determination of zinc and other metals with α, β, γ, δ-tetraphenylporphine (TPP), reported by Banks and Bisque[3]. Unfortunately, the determination had to be done by utilizing the absorption band of the zinc–TPP complex at 551 nm, where the molar absorptivity is only about 14,000, and it was necessary to use glacial acetic acid solvent, owing to the very poor solubility of TPP in aqueous solution. Accordingly, the porphyrin seemingly has no special advantages as an organic reagent for metal analysis compared with simpler chelating reagents. Recently, some water-soluble porphyrins have been synthesized which have hydrophilic groups, such as sulfonate[4,5], pyridinium[6], amino[7] and carboxylate[8]. By careful examination of spectra of these water-soluble porphyrins and their metal complexes, especially that of "Soret" bands, it was found that the spectral changes of Soret bands on complexation are large enough to allow them to be applied for analytical purposes. The molar absorptivities of porphyrins at their Soret bands are of the order of $2.0 \cdot 10^5$–$6.0 \cdot 10^5$. Therefore, it seemed likely that the Soret bands of porphyrins would provide very sensitive spectrophotometric determinations of metal ions. The present paper is concerned with the incorporation of copper ion into α, β, γ, δ-tetraphenylporphine trisulfonate (TPPS or H_2R)[4] in aqueous solution, and the application of this reaction for the direct spectrophotometric determination of 10^{-9} g ml^{-1} amounts of copper.

EXPERIMENTAL

Apparatus

Spectra were obtained with a Hitachi 124 Model double-beam spectrophotometer equipped with 1-cm cells. A Toa Denpa Model HM-5A pH meter was used for pH measurements.

Reagents

TPPS ($C_{44}H_{30}N_4S_3O_9 \cdot 4H_2O$) was prepared from tetraphenylporphine (TPP) by sulfonation. TPP was synthesized from pyrrole and benzaldehyde in propionic acid under reflux[9]. Sulfonation of TPP and purification of the TPPS were done as described by Pasternack *et al.*[4].

The standard TPPS solution (10^{-3} *M*) was prepared by dissolving 0.93 g of TPPS in distilled water and diluting to 1 l. The solution was standardized by photometric titration with the standard copper solution. The standard copper acetate solution (10^{-2} *M*) was standardized by titration with EDTA. Chloroacetate and acetate buffers were used over the pH range 2–6.

Standard procedure

Transfer the sample solution containing 0.3–3 μg of copper to a 100-ml beaker, and dilute, if necessary, to about 40 ml with water. Add 2.5 ml of 1 *M* acetate buffer (pH 4.0) and 5 ml of $1 \cdot 10^{-5}$ *M* standard TPPS solution. Boil for 1 min and allow to cool to room temperature. Add 1.5 ml of 1 *M* monochloroacetic acid solution to adjust the pH to 2.5. Transfer the solution to a 50-ml volumetric flask and dilute to the mark with water. Measure the absorbance at 434 nm for free TPPS and at 413 nm for the copper(II)–TPPS complex.

RESULTS

Absorption spectra

The absorption spectra of TPPS and the copper(II)–TPPS complex are shown in Fig. 1. At pH 6.5, the TPPS solution was reddish-purple and had absorption peaks at 413 (Soret band, $\varepsilon = 5.1 \cdot 10^5$), 517, 553, 580 and 634 nm; the TPPS solution was green at pH 2.5 and had absorption peaks at 434 (Soret

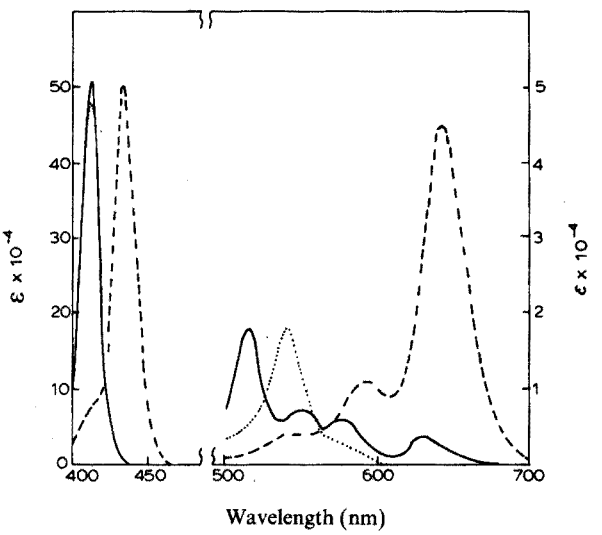

Fig. 1. Absorption spectra of TPPS and Cu–TPPS. Solid line, H_2R (pH 6.5); dashed line, H_4R^{2+} (pH 2.5); dotted line, CuR (pH 2.5).

band, $\varepsilon = 5.0 \cdot 10^5$), 595 and 645 nm. Other types of absorption spectra, *e.g.* corresponding to the dimeric TPPS species reported by Pasternack[4] (Soret band at 489 nm), were not observed in aqueous solution at any pH from 2 to 13, unless some type of salt, especially salting-out agents, was added.

The spectra of TPPS at pH 6.5 and 2.5 can be reasonably assigned to the free base form (H_2R) and the diacid form (H_4R^{2+}) of TPPS, respectively, because they are very similar to the spectra of H_2TPP and H_4TPP^{2+}, reported by Stone and Fleischer[10]. This assignment was confirmed by an analysis of the pH–absorbance plots (Fig. 2), by means of the following equation with a least-squares computer program:

$$A = \frac{\dfrac{\varepsilon_1[H^+]^2}{K_3K_4} + \dfrac{\varepsilon_2[H^+]}{K_3} + \varepsilon_3}{\dfrac{[H^+]^2}{K_3K_4} + \dfrac{[H^+]}{K_3} + 1} C_{TPPS} \tag{1}$$

where K_3 and K_4 are acid dissociation constants of H_4R^{2+} and H_3R^+, ε_1, ε_2 and ε_3 are the molar absorptivities of H_4R^{2+}, H_3R^+ and H_2R, respectively, and C_{TPPS} is the total concentration of TPPS.

$$H_4R^{2+} = H_3R^+ + H^+ \quad K_4 \tag{2}$$

$$H_3R^+ = H_2R + H^+ \quad K_3 \tag{3}$$

The acid dissociation constants were determined as $pK_4 = 4.86$ and $pK_3 = 4.95$ at

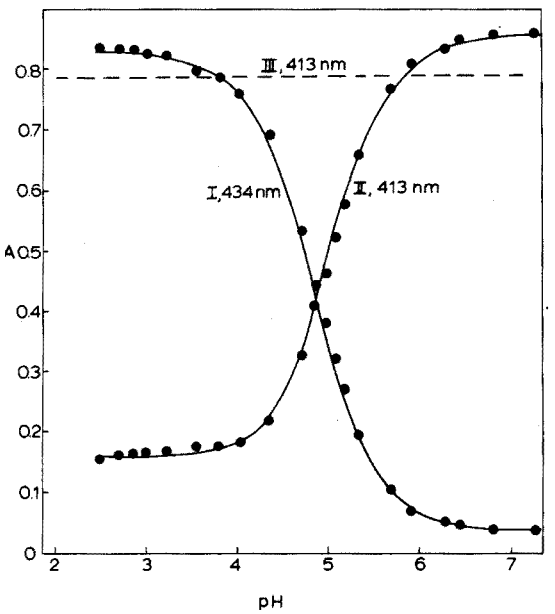

Fig. 2. Absorbance–pH curves of TPPS and Cu–TPPS. Curves I and II represent TPPS; the solid line indicates the theoretical value calculated from eqn. (1). Curve III represents Cu–TPPS.

25°C; the ε_2 values for H_3R^+ at 434 nm and 412 nm were $2.9 \cdot 10^5$ and $1.2 \cdot 10^5$, respectively. Thus, the theoretical curves for pH–absorbance relationship can be drawn from eqn. (1), and these are shown in Fig. 2 as solid lines. Excellent agreement is obtained between the theoretical curve and the experimental points. The first and second acid dissociation constants are very close to each other, hence the spectra of H_4R^{2+} and H_2R were clearly shown but that of H_3R^+ could not be detected separately.

The spectra of the copper(II)–TPPS complex had the Soret band ($\varepsilon = 4.76 \cdot 10^5$) at the same wavelength (413 nm) as the free base form of TPPS, H_2R. Therefore, very slight spectral changes were observed on reaction of copper(II) with H_2R at pH 6.5. Thus, the applications of the Soret band for metal analysis would be possible only when the predominant species of TPPS is the fully protonated cation, H_4R^{2+}, which has the Soret band at 434 nm (Fig. 1).

Absorbance–pH curve

The absorbance–pH curves were measured for TPPS and for its copper complex at their Soret bands. The curves of TPPS (Fig. 2, curves I and II) show that suitable conditions for the determination, *i.e.* where H_4R^{2+} predominates, should occur below pH 2.8; however, the formation rate of the copper complex was poor at pH 2.8. The complex was formed quantitatively within 1 min under boiling

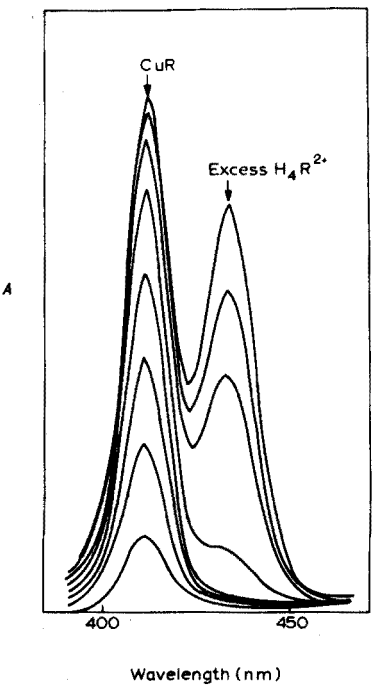

Fig. 3. Spectra of Cu–TPPS complex in various concentrations of TPPS. $[Cu^{2+}]$, $5.15 \cdot 10^{-7}$ *M*.

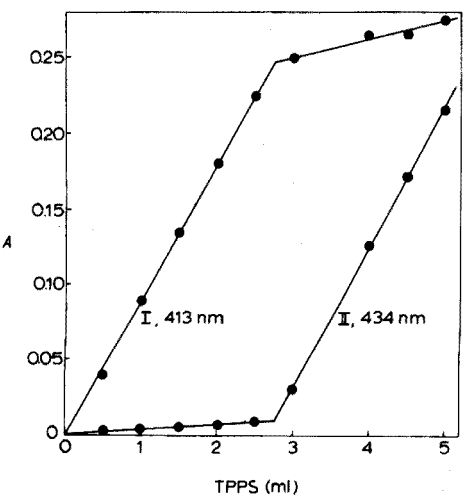

Fig. 4. Photometric titration plots. $[Cu^{2+}]$, $5.15 \cdot 10^{-7}$ *M* (1.65 μg/50 ml). [TPPS], $0.95 \cdot 10^{-5}$ *M*. Curve I, Cu–TPPS complex. Curve II, H_4R^{2+}.

conditions above pH 4, where the proton dissociation of H_4R^{2+} starts to take place. The copper complex once formed was stable and gave constant absorbance in the pH range 2–7 (Fig. 2, curve III). Thus, the application of the Soret band to the determination of copper(II) was possible by the procedure described above, *i.e.*, initial complex formation at pH 4 followed by acidification to pH 2.5.

Determination of copper

Photometric titration method. Aliquots of standard TPPS solution were added to the sample solution ($Cu = 5.15 \cdot 10^{-7}$ *M*) and the spectra were obtained by following the standard procedure (Fig. 3). These data were used to obtain photometric titration curves (Fig. 4). In each curve, the experimental points agreed very well with the theoretical curves, which were calculated with the assumption of quantitative formation of the complex. This result can be attributed to the very high stability of the copper–TPPS complex. The intercepts of curves I and II just coincided with each other at the same volume of TPPS solution added. Thus, by this titration method, 10^{-7}–10^{-5} *M* amounts of copper can be determined with excellent precision.

Calibration curve method. For the direct determination of copper, it was preferred to use the absorption band of the free H_4R^{2+} at 434 nm, because the band of the copper complex at 413 nm overlapped with the shoulder peak of H_4R^{2+} which showed somewhat poor reproducibility. A straight line calibration curve was obtained for copper concentrations of 0.006–0.06 μg ml^{-1}. The equation for the curve was

$$\text{Cu}(\mu\text{g ml}^{-1}) = 0.13\,(A_0 - A) \qquad (4)$$

where A_0 and A are the absorbance of reagent blank and sample, respectively, measured by the standard procedure at 434 nm in 1-cm cells against water as reference.

Influence of diverse ions.

Table I summarizes the results of the interference study. A change of 0.005 in absorbance value was set as the tolerance limit for reproducible results. Ca(II), Cd(II), Cr(III), Hg(II), K(I), Li(I), Mg(II), Mo(VI), Na(I), Pb(II), Sn(II), V(V) and W(VI) did not interfere up to amounts more than 1000 μg (about 600-fold excess). Al(III), Ag(I) and Ni(II) could be tolerated up to 100 μg (60-fold excess), and Co(II), Fe(III) and Mn(II) up to 10 μg (6-fold excess). Pd(II), Fe(II) and Zn(II) interfered with the determination. The interference of 10-μg amounts of palladium(II) was avoided by adding 1 ml of 0.01 *M* potassium iodide solution. The interference of iron(II) was eliminated by a preliminary oxidation to iron(III). Thus, only zinc(II) interfered with the determination; even equal amounts to copper(II) reduced the absorbance by about 0.035 unit. NO_3^-, Cl^-, SO_4^{2-}, Br^-, I^-, ClO_4^-, CH_3COO^- and $ClCH_2COO^-$ did not interfere with the determination up to 10^{-3} *M*.

Effects of salts

In the presence of concentrations of salts higher than 10^{-2} *M*, acidic TPPS solutions (pH below 4) showed Tyndall phenomena; the colloidal suspension showed

TABLE I

INFLUENCE OF DIVERSE IONS

(Copper concentration: 1.66 μg/50 ml = $5.2 \cdot 10^{-7}$ M = 33.2 p.p.b. $(A_0 - A) = 0.255$)

Ion	*Added as*	*Amount of foreign ions added*		
		10 μg	*100 μg*	*1000 μg*
Ag(I)	$AgNO_3$	—.	0.253	(0.240)
Al(III)	$Al(NO_3)_3$	—	(0.240)	—
Co(II)	$Co(NO_3)_2$	0.255	(0.345)	—
Fe(II)	Mohr's Salt	(0.297)	(0.383)	—
Fe(III)	Alum	0.250	—	—
Mn(II)	$MnCl_2$	0.257	(0.305)	(0.444)
Ni(II)	$Ni(NO_3)_2$	0.260	0.255	(0.311)
Pd(II)	$Pd(ClO_4)_2$	(0.405)	—	—
		0.257[a]	—	—
Zn(II)	$Zn(NO_3)_2$	(0.220[b])	—	—

[a] 1 ml of 0.01 M KI solution was added.
[b] 1.6 μg of Zn(II) was added.

a Soret band at 489 nm. The formation rates of the colloidal suspensions depended on both the concentrations and the kind of salt. The rate decreased in the following order: $Al(NO_3)_3 > Ca(CH_3COO)_2 > Na_2SO_4 > KNO_3 > KCl > KBr > KClO_4 > KI$. The presence of sodium acetate, sodium chloroacetate and sodium thiocyanate did not cause Tyndall phenomena. Except for the calcium and aluminum salts, salt effects were not observed at salt concentrations less than 10^{-3} M.

DISCUSSION

The Soret bands of H_4R^{2+}, H_2R and CuR were located at 434, 413 and 413 nm, respectively, so that useful spectral change could be expected only when H_4R^{2+} reacted with copper(II) to form CuR below pH 2.8. But the application of this direct reaction was not practical because of its small reaction rate, which changed as a function of pH. Yet CuR, once formed, was stable enough at least for 24 h even at pH 2 in chloroacetate buffer solution. Thus, complex formation at pH 4 followed by acidification to pH 2.5, was used for the determination.

No information is at present available for even approximate values of the stability constants of the extremely stable porphyrin complexes, which would make it possible to estimate the extent of possible interference of diverse metal ions and to design masking procedures. The relative order of the stability constants (K) and the formation rate constants (k) of the reactions of metal ions with various porphyrins and their analogues have been studied by several authors[1,7,11–13]. The following series of K and k may be deduced from consideration of the various data reported. For K: Pd(II) > Cu(II) > Ni(II) > Co(II) > Fe(II) > Zn(II) > Mg(II) > Cd(II) > Sn(II) > Ba(II) > Ag(I); and for k: Cu(II) > Zn(II) > Co(II) > Fe(II) > Ni(II), and Co(II) > Mn(II). The series of K and k values indicate that, in the

case of porphyrin complexes, the thermodynamic stability order and the kinetic order do not correspond to each other. As the interference study (see Table I) showed, the order of interfering metal ions was Pd(II) > Zn(II) > Fe(II) > Co(II) > Mn(II) > Ni(II). Thus, it may be deduced that the selectivity of the present method is largely dependent on the kinetic nature of the complex formation reaction. When the complex was formed at pH 6.5 and then the mixture was acidified to 2.5, the behavior of diverse metal ions was very different from that of the recommended procedure; for example, 500 μg amounts of Sn^{2+} and Hg^{2+} seriously interfered. Such pH depencence of interferences seems to support the speculation of kinetic reaction control.

TPPS was highly selective for copper(II); of the common metal ions, only palladium(II) and zinc(II) seriously interfered. Iodide could be used to mask palladium(II), but zinc(II) should be previously separated from copper(II).

Pasternack *et al.*[4] claimed that acidic TPPS solution containing 0.1 *M* potassium nitrate did not obey Beer's law, owing to the formation of dimeric TPPS species which had a Soret band at 489 nm. With the present procedure, however, Beer's law held over a 100-fold range (*ca.* 10^{-7}–10^{-5} *M*) of H_4R^{2+}, H_2R and CuR species, respectively; this indicates that these species are monomeric in acetate or chloroacetate buffer solutions. The systematic study of the salt effect on the acidic TPPS solution showed that formation of the TPPS species with a Soret band at 489 nm depended not only on the pH and salt concentrations of the solution, but also on the nature of salts, *i.e.*, the order of salt effect corresponded to the lyotropic series. Thus, in Pasternack's case, the effect of 0.1 *M* potassium nitrate caused the formation of the TPPS species with the Soret band at 489 nm which is responsible for the deviation from Beer's law. The presence of salts at more than 10^{-3} *M*, except sodium salts of acetate and chloroacetate, should be avoided in the determination.

The Soret band of the diacid form of TPPS (H_4R^{2+}) has an exceptionally large molar absorptivity ($5.0 \cdot 10^5$) at 434 nm; CuR also absorbs ($\varepsilon = 2.0 \cdot 10^4$) at this wavelength. Therefore, the effective change in absorbance by complexation at this wavelength should be proportional to $\varepsilon_{\text{effective}} = \varepsilon_{H_4R^{2+}} - \varepsilon_{CuR} = 4.8 \cdot 10^5$. Thus, trace amounts of copper(II) of the order of 10^{-2} μg ml^{-1} were directly determined by spectrophotometry with a sensitivity (Sandell index[14]) of 0.00013 μg Cu cm^{-2}, which is 17 times more sensitive than the dithizone method[14] (0.0022 μg Cu^{2+} cm^{-2}). The relative standard deviation for 0.03 μg Cu ml^{-1} was 3%.

As shown in Fig. 4, TPPS can also be applied for the photometric titration of dilute copper(II) solutions (10^{-7}–10^{-5} *M*). TPPS has several advantages compared with common titrants such as EDTA; *e.g.*, it forms an extremely stable complex with 1:1 molar ratio of metal to ligand, and has a very large molar absorptivity.

SUMMARY

Water-soluble porphyrin, α, β, γ, δ-tetraphenylphorphine trisulfonate (TPPS, H_2R), was found to be a very useful agent for both the direct spectrophotometric determination and the photometric titration of copper(II). The molar absorptivity of H_4R^{2+} at 434 nm is $5.0 \cdot 10^5$ and the spectrophotometric sensitivity is 0.00013

μg Cu cm^{-2} for $A=0.001$. Beer's law is followed in the range 0.006 μg–0.06 μg Cu ml^{-1}. Among twenty-two elements examined, only zinc(II) seriously interfered. Acid dissociation constants and salt effects on the spectra of TPPS were evaluated.

REFERENCES

1 J. E. Falk, *Porphyrins and Metalloporphyrins*, Elsevier, Amsterdam, 1964.
2 G. D. Dorough, J. R. Miller and F. M. Huennekens, *J. Amer. Chem. Soc.*, 73 (1951) 4315.
3 C. V. Banks and R. E. Bisque, *Anal. Chem.*, 29 (1957) 523.
4 R. F. Pasternack, P. R. Huber, P. Boyd, G. Engasser, L. Francesconi, E. Gibbs, D. Fasella, G. C. Venturo and L. DeC. Hinds, *J. Amer. Chem. Soc.*, 94 (1972) 4511.
5 E. B. Fleischer, J. M. Palmer, T. S. Srivastava and A. Chatterjee, *J. Amer. Chem. Soc.*, 93 (1971) 3162.
6 P. Hambright and E. B. Fleischer, *Inorg. Chem.*, 9 (1970) 1757.
7 T. P. Stein and R. A. Plane, *J. Amer. Chem. Soc.*, 91 (1969) 607.
8 F. R. Longo, M. G. Finarelli and J. B. Kim, *J. Heterocycl. Chem.*, 6 (1969) 927.
9 A. D. Adler, F. R. Longo, J. D. Finarelli, J. G. Gordmacher, J. Assour and L. Korsakoff, *J. Org. Chem.*, 32 (1968) 476.
10 A. Stone and E. B. Fleischer, *J. Amer. Chem. Soc.*, 90 (1968) 2735.
11 J. W. Barnes and G. D. Dorough, *J. Amer. Chem. Soc.*, 72 (1950) 4045.
12 B. D. Berezin, *Russ. J. Phys. Chem.*, 39 (1965) 576.
13 C. Grant and P. Hambright, *J. Amer. Chem. Soc.*, 91 (1969) 4195.
14 E. B. Sandell, *Colorimetric Determination of Traces Metals*, Interscience, New York, 3rd edn., 1965.

Analytica Chimica Acta, 74 (1975) 61–65

EXTRACTION–SPECTROPHOTOMETRIC DETERMINATION OF COPPER WITH 2-THIOPHENEALDEHYDE-2-BENZOTHIAZOLYLHYDRAZONE

TSUGIKATSU ODASHIMA

Department of Applied Chemistry, Faculty of Engineering, Tohoku University, Sendai (Japan)

HAJIME ISHII

Chemical Research Institute of Non-Aqueous Solutions, Tohoku University, Sendai (Japan)

(Received 18th June 1974)

Hydrazones, in particular, nitrogen-containing heterocyclic hydrazones have attracted much attention as analytical reagents, because of high sensitivity and selectivity, easy synthesis and good yield. Their properties have been described by many investigators[1–10], and some of them have been already used for the determination of traces of elements; for example, pyridine-2-aldehyde-2-quinolylhydrazone has been used for nickel[11], and quinoline-2-aldehyde-2-quinolylhydrazone for copper[12]. The present authors have synthesized 2-hydroxy-1-naphthaldehyde-2-benzothiazolylhydrazone and α-naphthaldehyde-2-benzothiazolylhydrazone by condensation of the corresponding aldehyde and hydrazines, and have reported the spectrophotometric determination of copper with these reagents[13,14]. Still more sensitive and selective reagents have been sought by suitable choice of aldehyde and hydrazine.

In the present paper, a new reagent, 2-thiophenealdehyde-2-benzothiazolylhydrazone(TBTH)(I)—prepared from 2-thiophenealdehyde and 2-hydrazinobenzothiazole—is reported as a spectrophotometric reagent for copper. TBTH reacts with copper(II) to form an insoluble complex, which can be extracted quantitatively into organic solvents, such as benzene, chloroform and methyl isobutyl ketone (MIBK). A method has been established for the direct spectrophotometric determination of microgram amounts of copper, after the extraction of copper(II) as its TBTH complex into benzene. The method is simple in that a single extraction suffices; common ions, except silver(I), mercury(II), vanadium(IV), thiocyanate, citrate and tartrate, do not interfere in the determination.

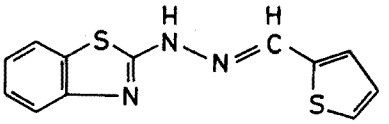

(I)

EXPERIMENTAL

Apparatus

Spectrophotometric measurements were made with a Hitachi Perkin-Elmer,

Model 139, spectrophotometer with 10-mm glass cells. The pH measurements were made with a Hitachi, Model 5-F, glass electrode pH meter.

Reagents

2-Thiophenealdehyde-2-benzothiazolylhydrazone (TBTH) solution. A $2.5 \cdot 10^{-4}$ *M* stock solution was prepared by dissolving 64.8 mg of TBTH in 1 l of benzene. The TBTH used was synthesized as follows. Dissolve 1.7 g of 2-hydrazinobenzothiazole in 100 ml of ethanol and mix with 10 ml of an ethanolic solution of 1.2 g of 2-thiophenealdehyde. Heat the mixture at 70–80°C on a water bath for 15 min. On cooling to room temperature, the hydrazone crystallized from the solution. The yield was 1.2 g after one recrystallization from ethanol (m.p. 215–217°C). Analytical results: calculated for $C_{12}H_9N_3S_2$ (m. w. 259.4), 55.6%C, 3.5%H, 16.2%N, 24.7%S; found, 55.4%C, 3.45%H, 15.5%N, 24.7%S.

Standard copper (II) solution. A stock solution containing about 1 mg Cu ml^{-1} was prepared by dissolving 3.93 g of copper(II) sulfate pentahydrate in 1 l of deionized water, sufficient sulfuric acid to give about 0.05 *M* acidity being added. This stock solution was standardized by titration with a 0.01 *M* EDTA solution and appropriately diluted to prepare working solutions.

Buffer solutions. In studies of experimental conditions, 1 *M* acetic acid – 1 *M* sodium acetate, 0.06 *M* disodium hydrogenphosphate—0.06 *M* potassium dihydrogenphosphate or 1 *M* aqueous ammonia – 1 *M* ammonium chloride systems were used according to the pH values required. In the recommended procedure, the mixture of 1 *M* acetic acid and 1 *M* sodium acetate (pH 5.1) was used.

Unless otherwise mentioned, all reagents used were of analytical-reagent grade.

Procedure

Take the sample solution containing 1–12 μg of copper(II) in a 50-ml separatory funnel. Add 1 ml of acetate buffer solution (pH 5.1). Adjust the volume to about 20 ml with deionized water. Add 10.0 ml of a $2.5 \cdot 10^{-4}$ *M* TBTH solution in benzene and extract the complex by shaking mechanically for 15 min. Transfer the organic phase to a 50-ml stoppered flask containing about 1 g of anhydrous sodium sulfate. Measure the absorbance of the organic phase at 422 nm against a reagent blank prepared at the same time as the sample solution as reference. The amount of copper can be obtained from the calibration curve.

RESULTS AND DISCUSSION

Absorption spectra

The absorption spectrum of the copper(II)–TBTH complex is illustrated in Fig. 1 along with that of TBTH in benzene. The absorption maximum of the complex occurs at 422 nm. There is no shift in this maximum wavelength used for the determination of copper, when either the pH value of the aqueous phase is varied from 5.4 to 10.3, or the molar ratio of copper to TBTH is varied from 1:10 to 10:1. These results suggest that only one species of the complex is extracted into benzene.

Effect of pH

The influence of pH on the degree of extraction was studied by extracting

copper(II) from a series of aqueous solutions buffered in the pH range 2.2–11.7. The absorbance was maximal and constant over the pH range 4.6–9.2. In more acidic or more alkaline solutions, the absorbance decreased, because of incomplete complex formation and of hydrolysis of the complex, respectively. The acetate buffer system was finally chosen in the recommended procedure.

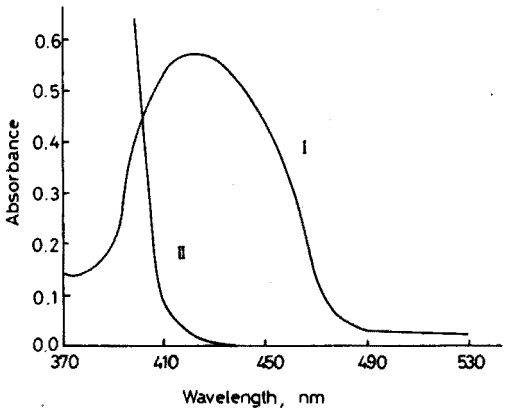

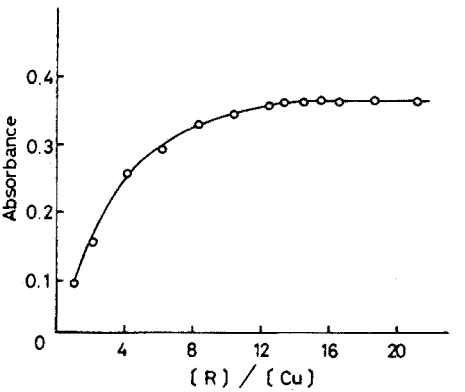

Fig. 1. Absorption spectra: Cu(II), 8.0 μg; TBTH, $2.5 \cdot 10^{-4}$ *M*; pH, 5.1; $V_{aq}/V_{org} = 3$ ($V_{org} = 10.0$ ml); shaking time, 30 min. (I) Cu(II)–TBTH complex in benzene against reagent blank. (II) Reagent blank against benzene.

Fig. 2. Effect of concentration of TBTH: Cu(II), 5.0 μg; pH, 5.1; $V_{aq}/V_{org} = 3$ ($V_{org} = 10.0$ ml); shaking time, 15 min; wavelength, 422 nm.

Effect of TBTH concentration

The absorbance of the extract was studied as a function of the mole ratio of TBTH to copper(II). The result is shown in Fig. 2. At least a 14-fold molar excess of TBTH is necessary to obtain constant and reproducible absorbance. An excess of the reagent up to 25-fold did not interfere with absorbance.

Effect of shaking time

The shaking time for the extraction was varied from 1 to 60 min. Extraction was quantitative with 15 min of shaking. Continued shaking up to 60 min produced no further change of absorbance.

Stability of the extracted complex

The absorbance of the complex extracted into benzene remained unchanged for at least 2 h.

Effect of phase volume ratio

The effect of the volume ratio of aqueous phase to organic phase was investigated by extracting copper(II) from various amounts of aqueous solution with 10.0 ml of benzene. Constant absorbance was obtained up to a volume ratio of 5:1.

Calibration curve

Beer's law was obeyed over a concentration range 1–12 μg of copper(II) in

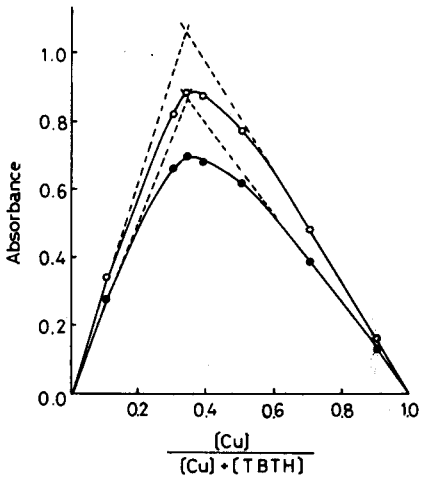

Fig. 3. Continuous variation plots at pH 5.1: total concentration of TBTH and copper, $3.1 \cdot 10^{-5}$ *M*; (○), 422 nm; (●), 402 nm.

10.0 ml of benzene for 10-mm cells. The molar absorptivity at 422 nm, as determined by the least-squares method, was $4.4 \cdot 10^4$ l mol^{-1} cm^{-1}. The sensitivity defined by Sandell[15] was $1.4 \cdot 10^{-3}$ μg Cu cm^{-2}.

Composition of the extracted species

In order to determine the composition of the extracted species, continuous variation plots were made. The results (Fig. 3) indicated a copper: TBTH ratio of 1:2.

Effect of diverse ions

Table I shows the effect of diverse ions on the recovery of copper. Silver(I),

TABLE I

EFFECT OF DIVERSE IONS[a]

Ion	*Ion added*	*Cu found (μg)*	*Relative error (%)*	*Ion*	*Ion added*	*Cu found (μg)*	*Relative error (%)*
Ag(I)	104 μg	5.9	17.8	Ti(IV)	113 μg	4.8	−4.0
Al(III)	76 μg	5.0	0.0	V(IV)	100 μg	3.9	−22.0
Ca(II)	99 μg	5.0	0.0	Zn(II)	103 μg	5.0	0.0
Cd(II)	102 μg	5.0	0.0	Br^-	80 mg	5.0	0.0
Co(II)	98 μg	5.1	2.0	Cl^-	36 mg	5.0	0.0
Cr(III)	100 μg	5.0	0.0	ClO_4^-	100 mg	5.0	0.0
Fe(III)	99 μg	5.0	0.0	I^-	127 mg	5.0	0.0
Hg(II)	110 μg	6.3	26.0	NO_3^-	62 mg	5.0	0.0
Mg(II)	75 μg	5.0	0.0	PO_4^{3-}	95 mg	5.0	0.0
Mn(II)	100 μg	5.0	0.0	SCN^-	58 mg	4.7	−6.0
Ni(II)	99 μg	5.0	0.0	Citrate	95 mg	1.7	−66.0
Pb(II)	97 μg	5.0	0.0	Tartrate	74 mg	4.1	−18.0

[a] 5.0 μg of Cu(II) taken.

mercury(II), vanadium(IV), citrate, tartrate and thiocyanate interfered with the determination, but the other common ions did not interfere. Interferences of the first two ions are attributed to the formation of extractable colored complexes, and could be avoided by adding 2 ml of 1 *M* potassium iodide. The interference of vanadium(IV) could be eliminated by oxidation to vanadium(V), by adding about 1 g of ammonium persulfate.

SUMMARY

A sensitive and selective extraction–spectrophotometric method is proposed for the determination of small amounts of copper. The method is based on the formation of a copper(II)–TBTH complex, which is extractable in benzene from the acetate buffered solution of pH 5.1. The extract is stable for at least 2 h. The complex system conforms to Beer's law for up to 12 μg of copper in 10.0 ml of the benzene extract at 422 nm. The molar absorptivity is $4.4 \cdot 10^4$ l mol^{-1} cm^{-1}. Common cations do not interfere.

REFERENCES

1 F. Lions and K. V. Martin, *J. Amer. Chem. Soc.*, 80 (1958) 3858.
2 J. F. Geldard and F. Lions, *J. Amer. Chem. Soc.*, 84 (1962) 2262.
3 J. F. Geldard and F. Lions, *Inorg. Chem.*, 2 (1963) 270.
4 R. W. Green, P. S. Hallman and F. Lions, *Inorg. Chem.*, 3 (1964) 376.
5 B. Chiswell and F. Lions, *Inorg. Chem.*, 3 (1964) 490.
6 B. Chiswell, F. Lions and M. L. Tomlinson, *Inorg. Chem.*, 3 (1964) 492.
7 M. L. Heit and D. E. Ryan, *Anal. Chim. Acta*, 32 (1965) 448.
8 J. E. Going and R. T. Pflaum, *Anal. Chem.*, 42 (1970) 1098.
9 M. Valcarcel and F. Pino, *Analyst. (London)*, 98 (1973) 246.
10 M. Lever, *Anal. Chim. Acta*, 65 (1973) 311.
11 B. K. Afghan and D. E. Ryan, *Anal. Chim. Acta*, 41 (1968) 167.
12 R. E. Jensen, N. C. Bergman and R. J. Helving, *Anal. Chem.*, 40 (1968) 624.
13 T. Odashima and H. Ishii, *Nippon Kagaku Kaishi*, 54 (1973) 729.
14 T. Odashima and H. Ishii, *Nippon Kagaku Kaishi*, accepted for publication.
15 E. B. Sandell, *Colorimetric Determination of Traces of Metals*, Interscience, New York, 2nd edn., 1950, p. 50.

Analytica Chimica Acta, 74 (1975) 67–73

PERIODATE OXIDATION ANALYSIS OF CARBOHYDRATES

PART I. SPECTROPHOTOMETRIC DETERMINATION OF GLYOXAL IN DIALDEHYDE FRAGMENTS FORMED FROM GLYCOSIDES WITH 2,4-DINITROPHENYLHYDRAZINE

SUSUMU HONDA, KAZUAKI KAKEHI, HIDETAKA YUKI and KIYOSHI TAKIURA
Faculty of Pharmaceutical Sciences, Osaka University, Toneyama, Toyonaka, Osaka-fu (Japan)
(Received 17th June 1974)

Periodate oxidation analysis is a powerful tool for the elucidation of carbohydrate sequences. Determination of periodate consumption[1–5] gives a fundamental knowledge of sequences, but the stoichiometry of this reaction is attained only under strict control of reaction conditions, since this reaction is very sensitive to pH and reaction temperature. Hence, simultaneous determination of primary oxidation fragments, such as formaldehyde[6,7] and formic acid[6], is often required for detailed sequence analysis.

When glycosides including oligo- and polysaccharides are oxidized with periodate, oligo- or polyaldehydic compounds are formed along with the one-carbon fragments mentioned above. These aldehydes may be hydrolyzed to yield various mono- and di-carbonyl compounds having more than two carbon atoms. Determination of these secondary fragments, without or after mutual separation, would produce valuable information which could not be obtained from the analysis of one-carbon fragments. This paper deals with the determination of glyoxal in dialdehyde fragments which were formed by oxidation of typical glycosides. The determination of this most characteristic two-carbon fragment derived from the C_1–C_2 part of glycosides, coupled with the determination of periodate consumption, makes it possible to estimate to what degree the oxidation—and any overoxidation from carbohydrate-ring rupture—proceeds.

Glyoxal in dialdehydes was conveniently converted, without a prior liberation process by acid hydrolysis, to its bis-hydrazone by the simple procedure of heating dialdehydes (isolated or *in situ*) with an aqueous dimethylsulfoxide solution of 2,4-dinitrophenylhydrazine hydrochloride. The bis-hydrazone thus formed gave intense color in alkaline conditions; this was measured spectrophotometrically. By this simplified procedure, glyoxal formed from $1 \cdot 10^{-2}$–$2 \cdot 10^{-1}$ μmole of glycoside samples could be determined accurately without interference from other oxidation fragments.

EXPERIMENTAL

Materials

A reagent-grade sample of 2,4-dinitrophenylhydrazine hydrochloride (Tokyo

Kasei Kogyo Co., Ltd.) was used without purification. For the glyoxal reference standard, a reagent-grade sample of glyoxal disodium bisulfite monohydrate (Tokyo Kasei Kogyo Co., Ltd.) was used. An authentic specimen of the bis-hydrazone of glyoxal was prepared by condensation of glyoxal trimer with the hydrazine hydrochloride in dimethylsulfoxide. (Analysis: $C_{14}H_{10}N_8O_8$ requires 40.2% C, 2.4% H, 26.8% N; found 40.2% C, 2.3% H, 26.5% N.)

Dimethylsulfoxide and ethanol used as solvents were of spectroscopic grade. All other reagents as well as samples of methyl and phenyl D-glucopyranosides were also of reagent grade. Methyl 4,6-O-benzylidene-D-glucopyranosides were synthesized and purified by the standard method[8].

7,9-Dihydroxy-6α- and β-methoxy-2-phenyl-*trans*-*m*-dioxano-(5,4e)(1,4)-dioxepan (dialdehyde I and II, respectively) were prepared by periodate oxidation of methyl 4,6-O-benzylidene-α and β-D-glucopyranosides, respectively, as described in the literature[9], and purified by recrystallization from aqueous acetone (m.p. 134–135°C for I and 118–119°C for II). (Analysis: $C_{14}H_{16}O_6 \cdot 2H_2O$ requires 53.2% C, 6.4% H; found (I) 53.0% C, 6.3% H; (II), 53.7%C, 6.3% H.)

Reagent solutions

Hydrazine solution. Dissolve 2,4-dinitrophenylhydrazine hydrochloride (100 mg) in dimethylsulfoxide (80 ml), and dilute to 100 ml with distilled water. This solution should be prepared daily, since it is decomposed gradually.

Alkali solution. Dissolve potassium hydroxide (12 g except for the experiment on the pH dependence of color formation) in 80% ethanol (100 ml).

Apparatus

A Shimazu UV-200 spectrophotometer with 1-cm glass cells was used.

Periodate oxidation of glycosides

To a 10^{-2} *M* solution (2.00 ml) of a glycoside sample, add a 10^{-1} *M* sodium metaperiodate solution (2.00 ml), and keep the mixture at 25°C in a thermostated water bath, shielding from the light. Remove a 1.00-ml aliquot and determine the amount of periodate consumed titrimetrically as described by Müller and Friedberger[1]. Dilute another 1.00-ml aliquot to 200 ml, and subject this dilute solution to glyoxal determination.

Standard procedure for the spectrophotometric determination of glyoxal

To a sample solution (5.00 ml) containing $1 \cdot 10^{-2}$–$2 \cdot 10^{-1}$ μmole of glyoxal in either free or conjugated form, add the hydrazine solution (1.00 ml). Heat the mixture for 90 min on a boiling water bath. Cool the reaction mixture rapidly to room temperature, and add the alkali solution (1.00 ml). After 1 h, read the absorbance at 576 nm, referenced by a reagent blank which is made with distilled water instead of the sample solution. The concentration of glyoxal is obtained from the absorbance against the calibration curve, prepared with standard solutions of glyoxal disodium bisulfite.

RESULTS AND DISCUSSION

Glyoxal forms its bis-hydrazone with 2,4-dinitrophenylhydrazine in acidic

conditions. Since the color of this hydrazone developed in alkaline media is very intense, 2,4-dinitrophenylhydrazine has been used for the spectrophotometric determination of glyoxal[10–12]. However, there is a problem of osazone formation with α-hydroxyaldehydes. Above all, the osazone formed from glycol aldehyde is identical with the bis-hydrazone of glyoxal. Osazones of other α-hydroxyaldehydes give absorption spectra similar to that of the bis-hydrazone of glyoxal. This interference from osazones makes it difficult to determine selectively glyoxal in periodate oxidation fragments of carbohydrates, especially when strongly acidic conditions are employed which accelerate the osazone formation. Unfortunately, previously reported procedures[10–12] are not selective to glyoxal for the aforementioned reason.

Our effort to eliminate this interference was successful, when glyoxal was coupled with the hydrazine under less acidic conditions (pH *ca.* 3.0). By heating sample solutions with the hydrazine reagent, prepared by dissolving the hydrazine hydrochloride in aqueous dimethylsulfoxide, the osazone formation was minimized, and the determination of glyoxal was possible in the presence of α-hydroxyaldehydes. As can be seen from Table I, the relative intensities, as referred to glyoxal, of glycol aldehyde at the wavelength of the absorption maximum for glyoxal (576 nm) was only 0.04. Other possible fragments of periodate oxidation gave smaller values.

TABLE I

COMPARISON OF THE INTENSITY OF COLOR AT 576 nm FORMED FROM α-HYDROXYALDEHYDES

(Concentration of α-hydroxyaldehydes, $2.00 \cdot 10^{-5}$ *M*)

α-Hydroxyaldehyde	*Relative intensity*
Glyoxal	1
Formaldehyde	0.01
Formic acid	0.00
Glycol aldehyde	0.04
DL-Glyceraldehyde	0.02
D-Erythrose	0.01
D-Xylose	0.01
D-Glucose	0.00

Figure 1 shows the absorption spectrum of the reaction mixture, against a reagent blank, obtained from glyoxal. The spectrum was identical with that for the authentic bis-hydrazone of glyoxal, indicating that the bis-hydrazone is the only chromogen formed. Since the apparent molar absorptivity of the chromogen, calculated on the basis of the amount of glyoxal used, was 64,000, and the molar absorptivity of the authentic bis-hydrazone, measured under the identical conditions, was 65,000, the formation percentage of the bis-hydrazone was estimated to be 98%.

The color formation was affected by the conditions used for condensation. When the reaction was conducted on a boiling water bath with the aforementioned hydrazine solution, the color developed gradually for 90 min to reach a plateau (Fig. 2).

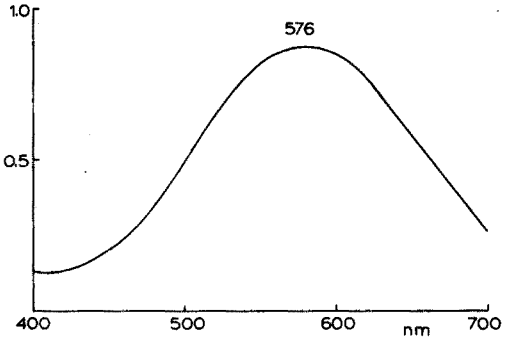

Fig. 1. Absorption spectrum of the chromogen formed from glyoxal. Concentration of glyoxal, $2.00 \cdot 10^{-5}$ *M*.

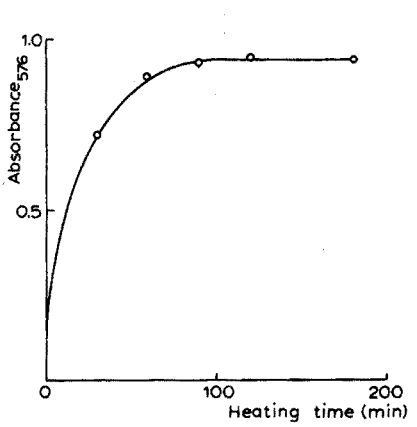

Fig. 2. Effect of heating time. Concentration of glyoxal, $2.00 \cdot 10^{-5}$ *M*.

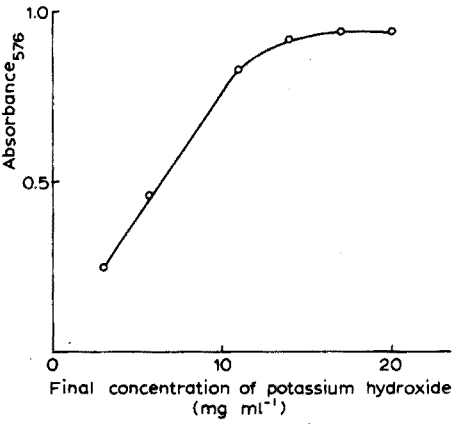

Fig. 3. Relationship between the color formation and the amount of alkali added. Concentration of glyoxal, $2.00 \cdot 10^{-5}$ *M*.

The alkalinity of the reaction solution was another factor to influence the color formation. Figure 3 shows the relationship between the color intensity and the amount of alkali added. The optimal condition was shown to be pH 14. This pH was attained by adding potassium hydroxide to a final concentration of 17 mg ml^{-1}, as in the standard procedure. The color developed by this procedure was stable for at least 24 h.

The calibration curve for free glyoxal, prepared by the standard procedure, was linear for concentrations ranging from $2 \cdot 10^{-6}$ *M* to $4 \cdot 10^{-5}$ *M*, which correspond to sample amounts of $1 \cdot 10^{-2}$–$2 \cdot 10^{-1}$ μmole.

Glyoxal in dialdehydic oxidation products exists in the conjugated form. Therefore, determination of glyoxal has been performed after liberation of glyoxal by acid hydrolysis[13]. However, this hydrolysis procedure may be omitted in the present method, since under the moderately acidic condition for condensation, hydrolysis occurred simultaneously. Thus, glyoxal in 7,9-dihydroxy-6α- and β-methoxy-2-phenyl-*trans*-*m*-dioxano-(5,4e)(1,4)-dioxepanes (dialdehyde I and II)—

crystalline model compounds of dialdehydes—was determined accurately as indicated in Table II. Data were reproducible and standard deviations did not exceed 2% for all levels of both compounds examined.

TABLE II

PRECISION OF THE DETERMINATION OF GLYOXAL IN DIALDEHYDES I AND II

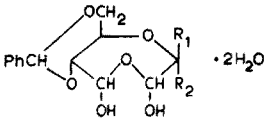

I R_1=H, R_2=OMe

II R_1=OMe, R_2=H

(5 determinations were done in each case)

Dialdehyde	*Amount of dialdehyde added·10^{-2} (μmole)*	*Ave. glyoxal formed ·10^{-2} (μmole)*	*Standard deviation*
I	1.00	1.00	0.00
I	1.90	1.88	0.01
I	2.50	2.46	0.05
II	1.00	1.00	0.00
II	1.90	1.83	0.03
II	2.50	2.52	0.03

In Table III the amounts of glyoxal in dialdehyde fragments, formed from selected glycosides by periodate oxidation in unbuffered solutions, are correlated to the amounts of periodate consumed. For methyl-4,6-O-benzylidene-D-glucopyranosides, both the periodate consumption and the glyoxal formation increased gradually giving an identical value of *ca.* 0.3 mole per mole of glycosides after 3 h. After 24 h they reached a theoretical value of 1. Both sets of data were in good agreement within experimental errors. The oxidation of methyl- and phenyl-β-D-glucopyranosides was so rapid as to be complete after 3 h. Thereafter, overoxidation, caused by C_1–O–C_5 bond cleavage, took place gradually, and excess of periodate, consumed by the oxidation of glyoxal (derived from the C_1–C_2 part) and D-glyceraldehyde (derived from the C_4–C_5–C_6 part) liberated, amounted to *ca.* 0.1–0.2 mole after 24 h. In the cases of the α-anomers, the reaction was much more rapid, and overoxidation had already occurred after 3 h. Since glyoxal and D-glyceraldehyde consume 1 and 2 molar amounts of periodate, respectively, the excess of the oxidant consumed during overoxidation should be equivalent to 3 times the amount of glyoxal destroyed. Comparison of the excess consumption of the oxidant with the loss in glyoxal content, both given in parentheses with positive and negative signs, respectively, indicates that the data accorded well with this prediction within experimental errors. Thus, periodate consumption increased throughout the courses of normal oxidation as well as overoxidation. The glyoxal content increased to the point where normal oxidation was complete, and then decreased as overoxidation proceeded.

TABLE III

PERIODATE OXIDATION OF SELECTED GLYCOSIDES

(Concentration of glycosides, $5.00 \cdot 10^{-3}$ *M*; reaction temperature, 25°C)

	Periodate consumption (mole/mole of glycoside)			*Glyoxal formed (mole/mole of glycoside)*[a] *Found*	
	Theor.	*Found*			
		3 h	*24 h*	*3 h*	*24 h*
Methyl 4,6-O-benzylidene-α-D-glucopyranoside	1	0.32	1.03	0.31	1.01
Methyl 4,6-O-benzylidene-β-D-glucopyranoside	1	0.30	1.01	0.30	0.99
Methyl α-D-glucopyranoside	2	2.03 (+0.03)[b]	2.16 (+0.16)[b]	0.98 (−0.02)[c]	0.95 (−0.05)[c]
Methyl β-D-glucopyranoside	2	1.95	2.12 (+0.12)[b]	0.98	0.97 (−0.03)[c]
Phenyl α-D-glucopyranoside	2	2.15 (+0.15)[b]	2.22 (+0.22)[b]	0.94 (−0.06)[c]	0.93 (−0.07)[c]
Phenyl β-D-glucopyranoside	2	2.00	2.20 (+0.20)[b]	0.98	0.93 (−0.07)[c]

[a] Theoretical value, 1.
[b] Excess consumption of periodate.
[c] Loss in glyoxal content.

SUMMARY

A simple procedure for the determination of glyoxal in dialdehyde fragments, formed from glycosides by periodate oxidation, is proposed. By heating sample solutions prepared by dilution of reaction mixtures for periodate oxidation, with an aqueous dimethylsulfoxide solution of 2,4-dinitrophenylhydrazine hydrochloride, followed by addition of an aqueous ethanolic solution of potassium hydroxide, intense color with an absorption maximum at 576 nm developed. The spectrophotometric method based on this color reaction makes it possible to determine selectively $1 \cdot 10^{-2}$–$2 \cdot 10^{-1}$ μmole amounts of conjugated glyoxal without a prior liberation process. Data for glyoxal content obtained by this procedure are discussed in relation to overoxidation.

REFERENCES

1 E. Müller and O. Friedberger, *Ber. Deut. Chem. Ges.*, 35 (1902) 2652.
2 L. Malaprade, *C.R.H. Acad. Sci.*, 186 (1928) 382; *Bull. Soc. Chim. France*, 43 (1928) 683.
3 P. F. Fleury and J. Lange, *J. Pharm. Chim.*, 17 (1933) 107; *J. Pharm. Chim.*, 17 (1933) 196.
4 J. S. Dixon and D. Lipkin, *Anal. Chem.*, 26 (1954) 1092.
5 K. Takiura and K. Koizumi, *Chem. Pharm. Bull.*, 10 (1962) 134.
6 M. Lambert and A. C. Neish, *Can. J. Res., Sect. B*, 28 (1950) 83.
7 J. R. Dyer, *Methods Biochem. Anal.*, 3 (1956) 111.
8 N. K. Richtmyer, *Methods Carbohyd. Chem.*, 1 (1959) 108.
9 R. D. Guthrie and J. Honeyman, *J. Chem. Soc.*, (1959) 2441.
10 T. Banks, C. Vaughn and L. M. Marshall, *Anal. Chem.*, 27 (1955) 1348.
11 E. Sawicki, T. R. Hauser and R. Wilson, *Anal. Chem.*, 34 (1962) 505.
12 N. Ariga, *Anal. Biochem.*, 43 (1971) 446.
13 C. S. Wise, C. L. Mehltretter and J. W. Van Cleve, *Anal. Chem.*, 31 (1959) 1241.

Analytica Chimica Acta, 74 (1975) 75–84

THE RAPID COLORIMETRIC DETERMINATION OF MOLYBDENUM WITH DITHIOL IN BIOLOGICAL, GEOCHEMICAL AND STEEL SAMPLES

B. F. QUIN and R. R. BROOKS

Department of Chemistry, Biochemistry and Biophysics, Massey University, Palmerston North (New Zealand)

(Received 17th May 1974)

The colorimetric method for the determination of molybdenum with toluene-3,4-dithiol (dithiol) is still used very extensively in spite of the tendency of classical methods to be replaced by instrumental techniques such as atomic absorption spectrometry. This is because the dithiol method is still one of the fastest, most precise and most sensitive methods of determining molybdenum. Since the introduction of the method by Hamence and Miller[1–3], it has been applied to a wide range of materials including plants[4–8], biological materials[9–11], soils[12–16], stream sediments[15,16], rocks[12,15–17], geochemical samples in general[14,18,19], tungsten ores[20], copper ores[21] and steel[22]. This large number of procedures has arisen partly as a result of individual workers developing specialized techniques which best seemed to fulfil their particular requirements without consideration of the parameters involved and without an attempt at development of a general method applicable to a much wider range of materials.

In view of the above, and because of the great importance of this colorimetric procedure, we have developed a simple, rapid and accurate method which is of general application to all the above materials, and which involves only changing the preliminary sample treatment. In developing this procedure, many combinations of types and concentrations of reagents were tested to determine which were most suitable. The results of these investigations are summarized in this paper.

EXPERIMENTAL

Equipment

A Bausch and Lomb Spectronic 20 spectrophotometer fitted with a red filter and an accessory phototube was used.

A muffle furnace was used for the fusion of geochemical samples and for the ashing of botanical and biological samples. Borosilicate glassware was used throughout.

Reagents

Analytical-reagent grade chemicals were used, except for zinc dithiol and isoamyl acetate.

Reducing solution. Prepare a solution containing 15% (w/v) of ascorbic acid and 2% citric acid in distilled water.

Potassium iodide solution. Prepare a 100% (w/v) solution of potassium iodide in distilled water. Add 0.5% (w/v) ascorbic acid.

Dithiol solution. Add 6 ml of ethanol to 1 g of zinc dithiol followed by 10 ml of water, 4 g of sodium hydroxide, and 2 ml of thioglycollic acid. Mix well, and dilute to 300 ml with distilled water. Store in a refrigerator.

Isoamyl acetate. Boiling range 125–142° C.

Standard molybdenum solution. Dissolve 0.1261 g of sodium molybdate dihydrate in 4 *M* hydrochloric acid and dilute to 500 ml with this acid to give a solution containing 100 μg Mo cm^{-3}. From this solution prepare solutions containing 10 μg and 1 μg of molybdenum per ml in 4 *M* hydrochloric acid.

Determination of molybdenum in botanical and biological samples

Weigh 2 g of dried material into a test tube (*e.g.* 150 × 16 mm) and ash to completion at 550 °C. Allow to cool, weigh (if ash percentage data are required), add 10 ml of 4 *M* hydrochloric acid and heat in a water bath at 80 °C for 15 min. Allow to cool to room temperature (<30 °C) and settle, then transfer 5 ml of the clear solution to a test tube (150 × 16 mm).

Add 1 ml of reducing solution, mix and allow to stand for 5 min. Add 3 ml of potassium iodide solution, mix, then add 0.02 ml of thioglycollic acid and mix again. Allow to stand for 30s, then add 1 ml of dithiol solution, mix and allow to stand for 1 min. Add 5 ml of isoamyl acetate, shake vigorously for 1 min, then measure the absorbance of the organic layer at 680 nm within 2 h. If the organic layer is cloudy, owing to the presence of dispersed water droplets, simply dip the colorimeter tube into hot water. If the absorbance is greater than that of the highest standard, repeat using a suitably smaller aliquot from the remaining sample solution, diluting this to 5 ml with 4 *M* hydrochloric acid and continuing from the addition of the ascorbic acid solution.

Standards. Make a series of standards representing 0, 0.2, 0.5, 1.0, 2.5, 5.0, 7.5, 10.0, 15.0 and 20.0 p.p.m. Mo by adding respectively to 10 test tubes 0, 0.2, 0.5, 1.0, 2.5, 5.0, 7.5, 10.0, 15.0 and 20.0 μg Mo. Dilute to 5 ml with 4 *M* hydrochloric acid and continue from the addition of the ascorbic acid solution.

The standards will keep for long periods, if required, if the potassium iodide is replaced by an equal volume of distilled water in the procedure.

Determination of molybdenum in geochemical samples

Weigh 0.2 g of sample (−100 mesh) into a test tube, add 1 g of potassium hydrogensulphate and mix. Fuse at 550 C for 10 min, or fuse over a Bunsen flame until a quiescent melt is obtained and continue heating for a further 2 min. Leach in a water bath with 10 ml of 4 *M* hydrochloric acid at 80 °C until the melt can be broken up with a glass rod. Allow to cool to room temperature (<30 °C) and settle. Transfer 5 ml of the clear solution to a test tube (150 × 16 mm), and continue as above from the addition of the ascorbic acid solution.

Standards. Make a series of standards representing 0, 2, 5, 10, 25, 50, 75, 100, 150 and 200 p.p.m. Mo by adding respectively to 10 test tubes 0, 0.2, 0.5, 1.0, 2.5, 5.0, 7.5, 10.0, 15.0 and 20.0 μg Mo. Dilute to 5 ml with 4 *M* hydrochloric acid and continue from the addition of the ascorbic acid solution.

Determination of molybdenum in steels

Dissolve 0.2 g of sample in 4 ml of hydrochloric acid (s.g. 1.18) and 1 ml of nitric acid (s.g. 1.42), taking to dryness over a boiling water bath. Add 2 ml of nitric acid and again take to dryness. Heat the residue with 10 ml of 4 *M* hydrochloric acid for 10 min at 80 °C, then cool, make up to 10 ml with distilled water, and centrifuge. Transfer 0.25 ml of the clear solution to a test tube (150 × 16 mm), add 4.5 ml of 4 *M* hydrochloric acid, and continue as above from the addition of the ascorbic acid solution.

Standards. Make a series of standards representing 0, 40, 100, 500, 1000, 1500, 2000, 3000 and 4000 p.p.m. Mo by adding respectively to 10 test-tubes 0, 0.2, 0.5, 1.0, 2.5, 5.0, 7.5, 10.0, 15.0 and 20.0 μg Mo. Dilute to 5 ml with 4 *M* hydrochloric acid and continue from the addition of the ascorbic acid solution.

RESULTS

Reproducibility and recovery tests

Table I shows the results of replicate analyses of various samples by the proposed procedure.

Recovery of molybdenum added to all types of samples was complete within the precision of the method (Table II).

TABLE I

ANALYTICAL DATA FOR REPLICATE DETERMINATIONS OF MOLYBDENUM

Sample	*Number of determinations*	*Mean Mo conc. (p.p.m.)*	*Range (p.p.m.)*	s_r (%)
Fish liver	5	2.4	2.3–2.6	±6.1
Clover	10	9.2	8.9–9.3	±1.5
Ryegrass	10	3.4	3.2–3.5	±3.6
Olearia range[a]	5	33.0	30.1–36.2	±7.3
Soil	10	0.95	0.91–0.97	±2.1
Soil[a]	10	10.4	10.1–10.7	±1.7
Scheelite ore[b]	5	6.5	6.3–6.6	±2.1
Copper–lead ore[c]	5	7.5	6.9–8.2	±6.8
A.R. grade sodium tungstate (< 100 p.p.m. Mo)	5	41	3.9–4.3	±3.9
B.S.C. No. 408 low alloy steel (0.14% Mo)	10	1380	1310–1420	±3.1

[a] From area of molybdenum mineralization, Nelson, New Zealand.
[b] From area of scheelite mineralization, Otago, New Zealand.
[c] From area of copper–lead mineralization, Coromandel, New Zealand.

The U.S. Geological Survey standard sample G-1 and W-1 were analysed by the proposed procedure with mean values of 6.2 and 1.3 p.p.m., respectively, being obtained. These values are in reasonably satisfactory agreement with the neutron activation results of Hamaguchi *et al.*[23], who reported 7.0 p.p.m. for G-1 and 1.3 p.p.m. for W-1.

Sensitivity

The proposed procedure allows for the determination of 0.05, 0.5 and 10 p.p.m. in botanical, geochemical and steel samples, respectively. Sensitivity may be increased 10-fold if required by using only 0.5 ml of isoamyl acetate in conjunction with micro-cells. Beer's law is obeyed over the range used. The same standard curve (A.U., 0.0–*ca.* 0.8) was obtained for 0–20 p.p.m. Mo in biological samples, 0–200 p.p.m. Mo in geochemical samples and 0–4000 p.p.m. Mo in steel samples.

DISCUSSION

Preliminary treatment of samples

Ashing of botanical and biological samples. Dry ashing at 550 °C gave very reproducible results (Table I) and unlike wet ashing with, for example, a mixture of nitric, sulphuric and perchloric acids[4,5,8,10,11], no chemicals are required and much less labour is involved. The involatile nature of the oxides and oxy-salts of molybdenum prevents any loss during ashing.

The ashing of 2 g of organic material in 150 × 16 mm test tubes, for example, takes a maximum of 20 h at 550 °C. If required, faster ashing may be achieved by using larger tubes or beakers.

TABLE II

MOLYBDENUM RECOVERED FROM VARIOUS SAMPLES

Sample	*Mo present (μg)*	*Mo added (μg)*	*Mo found*[b] *(μg)*	s_r *(%)*
Clover	9.2[a]	10.0	19.2	±0.8
Ryegrass	3.4[a]	10.0	113.3	±1.0
Soil	0.09[a]	10.0	10.1	±2.0
Granite	0.13[b]	10.0	10.1	±1.5
Scheelite ore	0.65[b]	10.0	10.7	±1.3
"Specpure" WO_3	0.00[b]	10.0	10.0	±0.5
A.R. grade tin(II) chloride	0.00[b]	10.0	9.9	±1.9
B.C.S. No. 408 low alloy steel	69[a]	10.0	78.5	±2.3

[a] Mean of 10 determinations.
[b] Mean of 5 determinations.

TABLE III

COMPARISON OF FUSION AND DIGESTION FOR GEOCHEMICAL SAMPLES

Sample	*Molybdenum (p.p.m., average of 5 determinations)*	
	$KHSO_4$ *fusion*	HF/HNO_3 *digestion*
Soil	3.1	3.2
Soil	210	205
Sodium tungstate (A.R.)	41	41
Rock	0.85	1.0
Stream sediment	21	20

Fusion of geochemical samples. Fusion with potassium hydrogensulphate at 550 °C may be carried out in borosilicate test tubes, which will last for 15–20 fusions before becoming very brittle. During the fusion, molybdenum is converted into soluble molybdate. Any organic matter present is completely decomposed. Stanton[15] has demonstrated that this fusion gives much more reproducible results than the low-temperature sodium carbonate–sodium chloride–potassium nitrate fusion of North[13], and gives similar results to the digestion with perchloric acid[16]. Table III shows a comparison of results by potassium hydrogensulphate fusion and digestion with a mixture of nitric and hydrofluoric acid.

Dissolution of steel samples. Inclusion of nitric acid in the initial step ensures complete dissolution of the sample during the time taken for the acid solution to evaporate (1–2 h). The second treatment, with nitric acid, ensures that all the molybdenum present is oxidised to molybdenum(VI).

Reactions involved during the formation and extraction of the molybdenum–dithiol complex

Molybdenum(VI) reacts rapidly at room temperature with dithiol to form the slightly soluble yellow-green dithiol complex[24]. After formation, the complex is quantitatively extracted into isoamyl acetate.

The prior addition of excess of ascorbic acid ensures the reduction of Fe(III) to Fe(II), and of Cu(II) to Cu(I); the citric acid complexes tungsten, and the addition of iodide precipitates the copper as copper(I) iodide. Thioglycollic acid is added to slow the extraction of iodine into the isoamyl acetate.

Parameters affecting the formation and extraction of the complex

The nature of the dithiol solvent. The possible methods of adding the dithiol are (a) as solid zinc dithiol[19], (b) as a solution of dithiol in isoamyl acetate[13,22], so that formation and extraction of the molybdenum–dithiol complex take place simultaneously, and (c) as a slightly basic aqueous solution of dithiol or its zinc derivative[4–12,14–18,20,21]. In this case, the complex is first formed as a slightly soluble suspension in the acid solution, and then extracted into an organic solvent.

Method (a) is unsuitable because dithiol oxidizes rapidly on exposure to air, and hence is more conveniently handled in solution.

Bowden[25] has criticised the use of the solution of dithiol in isoamyl acetate as in method (b), claiming that the reagent was unstable in this form, developing a high yellow-green colour (caused by formation of oxidation products of dithiol) after only 3 days, even if kept in a refrigerator. However, investigation showed that the reagent prepared in his way was at least as stable as the aqueous solution used in method (c), the solution being usable even after a year if stored in a refrigerator. This indicates that the dithiol used by Bowden must have been very impure.

A further criticism of method (b) was that extraction of molybdenum is very slow, being incomplete even after shaking for 15 min[4]. However, investigation showed that complete extraction of 10 μg of molybdenum into a 1% solution of dithiol in isoamyl acetate took only 4 min (Fig. 1).

In method (c), thioglycollic acid is added to the reagent solution to slow the oxidation of dithiol, and the solution may be used for some months if stored

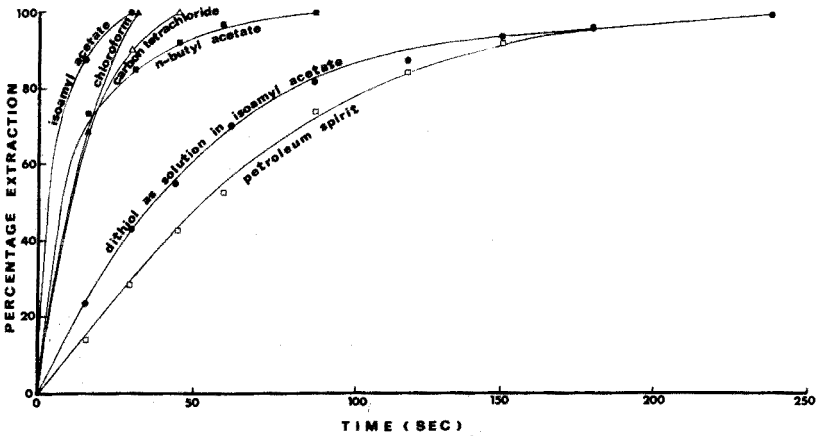

Fig. 1. Percentage extraction with time of molybdenum–dithiol complex into various solvents.

in a refrigerator. The dithiol, which is readily soluble in aqueous sodium hydroxide, precipitates to form a white colloidal suspension when this solution is added to the acidic sample solution.

In contrast to dithiol, the molybdenum–dithiol complex is soluble in many organic solvents, and hence several, including petroleum spirit[10,14–17,20], butyl acetate[9], isoamyl acetate[4,5,7,11–13,21,22], carbon tetrachloride[8], and chloroform[6,18] have been used for the extraction in method (c). These solvents were tested and all were found to completely extract the molybdenum, although the time for complete extraction varied considerably (Fig. 1).

Isoamyl acetate was chosen for the proposed procedure because of the rapid extraction obtained and because sampling of the organic layer was cleaner than with the denser-than-water carbon tetrachloride and chloroform. The rate of reaction is even faster at higher temperatures[26], but this also favours the reaction of tungsten with dithiol[5,24].

Acidity of the sample solution. Complete extraction of molybdenum (10 μg) was obtained from hydrochloric acid over the range 0.5–8 *M*. A final molarity of 2 *M* was chosen because (i) the complexing of tungsten by citric acid is not complete above 2.5 *M* (see below); (ii) the ability of ascorbic acid to reduce iron(III) is impaired in solutions greater than 4.5 *M*; and (iii) concentrations less than 2 *M* had very low tolerance towards tin interference (see below).

Interferences from other elements

The elements found to interfere were tungsten, iron, copper and tin.

Tungsten. Tungsten forms a blue-green dithiol complex with an absorption maximum at 630 nm (ref. 9). However, interference from tungsten is not a serious problem to overcome, because tungsten (as tungstate) is only slightly soluble in acid, and it reacts only very slowly with dithiol at room temperature. Sodium tungstate analysed by the proposed geochemical procedure but without citric acid (using 0.2 g), gave an absorbance equivalent to only 8 p.p.m. of molybdenum. However, it was considered desirable to remove tungsten interference altogether, so that the procedure could be used to determine molybdenum in tungsten ores. This was achieved by

the addition of 20 mg of citric acid which complexes tungsten, thus preventing the formation of tungsten dithiol. As shown in Table IV, it was essential to keep the final acid concentration at 2 *M*, as at higher acidities even greatly increased amounts of citric acid, as used by Marshall[6] and Stanton[15,16], do not achieve complete complexing of all the tungsten, and even 50 μg of tungsten interfered after 10-min standing[15]. Citric[9,20] and the similar tartaric[5,7,11,12] acid have been used to complex tungsten at low acidities in several earlier procedures[7].

Sodium tungstate (A.R.) was used in testing interference from tungstate as this gave higher solubility of tungsten than, *e.g.*, calcium tungstate (scheelite) or tungsten(VI) oxide. However, as this contained 41 p.p.m. molybdenum (Table I), it was necessary to determine how much of the absorption was due to molybdenum. This was done by measuring the A680/A630 absorption ratio for the molybdenum complex (1.56) and comparing this with the ratio achieved with sodium tungstate (Table IV).

TABLE IV

EFFECT OF FINAL ACID CONCENTRATION ON COMPLEXING OF TUNGSTEN WITH CITRIC ACID

Sample	*Final acid molarity (M)*	*Citric acid (mg)*	*Absorption ratio 680 nm/630 nm*
40 p.p.m. molybdenum standard	2	0	1.56
	2	20	1.56
	2	50	1.55
Sodium tungstate (A.R.)	3	0	0.74
	3	20	0.80
	3	50	0.83
	3	100	0.86
	2.5	0	0.92
	2.5	20	1.30
	2.5	50	1.35
	2.5	100	1.35
	2	0	1.12
	2	20	1.56
	2	50	1.56

Interference from tungsten is seen to be completely eliminated with 20 mg of citric acid. "Specpure" tungsten(VI) oxide was analysed and gave no measurable absorbance.

Iron. Iron has been said to interfere in a number of ways: (i) physically, by formation of an iron–dithiol complex[27]; (ii) colorimetrically, by the interference of iron(III) extracted into the organic solvent[12,15,18]; (iii) by suppression of the formation of the molybdenum–dithiol complex[15]; and (iv) by enhancement of the absorption of the molybdenum–dithiol complex[10].

(i) Iron(III) forms a black dithiol complex, slightly soluble in acid. Its formation is completely suppressed, provided that the final acid concentration is less than 3 *M*, by the presence of excess of ascorbic acid, which reduces Fe(III)

to Fe(II), without reducing Mo(VI). Iron(II) does not form a dithiol complex. Iron(III), if not reduced, may prevent complete formation of the molybdenum–dithiol complex, if present in sufficient concentration, by utilising all the available dithiol. The iron–dithiol complex is insoluble in isoamyl acetate and hence does not interfere colorimetrically.

(ii) Iron(III) will extract in small amounts into organic solvents including isoamyl acetate. Although all iron(III) is reduced by ascorbic acid in the proposed procedure, some of the small amounts of iron(II) that may also be extracted can be air-oxidised to iron(III). However, the absorption of the yellow iron(III) species is negligible at 680 nm and reportedly strong absorption is probably an artefact resulting from the use of spectrophotometers with poor diffraction gratings. The strong iron(III) absorption peak at 375 nm will show a peak at double this wavelength, *viz.* 750 nm, if a suitable filter is not used; this "peak" will result in significant absorption over the range 630–850 nm.

(iii) Stanton[15] reported that the presence of 2 mg or more of iron reduced the formation of the molybdenum–dithiol complex by approximately 10%, and recommended the addition of iron to standards and samples for the sake of reproducibility. Investigations of his procedure showed that this suppression was due to incomplete reduction of iron(III), because of the high acid concentration used.

When the proposed procedure is used, complete recovery of an added 10 μg of molybdenum was obtained from a 0.2 g sample of "Specpure" iron(III) oxide; the oxide alone gave no interference.

(iv) Several earlier procedures have suggested that the presence of small amounts of iron is essential to obtain complete formation of the molybdenum–dithiol complex[5,10,11], and/or that it increases the absorptivity of the complex[4,10]. However, investigation showed that the presence of 2 mg of iron(II) did not significantly increase the rate of extraction or formation of the molybdenum–dithiol complex at room temperature, whether the dithiol was added as an aqueous solution or as a solution in isoamyl acetate. It seems probable, therefore, than any effect of iron in earlier procedures was probably of a catalytic nature, as has been proposed by Gilbert[26].

As stated earlier, then, the proposed procedure is completely free from iron interference of any type.

Copper. Copper(II) interferes with the formation of the molybdenum–dithiol complex by rapidly forming a very stable purplish-black dithiol complex[27], and can therefore, if sufficient copper is present, utilise all the dithiol added. As with the iron(III)–dithiol complex, the copper complex is insoluble in isoamyl acetate and hence does not interfere colorimetrically. Simply adding more dithiol does not cure the problem however, as the suspension of copper–dithiol at the acid–ester interface can prevent complete formation and extraction of the molybdenum–dithiol.

The addition of potassium iodide suppresses copper interference by reducing any Cu(II) not reduced by ascorbic acid to Cu(I), and precipitating it as copper(I) iodide. This method of reducing copper interference has been employed by Stanton[15,16], whilst Clark and Axley[12] and Baker[18] have employed it instead of ascorbic acid to reduce iron(III). Stanton's method has a tolerance for 2 mg of

copper; although it is stated that more can be tolerated by the addition of more potassium iodide[15], investigation of this procedure showed that this was not the case, either because the ascorbic acid tended to prevent the oxidation of iodide to iodine by copper(II), or because large amounts of iodide tended to reduce molybdate to the green $MoOCl_5^{2-}$ species in strong acid[28]. The former case would permit more copper–dithiol to form; the latter would suppress the formation of molybdenum–dithiol.

The proposed procedure permits the complete extraction of molybdenum in the presence of up to 5 mg of copper (representing 0.5%, 5% and 100% in biological, geochemical and steel samples respectively). For practical purposes then, the procedure may be assumed to be free from copper interference since if in any of the former cases the limit is exceeded (as for example in copper ores), it is only necessary to reduce the sample size. This is far more convenient than having to extract the copper first, using reagents such as dithizone[4,9] or extracting molybdenum as the α-benzoinoxime[17,21] or cupferron[4,10] complex before converting it to the dithiol complex.

The proposed procedure, then, has a greater tolerance to copper than earlier procedures, permitting the determination of molybdenum in high-copper samples without prior separation.

Thioglycollic acid is added to slow the extraction of iodine into the isoamyl acetate. The absorption of the complex must be measured within 2 h of adding the ester, as the dithiol is slowly decomposed oxidatively as more iodine extracts, and eventually the colour of the iodine itself causes significant interference. The use of increased amounts of thioglycollic acid was found to result in incomplete extraction of the molybdenum–dithiol complex, owing to the reduction of molybdenum(VI).

Tin. Like copper, tin interferes by forming a dithiol complex[27], red in colour, which although insoluble in isoamyl acetate, can prevent the formation of the molybdenum complex by utilising the dithiol, or hindering the extraction by settling at the acid–ester interface. The proposed procedure will permit the complete extraction of molybdenum in the presence of up to 1 mg of tin. Although greater tolerance can be achieved by adding more dithiol (the tin complex is far less stable than that of copper), it is preferable to reanalyse high-tin samples by replacing the 3 ml of potassium iodide solution in the procedure by an equal volume of 8 *M* hydrochloric acid. When this is done, even tin compounds may be analysed for molybdenum, and added molybdenum is completely extracted (Table II). Although the red tin–dithiol complex forms after the addition of the dithiol, it decomposes on shaking with isoamyl acetate as the dithiol alone is extracted into the ester; the dithiol is then free to complex the molybdenum.

Other elements that were tested for interference and found to have no effect were arsenic, antimony and selenium.

CONCLUSION

It is concluded that, in terms of rapidity, recovery, and particularly versatility, the proposed procedure represents a significant improvement over existing colorimetric methods for the determination of molybdenum. If fusions are done in a furnace, up to 150 geochemical samples can be analysed per man-day, while ashed

biological and botanical samples may also be analysed at this rate. The procedure described for ashing dried vegetation involves a minimum of labour and enables large numbers of samples to be treated simultaneously.

SUMMARY

A rapid method for the determination of molybdenum in botanical, biological, geochemical and steel samples with dithiol, is described. Botanical and biological samples are ashed at 550 °C before leaching with 4 *M* hydrochloric acid, while geochemical samples are fused with potassium hydrogensulphate, and steels are decomposed with nitric and hydrochloric acids. The dithiol complex of molybdenum is formed by the addition of an alkaline solution of dithiol to the sample solution, and then extracted into isoamyl acetate. Ascorbic acid and citric acid are used to eliminate interferences from iron and tungsten, and the addition of potassium iodide gives the procedure very high tolerance to copper. Up to 150 geochemical samples or ashed botanical or biological samples can be analysed per man-day. Sensitivity of the method is 0.05, 0.5 and 10 p.p.m. for biological, geochemical and steel samples, respectively. The relative standard deviation is better than $\pm 7\%$ over the standard range used, and recovery of added molybdenum is complete.

REFERENCES

1 J. H. Hamence, *Analyst (London)*, 65 (1940) 152.
2 C. C. Miller and A. J. Lowe, *J. Chem. Soc., London*, (1940) 1258.
3 C. C. Miller, *J. Chem. Soc., London*, (1941) 792.
4 C. S. Piper and R. S. Beckwith, *J. Soc. Chem. Ind., London*, 67 (1948) 374.
5 J. B. Bingley, *J. Agr. Food Chem.*, 7 (1959) 269.
6 N. J. Marshall, *Econ. Geol.*, 59 (1964) 142.
7 U. C. Gupta and D. C. Mackay, *Soil Sci.*, 99 (1965) 414.
8 H. S. Sekaalo, *Analyst (London)*, 96 (1971) 346.
9 C. F. Bickford, W. S. Jones and J. S. Keene, *J. Amer. Pharm. Ass.*, 37 (1948) 255.
10 S. H. Allen and M. B. Hamilton, *Anal. Chim. Acta*, 7 (1952) 483.
11 J. B. Bingley, *J. Agr. Food Chem.*, 11 (1963) 130.
12 L. J. Clark and J. H. Axley, *Anal. Chem.*, 27 (1955) 2000.
13 A. A. North, *Analyst (London)*, 81 (1956) 660.
14 J. H. Watkinson, *New Zealand J. Sci.*, 1 (1958) 201.
15 R. E. Stanton and A. J. Hardwick, *Analyst (London)*, 92 (1967) 387.
16 R. E. Stanton, *Australas. Inst. Mining Met., Proc.*, 235 (1970) 101.
17 P. G. Jeffery, *Analyst (London)*, 81 (1956) 104.
18 W. E. Baker, *Australas. Inst. Mining Met., Proc.*, 214 (1965) 125.
19 M. F. Stubbs, *Analyst (London)*, 93 (1968) 59.
20 P. G. Jeffery, *Analyst (London)*, 82 (1957) 558.
21 H. R. Skewes, *Aust. J. Appl. Sci.*, 10 (1959) 464.
22 J. E. Wells and R. Pemberton, *Analyst (London)*, 72 (1947) 185.
23 H. Hamaguchi, R. Kuroda, T. Shimuzu, I. Isukahara and R. Yakamoto, *Geochim. Cosmochim. Acta*, 26 (1962) 503.
24 E. B. Sandell, *Colorimetric Determination of Traces of Metals*, Interscience, New York, 1959.
25 P. Bowden, *Analyst (London)*, 89 (1964) 771.
26 T. W. Gilbert, Jr., Ph.D. Thesis, University of Minnesota, 1956.
27 R. E. D. Clark, *Analyst (London)*, 83 (1958) 396.
28 C. K. Jorgensen, *Absorption Spectra and Chemical Bondings in Complexes*, Pergamon, Oxford, 1962.

Analytica Chimica Acta, 74 (1975) 85–99

A STUDY OF VANADIUM(IV)–3-METHYLCATECHOL–QUATERNARY AMMONIUM SYSTEMS

ITS ANALYTICAL IMPLICATIONS

A. M. NARDILLO and J. A. CATOGGIO

Departamento de Química Analítica, Facultad de Ciencias Exactas, Universidad Nacional de La Plata, La Plata (Argentina)

(Received 14th October 1973)

Both vanadium(IV) and vanadium(V) react with catechol and its alkyl and halogenated derivatives in neutral or nearly neutral aqueous solutions in the presence of sodium sulfite, to give one or more complexes with two absorption maxima in the visible spectrum; the principal maximum appears at 590 nm, and the secondary one at 370–380 nm. It has already been proved that the final reaction product in aqueous media is the same for both oxidation states of the original metal ion. This has been attributed to reduction of vanadium(V) to vanadium(IV), by reaction with catechol[1–4], or with derivatives such as tiron[5] or dihydroxybenzoic acids[6] apart from the effect of sodium sulfite itself[7,8].

If the behavior of 3-methylcatechol were comparable to that of catechol under similar conditions[1,2,9–11], then at pH 7.0 the anionic complexes formed between vanadium(IV) and 3-methylcatechol should predominate over the neutral complexes. The anionic vanadium(IV)–3-methylcatechol complexes can be extracted into 1,2-dichloroethane in the presence of organic cations, *e.g.* quaternary ammonium[12], phosphonium and arsonium ions; similar behavior is shown by the vanadium(IV)–catechol system[13].

The visible absorption spectrum of the extracted species in 1,2-dichloroethane is entirely analogous to that of the aqueous phase before the large cation is added; a major peak is found around 600 nm and a minor one at about 400 nm. However, after a while, the absorption band at 390–400 nm progressively enlarges. For the extract of an aqueous solution containing $5 \cdot 10^{-5}$ *M* vanadium(IV), $2 \cdot 10^{-1}$ *M* 3-methylcatechol and $1 \cdot 10^{-2}$ *M* tetrabutylammonium iodide (TBAI), this new maximum exceeds the main orginal peak at 600 nm within 15 min; after 1 h, the concentration of the new species absorbing at 390–400 nm becomes large enough to begin contributing slowly to the absorption at 600 nm.

The appearance of this band has been mentioned for the vanadium–catechol system, though no interpretation was offered[14]. Analogous behavior has been described for the dichloroethane extract of the system vanadium(IV)–catechol–antipyrine from aqueous medium at pH 6.0, the phenomenon being attributed[13] to the presence of "non-optimum excess amounts of the ligands". It has been also stated[2] that for $2 \cdot 10^{-3}$ *M* vanadium solutions above pH 6.0, a yellow compound ($\lambda_{max.}$ 380 nm), extractable into 1,2-dichloroethane, is formed between vanadium and catechol, in

addition to the well-known blue complexes; an equilibrium was assumed to exist between the blue and yellow compounds, through a polymerization process, the yellow species being regarded as a dimer.

Several questions arise in connection with these cited studies. For analytical purposes, it was considered essential to establish an appropriate procedure and reagents so that adequate stability of the vanadium ion pair in the organic solvent could be attained. Moreover, the nature of the product(s) generated in the organic extract from an aqueous solution of the vanadium–3-methylcatechol–quaternary ammonium system at pH 7.0 had to be investigated, and, if possible, a procedure for the metal determination devised. A progressive experimental study was therefore undertaken based on the following steps: (1) extractions into 1,2-dichloroethane of the vanadium(IV)–3-methylcatechol complex with a large cation, (2) analogous extractions of vanadium-free blanks, (3) dissolution in 1,2-dichloroethane of the insoluble products formed in the aqueous solutions of the systems in (1) and (2), and (4) experimental verification of related systems reported in the literature, under varying conditions. The study was conducted from two different points of view: first, qualitatively in connexion with the appearance of the absorption band at 390–400 nm; and secondly, a time study concerned with the evolution of the absorption bands. It must be stated in advance that times recorded here are only of relative value and may change by $\pm 30\%$, because no special control of oxygen content was made, and the general process is undoubtedly oxidative in nature.

EXPERIMENTAL

Instrumentation

A Bausch–Lomb Spectronic 600 unit was used for the u.v.–visible range. I.r. spectra were run in a Perkin-Elmer 257 spectrometer. pH measurements were made with a Leeds–Northrup model 7404.

Reagents

Vanadium(IV) solutions were prepared by bubbling sulfur dioxide through sodium metavanadate (C. Erba, p.a.) solution in 1 *M* sulfuric acid.

3-Methylcatechol (Aldrich) was purified by sublimation (m.p. 68°C).

Quaternary ammonium and phosphonium salts. Tetrabutylammonium iodide TBAI, and triphenylbutylphosphonium bromide, TPBPB (Aldrich); phenyltrimethylammonium iodide, PTMAI, and methyltrioctylammonium bromide, MTOAB (Eastman Kodak); methyltributylammonium iodide, MTBAI, lauryltrimethylammonium bromide LTMAB, and dibenzyldimethylammonium chloride, DBDMAC (K & K).

TBA nitrate (TBAN) was prepared by adding an equivalent amount of silver nitrate to a TBAI solution, and vacuum-evaporating the filtered clear solution. TBA chloride (TBAC) was obtained by percolating a TBAI solution through a 200–400 mesh Dowex 1-X8 (chloride form) anion-exchange column, and vacuum-evaporating the TBAC fraction.

Extractions

Suitable amounts ($0.5–1.0 \cdot 10^{-4}$ *M*) of vanadium(IV) for spectrophotometric measurements were added to aqueous $2 \cdot 10^{-1}$ *M* 3-methylcatechol solution, and

the pH was adjusted at 7.0 by addition of solid sodium sulfite; the required amount of quaternary ammonium or phosphonium salt was then added to attain the concentration sought, and finally 1,2-dichloroethane was added in a 1:1 volume ratio. The phases could be clearly separated by centrifugation after shaking for 2 min. In every case, 4.0-ml fractions of organic extract were kept in 6–7-ml test tubes tightly plugged with polyethylene stoppers. Aqueous solutions of 3-methylcatechol plus vanadium(IV) were adjusted to pH 7.0 with sodium sulfite exclusively; attempts to begin neutralization with sodium hydroxide led to poorer stability of the blue vanadium complex in the organic solvent. Usually, the final solutions contained at least 1% (w/v) sodium sulfite, though occasionally more was required to achieve pH 7.

Blank tests were run similarly; an equivalent volume of 1 *M* sulfuric acid was used instead of the acid vanadium(IV) solution.

Preparation of the vanadium(IV)–3-methylcatechol–quaternary ammonium ion pair.

To an acidic solution of vanadium(IV), the following reagents were successively added: solid sodium sulfite, 3-methylcatechol, plus sodium sulfite to give pH 7.0 and, finally, TBAI; the amounts used were such that the final concentrations were $5 \cdot 10^{-3}$ *M* vanadium, $2 \cdot 10^{-2}$ *M* 3-methylcatechol and $1 \cdot 10^{-2}$ *M* TBAI. The precipitate thus formed was separated by filtration, washed with cold water and dried at room temperature under vacuum for 24 h.

A similar procedure was followed to obtain the insoluble product formed by interaction between 3-methylcatechol and TBAI at pH 7.0.

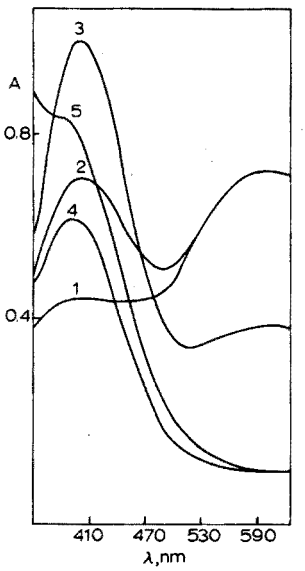

Fig. 1. Spectrophotometric behavior as a function of time of the V(IV)–3-methylcatechol–TBAI complex in the 1,2-dichloroethane extract from an aqueous solution containing $1 \cdot 10^{-4}$ *M* V(IV), $2 \cdot 10^{-1}$ *M* 3-methylcatechol and $1 \cdot 10^{-2}$ *M* TBAI at pH 7.0. Curve (time elapsed, cell path): (1) 5 min, 1 cm; (2) 45 min, 1 cm; (3) 75 min, 0.5 cm; (4) 3 h, 1 mm; (5) 5 h, 1 mm.

TABLE I

STABILITY OF THE VANADIUM(IV)–3-METHYLCATECHOL–QUATERNARY AMMONIUM SYSTEM EXTRACTED INTO 1,2-DICHLOROETHANE

($5 \cdot 10^{-5}$ *M* V(IV), $2 \cdot 10^{-1}$ *M* 3-methylcatechol in aqueous solution at pH 7.0. Stability is defined as the time required for the absorption band at 390–400 nm of the organic extract, to attain an absorbance of 0.2 at 390 nm.)

Quaternary ammonium salt (mol l^{-1})	*Stability*		
	TBAI	*TBAC*	*LTMAB*
$2 \cdot 10^{-3}$			3 h[a]
$3 \cdot 10^{-3}$	30 min		
$5 \cdot 10^{-3}$	30–40 min	25–30 min	8 h
$1 \cdot 10^{-2}$	50–60 min	90 min	40 h
$2 \cdot 10^{-2}$	4 h	6 h	
$3 \cdot 10^{-2}$	6 h		
$5 \cdot 10^{-2}$	12 h		4 days
$1 \cdot 10^{-1}$	24 h		

[a] Incomplete extraction of vanadium.

RESULTS

Extraction of vanadium(IV)–3-methylcatechol–quaternary ammonium complex

Effect of the quaternary ammonium salt concentration. The effect of TBAI concentration on the stability of the ion-pair extract in 1,2-dichlorethane was studied, beginning with the minimal amount required for quantitative extraction. The same qualitative behavior as mentioned in the introduction was verified as a function of time elapsed (Fig. 1). The extracted ion pair was more unstable, the lower the initial concentration of quaternary ammonium salt (Table I).

Tests with LTMAB showed similar behavior to that observed with TBAI, even though the extracted ion pair formed with LTMA was more stable (Table I).

Effect of the quaternary ammonium salt anion. Similar behavior was obtained when TBA chloride or nitrate replaced the iodide. Some stability results for TBAC are given in Table I. These experiments indicate that the quaternary ammonium salt anion is not a determining factor in the decomposition of the system.

Effect of the quaternary ammonium cation. Different cations, *i.e.* MTBAI, MTOAB, DBDMAC and TPBPB at $1 \cdot 10^{-2}$ *M* and PTMAI at $2 \cdot 10^{-2}$ *M*, were tested individually. The behavior in every case was analogous to that obtained with TBAI; but the band at 400 nm appeared at different intervals of time.

Nature of the process. It was proved experimentally that the organic extract in 1,2-dichloroethane from the aqueous vanadium–3-methylcatechol–TBA system at pH 7.0, absorbs oxygen. This was verified by checking the decrease in air volume (more than 11% in 12 h), when a freshly prepared extract was placed in a modified Warburg device; the organic phase showed the same color shift as usual. The two phenomena are undoubtedly related and define the process as an oxidation.

The vanadium–3-methylcatechol–LTMA system was then extracted from an aqueous solution at pH 7.0, into dichloroethane through which sulfur dioxide

had previously been bubbled; the quaternary ammonium iodides must not be used under these circumstances, because iodide gives an intensely yellow extractable reaction product in acidic solutions with sulfur dioxide, which does not disappear in neutral medium.

In the presence of sulfur dioxide, the absorbance of the ion pair extracted with $5 \cdot 10^{-3}$ *M* LTMAB into 1,2-dichloroethane did not change within the 350–625-nm region for several days. This test, compared with data included in Table I, confirms the oxidative nature of the decomposition process.

Extraction of vanadium-free systems

It is important to note that even the blanks corresponding to the above tests on the effect of TBAI concentrations showed analogous behavior to the vanadium–3-methylcatechol–TBAI extract (Fig. 2), though much more slowly. This made it advisable to study the effect on the blanks of the same variables as described above.

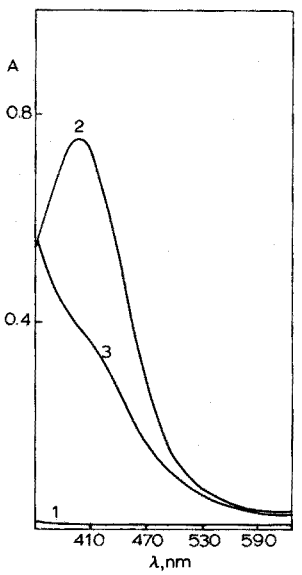

Fig. 2. Spectrophotometric behavior as a function of time of the 3-methylcatechol–TBAI system in the 1,2-dichloroethane extract from an aqueous solution containing $2 \cdot 10^{-1}$ *M* 3-methylcatechol and $1 \cdot 10^{-2}$ *M* TBAI at pH 7.0. Curve (time elapsed, cell path): (1) 15 min, 1 cm; (2) 10.5 h, 0.5 cm; (3) 12 h, 1 mm.

Tests on the effect of variable TBA concentration (Table II) showed that the system becomes more unstable at intermediate concentrations. This peculiar behavior can be interpreted by associating the decrease in stability with the beginning of an extraction of rather loose ion pairs of the cation, either with the 3-methylcatechol anion or with the original anion (iodide); such ion pairs might catalyse the decomposition process. A higher concentration of the cation would in turn inhibit such decomposition, because of stabilization of the ion pair through mass action.

TABLE II

STABILITY OF THE 3-METHYLCATECHOL–QUATERNARY AMMONIUM SYSTEM EXTRACTED INTO 1,2-DICHLOROETHANE

(Aqueous $2 \cdot 10^{-1}$ *M* 3-methylcatechol solution at pH 7.0. Stability is defined as in Table I)

Quaternary ammonium salt (mol l^{-1})	*Stability (h)*		
	TBAI	*TBAC*	*TBAN*
$1 \cdot 10^{-4}$	50		
$1 \cdot 10^{-3}$	50		
$5 \cdot 10^{-3}$	4	10	10
$1 \cdot 10^{-2}$	8	10	
$5 \cdot 10^{-2}$	50		
$1 \cdot 10^{-1}$	50		

When $1 \cdot 10^{-2}$ *M* TBA chloride or nitrate was used, large qualitative differences were observed compared to the behavior with TBAI. Even though the band at 390–400 nm appeared, it attained absorbance values of 0.3 at most at 390 nm (as opposed to values around 3.0—adjusted to the same path length—for the same wavelength and time with equal concentration of TBAI) before being overlapped by the absorbance increase in the u.v. range. The time of appearance of the 390-nm band also differed for the chloride and nitrate, compared to the iodide (Table II). These tests suggest that iodide plays a specific role in the decomposition of the extracted system.

Tests were therefore run with $1 \cdot 10^{-2}$ *M* TBMAI and $2 \cdot 10^{-2}$ *M* PTMAI, both of which showed the same qualitative behavior as TBAI, and also with $1 \cdot 10^{-2}$ *M* DBDMAC, MTOAB, LTMAB or TPBPB, which behaved similarly to the TBAC or TBAN. This seems to confirm the idea that iodide has a specific action.

Variations in the time of appearance of the band at 400 nm in the absence of iodide can be ascribed to the varying nature of the cation which would affect the stability constant of the corresponding ion pair.

Studies of the insoluble products in absence of vanadium

As shown above, when $2 \cdot 10^{-1}$ *M* 3-methylcatechol and 10^{-2} *M* TBAI are mixed in aqueous solution at pH 7.0, a white precipitate forms which is extracted by 1,2-dichloroethane; and the plain 3-methylcatechol solutions in 1,2-dichloroethane were stable with time. It was therefore considered that the instability of the blanks was related to the insoluble product in aqueous solution. The pK_1 value for 3-methylcatechol is 9.51[15], and the pH of extraction is 7.0, hence the precipitate might be considered as tetrabutylammonium 3-methylcatecholate. Elemental analysis of the precipitate gave the following values: 72.57% C, 9.82% H, 2.35% N. These results correspond to a mixture of 61.6% tetrabutylammonium 3-methylcatecholate with 38.4% 3-methylcatechol; which, perhaps coincidentally, approximates a 1:2 molar ratio.

The precipitate was centrifuged from the aqueous solution and dried under vacuum at room temperature. A $5 \cdot 10^{-3}$ *M* (expressed as tetrabutylammonium 3-methylcatecholate) solution was prepared in 1,2-dichloroethane. This solution

showed no absorbance in a 1-cm cell between 350 and 625 nm when freshly prepared; but after 1–2 h, a band appeared at 390–400 nm which attained an absorbance of 0.2 at 390 nm before it became overlapped by an increasing band in the u.v. range. The behavior matched that observed for the organic extracts of 3-methylcatechol–quaternary ammonium systems in the absence of iodide. No change in behavior was observed when $6 \cdot 10^{-3}$–10^{-1} *M* 3-methylcatechol was added to the TBA–3-methylcatecholate solution in dichloroethane.

The effect of iodide on the behavior of the precipitate ("catecholate") was then investigated. Aliquots of an extract in 1,2-dichloroethane from an aqueous 10^{-2} *M* TBAI solution were treated with (a) $5 \cdot 10^{-3}$ *M* catecholate plus 10^{-2} *M* 3-methylcatechol; (b) $5 \cdot 10^{-3}$ *M* catecholate; and (c) 10^{-2} *M* 3-methylcatechol. In case (a), the behavior was similar to that of the organic extract of an aqueous solution at pH 7.0 of $2 \cdot 10^{-1}$ *M* 3-methylcatechol and 10^{-2} *M* TBAI. In case (b), a band appeared initially at 390–400 nm but the λ_{max} shifted with time and remained at 350–360 nm for several days. Case (c) showed a remarkable stability, the band at 390–400 nm only developing after four days.

The catecholate formed in aqueous medium therefore appears to be the starting species for the decomposition of the blanks; its concentration in the organic phase in a single extraction depends on the quaternary ammonium concentration, and iodide, extracted as an ion pair, catalyses the decomposition. The excess of 3-methylcatechol plays a relatively important role, behaving as a substrate for the generation of the yellow compound, and possibly regulating the solvent "acidity". A high concentration of the quaternary ammonium ion stabilizes the system by inhibiting the dissociation of the catecholate.

Studies of the insoluble products in the presence of vanadium

The vanadium(IV) complex with 3-methylcatechol in aqueous solution at pH 7.0 is anionic (an anion exchanger discolors the solution while turning bluish); in the presence of TBAI or any heavy quaternary ammonium ion, an insoluble product is formed. This precipitate is completely soluble in organic solvents, and, if it is separated by solvent evaporation, remains insoluble in water at pH 7.0, any turbidity disappearing from both phases when the aqueous suspension is shaken with dichloroethane. The precipitate and the extracted species therefore seem identical.

The results of elemental analysis of the synthetic ion pair thus obtained did not match exactly any of the most probable stoichiometries, be it VL_3M_2 (where L may be 3-methylcatechol or catechol and M is thallium, Henry *et al.*[16] having failed to prepare the corresponding potassium, ammonium or guanidinium salts), or VOL_2M_2, as given for vanadium complexes with catechol and diphenylguanidinium[1], where M is the diphenylguanidinium cation. Percentages found for the synthetic ion pair formed with tetrabutylammonium iodide, and those corresponding to the theoretial species, are:

	% *C*	% *H*	% *N*	% *V*
Synthetic ion pair	68.8	9.7	2.9	5.40
$(TBA)_2VL_3$	70.55	10.05	3.10	5.65
$(TBA)_2VOL_2$	69.40	10.63	3.51	6.40

The solid ion-pair compound was studied in 1,2-dichloroethane, under different conditions, as described in the following paragraphs.

(a) Without further reagent addition. The absorption spectrum of the synthetic ion pair, immediately after dissolution in 1,2-dichloroethane, is similar to that of the product extracted with this solvent from an aqueous solution at pH 7.0 containing vanadium(IV), and excesses of 3-methylcatechol and tetrabutylammonium iodide. The absorbance around 600 nm diminishes slowly with time and a band with maximal absorbance at 380–390 nm appears gradually (Fig. 3). This behavior is similar to that exhibited by the extract from an aqueous solution, but some differences are apparent. (i) The absorbance around 600 nm increases with time in the extract from aqueous solution, while that of the synthetic ion-pair decreases. (ii) The absorbing band of the reaction product lies at 390–400 nm in the extract but at 380–390 nm for the dissolved synthetic ion-pair. (iii) The maximum at 390–400 nm is overshadowed by the steady increase in absorbance from the u.v. for the extract, whereas the maximum at 380–390 nm remains almost stable in the same period for the dissolved synthetic ion-pair. (iv) After the new band has appeared, the absorbance at 390 nm rapidly becomes greater than the original band at 600 nm in the case of the extract; for the dissolved synthetic ion-pair, this increase is slow and the final absorbance at 390 nm never exceeds that at 600 nm. Difference (iv) can be explained by assuming that 3-methylcatechol—absent from solutions of the synthetic ion-pair but present in extracts—participates in the

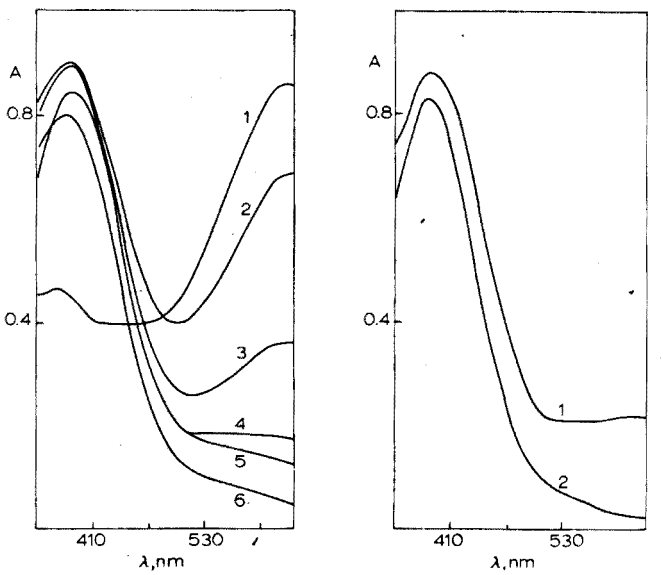

Fig. 3. Spectrophotometric behavior as a function of time of the synthetic ion-pair dissolved in 1,2-dichloroethane. Curve (time elapsed, cell path): (1) 10 min, 1 cm; (2) 5 h, 1 cm; (3) 24 h, 1 cm; (4) 2 days, 1 cm; (5) 7 days, 1 cm; (6) 12 days, 1 cm.

Fig. 4. Absorption spectra of synthetic ion-pair (1) 14 h after its dissolution in 1,2-dichloroethane; (2) after treatment of this solution with 0.1 *M* HCl, washing with Na_2SO_4 solution and drying with anhydrous Na_2SO_4.

absorbance increase.

The organic solution of the synthetic ion-pair, after *ca.* 14 h, was treated as follows: it was contacted three times with equal volumes of 0.1 *M* hydrochloric acid, the aqueous layers being retained; the organic phase was then washed several times with sodium sulfate solution until acid-free, and finally dried over anhydrous sodium sulfate. The absorption spectrum in the visible range was recorded for the clear organic extract thus obtained: the maximum at 380–390 nm shifts very slightly towards the u.v. and absorbance diminishes by around 10%, compared to the spectrum before acid treatment, while there is practically no absorbance at 600 nm (Fig. 4).

Qualitative tests for vanadium in the acidic aqueous layer were positive; the same tests applied to the mineralized residue of the acid-treated organic phase after evaporation, gave negative reactions. Thus the yellow product, absorbing at 380–390 nm, and formed in the solution of the synthetic ion-pair in dichloroethane, does not contain vanadium.

In order to ascertain the nature of the product(s) arising from the synthetic ion-pair in dichloroethane, the organic solution after the above-mentioned treatment and washing was evaporated to dryness at room temperature under vacuum. The i.r. spectrum (Fig. 5) shows the presence of C=O groups (1,660 cm^{-1}), typical of quinones[17,18] though the bands at 1,735 cm^{-1} and 1,590 cm^{-1} may indicate polymerization of these quinones[19].

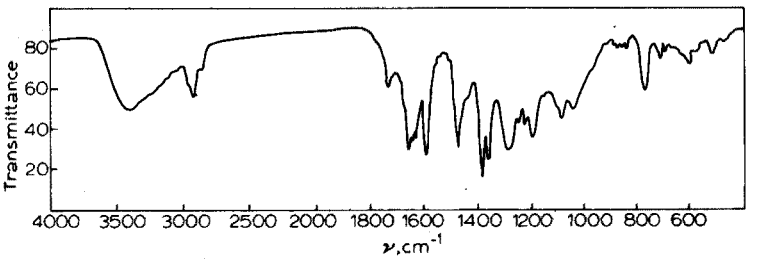

Fig. 5. I.r. spectrum of the residue from vacuum evaporation of the washed solution of synthetic ion-pair in 1,2-dichloroethane (KBr pellet).

Because the process is oxidative (see above), the synthetic ion-pair was dissolved in dichloroethane through which sulfur dioxide had been bubbled. The maximum at 600 nm then slowly diminished and finally disappeared (possibly because of a change in acidity) but no band appeared at 400 nm, which proves that sulfur dioxide efficiently inhibits oxidation of 3-methylcatechol anions.

(b) With further reagent addition. The synthetic ion-pair was dissolved in $4 \cdot 10^{-3}$–$1.2 \cdot 10^{-1}$ *M* 3-methylcatechol in dichloroethane. These conditions are approximately the same as in an actual extraction. The absorbance spectra (Fig. 6) show that the absorbance at 600 nm does not diminish as a function of time.

This eliminates discrepancy (i) but not (ii), as the absorption maximum for the decomposition product(s) shifts towards longer wavelengths (435–440 nm; Fig. 6), in contrast to the behavior of the organic phase from a liquid–liquid extraction. The higher the concentration of 3-methylcatechol, the faster is this shift. Overlapping

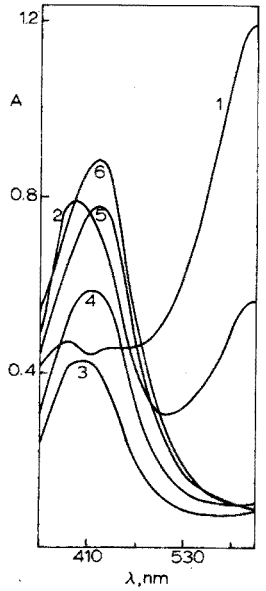

Fig. 6. Spectrophotometric behavior as a function of time of synthetic ion-pair dissolved in $4 \cdot 10^{-3}$ *M* 3-methylcatechol in 1,2-dichloroethane. Curve (time elapsed, cell path): (1) 15 min, 1 cm; (2) 5 h, 0.5 cm; (3) 24 h, 1 mm; (4) 2 days, 1 mm; (5) 7 days, 1 mm; (6) 12 days, 1 mm. (Note different path lengths).

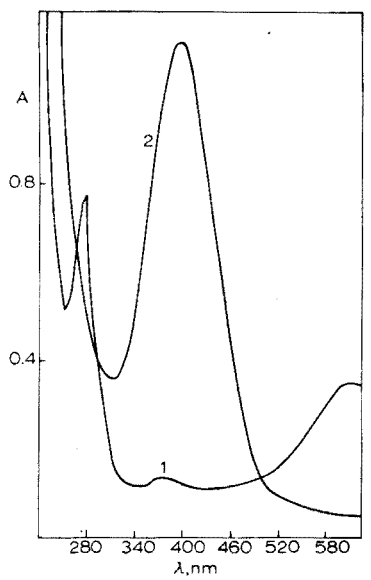

Fig. 7. Spectrophotometric behavior as a function of time of synthetic ion-pair dissolved in $4 \cdot 10^{-3}$ *M* 3-methylcatechol in 1,2-dichloroethane. Curve (1) 30 min; (2) 5 days. Path length 0.5 cm.

of the new band with time was not observed, so that the above point (iii) remains unsolved.

It should be noted that even though the absorbance around 400 nm increases more quickly after the degradation band appears, than in the case of the plain synthetic ion-pair, the rate of increase is still lower than that found in the ion-pair extracted from aqueous solution.

Finally, Fig. 6 indicates that further addition of 3-methylcatechol increases the absorbance at 600 nm compared to plain synthetic ion-pair (Fig. 3). This might be explained by progressive dissociation of the ion pair and the anion:

$$(NR_4)_3VL_3 \rightleftharpoons VL_3^{2-} + 2\,NR_4^+ ; \quad VL_3^{2-} \rightleftharpoons VL_2 + L^{2-}$$

both of which reactions would be shifted to the left by excess of ligand.

The participation of the diphenol in the phenomena studied—through autoxidation, oxidation catalysed by the vanadium complex, or chemical reaction with a supposed quinone[20]—was also verified by the decrease of absorbance in the 270–290 nm range, characteristic of the diphenol and its ions[21] (Fig. 7). This consumption of the diphenol is, of course, accompanied by an increase in the absorbance band around 400 nm (*cf.* Figs. 3 and 6).

(c) With previous equilibration of solvent. The synthetic ion-pair was dissolved in Na_2SO_4–dried 1,2-dichloroethane which had been equilibrated with $2 \cdot 10^{-1}$ *M* 3-methylcatechol and aqueous $1 \cdot 10^{-2}$ *M* TBAI solution at pH 7.0. Under these conditions, which reproduce the actual extraction conditions, the spectrophotometric behavior is very similar to that of the vanadium–3-methyl-

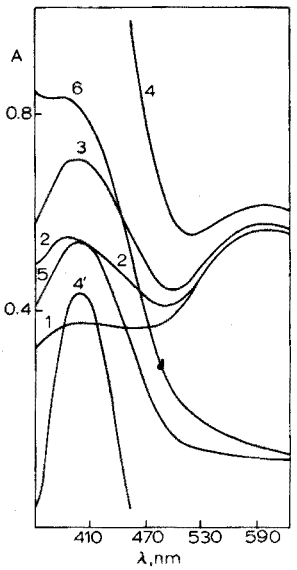

Fig. 8. Spectrophotometric behavior as a function of time of synthetic ion-pair plus $1 \cdot 10^{-2}$ *M* catecholate dissolved in 1,2-dichloroethane after equilibration with aqueous $2 \cdot 10^{-1}$ *M* 3-methylcatechol solution at pH 7.0. Curve (time elapsed, cell path): (1) 5 min, 1 cm; (2) 25 min, 1 cm; (3) 45 min, 1 cm; (4) 1 h 30 min, 0.5 cm; (4) 1 h 30 min, 0.5 cm (ordinate scale range 1.0–2.0); (5) 2 h 30, 1 mm; (6) 4 h, 1 mm.

catechol–TBA species extracted from aqueous solution at pH 7.0. The 390–400 nm band not only appears (ii) but after about 4 h is overlapped by a strong increase in the u.v. absorbance (iii). A higher concentration of quaternary ammonium salt ($5 \cdot 10^{-2}$ *M*) stabilizes the system (Table I).

(d) With addition of catecholate. In this case, the synthetic ion-pair and the catecholate (in amounts adequate to achieve 10^{-2} *M* as tetrabutylammonium 3-methylcatecholate) were dissolved in dichloroethane which had been equilibrated with $2 \cdot 10^{-1}$ *M* 3-methylcatechol solution at pH 7.0 and dried with anhydrous sodium sulfate. Again the behavior was practically the same as for the liquid–liquid extraction system (Fig. 8), as happened in experiment (c). If a lower concentration ($4 \cdot 10^{-3}$ *M*) of catecholate is used, the behavior of the extract is reproduced qualitatively but the appearance of the generated band is delayed.

Studies of analogous systems

There are obvious differences between the conclusions deduced from the above experiments and those reported in the literature[3] for analogous systems, hence some of latter tests were re-examined. Basically, aqueous $2 \cdot 10^{-3}$ *M* vanadium(IV) and $2 \cdot 10^{-2}$ *M* catechol solutions at pH 7.0 were extracted into dichloroethane; pH adjustment was done with sodium sulfite and with sodium hydrogencarbonate. When neutralization is done with sodium sulfite, the organic extract remains colorless, in contrast to the yellow color originally reported; the u.v. spectrum of the organic phase shows the presence of catechol and no vanadium appears in the aqueous phase resulting from stripping with acid. When sodium hydrogencarbonate is used to adjust pH, the organic phase is yellow, and absorption maxima are found around 275 nm (catechol) and 390 nm ("vanadium-containing yellow dimer"[2]). An aliquot of this yellow extract was discolored by contacting with aqueous sodium sulfite or hydrogensulfite solution. Vanadium could not be detected with either 3-methylcatechol or oxine, in the residue of the yellow extract after organic matter had been destroyed by nitric–sulfuric acid treatment. A second contact of fresh 1,2-dichloroethane with the first lean aqueous phase, gave a new yellow extract with same spectrophotometric behavior and absence of vanadium in the residue.

These tests confirm that the yellow compound quoted in the literature is not a vanadium-containing dimer[2] but a quinone derivative (λ_{max} 380–390 nm) identical to the one described in this paper.

According to Shnaiderman *et al.*[13], extracts into dichloroethane from solutions containing $2 \cdot 10^{-4}$ *M* vanadium(IV), $4 \cdot 10^{-2}$ *M* catechol and 0.2 *M* antipyrine at pH 3.8–4.4, show two absorption maxima; the main one at 600–610 nm, and a second at 375–400 nm. At higher pH values, both absorbances increase, but the band at 375–400 nm becomes proportionally larger. When mixtures containing $3 \cdot 10^{-4}$ *M* vanadium(IV), $2 \cdot 10^{-1}$ *M* catechol, and 0.2 *M* antipyrine at pH 3.8 were extracted, the spectrum of the extract between 350 and 625 nm was almost the same as that described by Shnaiderman *et al.*[13]. But after around 40 h, a band is generated at 380–390 nm while the absorbance at 600 nm steadily diminishes from its initial value (0.850); after 7 days, the absorbance at 390 nm reaches 4.0, whereas that at 600 nm is 0.650. After the aged extract has been stripped with dilute hydrochloric acid and washed until acid-free, the organic solvent has the same color and absorbance around 390 nm as before stripping; and vanadium is found only in the acid aqueous

phase, not in the yellow extract.

Analogous tests, starting at pH 4.5 and 6.0, lead to similar evolution, although development is faster and absorbance values at 600 nm slightly higher.

Attempts were made to reproduce most of the conditions (counter-ion, pH) used for the extraction of the vanadium(IV)–catechol complexes with $5 \cdot 10^{-3}$ *M* and $1 \cdot 10^{-2}$ *M* n-butyltriphenylphosphonium bromide[2], and to compare the results with the same concentrations of LTMAB; aqueous solutions were at pH 3.3, sodium sulfite being used instead of ammonia and formate buffer, and 1,2-dichloroethane instead of chloroform. The ion pair formed with the phosphonium cation showed larger absorbance values ($\varepsilon = (11.14 \pm 0.08) \cdot 10^3$ at 620 nm)[13] and therefore better sensitivity than that with the quaternary ammonium ion ($\varepsilon = 7.5 \cdot 10^3$) in the organic solvent.

Stability improves with increasing concentrations of the quaternary ammonium salt; the absorbance at 610 nm remains unaltered for at least 24 h; the band developed at 380–390 nm within the first 24 h when the phosphonium salt is used (the absobance is inversely proportional to the counter-ion concentration) does not affect the absorbance either at 380 nm or at 610 nm for several hours. These effects can be ascribed to the stabilizing effect of sulfur dioxide. The emulsion formed when quaternary ammonium salts are used at pH 3.3 is no deterrent, because it can readily be broken by centrifugation.

Shnaiderman *et al.*[2] claim that tungsten interferes. It was shown here that $5 \cdot 10^{-5}$ *M* vanadium(IV) can be determined by selectively extracting the ion-pair from $2 \cdot 10^{-1}$ *M* 3-methylcatechol–$1 \cdot 10^{-2}$ *M* LTMAB solution at pH 7.0 (attained with sodium sulfite) into 1,2-dichloroethane, for W(VI):V(IV) ratios up to 45:1, if the absorbance of the organic extract is measured at 610 nm. Tungsten affects stability unfavorably, but absorbances at 610 nm are stable for at least 2 h.

DISCUSSION

The qualitative behavior of blanks with different anions associated with the same quaternary ammonium cation, or with different quaternary ammonium cations in the presence or absence of iodide, proves that iodide has a catalytic effect, similar to that of the vanadium ion pair, in the evolution of the organic extracts from neutral aqueous 3-methylcatechol–quaternary ammonium solution. For the vanadium(IV)–3-methylcatechol–quaternary ammonium ion-pair extracted at pH 7.0, iodide is not a determining factor. The decomposition observed is proved to be an oxidative process, not only by the consumption of oxygen, but also by the inhibition of the degradation process in the organic solvent by sulfur dioxide.

The various tests conducted with the synthetic ion-pair show that the yellow product(s) with an absorption maximum at 380–390 nm, which is generated in the organic extracts from both vanadium(IV)–3-methylcatechol–quaternary ammonium and 3-methylcatechol quaternary ammonium systems, is a quinone (Fig. 5), which is probably polymerized, but is definitely not a vanadium-containing compound. Moreover, the concentration of catecholate determines the delay in the onset of the degradation process, and, together with the concentration of excess diphenol, the speed of that degradation. The vanadium ion pair catalyzes the process, superseding the iodide effect, which was verified for the blanks.

From the behavior of blank and ion-pair extracts, it can be concluded that a large excess of quaternary ammonium salt in the original solution (or solvent) stabilizes the extracted system.

CONCLUSIONS

Quaternary ammonium ions offer poorer sensitivity than phosphonium ions as ion-pair reagents in the extraction of vanadium(IV)–3-methylcatechol complexes. The addition of sodium sulfite to attain the required pH stabilizes both systems, especially the one in which the quaternary ammonium counter-ion intervenes; decomposition products do not affect absorbance readings for several hours in the presence of sulfur dioxide. Quaternary ammonium ions are more efficient and selective than phosphonium ion in extracting vanadium from neutral mixtures with tungsten(VI).

For the separation and determination of vanadium by extraction with a quaternary ammonium salt into 1,2-dichloroethane and spectrophotometric measurement, the following conditions are recommended. Excess of acid should be neutralized with sodium sulfite, which inhibits the oxidative process which otherwise develops in the organic extract. Iodide ion should be excluded as anion in the quaternary ammonium salt, because of its catalytic action on the oxidation of the extracted system. Quaternary ammonium salts such as LTMAB should be preferred so as to assure quantitative extraction with minimal excess, thus avoiding emulsions; the vanadium–quaternary ammonium ratio should not exceed 1:200.

As is shown in the Discussion the absorption band at 390–400 nm is not suitable for the direct determination of vanadium as it does not belong to a vanadium compound, although it might be used in an indirect method based on the catalytic activity of the vanadium ion-pair in the oxidation process.

SUMMARY

The extraction into 1,2-dichloroethane of the blue vanadium(IV)–3-methylcatechol–quaternary ammonium ion pair from aqueous solution at pH 7.0, has been studied. Solutions should be neutralized with sodium sulfite, and large excesses of ligand and quaternary ammonium ion are necessary: a convenient ratio is vanadium–3-methylcatechol–lauryltrimethylammonium (LTMA) equal to 1:4,000:200. Vanadium(IV) ($5 \cdot 10^{-5}$ *M*) can be determined in the presence of 45-fold organic extract from amounts of tungsten(VI) when LTMA is used. Yellow species which appear with time in the organic extract, are oxidation products of the diphenol, oxidation being catalysed by the vanadium-containing ion pair (or by iodide); the ligand anion acts as active intermediate. The products extracted from similar systems —vanadium–catechol and vanadium–catechol–antipyrine—which have been described as vanadium compounds, do not contain vanadium but are oxidation products (probably polymerized quinones) entirely analogous to those found in the vanadium–3-methylcatechol system.

REFERENCES

1 A. I. Busev and Z. P. Karyakina, *Russ. J. Inorg. Chem.*, 13 (1968) 839.
2 S. Ya. Shnaiderman, A. N. Demidovskaya and V. G. Zaletov, *Russ. J. Inorg. Chem.*, 17 (1972) 348.
3 S. Ya. Shnaiderman, G. N. Prokof'eva, A. N. Demidovskaya and E. P. Klimenko, *Zh. Obshch. Khim.*, 42 (1972) 24; *Chem. Abstr.*, 77 (1972) 10329t.
4 E. P. Klimenko and S. Ya. Shnaiderman, *Russ. J. Inorg. Chem.*, 17 (1972) 1274.
5 D. Braun-Steinle and S. Fallab, *Chimia*, 23 (1969) 269.
6 S. Ya. Shnaiderman and G. N. Prokof'eva, *Russ. J. Inorg. Chem.*, 17 (1972) 1643.
7 V. Patrovsky, *Collect. Czech. Chem. Commun.*, 31 (1966) 3392; *Chem. Abstr.*, 65 (1966) 14427b.
8 V. Patrovsky, *Talanta*, 16 (1969) 456.
9 S. Ya. Shnaiderman, *Russ. J. Inorg. Chem.*, 8 (1963) 239.
10 K. Lal and R. P. Agarwal, *Bull. Chem. Soc. Jap.*, 40 (1967) 1148.
11 S. Ya. Shnaiderman, E. P. Klimenko, E. N. Knyazeva and N. V. Chernaya, *Russ. J. Inorg. Chem.*, 14 (1969) 648.
12 A. M. Nardillo and J. A. Catoggio, *Anal. Chim. Acta*, to be published.
13 S. Ya Shnaiderman, E. P. Klimenko and A. N. Demidovskaya, *Rus.. J. Inorg. Chem.*, 14 (1969) 382.
14 M. Vrchlabsky and L. Sommer, *Talanta*, 15 (1968) 887.
15 J. Sunkel and H. Staude, *Ber. Bunsenges. Phys. Chem.*, 72 (1968) 567.
16 R. P. Henry, P. C. H. Mitchell and J. E. Prue, *J. Chem. Soc. A*, (1971) 3392.
17 M. L. Josien, N. Fuson, J. M. Lebas and T. M. Gregory, *J. Chem. Phys.*, 21 (1953) 331.
18 W. Otting and G. Staiger, *Chem. Ber.*, 88 (1955) 828.
19 H. J. Teuber and G. Staiger, *Chem. Ber.*, 88 (1955) 802.
20 H. Musso, *Angew. Chem.*, 75 (1963) 965.
21 J. Sunkel and H. Staude, *Ber. Bunsenges. Phys. Chem.*, 73 (1969) 203.

Analytica Chimica Acta, 74 (1975) 101–106

COMPOSITION AND STABILITY OF SOME METAL CITRATE AND DIGLYCOLATE COMPLEXES IN AQUEOUS SOLUTION

TERRENCE B. FIELD, JOHN COBURN, JANET L. McCOURT and W. A. E. McBRYDE
Department of Chemistry, University of Waterloo, Waterloo, Ontario N2L 3G1 (Canada)
(Received 3rd June 1974)

There has been some renewed interest in the metal complexes formed by citrate ion in aqueous solution, arising from the consideration of citric acid as a potential detergent builder. Diglycolic acid has also been considered for the same purpose, and corresponding data for the stability of its complexes would be useful. Of these ligands, citrate at least is known to form protonated species MHL or MH_2L where H_3L represents citric acid. When complex formation is measured by proton displacement in the manner first advocated by Bjerrum[1], interpretation of the experimental results is made more difficult when an unknown amount of the hydrogen-ion balance is incorporated in such protonated complexes.

The authors have had access to the powerful computer program SCOGS[2] which utilizes pH-titration data for systems consisting of metal, acid and ligand, and fits stability constants for proposed complex species to the data by a non-linear least-squares method. The special advantage of this computer method for the systems to be studied is that it can handle protonated or deprotonated complex species, hydrolysis products, and so forth. Accordingly suitable pH titrations of solutions containing citric or diglycolic acid have been done with and without metal present, and with an added indifferent electrolyte (KNO_3) added to try to achieve constant ionic strength. The results of these titrations were then interpreted in terms of possible complex species, those complexes and their formation constants being preferred and reported which gave minimum sum of squares of deviations between calculated and experimental titres.

EXPERIMENTAL

The pH titrations were carried out in a vessel thermostatted at 25.0°C (ref. 3) with standard alkali or acid added by a calibrated syringe with micrometer drive. The solutions of metal nitrates were prepared from analytical reagent salts and standardized by EDTA titrations[4]. Molar alkali solution for titration was prepared by dilution of ampoules of B.D.H. concentrated volumetric solution, standardized with acid phthalate, and stored under CO_2-free nitrogen. Recrystallized potassium nitrate was added to all solutions as background electrolyte at a molarity of 0.1. The citric acid (B.D.H.) and diglycolic acid (J. T. Baker) were of reagent grade, and were used without further purification when their sufficient purity had been established by titration.

The pH measurements were made either with an Orion Model 801 meter

equipped with Beckman electrodes or a Radiometer Model PHM52 meter with Radiometer electrodes. The pH scale was established for these two assemblies with N.B.S. buffer solutions, and any observed departure from the Nernst slope for readings between pairs of buffers was compensated by means of the temperature-adjustment control on each meter. All pH-meter readings were converted to hydrogen-ion concentrations by means of an empirically determined factor $\Gamma = 10^{-pH}/[H]$, measured under the same conditions and with the same electrodes as applied to particular titrations[5]. During titrations the apparatus was continuously purged with CO_2-free nitrogen.

In the absence of metal ion, the pH titrations yield acidity constants for the ligands, and when metal ions are present the titration curve is modified according to the amount of hydrogen ion set free by complex formation. In either case the observations yield stoichiometric equilibrium constants valid within the particular salt background used. It may be noted in connection with acidity constants that these are here given as protonation constants, and numbered in order of increasing numbers of protons bound. This practice places these constants in a formally analogous relationship with the numbering of complex stability constants, and aids in the writing of generalized statements in computer programming.

It may be mentioned that the titrations to determine metal complex stability constants were carried out with an excess of metal over the ligand present in order to secure a sufficient degree of conversion to complexes. In the inverse situation, the titration curve of citric acid is not sufficiently displaced by the presence of a smaller amount of metal to give a precise indication of the extent of complex formation. It follows that under the experimental conditions used in this study, no evidence of complexes with higher than 1:1 stoichiometry was detected.

RESULTS AND DISCUSSION

The results obtained from this study are summarized in Tables I–III. They are reported as averages from the data of several titrations in each case, together with a standard deviation on each reported constant. In the various titrations from which results are combined the concentrations of metal (if present) and

TABLE I

ACIDITY CONSTANTS FOR CITRIC AND DIGLYCOLIC ACIDS

(Concentration quotients, 25°C, 0.1 *M* KNO_3 background)

	$\log \beta_1^0$	$\log \beta_2^0$	$\log \beta_3^0$
Citric acid	5.70±0.02	10.06±0.02	12.87±0.08
Diglycolic acid	3.95±0.01	6.73±0.01	

ligand were systematically varied, and there was no evidence that any of the β values derived from the experimental results showed any dependence on the overall concentration of the reagents. Typically, the levels of metal or ligand concentration were in the range $1\text{–}6 \cdot 10^{-3}$ *M*.

TABLE II

STABILITY CONSTANTS FOR METAL CITRATES

(Concentration quotients, 25°C, 0.1 *M* KNO_3 background)

	MHL $log\ \beta_{111}$	*ML* $log\ \beta_{101}$
Calcium	8.02±0.15	3.50±0.06
Magnesium	7.66±0.19	3.38±0.07
Zinc	8.98±0.07	5.10±0.05
Nickel	9.04±0.07	5.40+0.04

TABLE III

STABILITY CONSTANTS FOR METAL DIGLYCOLATES

(Concentration quotients, 25°C, 0.1 *M* KNO_3 background)

	MHL $log\ \beta_{111}$	*ML* $log\ \beta_{101}$
Calcium	6.56±0.04	3.54±0.02
Magnesium	5.88±0.02	2.15±0.01
Zinc	6.03±0.05	3.59±0.01

The values of the equilibrium constants are those which give the minimum standard deviation in titre (s.d.t.) for the titrations from which they are derived. They also refer to the choice of species, from various possibilities tried out, which give the lowest s.d.t. Thus, for instance, in the case of diglycolic acid the complexes ML and MHL taken together gave in every titration or combination of titrations a lower s.d.t. than that calculated when ML was the only species assumed to be present. This is the evidence on which our assumption of the formation of protonated diglycolate species is based.

The acidity constants listed in Table I are concentration quotients applicable only in solutions of comparable ionic strength. Owing to the multiple charge borne by some of the ions generated by these acids, and the effect of this on activity coefficients, the stoichiometric ionization constants, particularly of citric acid, show a marked dependence on the ionic strength (*cf.* thermodynamic values[6]). The values reported here appear to be in satisfactory accord with those reported under nearly comparable conditions by Campi *et al.*[7] and by Li *et al.*[8]. A recent summary of the literature on citrate equilibria by Pearce[9] including his own measurements lists five sets of stoichiometric acidity constants for ionic strength 0.1 and at specified temperatures ranging from 20 to 30°C. The present results for pK_1 are slightly lower, but the others are in excellent agreement with this summary. Pearce has applied a correction to the values of pK_3 for complexation of citrate ion by potassium or sodium ion; this refinement has not been introduced in the present work.

With respect to the citrate complexes, it is clear that protonated species do occur, certainly MHL and possibly MH_2L. The titration data failed to produce

evidence to support the existence of the latter, but Campi *et al.*[7] and Pearce[9] have reported stability constants for this with certain metals. The pH-titration method for studying metal complex formation is much less capable of defining the state of equilibrium when protonated species occur. This can be seen from the relationship

$$C_H - [H] + [OH] = \Sigma q\beta_{pqr}[M]^p[H]^q[L]^r + \Sigma j\beta_j^0[H]^j[L]$$

in which C_H is the total net concentration of ionizable hydrogen at any point. If $q=0$ throughout, [L] is explicitly known, given the β_j^0 values. If $q \neq 0$, the above relationship does not define [L], and one must resort to best-fit solutions of several mass-balance equations to define [M] and [L]. Experience has shown that in such cases various sets of p, q, and r can be found which satisfy the data roughly as well, so that a clear choice of constituent species cannot be made.

It is a further limitation on any method of determining equilibrium constants that there be a sufficient and thus precisely defined concentration of each species involved. In the case of the species MH_2L, if it exists, the pK for its dissociation to MHL may be so small that to obtain a reasonably amount of this complex would require working at a pH so low as to preclude much formation of any metal complex. With the aid of Pearce's formation constants and the computer program SPECON[10], the concentration of each species formed between pH 2 and pH 6 was calculated for a number of selected values of C_M and C_L. For the case where $C_L = 1.0 \cdot 10^{-3}$ and $C_M = 5.0 \cdot 10^{-3}$ (corresponding to one of our titrations), the maximum value of $[MH_2L]$ was $3.8 \cdot 10^{-5}$ M (at pH 3.5). This is not enough conversion of either ligand or metal to yield a precise definition of β_{121}. Even when C_H was raised to $1.0 \cdot 10^{-2}$, only 7% of the ligand was converted to $[MH_2L]$ at its maximum concentration.

The values of log β_{101} for calcium and magnesium complexes are in good agreement with those of Campi *et al.*[7] and Pearce[9], though slightly higher than those of Li *et al.*[8]. The corresponding values for nickel and zinc accord with those reported by Campi and coworkers. The present values for log β_{111} for these complexes tend throughout to be slightly higher than Campi's, and rather closer to Pearce's for the first two metals. The discrepancy may be linked to the inability to characterize MH_2L as a discrete species; if some of this was formed in the present expériments, the effect on the data would be to augment the estimate of [MHL] and hence of β_{111}.

Values of stability constants of the diglycolate complexes may be compared with those previously published by Tichane and Bennett[11] and by Yasuda *et al.*[12]. Apart from the indication of protonated species at low pH and the proposed stability constants for these, the results appear to be in general agreement with earlier work. It is not clear why the value of β_{101} for magnesium diglycolate is so much lower than that for the calcium complex; a similar relationship is not apparent from a comparison of the citrate complexes, nor, for that matter, other complexes of carboxylic acids, α-hydroxy- or α-aminocarboxylic acids (*e.g.* iminodiacetic acid).

The efficacy of citric acid, diglycolic acid, and NTA as chelating agents to be added to detergents to sequester metal ions may be compared by calculating the concentration of free metal for a selected set of values of total metal and ligand concentrations and of pH. An illustrative example is given in Table IV based, unless

TABLE IV

PERCENTAGE OF METAL UNCOMPLEXED AT pH 6

($C_M = C_L = 0.001$ *M*)

M/L	*Citric acid*	*Diglycolic acid*	*Nitrilotriacetic acid*
Calcium	50.7	41.4	77.3
Magnesium	55.4	89.0	96.5
Zinc	10.8	40.3	1.20
Nickel	7.78	76.8[a]	0.45
Copper(II)	0.69[b]		0.065[c]
Iron(II)	14.9[b]		9.52[d]
Iron(III)	0.00023[b]		0.0019[e]

[a] Value calculated by constants other than those in Tables I–III; see ref. 12.
[b] Values calculated by constants other than those in Tables I–III; see ref. 13.
[c] Value calculated by constants other than those in Tables I–III; see ref. 14.
[d] Value calculated by constants other than those in Tables I–III; see ref. 15.
[e] Value calculated by constants other than those in Tables I–III; see ref. 16.

noted otherwise, on the constants of Tables I–III. The results show that while citrate cannot match the performance of NTA for sequestering transition metal ions, it may be superior to the latter for the ions of the Group IIA metals. As an agent for the reduction of free metal ion concentration, a mixture of citrate and NTA might prove more efficaceous than either substance alone.

SUMMARY

Metal complexes formed in solution by citric acid or diglycolic acid with calcium, magnesium, zinc or nickel ions have been studied by pH titrations. Normal and protonated complexes of 1:1 stoichiometry are formed, the compositions and stability constants of which are reported which are in best agreement with the experimental data. The effectiveness of these ligands for the sequestration of metal ions is compared with that of NTA.

REFERENCES

1 J. Bjerrum, *Metal Ammine Formation in Aqueous Solution*, P. Haase and Son, Copenhagen, 1941.
2 I. G. Sayce, *Talanta*, 15 (1968) 1397.
3 D. D. Perrin and I. G. Sayce, *Chem. Ind. (London)*, (1966) 661.
4 G. Schwarzenbach and H. Flaschka, *Complexometric Titrations*, Methuen, London, 5th German edn. translated by H. M. Irving, 1969.
5 W. A. E. McBryde, *Analyst (London)*, 94 (1969) 337; 96 (1971) 739.
6 R. G. Bates and G. D. Pinching, *J. Amer. Chem. Soc.*, 71 (1949) 1274.
7 E. Campi, G. Ostacoli, M. Meirone and G. Saini, *J. Inorg. Nucl. Chem.*, 26 (1964) 553.
8 N. C. Li, A. Lindenbaum and J. M. White, *J. Inorg. Nucl. Chem.*, 12 (1959) 122.
9 K. N. Pearce, Ph.D. Thesis, Massey University, New Zealand, 1972.
10 D. D. Perrin, *Suom. Kemistilehti A*, 42 (1969) 205.
11 R. M. Tichane and W. E. Bennett, *J. Amer. Chem. Soc.*, 79 (1957) 1293.
12 M. Yasuda, K. Yamasaki and H. Ohtaki, *Bull. Chem. Soc. Jap.*, 33 (1960) 1067.

13 T. B. Field, J. L. McCourt and W. A. E. McBryde, *Can. J. Chem.*, 52 (1974) 3119.
14 W. A. E. McBryde, J. L. McCourt and V. Cheam, *J. Inorg. Nucl. Chem.*, 35 (1973) 4193.
15 G. Schwarzenbach, G. Anderegg, W. Schneider and H. Senn, *Helv. Chim. Acta*, 38 (1955) 1147.
16 E. Bottari and G. Anderegg, *Helv. Chim. Acta*, 50 (1967) 2349.

Analytica Chimica Acta, 74 (1975) 107–117

THE RAPID SUB-PICOGRAM DETERMINATION OF VOLATILE ORGANO-MERCURY COMPOUNDS BY GAS CHROMATOGRAPHY WITH A MICROWAVE EMISSION SPECTROMETRIC DETECTOR SYSTEM

YAIR TALMI

Analytical Chemistry Division, Oak Ridge National Laboratory, Tennessee 37830 (U.S.A.)

(Received 3rd June 1974)

There is a great demand for rapid analytical methods that provide the sensitivity and selectivity required for the determination of CH_3HgX in environmental samples. The most widely accepted methods are based on the Westöö procedure[1], which involves formation of a water-soluble adduct of methylmercury and cysteine, its extraction into water, acidification, and finally reaction of the liberated CH_3HgX with an aromatic solvent. The CH_3HgX (where X designates Cl, Br, or I) is then determined by a gas chromatograph equipped with an electron capture detector (g.c.–e.c.). This technique exhibits the following disadvantages. (1) The poor selectivity of the detector to CH_3HgX requires relatively time-consuming and elaborate clean-up procedures. (2) Large volumes of high-purity

TABLE I

THE APPLICABILITY OF E.C. AND M.E.S. DETECTORS TO THE DETERMINATION OF VOLATILE ORGANO-MERCURY COMPOUNDS

	E.c.	*M.e.s.*
Selectivity	Poor. Restricted to RHgX compounds	Highly selective to all Hg compounds
Sensitivity	Sub-nanogram for CH_3HgX; poor for $(CH_3)_2Hg$	Picogram level for all Hg compounds regardless of chemical form
Solvent	Highly polar solvents are generally avoided	Any solvent can be used
Stability	Detectors are readily fouled by contaminants from bleeding columns; frequent cleaning of detector is required	Stable over long periods of time. Detector is relatively unaffected by column bleeding; cleaning procedures are seldom required
Service and repairs	Usually by the manufacturer only	Very simple; usually by the user (except for the microwave generator)
Sample preparation	CH_3HgX: digestion; extraction into benzene; partitioning to aqueous thiosulfate solution; reextraction into benzene	CH_3HgX: digestion; extraction into benzene
Rate of sample injection	Usually 2–5/h, due to interferences from eluted substances	Up to 40/h

solvents are required. (3) The choice of solvent is limited by the detection characteristics of the electron-capture detector, and the detectors are easily fouled by many eluents. (4) Sample injection rate is slow because all interferences must emerge from the column before a subsequent injection can be made.

An alternative procedure in which the electron-capture detector is replaced by a microwave emission spectrometer (m.e.s.)[2] was described by Bache and Lisk[3]. A modified version of this system has been constructed and optimized in this Laboratory[4]. By taking advantage of the detector selectivity, the analytical procedure was substantially simplified and the sensitivity enhanced. Typical analysis time for a biological sample, excluding homogenization, was about 15 min. Benzene extracts of CH_3HgCl in biological samples did not require any clean-up and could be analyzed at a rate of up to 30 per h. The absolute sensitivity of the system for many volatile organo-mercury compounds, including $(CH_3)_2Hg$, ranged from 0.5 to 10 pg. The following discussion describes the applicability of the g.c.–m.e.s. system to the determination of trace quantities of volatile organo-mercury compounds, in particular CH_3HgX, and compares it with that of the widely accepted g.c.–e.c. system. Table I summarizes some of the basic features of each system.

EXPERIMENTAL

Apparatus

The g.c.–m.e.s. system is basically similar to that described by McCormack *et al.*[2], although various instrumental modifications have been incorporated. The gas chromatograph used in this study is a modified Tracor MT-220. A Pyrex capillary

TABLE II

G.C.–M.E.S. OPERATING CONDITIONS

Parameter[a]	*Determination of CH_3HgX in benzene and air*	*Determination of CH_3HgX in water and air*	*Determination of $(CH_3)_2Hg$ in wate and air*
Column packing	4% FFAP on 80–100 mesh Gas-Chrom Q	1% FFAP on 80–100 mesh carbon beads	Chromosorb 101
Column length (ft)[b]	3	3	2
Quartz capillary, i.d., o.d. (mm)	0.5, 6.5	0.5, 6.5	2, 8
Carrier gas	Argon	Argon	Helium
Carrier gas flow Rate (ml min^{-1})	90	95	80
Pressure at the outlet of capillary (torr)	750	750	1–10[c]
Column temp. (°C)	150	135	115
Injector temp. (°C)	200	200	135

[a] Common parameters for all experiments: microwave generator output, 30 W; monochromator slit wi 35 μm; slit height, 12 mm. Analytical spectral line, 253.7 nm. Lens focal length, 4 in.; diameter, 2 Photomultiplier (1-P28) voltage, 650 V.

[b] Pyrex column dimensions: i.d. 3 mm, o.d. 6.5 mm.

[c] The capillary was continuously pumped by means of a rotary pump in order to sustain the helium plas

splitter directs the g.c. effluent to a flame ionization detector that serves as a comparative, nonselective detector, and also to the m.e.s. detector. The m.e.s. detector is a highly transparent quartz capillary (Thermal American Fuzed Quartz Co.) that conducts the effluent gas from the g.c. oven to the center of a tapered microwave cavity (7097-1001 G1 7097-5002 G1, Raytheon Corp.). The upstream end of the quartz capillary is held in close contact with the outlet of the Pyrex g.c. column by a 1/4-in. nut (Swagelok) with a Teflon front ferrule. Thus, the possibility of contact of the separated components with metallic surfaces is eliminated. An argon or helium plasma discharge is formed by a 100-W microwave generator (Scintillionics Model HV 15A) which is confined within the quartz capillary. The eluted organo-mercury compounds are determined by detection of their characteristic atomic emission intensities at the mercury 253.7-nm line with a 0.5-m Jarrel-Ash monochromator, model 82000. The grating (1180 grooves/mm) is blazed at 190 nm. The operating conditions for CH_3HgCl and $(CH_3)_2Hg$ are summarized in Table II. For the measurement of trace quantities of CH_3HgX in aqueous solutions, a special g.c. column was developed. (Here X designates Cl, Br, I, or OH because these species are eluted simultaneously.) Graphitized carbon beads (80–100 mesh), used as the solid support were coated with 1% FFAP.

Reagents

Commercially available reagents were used without further purification. The organo-mercury compounds were obtained from Alfa Inorganics; the carbon beads were provided by the Metals and Ceramics Division of Oak Ridge National Laboratory.

Procedures

Aqueous samples (indirect). Transfer 10–75 ml of the sample to a 125-ml separatory funnel and add 1 ml of 0.1 *M* sodium iodide solution. Extract the CH_3HgI formed into 2 ml of benzene by shaking the solution for 2 min. Dry the separated benzene layer over anhydrous sodium sulfate. Inject 1–10-μl aliquots of the benzene layer into the g.c., and record the emission intensity at 253.7 nm. Peak heights of unknown samples are compared with those from pure CH_3HgCl benzene standard solutions.

Aqueous samples (direct). Water samples can be injected directly into the graphitized carbon bead-packed g.c. column. The water is completely eluted from the column within 10–15 s, and sharp quantitative peaks are obtained for the CH_3HgX eluted thereafter.

Biological samples. Accurately weigh 0.5–2.0 g of tissue and transfer to a tissue homogenizer (Waring blender with 20-ml micro-container, No. 22-1630 ACE Scientific or equivalent) with sufficient water to cover the sample. After grinding for 3–12 min, transfer the sample to a prebaked 40-ml bottle with a polyethylene-lined cap. Rinse the blender several times to ensure quantitative transfer of the sample into the bottle. Accurately weigh the final homogenate in order to determine the weight per cent of the tissue.

Transfer 1.0–2.0-g aliquots of the homogenate sample to 25-ml bottles, capped with disposable Teflon-coated rubber septums by means of Pasteur pipets. Then accurately weigh these samples. Add 2 ml of water and 1 ml of concentrated

hydrochloric acid to each duplicate, and shake for 3 min. Add 2 ml of benzene to each sample, and shake for 3 min. Centrifuge the samples in the bottles for about 5 min.

Remove 1–10-μl benzene aliquots directly from the benzene layer, through the septum, and analyze. Alternatively, separate the benzene layer and transfer to a 4-ml bottle containing anhydrous Na_2SO_4 and capped with a Teflon-coated rubber septum. These samples are stable for at least two weeks, so that an immediate determination is not required.

Hard tissues. The determination of CH_3HgX at the 0.01–0.03 p.p.m. level in small samples of insects (50–200 mg) required a very thorough homogenization procedure. Unfortunately, minigrinders proved to be inadequate for this task, and because a freezer-mill was not available, the samples were homogenized in the following manner. Weigh the sample in a 25-ml prebaked bottle, and set it in the center of a 100-ml polyethylene beaker. Add enough liquid nitrogen to both the bottle and the beaker to maintain a level of about 15–20 mm. Then crush the frozen sample with a Pyrex rod until a fine powder is obtained. After the sample thaws, add 2–5 ml of water and 1 ml of concentrated hydrochloric acid to the bottle and shake for 3 min. Then complete the procedure described above for biological tissues.

RESULTS AND DISCUSSION

Liberation and extraction of CH_3HgX

The excellent selectivity provided by the m.e.s. detector permits the elimination of the clean-up procedure so essential in the Westöö procedure. Nevertheless, the elimination of the thiosulfate partitioning step results in smaller (solvent/aqueous sample) volume ratios and thus ensures better control over the extraction procedure.

TABLE III

EXTRACTION OF VARIOUS METHYLMERCURY(II) SALTS BY BENZENE

Volume ratio (H_2O/benzene)	*Concentration of added CH_3HgCl $M \cdot 10^{-9}$ (p.p.m.)*[3]	*Concentration of added NaX (M)*	*Extracted species*	*Recovery (first extn.) (%)*	*Recovery (second extn.) (%)*
10	4(0.001)			86	12
20	2(0.0005)	0.005 NaI	CH_3HgI	85	12
40	1(0.00025)			87	13
10	4(0.001)			82	15
20	2(0.0005)	0.005 NaBr	CH_3HgBr	83	15
40	1(0.00025)			81	16
10	4(0.001)			63	27
20	2(0.0005)	0.005 NaI	CH_3HgCl	62	24
40	1(0.00025)			64	25
10	4(0.001)			54	25
20	2(0.0005)	None	CH_3HgOH	52	26
40	1(0.00025)			53	24

Both hydrobromic and hydroiodic acids have been suggested as alternatives to hydrochloric acid for the liberation of CH_3HgX from the protein substrate, because bromide and iodide are stronger nucleophiles and thus can participate more effectively in the cleavage reaction. Furthermore, the subsequent conversion of CH_3HgCl into its bromide or iodide homolog results in a more favorable distribution coefficient between the aqueous and aromatic phases[5,6]. Consequently, the procedure for CH_3HgX in water samples at the pH range 5–9 significantly benefited from the addition of bromide or iodide, as shown in Table III. However, the substitution of HBr or HI for HCl can lead to a severe deterioration of accuracy. Both acids are partially oxidized to form free bromine and iodine. Although chromatographic interferences from these species are insignificant, owing to the high selectivity of the detector, these free halogens will rapidly decompose CH_3HgX according to the following photochemically induced reaction:

$$CH_3HgCl(aq)+X_2 \rightleftarrows CH_3X+\tfrac{1}{2}HgX_2(s)+\tfrac{1}{2}HgCl_2$$

where X designates Br or I.

Sensitivity

The g.c.–e.c. detection limits reported for CH_3HgX range from 0.001 ng[7]

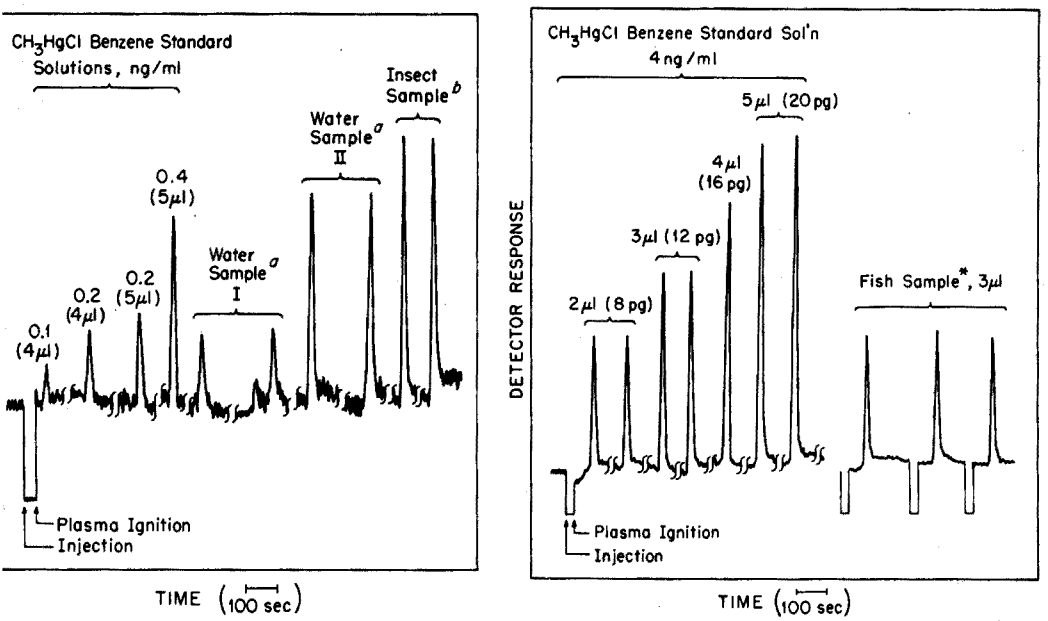

Fig. 1. Detection of CH_3HgCl at the detection limit level.
[a] Water samples, 50 ml, were extracted with 2 ml benzene following the addition of NaI.
[b] 0.2 gm of the ground insect were treated as described above and extracted into 2 ml benzene. Benzene aliquots, 5 μl, were injected.

Fig. 2. Detection of CH_3HgCl at the p.p.b. level.
Three, 0.5 gm, samples of fish homogenate were treated with HCl and extracted into 2 ml benzene. Benzene aliquots, 2 μl, were injected.

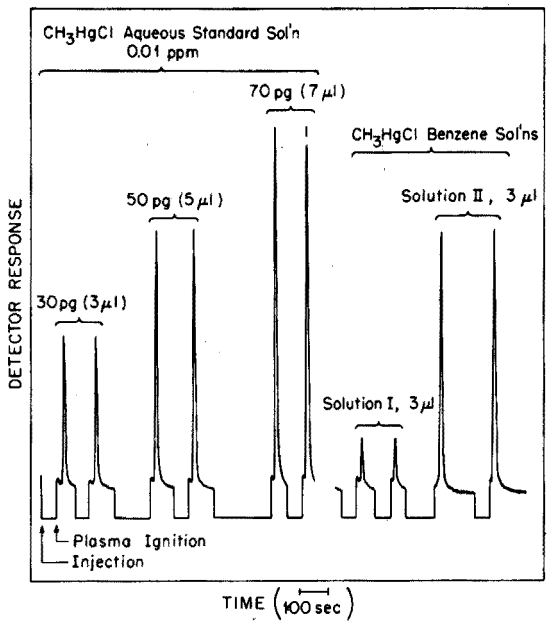

Fig. 3. Comparison between the CH_3HgCl chromatograms obtained from aqueous and benzene solutions. Solution I: 1 ml of the air phase in equilibrium with a 1000 ppm CH_3HgCl water solution were dissolved in 10 ml benzene. Solution II: 1 ml of the air phase in equilibrium with CH_3HgCl salt crystals were dissolved in 10 ml benzene.

to 0.4 ng[8]. Relative sensitivities range from 0.02 p.p.m. for a 0.2-g sample[9] to 0.02 p.p.m. for a 10-g sample[8] depending on the analytical procedure, the nature of the sample analyzed, and the operating conditions selected. The g.c.–m.e.s. detection limits for CH_3HgX and $(CH_3)_2Hg$ are 0.0005 and 0.002 ng, respectively, where detection limit is defined as the amount of analyte which produces a signal with amplitude four times that of the background standard deviation. These values refer to untreated benzene extracts of biological tissues and thus should be considered as the practical usable detection limits. Relative sensitivity for 50-ml water samples is 1 ng l^{-1}, while the value for biological samples should be better than 0.001 p.p.m. Both values are based on use of the direct hydrochloric acid–benzene procedure discussed above, which does not involve preconcentration steps. When the Westöö procedure is used, large samples (10 g) can be analyzed, and the relative sensitivity should be better than 0.0001 p.p.m. Unfortunately, because fish samples with CH_3HgX concentration below 0.006 p.p.m. were unavailable, confirmation of these values was not possible. Figures 1 and 2 demonstrate the practical applicability of the g.c.–m.e.s. system to the determination of CH_3HgCl at low concentration levels. Figure 3 shows the performance at a high concentration level.

Selectivity

Because of the rather poor e.c. detector selectivity for organo-mercury compounds, many substances give false methylmercury peaks that consequently

reduce the sensitivity of the technique. Failure to eliminate these interferences also lengthens the time intervals required between sample injections; but to reduce the degree of these interferences, time-consuming and elaborate clean-up procedures are necessary. The m.e.s. detector provides much better selectivity. At the 253.7-nm atomic emission line, the selectivity for mercury when comparing either CH_3HgX or $(CH_3)_2Hg$ with chloroform or hexadecane was well above 10,000:1, in agreement with Bache and Lisk. Thus, more than 30 samples per hour can be injected without previous clean-up procedures; the baseline remains unchanged over long working periods and seldom requires any resetting. Because the detector is mercury-dependent, the sensitivity for all volatile organo-mercury compounds was within a factor of 5 regardless of the chemical form.

Accuracy and precision

Both accuracy and precision of the g.c.–m.e.s. technique are affected by factors such as the efficiency of sample homogenization, CH_3HgX liberation and extraction, and by the performance of the separation and measurement systems. In the absence of certified biological standards for CH_3HgX, accuracy was determined from the recovery measurements described in Tables III–V. Percentage recovery of CH_3HgX by a single extraction ranged from 70 to 81%, with an average of 76% depending on the nature of the sample analyzed and on the concentration of CH_3HgX. The adequate reproducibility of CH_3HgX recovery permits use of the simplified single extraction method where results are corrected by a proper recovery factor[1]. Accuracy was also estimated through a comparison of CH_3HgX concentrations determined in fish samples by the g.c.–m.e.s. system with those obtained by other techniques (Table VI). The m.e.s. detector responds linearly in the range 0.005–100 ng of injected CH_3HgCl samples. Although the detector response did not fluctuate by more than $\pm 10\%$ during 8-h working periods, a standard solution should be injected after every 3–4 sample injections to maximize accuracy.

'ABLE IV

'HE EFFECT OF DIGESTION AGENT COMPOSITION ON THE RECOVERY OF CH_3HgX FROM 'ISH

let weight[a] *g)*	*Volume of H_2O added (ml)*	*Digestion agent (ml)*	*Volume of benzene (extractant) (ml)*	*% Recovery 1st extn.*[c]
.17	1	HCl, 2	3	68
.16	1	HCl, 2	3	66
.13	2	HCl, 1	3	74
.15	2	HCl, 1	3	75
.15	2	HCl, 1	3	75
.16	2	HCl, 1	4	76
.16	0	($CuSO_4$, 1, NaBr, 2)[b]	3	84
.14	0	($CuSO_4$, 1, NaBr, 2)	4	84

All samples were aliquots of the same homogenate. The homogenate contained 12.5% trout-muscle tissue. $CuSO_4$ designates aqueous 0.1 *M* $CuSO_4 \cdot 5H_2O$ solution. NaBr designates aqueous 1 *M* H_2SO_4–3 *M* NaBr olution.

Two homogenate aliquots were extracted four times with 3-ml portions of benzene. The CH_3HgCl recovery a the combined extracts was considered complete and served as the basis for the above recovery calculations.

TABLE V

RECOVERY OF CH_3HgCl SPIKED INTO VARIOUS BIOLOGICAL SAMPLES

Sample[a] (g)	*CH_3HgCl added (ng)*	*Number of samples (same homogenate)*	*Recovery first extn. (%)*
0.5, Freeze-dried tuna	200	3	98±3.5
0.3,[b]	10	2	80±4.5
Muscle	5	3	81±5.3
0.1,[b]	4	2	79±3.1
Liver			
0.1,[b]	3	3	78±5.8
Brain			
0.1,[b]	2	2	77±6.0
Gonad			
0.2, Insect (whole)	3	3	77±4.5

[a] 1 ml of concentrated HCl and 2 ml of water were added to each sample.
[b] From a rainbow trout from the Great Smoky Mountains National Park.

TABLE VI

CONCENTRATION OF CH_3HgX IN E.P.A. ROUND-ROBIN FREEZE-DRIED FISH SAMPLES

Sample no.	*Mean*	*Minimum*	*Maximum*	*S*	*G.c.–m.e.s.[a] (mean)*	*G.c.–m.e.s.[b] (mean)*
72C-1222	1.75	0.22	2.24	0.57	1.85	2.15–2.18
72C-1223	5.06	0.60	6.67	1.70	5.80	5.75–5.78
72C-1224	6.07	0.70	8.00	1.85	6.90	6.74–7.06

[a] Only 0.1 g was available for each sample.
[b] These results were reported by M. E. Vett and S. A. Newton, Lawrence Berkeley Laboratory, who used the following analytical procedure: double extraction of the ground tissue with acetone to remove water and lipids followed by acidification with HCl and extraction of the CH_3HgCl with benzene.

The relative standard deviation for the determination of CH_3HgX in biological samples ranged from 2 to 20%, depending mainly on the nature of the matrix. Analysis of variance was performed to evaluate the respective random error contributions from the sampling procedure (*i.e.*, homogenization, CH_3HgX liberation and extraction, and sample heterogeneity) and from the measurement procedure (*i.e.*, syringe reading error, column interferences, and detector errors). Fish muscle (18 g), freeze-dried tuna (6 g) and CH_3HgCl-spiked spring water (3 l) were chosen for this analysis. The solid samples were each divided into six portions of approximately equal weight. Each portion was homogenized with 10 ml of water, and four 2-g aliquots were then taken for CH_3HgCl determination. Similarly, the water sample was divided into six 500-ml portions, and four 50-ml aliquots from each portion were analyzed for their CH_3HgCl content. Altogether, 24 aliquots were randomly analyzed for each sample. The sampling variance and the measurement variance were calculated for each sample[10–13]. Application of the F test, at 95% confidence level, to each sample (Table VII) led to the following conclusions.

BLE VII

ALYSIS OF VARIANCE

mple	Source of error	Degrees of freedom	Variance S^2	Variance ratio F (S^2 sampling/S^2 measurement)	$_{0.975}F$
h muscle	Sampling	5	16.3	$F_1 = \frac{16.3}{3.2} = 5.1$	
	Measurement	18	3.2	$F_1 > {}_{0.975}F(5,18)$	
eze-dried tuna	Sampling	5	8.2	$F_2 = \frac{8.2}{3.0} = 2.7$	$_{0.975}F(5,18) = 3.38$
	Measurement	18	3.0	$F_2 < {}_{0.975}F(5,18)$	
I_3HgCl-spiked	Sampling	5	3.4	$F_3 = \frac{3.4}{2.9} = 1.2$	
ing water	Measurement	18	2.9	$F_3 < {}_{0.975}F(5,18)$	

With the muscle sample, the sampling error was significantly greater than the measurement error because of the difficulty in homogenizing the sample. There is no reason to believe that the sampling error was greater than the measurement error with either the water or the tuna samples. This was also observed with a well-homogenized fish liver sample. Thus, the main contribution to the sampling

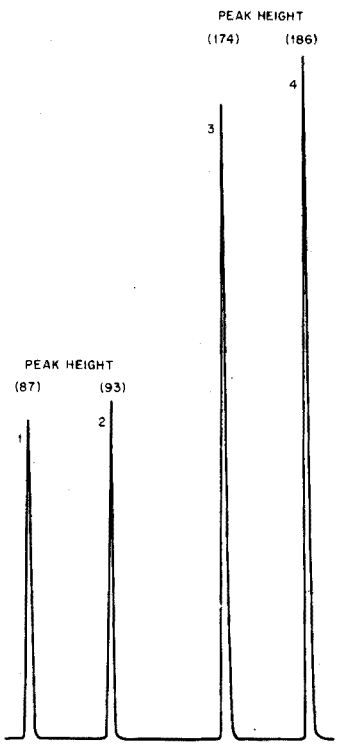

Fig. 4. Comparison between the $(CH_3)_2Hg$ chromatograms obtained from air and aqueous phases in equilibrium. Aqueous 100 p.p.b. $(CH_3)_2Hg$ solutions. (1) and (3): 3 and 6-μl aliquots (aqueous phase); (2) and (4): 10 and 20-μl aliquots (air phase).

error seems to originate from the incomplete homogenization of the tissue, although contribution from sample heterogeneity should not be altogether ruled out. Sampling errors became more severe with skin, whole fish, and whole insect samples, which suggests that development of more efficient homogenization procedures is highly desirable.

Direct determination of CH_3HgX and $(CH_3)_2Hg$ in aqueous solution

Various studies of the physico-chemical properties of CH_3HgX and $(CH_3)_2Hg$ require the direct measurement of these species in water samples[14]. The 1% FFAP-coated, graphitized, carbon-bead g.c. column was developed for CH_3HgX measurements. Air, benzene, or water are instantly eluted from the column without any noticeable tailing effect. The retention time values, response and shape of the CH_3HgCl chromatographic peaks, and the chromatographic resolution are practically the same for all three matrices. Figure 3 compares the chromatographic peaks obtained for benzene and aqueous solutions of CH_3HgCl. The benzene samples shown were part of a detailed study[14] to determine the vapor pressure of CH_3HgCl. Samples of air phases in equilibrium with either solid CH_3HgCl or its aqueous 1000-p.p.m. solution were collected and transferred to known volumes of benzene. The CH_3HgCl concentrations of these benzene samples were then determined. Further information on the properties and preparation of the graphitized solid support will be given in a future publication.

TABLE VIII DETERMINATION OF LOW-LEVEL CH_3HgX IN BIOLOGICAL SAMPLES[a]

Sample	*Concentration (fresh weight) as mercury (p.p.m.)*[b]			
	Net weight of tissue in homogenate (g)	*Total mercury*	*Methyl mercury, direct analysis*[e]	*Methyl mercury, Westöö method*
Brook trout[c]				
Brain	0.05	0.052	0.038	
Gills	0.30	0.012	0.011	
Intestines	0.35	0.015	0.012	
Liver	0.45	0.046	0.042	0.045
Muscle	0.34	0.027	0.023	0.020
Skin	0.36	0.014	0.009	0.011
Insect[d] *combined sample*				
1	0.052	0.024	0.026	
2	0.069	0.029	0.034	
3	0.045	0.110	0.108	
Insects, individual whole insect				
4	0.095	0.021	0.021	
5	0.075	0.029	0.034	
6	0.154	0.019	0.040	

[a] Samples obtained from J. W. Huckabec (Environmental Sciences Division, ORNL).
[b] All results were calculated on the assumption that % recovery in the first extraction is 75%, and thus a correction factor of 1.33 was applied.
[c] From the Piogah, North Carolina, Fish Hatchery.
[d] Each homogenate sample combines a few different insects collected at the same area.
[e] As described in the *Procedures* section.

Similarly, the Chromosorb-101 column was found useful for the determination of $(CH_3)_2Hg$ in both water and air samples. Figure 4 shows the chromatographic peaks obtained for samples taken from a 100-p.p.b. $(CH_3)_2Hg$ water solution and air phase in equilibrium with it. The measurements were made to determine the distribution coefficient of $(CH_3)_2Hg$ between air and water phases.

Analysis of biological samples

Table VIII summarizes some of the analytical results obtained for the determination of CH_3HgX in fish and insect samples. A comparison is given between the concentrations of total mercury and CH_3HgX in various fish tissues as well as in individual and combined insect samples. The reasonable agreement between total and methylmercury concentration levels in the insect samples is exceptionally satisfactory considering the complex nature of the matrix, the small sample size, and the difficulties involved in the liquid nitrogen homogenization procedure. For comparison, three samples were also analyzed by the Westöö procedure.

This research was supported by the National Science Foundation–RANN (Environmental Aspects of Trace Contaminants) Program under NSF interagency agreement No. 389 with the U.S. Atomic Energy Commission.

SUMMARY

The applicability of a gas chromatograph with a microwave emission spectrometric detector (g.c.–m.e.s.) to the determination of trace amounts of volatile organo-mercury compounds in environmental samples is described. The high selectivity of the detector to mercury compounds allows the procedures to be drastically simplified. Thus, the total analysis time for methylmercury in fish is less than 15 min and more than 30 samples of CH_3HgCl (benzene extracts) can be analyzed per hour. The detection limit is 0.5 pg for CH_3HgCl (or C_2H_5HgCl) and 2 pg for $(CH_3)_2Hg$. The relative sensitivity for CH_3HgCl in water samples is 1 ng l^{-1} and for fish samples is 1 ng g^{-1}. Direct determinations of CH_3HgCl and $(CH_3)_2Hg$ in aqueous solutions are also discussed.

REFERENCES

1 G. Westöö, *Acta Chem. Scand.*, 20 (1966) 2131.
2 A. J. McCormack, S. C. Tong and W. D. Cooke, *Anal. Chem.*, 37 (1965) 1470.
3 C. A. Bache and D. J. Lisk, *Anal. Chem.*, 43 (1971) 950.
4 Y. Talmi and R. Crosmun, *Ecology and Analysis of Toxic Contaminants*, ORNL-NSF-EATC-1, March 1973.
5 R. B. Simpson, *J. Amer. Chem. Soc.*, 83 (1961) 4711.
6 J. A. Ealy, M. S. Dissertation, University of Tennessee, Knoxville, 1971.
7 K. Sumino, *Kobe J. Med. Sci.*, 14 (1968) 115.
8 L. B. Kamps and B. McMahon, *J. Ass. Offic. Anal. Chem.*, 55 (1972) 590.
9 P. A. Krenkel, *Critical Review in Environmental Control*, Vol. 3, Issue 3, CRC, 1973, pp. 303–373.
10 H. A. Laitinen, *Chemical Analysis*, McGraw-Hill, New York, 1960.
11 A. B. Calder, *Anal. Chem.*, 36 (1964) 25A.
12 W. J. Youdon, *Statistical Methods for Chemists*, Wiley, New York, 1951.
13 R. K. Skogerboe, *Flame Emission and Atomic Absorption Spectrometry*, Marcel Dekker, New York, 1969.
14 Y. Talmi and R. E. Mesmer, *Water Res.*, submitted for publication.

Analytica Chimica Acta, 74 (1975) 119–124

PYROLYSIS–GAS CHROMATOGRAPHY OF VINYL CHLORIDE–METHYL METHACRYLATE AND VINYL CHLORIDE–ACRYLONITRILE COPOLYMERS

M. TANAKA, F. NISHIMURA and T. SHONO

Department of Applied Chemistry, Faculty of Engineering, Osaka University, Yamadakami, Suita, Osaka 565 (Japan)

(Received 11th June 1974)

Progress in polymerization techniques has gradually made it possible to control the sequential structures of polymers. A typical example is the complexed copolymerization[1] of vinyl compounds with alkylaluminum halides or related metal halides. This complexed copolymerization gives equimolar copolymers with an alternating sequential structure. Some of these alternating copolymers have excellent properties[2,3], because of the regularity in their structural units. In the future, the sequential structure of polymers may be more easily controlled, and it must become increasingly important to analyze the microstructure. Pyrolysis–gas chromatography is one of the most powerful methods for the analysis of the microstructure of polymers.

The pyrolysis–gas chromatographic behaviours of *cis*-1,4-, *trans*-1,4- and 1,2-polybutadienes[4] and of random and alternating copolymers of acrylonitrile and butadiene have already been reported[5]. In this paper, the relationships between pyrolytic products and microstructures have been investigated by means of pyrolysis–gas chromatography for copolymers of vinyl chloride with methyl methacrylate or acrylonitrile.

EXPERIMENTAL

Materials

Random copolymers of vinyl chloride (VC)–methyl methacrylate (MMA) and of VC–acrylonitrile (AN) were synthesized by bulk polymerization with azo-bis(isobutyronitrile) as initiator. Alternating VC–MMA copolymer[6] was prepared in the presence of ethylaluminum dichloride–vanadium oxytrichloride, and alternating VC–AN copolymer[7] in the presence of ethylaluminum dichloride by established methods.

Table I shows the copolymer compositions calculated from the elemental analyses.

Apparatus and technique

A curie-point pyrolyzer (Nippon Bunseki Kogyo JHP-2) was used to decompose the polymers. This gives reproducible pyrograms because the fast temperature rise (curie-point of the ferromagnetic wire) results in more specific products

TABLE I

ANALYTICAL DATA FOR VC–MMA AND VC–AN COPOLYMERS

Sample[a]	*C (%)*		*H (%)*		*N (%)*		*VC (mole-%)*
	Found	*Calcd.*	*Found*	*Calcd.*	*Found*	*Calcd.*	
VC–AN Copolymer							
R_1	60.9	61.0	5.5	5.5	20.2	20.2	20.8
R_2	55.7	55.7	5.3	5.3	15.5	15.5	37.5
R_3	51.7	52.0	5.2	5.2	12.1	12.1	50.7
R_4	49.1	49.0	5.1	5.2	9.4	9.5	60.3
R_5	42.1	42.1	5.0	5.0	3.3	3.3	85.6
A	52.0	52.0	5.1	5.2	12.3	12.2	49.9
VC–MMA Copolymer							
R_1	56.4	56.7	7.8	7.6			22.5
R_2	52.4	52.6	7.1	7.0			45.7
R_3	50.6	50.7	6.7	6.7			55.0
R_4	48.1	48.3	6.5	6.3			65.6
A	51.9	51.8	6.8	6.9			49.4

[a] R = Random copolymer, A = alternating copolymer.

and any contamination from previous samples can be avoided by using a new wire each time. The pyrolyzer was coupled to a gas chromatograph (Shimazu GC-4BM) equipped with a dual flame-ionization detector. The samples were 10–20 μg in size.

The separation column was stainless steel tubing (75 cm × 3 mm i.d.), packed with Porapak N (100–120 mesh). A column (5 cm × 3 mm i.d.) packed with a mixture of K_2CO_3 and Diasolid H (60–80 mesh) in a 1:2 weight ratio was placed between the pyrolyzer and the separation column to precut acidic products on pyrolysis. The separation column was operated at 170°C and the detector block was maintained at 220°C. The flow rate of carrier gas (nitrogen) was 30 ml min^{-1}, and the hydrogen and air pressures were 0.5 kg cm^{-2} and 1.0 kg cm^{-2}, respectively. The peak areas were measured by a digital integrator (Shimazu ITG-4A).

Identification of the peaks was carried out by comparison with the retention data of known substances and/or by direct combination of the pyrolysis–gas chromatograph with a mass spectrometer (Nippon Bunko–Finnigan GC-9500-3100 D).

RESULTS AND DISCUSSION

VC–MMA copolymer

Zutty and Welch[8] reported that when VC–MMA copolymers are heated at 150–200°C, an intramolecular lactonization from adjacent co-monomers occurs, forming γ-butyrolactone groups in the polymer backbone concomitant with the quantitative elimination of methyl chloride (eqn. 1).

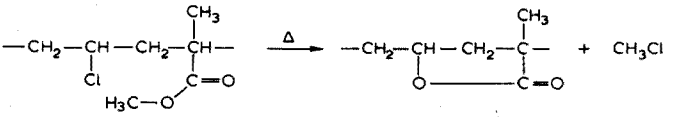

(1)

The extent of this cyclization depends on the arrangement of the monomer units in the copolymers. The copolymers listed in Table I were heated under vacuum at 200°C until lactonization was complete, and no further weight loss was observed. From this weight loss, the fraction of the methyl methacrylate units cyclized, f_c(MMA), was calculated. These experimental f_c(MMA) values were in good agreement with the theoretical ones given from a statistical treatment[9,10] based on the expected number of adjacent MMA and VC residues, as shown in Table II.

Figure 1 shows typical pyrograms of random (R_2) and alternating VC–MMA copolymers (pyrolysis at 541°C). The yields of MMA monomer, methyl chloride

TABLE II

LACTONIZATION OF VC–MMA COPOLYMERS

Sample	*Composition MMA (mole-%)*	*f_c(MMA)*[a]	
		Experimental	*Theoretical*[b]
R_1	77.51	0.235	0.276
R_2	54.34	0.567	0.629
R_3	45.03	0.731	0.757
R_4	34.44	0.873	0.870
A	50.60	0.860	0.865

[a] f_c(MMA) represents the fraction of the methyl methacrylate units cyclized.
[b] See Refs. 9 and 10 for details.

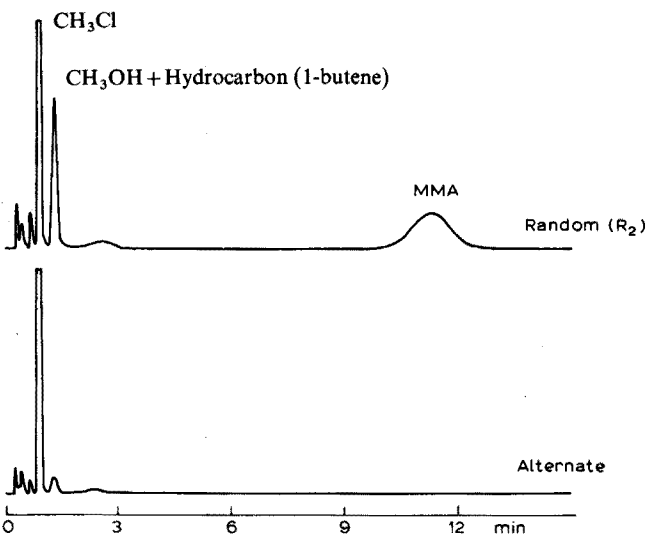

Fig. 1. Pyrograms of VC–MMA copolymer at 541°C.

TABLE III

PYROLYSIS PRODUCTS OF VC–MMA COPOLYMERS AT 541°C

Sample	*Yield of pyrolysis products (mole-%)*[a]		
	MMA	CH_3Cl	CH_3OH[b]
R_1	26.1	24.7	9.2
R_2	7.5	66.9	14.0
R_3	3.9	72.1	11.1
R_4	0.5	60.5	3.9
A	0.6	71.5	0.5

[a] Mole-% to MMA in copolymer.
[b] Obtained indirectly from the decrease in peak area after methanol had been removed with an absorber (15 cm × 3 mm i.d.) packed with 25% PEG-20M on Celite 545 (60–80 mesh) containing 3 wt.% boric acid, placed before the separation column.

and methanol on the pyrogram are summarized in Table III, and expressed in terms of mole percentage to MMA in the copolymer. In the case of the random copolymers, it is reasonable that the MMA yield decreases with the decrease of MMA content in the sample. The yields of methyl chloride and methanol reach maxima near 50 mole-% of MMA content. But the alternating copolymer gives only negligible amounts of MMA and methanol, though it yields methyl chloride in amounts between those of R_2 and R_3.

These results may be interpreted as follows. The alternating copolymer contains only a VC–MMA unit in its chain, and has a larger f_c(MMA) value than the random copolymers with compositions close to the alternating one, as shown in Table II. It is therefore assumed that the production of MMA monomer from the alternating copolymer is reduced because of both the absence of the unzipping reaction from the successive MMA unit and the lesser extent of the uncyclized MMA units. There is no difference in the methyl chloride yields of the random and alternating copolymers, hence methyl chloride must be produced by other mechanisms predominantly occurring in the random copolymer in addition to the lactonization reaction. Reactions (2) and (3) were proposed by McNeil and Neil[11] from the results of the pyrolysis for PVC–PMMA blends, but they could not confirm the production of methanol. In the present tests of pyrolysis at 541°C, the 1:1 PVC–PMMA blend gave methyl chloride, methanol and MMA in molar ratios of 0.393, 0.166 and 1.000, respectively; but methyl chloride and methanol were obtained from neither PVC nor PMMA. As shown in eqns. (3), methanol is given by the attack of hydrogen chloride from dehydrochlorination of VC units on the MMA–MMA unit together with equal amounts of methyl chloride. If the methanol yield (Table III) is considered, the contribution of eqn. (3) to the formation of methyl chloride cannot be neglected in the case of the random copolymers. It was found, as mentioned above, that the microstructural differences are reflected on the pyrograms.

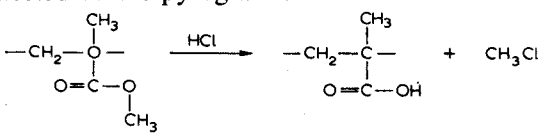

(2)

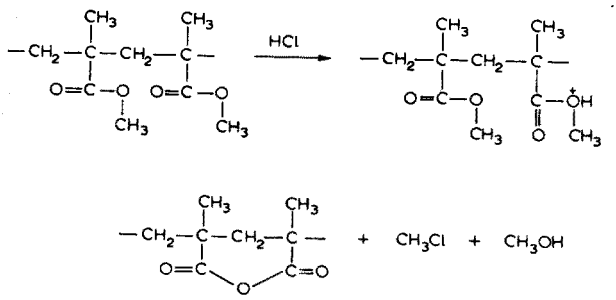

(3)

VC–AN copolymer

The thermal degradation of polyacrylonitrile and acrylonitrile containing copolymers has been studied extensively[12–14], and many kinds of degradation products including dimers have been found. In the present work, the random and alternating VC–AN copolymers listed in Table I were pyrolyzed at 536°C, but did not give dimers as degradation products (Fig. 2). The main products of the random copolymers are AN monomer and acetonitrile. Figure 3 shows the relationship between the molar ratio of acetonitrile to AN monomer on the pyrogram and the VC content of the copolymer. This ratio increases suddenly as the VC content exceeds 50 mole-%. It is suggested that AN monomer is produced from AN–AN units at least. In fact, the alternating copolymer having only a VC–AN unit gives no peak of AN monomer on the pyrogram, but only acetonitrile.

It is interesting to note that methyl chloride is obtained from the alternating samples as a main product but hardly at all from the random samples. The alternating copolymer gives a resinous solid on heating at 320°C for 3 min under

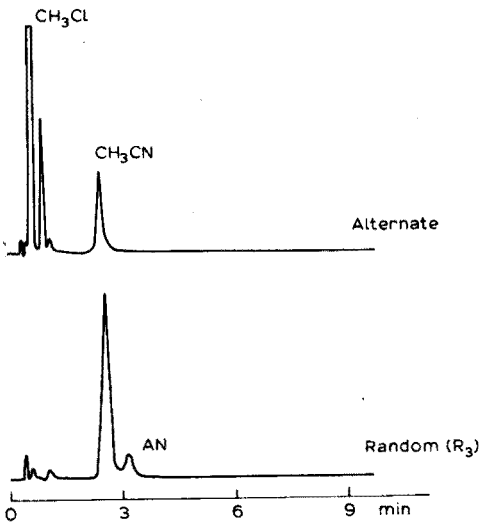

Fig. 2. Pyrograms of VC–AN copolymer at 536°C.

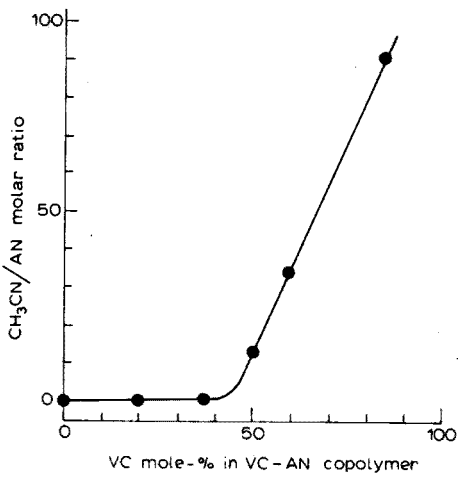

Fig. 3. CH_3CN/AN molar ratio of VC–AN copolymers (random) on pyrograms at 536°C.

a nitrogen atmosphere. When this resinous solid is pyrolyzed at 536°C, the main product is acetonitrile and only a little methyl chloride is formed. It is assumed from this result that methyl chloride is eliminated first, and that the residual substance has a structure from which acetonitrile is produced easily on pyrolysis.

Further work is being done to elucidate the specific degradation mechanism of the alternating VC–AN copolymer.

SUMMARY

Pyrolysis–gas chromatographic investigations have been carried out on VC–MMA and VC–AN copolymers with a curie-point pyrolyzer. The pyrograms distinctly show the difference in sequential structures of these copolymers. MMA monomer and methanol are scarcely formed from the alternating VC–MMA copolymer; the alternating VC–AN polymer yields mainly methyl chloride, which is not obtained from the random samples. The microstructure of copolymers in relation to their degradation products is discussed.

REFERENCES

1 M. Hirooka, H. Yabuuchi, S. Kawasumi and K. Nakaguchi, *J. Polym. Sci., Polym. Chem. Ed.*, 11 (1973) 1281.
2 M. Hirooka, *23rd IUPAC Congress*, M-5, 1971.
3 M. Hirooka, K. Mashita, S. Imai and T. Kato, *103rd Meeting of Rubber Division, ACS*, May 1973.
4 T. Shono and K. Shinra, *Anal. Chim. Acta*, 56 (1971) 303.
5 T. Shono, M. Tanaka, K. Terashita and K. Shinra, *Jap. Anal.*, 21 (1972) 326.
6 F. Shepherd and H. J. Harwood, *Polym. Lett.*, 9 (1971) 419.
7 J. Furukawa, E. Kobayashi and J. Yamauchi, *Polym. J.*, 2 (1971) 407.
8 N. L. Zutty and F. J. Welch, *J. Polym. Sci., Part A*, 1 (1963) 2289.
9 P. J. Flory, *J. Amer. Chem. Soc.*, 61 (1939) 1518.
10 T. Alfrey, Jr., C. Lewis and B. Magel, *J. Amer. Chem. Soc.*, 71 (1949) 3793.
11 I. C. McNeil and D. Neil, *Europ. Polym. J.*, 6 (1970) 569.
12 A. R. Monahan, *J. Polym. Sci., Part A-1*, 4 (1966) 2391.
13 S. Tsuge, T. Okumoto and T. Takeuchi, *J. Chem. Soc. Jap., Ind. Chem. Sect.*, 71 (1968) 1634.
14 Y. Yamamoto, S. Tsuge and T. Takeuchi, *Kobunshi Kagaku*, 29 (1972) 407.

Analytica Chimica Acta, 74 (1975) 125–132

THE EXTRACTION OF CHROMIUM(VI) FROM SULPHURIC ACID SOLUTIONS BY 4-(5-NONYL)PYRIDINE AND ITS SEPARATION FROM FISSION PRODUCTS

M. IQBAL and M. EJAZ

Pakistan Institute of Nuclear Science & Technology, P.O. Nilore, Rawalpindi (Pakistan)

(Received 20th April 1974)

Pyridine[1–4] and its methyl-substituted derivatives[5,6] have long been used for the extraction and separation of oxyanions of manganese, rhenium and technetium from alkaline solutions. The extraction of other metals that form oxyanions in their highest oxidation state, *i.e.* Cr, Mo and W, is very poor when these reagents are used. Moreover, the reagents are not applicable for extractions in acidic media, because their solubility in acidic solutions is so high that no phase separation occurs. In the present study, the extraction of chromium(VI) was investigated with a new liquid anion exchanger, a high-molecular-weight heterocyclic pyridine amine—4-(5-nonyl)pyridine (NPy). It is liquid at ordinary temperature and is relatively insoluble in water but easily soluble in a large number of organic solvents, such as benzene, carbon tetrachloride, etc. This solubility is shared by the metal ion-association complexes.

EXPERIMENTAL

Reagents

4-(5-Nonyl)pyridine(K&K Labs Inc., Plainview, N.Y.) was purified by vacuum distillation before use. 4-(5-Nonyl)pyridine is a pale yellow oily liquid (b.p. 94°C at 0.8 mm Hg; refractive index n_D^{20} 1.485; d^{20} 0.9208 g cm^{-3}. Its solubility in water was found to be 1.2 g l^{-1}. The purity of the reagent was checked with a Varian Aerograph Chromatography unit, on a 10% carbowax 20M column at 220°C; a single peak was found. The detector employed was an alkali flame-ionization type.

Nitric, hydrochloric and sulphuric acid solutions were generally prepared from BDH volumetric solution ampoules and all other chemicals used in this work were of AnalaR grade.

^{51}Cr tracer as dichromate was obtained from the Radiochemical Centre, Amersham. Sodium chromate was used in the experiments where the total concentration of chromium(VI) was raised to $5 \cdot 10^{-2}$ *M*. The uranium, thorium and fission product tracers used were ^{233}U, ^{234}Th, ^{99m}Tc, ^{99}Mo, ^{95}Nb, ^{95}Zr, ^{106}Ru, ^{144}Ce, ^{137}Cs, and ^{90}Sr.

Radiochemical analysis and instrumentation

The equipment used for general α-ray measurement included an argon

gas-flow proportional counter (Harwell type 3-7/11558) in conjugation with an Ekco fast scaler (type N 530 F; high voltage was taken from the scaler) and a Nuclear Chicago Corporation scintillation counter (Model DS-S Serial 1709).

Solid β-emitting samples were measured with the aid of an end-window Geiger Assembly equipped with a G.E.C. tube type EHM 2/S.

Count rates for γ-rays were determined with a Nuclear Chicago single-channel analyser, model 872 coupled with 3 × 3-in. thallium-doped sodium iodide well-type scintillation counter. γ-Spectra were taken with a Nuclear Data ND-4410 computer system 512/1024 multichannel analyser model 2560. The detector used with this analyser was a 4 × 3-in. NaI(Tl) crystal.

Measurement of distribution coefficients

The distribution coefficient of chromium(VI) between equal volumes of aqueous and organic phases (equilibrated previously with aqueous solution of the same composition as the solution from which chromium was extracted) was found by shaking the phases for 5 min. This was sufficient time for equilibration. To avoid errors from loss of radioactive material, the material balance was checked, with those points having a balance of less than 90% being repeated.

RESULTS AND DISCUSSION

The dependence of D values of trace and macroamounts of chromium(VI) on sulphuric acid concentrations is shown in Fig. 1 for 0.10 M 4-(5-nonyl)-pyridine in benzene. Simple equilibrium in the aqueous phase could be expected for initial trace concentrations of chromium(VI), but a third phase was formed above 0.2 M sulphuric acid. It is interesting that the third phase disappeared

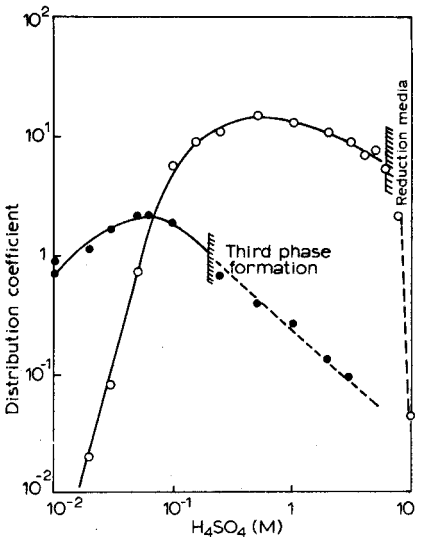

Fig. 1. Variation of the partition coefficient of chromium(VI) with sulphuric acid concentration in the equilibrium aqueous phase. (●) Trace Cr(VI), (○) 0.05 M Cr(VI).

for initial aqueous chromium(VI) concentrations greater than 0.02 *M* and the log D_{Cr} *vs.* log $(H_2SO_4)_w$ curve shifted markedly towards higher distribution ratios above 0.1 *M* sulphuric acid.

Since for trace concentrations of chromium(VI) the concentration of $HCr_2O_7^-$ and $Cr_2O_7^{2-}$ is negligibly small[7,8], it is probable that in low sulphuric acid concentration, species of the type ($2\ BH^+$, CrO_4^{2-}) and (BH^+, $HCrO_4^-$) are extracted in the organic phase. The formation of a third phase above 0.2 *M* sulphuric acid may be at least partially due to the lower solubility of $(NPyH)^+$-HSO_4^- in benzene, as the amine hydrogen sulphates are generally less soluble than the corresponding sulphates[9], probably because the former are more aggregated. Since the third phase was found to contain chromium(VI), it may be suggested that two types of chromium complexes are formed with the reagent; possibly these are not mutually miscible so that a third phase is formed. It is also possible that the formation of mixed quadrupoles between the free amine hydrogensulphate and amine perchromate ion pairs, of the type $[NPy \cdot H^+ \cdot HSO_4^- \cdot NPy \cdot H^+ \cdot HCrO_4^-]$, may contribute to the third phase formation. The disappearance of the third phase and the increase of *D* values at comparatively high chromium(VI) concentrations (0.05 *M*) may be due to the decrease in the concentration of free amine hydrogen sulphate and the reduction in the concentration of chromate ions, which have been reported[10] to be extracted less than $HCrO_4^-$, with subsequent reduction in the concentration of mixed quadrupoles.

The dependence of the distribution ratio of chromium(VI) on the 4-(5-nonyl)pyridine concentration is shown in Fig. 2 for two concentrations of the aqueous sulphuric acid.

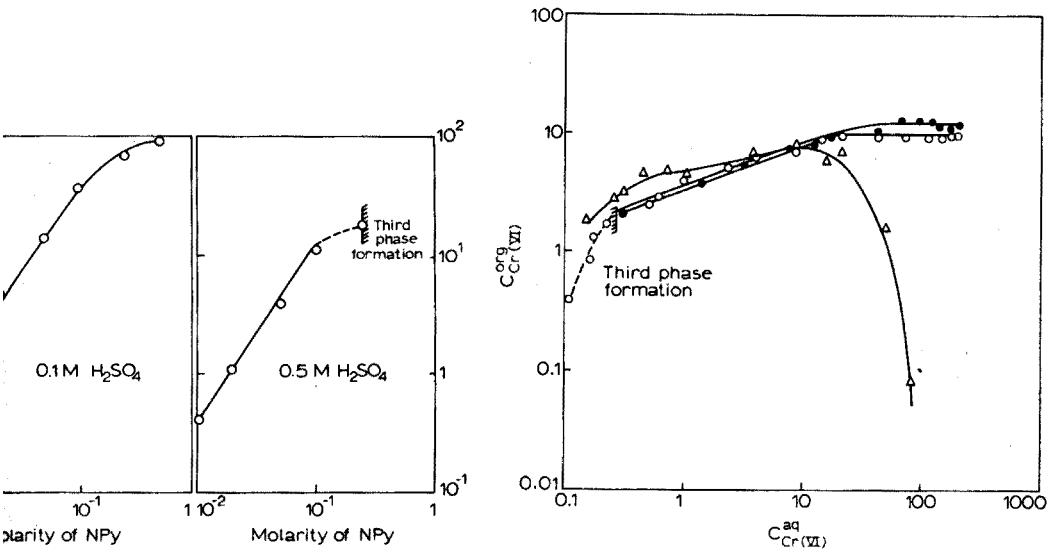

Fig. 2. Variation of the partition coefficient of chromium(VI) with concentration of 4-(5-nonyl)-pyridine in the organic solvent (benzene).

Fig. 3. Extraction of chromium(VI) by 0.1 *M* 4-(5-nonyl)pyridine in benzene as a function of metal concentration from 0.5 *M* (△), 3 *M* (○) and 5 *M* (●) H_2SO_4.

The slope of the linear parts of the plots of log $D_{Cr(VI)}$ against log [NPy]obtained at 0.1 *M* and 0.5 *M* sulphuric acid for trace amounts of chromium(VI) is *ca.* 1.5, which indicates the extraction of a mixture of compounds which contain one or two molecules of the extractant.

Saturation experiments were undertaken to find the maximal extraction capacity of the 0.1 *M* amine in benzene for chromium(VI) from different concentrations of sulphuric acid. The results are shown in Fig. 3. From 0.5 *M* sulphuric acid, a limiting loading by chromium(VI) corresponded to 7.5 g, when the initial aqueous concentration was in the range of 15–25 Cr l^{-1}. The loading decreased sharply at higher concentrations of chromium(VI). Possibly, the large amounts of chromium(VI) in the aqueous phase lead to polymeric species[11] ($2\ HCrO_4^- \rightleftharpoons Cr_2O_7^{2-} + H_2O$) with a subsequent decrease in the H^+ ion concentration such that the stability of the amine salt of the type $(NPyH)^+$ is considerably decreased. This explanation appears plausible because loading experiments performed from more dilute acid (0.1 *M*) decreased the extraction drastically at initial aqueous chromium(VI) concentration greater than 5 g l^{-1}. From 3 *M* sulphuric acid the limiting loading of 0.1 *M* 4-(5-nonyl)pyridine corresponded to 10 g l^{-1}, suggesting extraction of $HCr_2O_7^-$, while from 5 *M* sulphuric acid the chromium(VI) uptake increased above the Cr/NPy ratio of 2 and corresponded to 13.5 g l^{-1}.

The effect of addition of neutral sulphate ions to constant aqueous phase sulphuric acid concentrations of 0.5 *M*, 3 *M* and 5 *M* is shown in Fig. 4. From 0.5 *M* sulphuric acid, the *D* values have a decreasing trend, while from 3 *M* sulphuric acid, the distribution coefficient remains more or less the same. It is

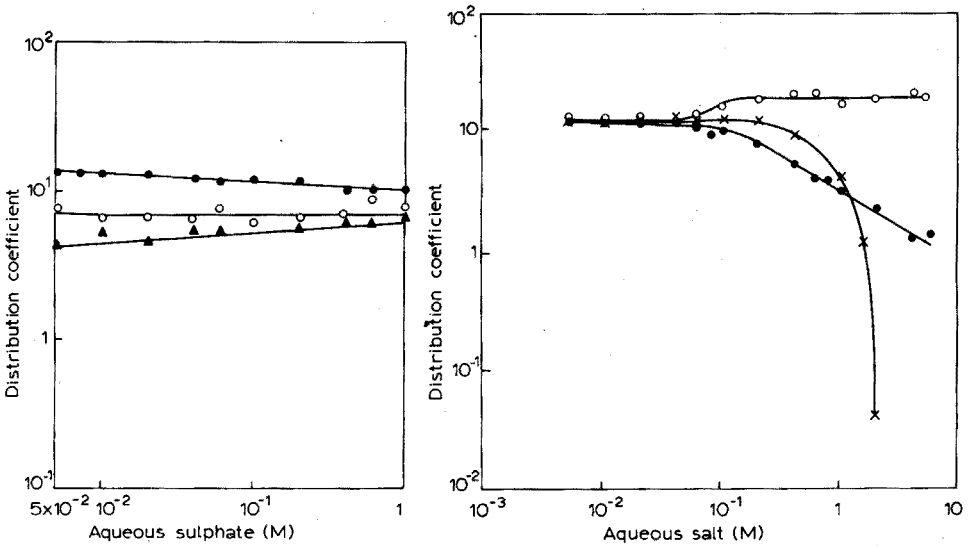

Fig. 4. Dependence of the partition coefficient of chromium(VI) on sodium sulphate concentration in the equilibrium aqueous phase at different sulphuric acid concentrations. (●) 0.5 *M* H_2SO_4, (○) 3 *M* H_2SO_4, (▲) 5 *M* H_2SO_4.

Fig. 5. Extraction of chromium(VI) by 0.1 *M* 4-(5-nonyl)pyridine in benzene as a function of the initial concentration of fluoride (×), chloride (○) and nitrate (●) ions from 0.5 *M* sulphuric acid.

interesting to note that the extraction increases with increasing concentration of sodium sulphate in the aqueous phase when the acid concentration is 5 *M*. Possibly the stability of the amine cation $(NPyH)^+$ and the formation of some anionic sulphate complexes of chromium(VI) under these conditions and their subsequent extraction by ion-association have an effect.

Figure 5 shows the effect of sodium nitrate, fluoride and chloride on the extraction of 0.05 *M* chromium(VI) with 0.1 *M* 4-(5-nonyl)pyridine in benzene from 0.5 *M* sulphuric acid. Nitrate and fluoride ions decrease the extraction coefficient above 10^{-1} *M*, probably owing to their competition for the amine cation, whereas excess of chloride ions increases the distribution coefficient; the latter may be due to a simple salting-out action or to the formation and extraction of some anionic chlorocomplexes of the type $CrO_2Cl_n^{-(n+2)}$ where $n=3,4$, like those of molybdenum and tungsten. However, chromium(VI) has been reported[12] not to form chlorocomplexes in aqueous solutions and even if these are formed, their extraction appears doubtful since extraction studies of uranium[13] have shown that unlike the anionic nitrate complexes, the anionic chlorocomplexes of uranium are not extractable.

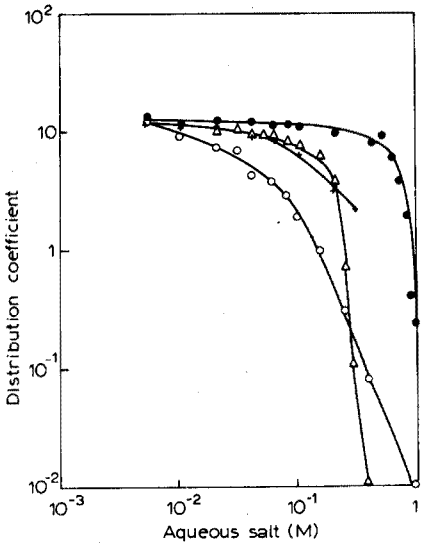

Fig. 6. Extraction of chromium(VI) from 0.5 *M* H_2SO_4 by 0.1 *M* 4-(5-nonyl)pyridine in benzene as a function of the concentration of oxalate (○), citrate (△), tartrate (+) and acetate (●) ions.

Figure 6 shows the isotherms of chromium(VI) distribution as a function of potassium oxalate, ammonium acetate, sodium citrate or potassium tartrate concentration in the aqueous phase containing 0.5 *M* sulphuric acid.

The decrease in extraction follows the sequence: oxalate > tartrate > citrate > acetate. In the case of oxalate, the colour of the aqueous phase turns violet above 0.01 *M*. At 1 *M* concentrations the violet colour becomes dark brown. This indicates that some unextractable complexes of chromium(VI) are formed in oxalate solutions.

The effects of EDTA and potassium thiocyanate on the distribution of chromium(VI) from 0.5 *M* sulphuric acid are shown in Fig. 7. In the case of EDTA the colour of the aqueous phase becomes violet in the range 0.01–0.2 *M* and above 0.6 *M* a precipitate forms in the aqueous phase. In the case of

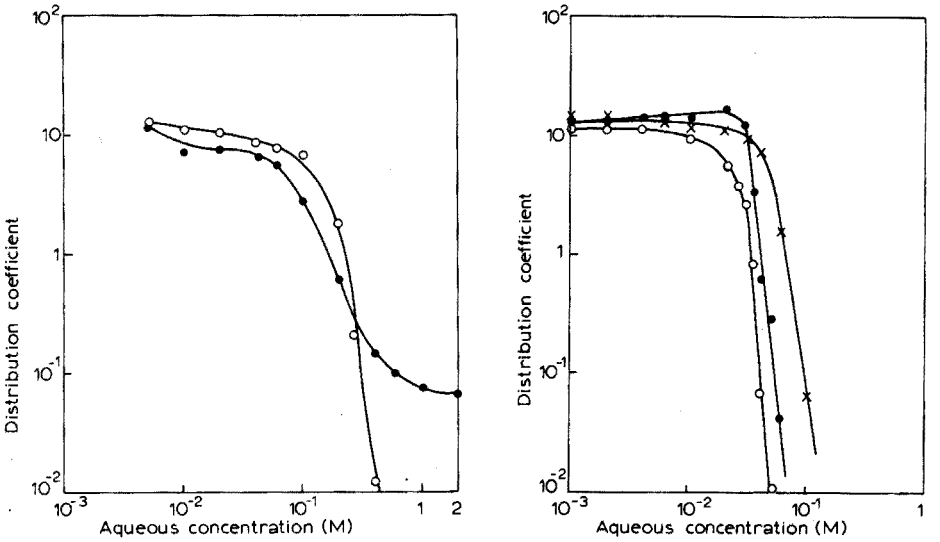

Fig. 7. Effect of EDTA (○) and potassium thiocyanate (●) on the distribution of chromium(VI) from 0.5 *M* sulphuric acid by 0.1 *M* 4-(5-nonyl)pyridine in benzene.

Fig. 8. Variation of the distribution coefficient of chromium(VI) with concentration of reducing agents from 0.5 *M* sulphuric acid for extraction by 0.1 *M* 4-(5-nonyl)pyridine in benzene. (●) Hydrazine hydrochloride, (×) thiosulphate, (○) ascorbic acid.

TABLE I

DISTRIBUTION COEFFICIENT OF VARIOUS METAL IONS BETWEEN 0.1 *M* 4-(5-NONYL)-PYRIDINE IN BENZENE AND 3 *M* SULPHURIC ACID

Metal ion	*Amount present in the initial aqueous phase (mole l^{-1})*	*D values*
^{99m}Tc(VII)	C.F.	~0.03
^{99}Mo(VI)	10^{-5}	~0.01
^{233}U(VI)	10^{-3}	$<10^{-2}$
^{95}Nb(V)	C.F.	$<10^{-2}$
^{234}Th(IV)	C.F.	$<10^{-3}$
^{95}Zr(IV)	10^{-9}	$<10^{-2}$
^{106}Ru	10^{-5}	~0.02
^{144}Ce(III)	10^{-9}	$<10^{-3}$
^{90}Y(III)	C.F.	$<10^{-3}$
^{51}Cr(III)	$2\cdot10^{-5}$	$<10^{-3}$
^{90}Sr(II)	10^{-9}	$<10^{-3}$
Mn(II)	10^{-4}	$<10^{-3}$

thiocyanate, the colour of the aqueous phase changes from light green to violet; the decrease in extraction with increase in thiocyanate concentration may be associated with the formation of poorly extracted complexes[11].

Figure 8 shows the effect of reducing agents on the extraction of 0.05 *M* chromium(VI). It is evident that ascorbic acid, hydrazine hydrochloride and sodium thiosulphate at concentrations greater than 0.1 *M* can reduce the amount of chromium(VI) taken.

The selectivity of the extraction separation of chromium(VI) with 0.1 *M* 4-(5-nonyl)pyridine in benzene was studied from 3 *M* sulphuric acid. The behaviour of a number of metal ions including uranium, thorium and important fission products, was studied. Each element was studied individually by the standard procedure described. The data are presented in Table I. Separation of spiked ^{51}Cr(VI) (the concentration of chromium in the initial aqueous phase was 0.05 *M*) from 3 months-old fission products was carried out, and chromium was back-extracted with 4% ammonia solution. Clear separation was achieved. This is shown by the γ-spectra in Fig. 9.

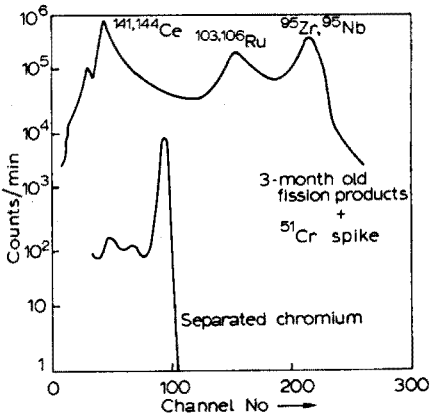

Fig. 9. Separation of spiked chromium(VI) from fission products and their γ-spectra.

Back-extraction of chromium(VI)

The distribution coefficients of chromium(VI) in Fig. 1 show that it is possible to back-extract the chromium(VI) from the solvent phase with either high or very low acid concentrations. It is also possible to back-extract by stirring the organic phase with a reducing agent; the low distribution ratio for trivalent chromium causes it to concentrate in the aqueous phase. Ascorbic acid, hydrazine hydrochloride and thiosulphate will reduce chromium(VI). Dilute ammonia was also found suitable for back-extraction.

SUMMARY

4-(5-Nonyl)pyridine, a new liquid anion exchanger, has been studied for the extraction of chromium(VI) from sulphuric acid solutions. The optimal acidity is 0.1–1 *M*, depending on the concentration of chromium. Common anions have

little effect on extraction in concentrations up to 0.1 *M*. Reducing agents such as ascorbic acid and thiosulphate prevent extraction at concentrations above 0.1 *M*. Separation of chromium(VI) from fission products was achieved.

REFERENCES

1 W. Goishi and W. F. Libby, *J. Amer. Chem. Soc.*, 74 (1952) 6109.
2 J. B. Gerlit, *Proc. Int. Conf. Peaceful Uses At. Energy, Geneva, 1955*, Vol. 7, 1956, pp. 145–151.
3 G. E. Boyd and Q. V. Larson, *Anal. Chem.*, 64 (1960) 988.
4 D. T. Meshri and B. C. Haldar, *J. Sci. Ind. Res.*, 20B (1961) 551.
5 S. J. Rimshaw and G. F. Malling, *Anal. Chem.*, 33 (1961) 751.
6 A. A. Zaitsev, I. A. Lebedev, S. V. Pirozhkov and G. N. Yakovlev, *Russ. J. Inorg. Chem.*, 8 (1963) 1260.
7 J. Ying-Peh Tong and E. L. Prue, *J. Amer. Chem. Soc.*, 75 (1953) 6180.
8 C. W. Davies and J. E. Prue, *Trans. Faraday Soc.*, 51 (1955) 1045.
9 A. S. Kertes and Y. Marcus, *Ion Exchange and Solvent Extraction of Metal Complexes*, Interscience, Wiley, New York, 1969, p. 748.
10 V. I. Kuznetsov and L. I. Moyseyev, *Radiokhimiya*, 6 (1964) 280, 433.
11 K. A. Muirhead, G. P. Haight Jr. and J. K. Beattie, *Inorg. Chem.*, 12 (1973) 1116.
12 Y. Marcus, *Coord. Chem. Rev.*, 2 (1967) 259.
13 M. Ejaz, unpublished work.

Analytica Chimica Acta, 74 (1975) 133–137

SOLVENT EXTRACTION OF SELENIUM, CHROMIUM, IRON AND ZINC FROM ASHED SERUM SAMPLES

SHARON S. LEITNER*

Department of Pathology, University of Florida, Gainesville, Florida 32601 (U.S.A.)

and JOHN SAVORY

Departments of Medicine, Biochemistry, and Pathology, University of North Carolina, Chapel Hill, N.C. 27514 (U.S.A.)

(Received 12th December 1973)

Solvent extraction is an attractive technique for isolation and concentration of metals from biological samples. The metals thus isolated can be determined by various approaches such as atomic absorption spectrometry[1,2], gas chromatography[3–7], or x-ray fluorescence[8]. The present investigation was initiated to obtain conditions whereby several trace elements could be extracted quantitatively from biological samples and the extract then analyzed by neutron activation or atomic absorption.

A recent report[9] from these laboratories discussed the extraction of Cd, Se, Ag, Rb, Zn, and Fe from serum by means of four chelating systems: ammonium pyrrolidinedithiocarbamate (APDC), diethyldithiocarbamate (DDTC), acetylacetone, and dithizone. The most efficient extraction mixture was APDC in methylisobutylketone (MIBK) although in no instance were quantitative extractions obtained. In the present study, the APDC–MIBK system was used with longer extraction times and higher temperatures than before, since it has been demonstrated[7] that such changes in extraction conditions greatly enhanced the extraction of chromium from serum by trifluoroacetylacetone.

EXPERIMENTAL

Irradiation and counting apparatus

Serum samples and standards were counted on a 55-cm^3 nominal active volume Ge(Li) detector (Model LGCC 8.0–27, Nuclear Diodes, Inc., Prairie View, Ill. 60069) equipped with a Model 103 preamplifier (Nuclear Diodes, Inc.), a high voltage power supply (Model 456, Ortec, Inc., Oak Ridge, Tenn. 37830) and a spectroscopy amplifier (Model 451, Ortec, Inc.). The amplified detector output was processed through a 2048-channel analyzer system[10] with a PDP 8/L laboratory computer (Digital Equipment Co., Maynard, Mass. 01754) for memory which operated under software control. In addition to the computer, the system contained a Wilkinson-type 8192-channel analog-to-digital converter (Model 629, Northern Scientific, Inc., Middletown, Wisc. 53562), experimental logic interface

* Present address: Clinical Laboratories, St. Lukes Hospital, Jacksonville, Florida 32206, U.S.A.

and digital timer, a magnetic tape unit (Tennecomp, Inc., Oak Ridge, Tenn. 37830) and an ASR Model 33 Teletype.

Apparatus for sample treatment

Serum samples were placed in shallow glass sample boats and dried in a heated vacuum disiccator (Model 68351, Precision Scientific Co., Chicago, Ill. 60647) fitted with a vacuum trap immersed in dry ice–acetone. The dried serum was ashed in a five-chamber radio-frequency low-temperature dry asher (Model LTA-600, Tracerlab, Richmond, Calif. 94802) also fitted with a vacuum trap packed in dry ice placed between the exhaust manifold of the asher and the line to the vacuum pump. Serum extractions were carried out in 16 × 75 mm Pyrex screw cap vials (Corning Glass Works, New York 14830) which were placed in a 24-hole aluminum block heated with two 100-W adjustable heating cartridges. All counting was accomplished in glass screw-cap scintillation vials.

Reagents and solutions

Reagent-grade methyl isobutyl ketone (MIBK) was redistilled twice before use. Potassium hydrogenphthalate buffer solution of pH 4.0 (Hartman-Leddon Co., Philadelphia, Pa. 19143) was purified by extraction with MIBK. A 1% (w/w) solution of APDC in MIBK was prepared immediately before use.

Radioactive tracer-spiked serum was prepared with serum pooled from non-icteric, non-lipemic samples from hospital patients. Solutions of $^{51}CrCl_3$; $^{59}FeCl_3$; $^{86}RbCl$; $H_2{}^{75}SeO_3$; and $^{65}ZnCl_2$ in 0.5 *M* hydrochloric acid and $^{11m}AgNo_3$ in 1.0 *M* nitric acid. (New England Nuclear, Boston, Mass. 02118) were diluted and mixed to form a spike solution which was added to serum to obtain final concentrations of tracers which were at or below the reported normal serum levels (Se, 200; Cr, 20; Fe, 125,000; Ag, 6,000 ng ml^{-1}). The serum and spike were mixed gently and left at room temperature for at least 30 min to allow equilibration.

Procedures

Serum ashing and extraction. Radioactive tracer spiked serum samples were pipetted into sample boats in 1-ml aliquots, dried at 30°C overnight in the heated vacuum desiccator, and ashed for 10 h in the low-temperature asher at a radio-frequency power of 300 W, a minimized reflected power (about 30 W), an oxygen line pressure of 7 p.s.i., an oxygen flow rate of 7.5 scale divisions, and an operating chamber pressure of 1 mm Hg. Each sample was dissolved in 1 ml of pH 4 potassium hydrogenphthalate buffer and transferred with two 0.5-ml buffer rinses to another container with a transfer pipet. The spiked samples were transferred to scintillation vials and counted, then transferred to 16 × 75-mm screw-cap Pyrex test tubes for extraction. APDC in MIBK (2 ml of 1% w/w) was added to each tube, the threads were wrapped with a 5 × 0.5-in. strip of teflon tape and the tubes capped tightly. The extraction mixtures were shaken for 45 min at specified temperatures on the heating shaking apparatus, and then centrifuged to enhance layer separation. The organic layers of tracer spiked samples were transferred with two 10-drop rinses of MIBK to scintillation vials and counted.

Counting. The radioactive tracer spiked serum samples were counted with the

Ge(Li) detector and 2048-channel analyzer system before and after extraction. Sufficient resolution was obtained with a single 0–1.3 MeV spectrum taken from each sample. Peak search and peak area calculations were software-controlled. Peak boundaries indicated by the peak searches were verified by examination of the digital data. Identification of peaks was made by comparison of sample spectra with spectra of single tracer solutions. The PDP 8/E laboratory computer was programmed to make decay corrections and calculate extraction efficiencies.

Organic extracts, aqueous layers, emptied scintillation vials (in which pre-extraction solutions were counted) and emptied sample boats of the tracer spiked samples were counted to determine percentages of metals lost in the sample boats and in solution transfer. Two spectra of different energy ranges were taken from each sample and calculations were carried out on the laboratory computer.

RESULTS AND DISCUSSION

Previous work[9] provided information concerning the extraction of metals from ashed serum with several systems; the ash was shaken with the extractant for 30 s at room temperature. The APDC–MIBK system was the most effective, but the greatest extraction obtained was only 52%. The present study used APDC in MIBK with prolonged extraction times and elevated temperatures. Radioactive tracer spiked serum was dried, ashed, dissolved, and extracted for 45 min at 25°C, 40°C, 55°C, or 70°C on the heating shaking apparatus. Three serum samples were used at each temperature. Dissolved serum ash was counted before extraction and the organic layer was removed and counted after extraction. The mean extraction efficiencies for the four temperatures are summarized in Table I, along with the efficiency of extraction of the metals reported previously[9]. The highest extraction percentages were obtained at 40°C. Some of the fluctuation in extraction percentages for each metal over the temperature range is of course due to experimental error. There remain, however, significant changes which must be attributed to metal–chelate interaction.

TABLE I

SUMMARY OF EXTRACTION EFFICIENCIES FOR THE PRESENT METHOD

Metal	*Percent extracted (mean ± s)*				
	Previous study[9]	*25°C*	*40°C*	*55°C*	*70°C*
Se	12.5±10.9	4.8±0.4	6.3±0.6	6.4±1.4	7.2±1.1
Cr	16.7±6.6	0	42.0±7.6	13.0±6.2	17.0±3.6
Fe	52.5±23.1	91.0±2.1	82.0±46	87.0±11.0	49.0±2.3
Zn	51.5±23.3	54.0±4.6	84.0±3.4	36.0±4.3	43.0±6.2

The extraction of selenium was not improved significantly over the previous study although the percentage extracted did increase slowly with increasing temperature. An extraction time of 45 min gave no recovery of chromium at 25°C, in contrast to a 16% recovery obtained with an extraction time of 30 s.

However, an increase in temperature to 40°C markedly enhanced the extraction of chromium, although further increases in temperature from 40°C to 70°C resulted in a decrease in the extraction percentage. Like chromium, zinc was extracted best at 40°C, whereas iron was extracted efficiently in the 25–55°C range with a considerable decrease as the temperature was raised to 70°C.

The validity of the extraction efficiency data given in Table I depends on minimal losses of metals during the processing steps. Losses during drying were minimized by carrying out this step at 30°C, which is a sufficiently low temperature to eliminate losses by volatilization. Additional sources of error from metal loss were investigated by counting emptied scintillation vials (in which pre-extraction solutions were counted) and emptied sample boats used in analysis of the radioactive tracer spiked samples. Organic extracts and aqueous layers were also counted to give an estimate of the total amount of activity present in each sample. Activities of each container used in analysis of a sample were added, and percentages of metal recovered from each container were calculated. Table II gives the mean recovery percentages for each metal. Amounts of metal left behind in vials from which solutions were transferred were minimal. Metal losses in the sample boats were greater, though still small. Thus, losses of metals during the processing steps do not contribute to the extraction efficiency data.

TABLE II

METAL LOSSES IN PROCESSING STEPS

Metal	*Losses in counting vial (%)*[a]	*Losses in sample boat (%)*[a]
Cr	0.11 ± 0.04	0.73 ± 0.42
Fe	0.12 ± 0.07	2.28 ± 1.03
Zn	0.01 ± 0.02	0.68 ± 0.32

[a] Mean of 3 analyses, expressed as mean $\pm s$.

Results from all these studies demonstrate the difficulties of obtaining quantitative extractions of metals from biological samples. It appears that solvent extraction has very limited scope for multi-element measurements in biological samples. Thus, techniques such as neutron activation analysis, which require prior treatment of the samples, will have to rely on other procedures for isolating the metals of interest.

This investigation was supported by National Institutes of Health Grant 5 R01 GM 17203-02.

SUMMARY

The extraction by APDC in MIBK of Se, Cr, Fe and Zn from serum ashed in a low-temperature dry asher is described. Extraction temperatures of 25, 40, 55, and 70°C were studied; 40°C provided the best overall extraction efficiencies. However, in no case could quantitative extractions be obtained. Losses

of metals during the processing steps were shown to be insignificant.

REFERENCES

1 F. J. Feldman, E. C. Knoblock and W. C. Purdy, *Anal. Chim. Acta*, 38 (1967) 489.
2 S. Nomoto and F. W. Sunderman, Jr., *Clin. Chem.*, 16 (1970) 477.
3 R. W. Moshier and J. E. Schwarbert, *Talanta*, 13 (1966) 445.
4 W. G. Scribner and A. M. Kotecki, *Anal. Chem.*, 37 (1965) 1304.
5 W. G. Scribner, W. J. Treat, J. D. Weis and R. W. Moshier, *Anal. Chem.*, 37 (1965) 1136.
6 W. I. Stephen, I. J. Thomson and P. C. Uden, *Chem. Commun.*, (1969) 269.
7 J. Savory, P. Mushak and F. W. Sunderman, Jr., *J. Chromatogr. Sci.*, 6 (1969) 674.
8 B. Armitage and H. Zeitlin, *Anal. Chim. Acta*, 53 (1971) 47.
9 D. E. Appleby and J. Savory, *Anal. Chim. Acta*, 62 (1972) 317.
10 D. B. Cottrell, Dissertation for the Degree of Doctor of Philosophy, University of Florida, Gainesville, Fla., 1973.

Analytica Chimica Acta, 74 (1975) 139–146

TITRIMETRIC DETERMINATION OF LONG-CHAIN AMINES AND QUATERNARY AMMONIUM SALTS

ST. J. H. BLAKELEY and V. J. ZATKA

J. Roy Gordon Research Laboratory, The International Nickel Company of Canada, Ltd., Sheridan Park, Mississauga, Ontario L5K 1Z9 (Canada)

(Received 16th May 1974)

High-molecular-weight organic quaternary ammonium (R_4N^+) salts are very useful solvent-extraction reagents as indicated by recent reviews[1–3]. Of special interest are thiocyanate salts which can be readily obtained from the commercially available quaternary ammonium chlorides such as Aliquat 336 (General Mills Inc.), Adogen 464 (Ashland Chemicals) or Arquad (Armour Industrial Chemical Co.). They show particular properties which can be applied to the solvent extraction of cobalt[4], indium[5], manganese[6] and possibly many others. The commercial products, however, are seldom pure and usually contain varying amounts of the parent long-chain tertiary amine. In a solvent extraction process, amines affect the extraction equilibria and, in a continuous operation, their concentration may change. An analytical method to determine amines and quaternary ammonium salts in the presence of either each other or any metal which might be extracted in the organic phase is extremely desirable. Procedures used routinely for the determination of the quaternary ammonium ions, such as the sodium lauryl sulfate titration[7], either are not selective and report the amine as well[8], or, as with the bromophenol blue solvent-extraction technique[9,10], cannot be adapted readily to the amine determination in the presence of a large excess of the quaternary ammonium ion.

The titrimetric determination of amines in non-aqueous media is well established. The method can be applied to amine analysis in $R_4N^+X^-$ systems, provided that the anion X^- is derived from a strong acid which is sufficiently ionized in the non-aqueous medium. In glacial acetic acid such anions are perchlorate, iodide, bromide and chloride[11,12] and the corresponding quaternary ammonium salt will not take part in the reaction. However, if the conjugate acid HX is only slightly dissociated, the anion is protonated as in the titration of thiocyanate with perchloric acid.

$$R_4N^+SCN^- + H^+ + ClO_4^- \rightarrow HSCN + R_4N^+ClO_4^- \quad (1)$$

Thus reaction (1) can be used for the determination of the sum of quaternary ammonium ion and free amine. If the R_4N^+ salt is converted to the perchlorate or iodide, then the amine alone can be determined with no interference by the R_4N^+. However, by converting the R_4N^+ ion to the iodide form, the sequential determination of both amine and R_4N^+ is possible.

After titration of the amine, mercury(II) acetate[11], is added to convert the

quaternary ammonium iodide to the strongly basic quaternary ammonium acetate and undissociated mercury(II) iodide according to:

$$2(R_4N^+I^-)+Hg(CH_3COO)_2 \rightarrow 2(R_4N^+CH_3COO^-)+HgI_2 \quad (2)$$

The mercury(II) iodide remains dissolved in the excess of mercury acetate and does not interfere with the titration of the quaternary acetate with perchloric acid:

$$R_4N^+CH_3COO^-+H^++ClO_4^- \rightarrow CH_3COOH+R_4N^+ClO_4^- \quad (3)$$

The present paper describes the sequential determination of amine and quaternary ammonium ion in the Aliquat thiocyanate extractant or in any other long chain quaternary ammonium system. Any metal ions which may be present in the organic extractant from a previous operation are removed by stripping with dilute ammonia solution before the acidimetric titration. Both visual and potentiometric end-point indication can be used.

EXPERIMENTAL

Apparatus

For the potentiometric indication with glass and calomel electrodes, the saturated potassium chloride filling solution in the reference electrode has to be replaced with an aqueous 0.1 *M* lithium chloride solution to prevent plugging its junction capillary with potassium perchlorate.

Reagents

Ammoniacal stripping solution. 0.5 *M* Sodium chloride in (1+2) ammonia solution.

Potassium iodide (ammoniacal). 1.5 *M* KI in (1+3) ammonia solution.

Sodium perchlorate (ammoniacal). 0.5 *M* $NaClO_4$ in (1+2) ammonia solution.

Standard perchloric acid (0.1 M) in acetic acid. Add 8.5 ml of 72% $HClO_4$ to 900 ml of glacial acetic acid, mix, add gradually 25 ml acetic anhydride and dilute to 1 l with acetic acid. Standardize the next day against potassium hydrogenphthalate in acetic acid with crystal violet as indicator.

For the amine titration prepare 0.05 *M* $HClO_4$ by dilution of the standard 0.1 *M* acid with glacial acetic acid.

Test chemicals. Tris(hydroxymethyl)aminomethane and toluene were analytical grade chemicals (J. T. Baker); tri-n-butylamine (Eastman Practical grade) was distilled before use; tetrabutylammonium bromide and tetraheptylammonium iodide (Eastman) were used without purification.

Alamine 336 (essentially tricaprylamine, av.m.w. 392[3]), and Aliquat 336 (tricaprylmethylammonium chloride, av.m.w. 475) were commercial products (General Mills Chemicals Inc., Kankakee, Ill.).

Aliquat thiocyanate (30% solution in toluene). Prepare from a 30% solution of the Aliquat 336 by three consecutive equilibrations with equal volumes of 1 *M* thiocyanate. Wash the organic phase with water and clarify by filtration or centrifuging. Thiocyanate in the organic phase was determined potentiometrically with silver nitrate after dilution of the sample with 2-propanol.

Recommended procedures

Sequential determination of amine and quaternary ammonium ion in Aliquat extracts. Dilute 5.0 ml of sample with 25 ml of toluene in a separatory funnel. If the presence of metal ions is suspected in the sample, extract twice with 50 ml of the ammoniacal stripping solution, discarding the aqueous phase. Load with iodide by four consecutive shakings with 50 ml of ammoniacal iodide solution for 2 min each time. Wash the organic phase three times with 80 ml of water; use a swirling motion to prevent emulsion formation.

Dry the stem of the separatory funnel, insert a tight glass-wool plug and slowly filter the organic phase into a glass vial. Clarify the filtrate by adding anhydrous sodium sulfate and centrifuging, if necessary. Measure a 10.0-ml aliquot, dilute with 15 ml of glacial acetic acid, and after addition of crystal violet indicator (0.5% w/v in acetic acid), titrate the free amine with standard 0.05 *M* perchloric acid to a blue-green color.

Add 15 ml of mercury(II) acetate solution (5% w/v in acetic acid) and continue the titration, this time with 0.1 *M* acid, to the same end-point color. Correct both acid volumes for the respective blanks as obtained in titrating 10 ml of toluene instead of the sample aliquot. From the corrected volumes of both acids calculate the contents of amine, and R_4N^+, respectively.

Determination of the sum of amine and quaternary ion in Aliquat thiocyanate extracts. Dilute 5.0 ml of sample with 25 ml of toluene and, if extracted metals are present in the sample solution, scrub 3 or 4 times with 50 ml of ammoniacal stripping solution and wash as before. Shake the organic phase twice with 30 ml of 1 *M* thiocyanate for 1 min each time. Wash twice by swirling with 80 ml of water and discard the washings.

Dry the stem of the separatory funnel, filter, dry the filtrate, and titrate a suitable aliquot with 0.1 *M* perchloric acid as above. Correct for the blank titration and calculate the total of amine plus quaternary ammonium ion.

Determination of amine only in Aliquat extracts. Dilute 5.0–10.0 ml of extract with 25 ml of toluene and scrub with 50 ml of the ammoniacal perchlorate solution. For a complete removal of metals repeat 4 to 5 times, shaking always for 1 min and discharging the aqueous phases. Wash the organic layer three times with 80 ml of water, using a swirling motion to prevent emulsion formation, dry and titrate with 0.05 *M* perchloric acid. If the organic layer was properly loaded with perchlorate, no acid consumption should occur after addition of mercury(II) acetate.

RESULTS AND DISCUSSION

Perchloric acid titration

The direct acidimetric titration involves all free amines, primary through tertiary, and, in addition, any anion derived from an acid not sufficiently ionized in acetic acid medium, such as thiocyanate. Thus, Aliquat thiocyanate can be assayed acidimetrically; the results, corrected for the amine present, are in agreement with the argentimetric thiocyanate determination (Table I). Since iodide, bromide, chloride. and perchlorate do not interfere, it is possible to monitor acidimetrically their extraction equilibria with the thiocyanate (Table II). In the presence of chlorides the

visual end-point is less sharp as hydrochloric acid is the least dissociated of the three halide acids[1,2], and a potentiometric indication becomes necessary. Results summarized in Table I show good recoveries in titrations of individual compounds as well as mixtures.

TABLE I

ACIDIMETRIC DETERMINATION OF AMINE AND QUATERNARY AMMONIUM SALT IN ACETIC ACID

Added (meq)		*Found*			
		Amine		R_4N^+	
		meq	*% Recovery*	*meq*	*% Recovery*
Tris(hydroxymethyl)-aminomethane	0.7211	0.7233	100.3	—	—
Tributylamine	0.9360	0.9350	99.9	—	—
Alamine	0.4969	0.4946	99.5	—	—
	0.8098	0.8072	99.7	—	—
	0.8098[a]	0.8146[b]	100.6	—	—
Tetrabutylammonium bromide	0.9038	0.0005	—	0.8999	99.6
Tetraheptylammonium iodide	0.5988	0.0005	—	0.6013	100.4
	0.5788	0.0005	—	0.5780	99.8
Aliquat thiocyanate	0.8767[c]	0.0085	—	0.8788	100.2

[a] 0.8 meq of Aliquat chloride added.
[b] Including 1% amine impurity in added Aliquat.
[c] Determined by titration of SCN^- with $AgNO_3$.

TABLE II

SUBSTITUTION OF THIOCYANATE IN ALIQUAT PHASE WITH PERCHLORATE OR IODIDE

(Aliquat thiocyanate (30%) diluted (1 + 5) with toluene; $V_{org} = V_{aq}$; 2 min equilibration)

No. of contacts	*Equilibrated with 0.5 M $NaClO_4$; SCN^- (meq)*[a]	*Equilibrated with 1 M KI*			*Equilibrated with 1.5 M KI*		
		SCN^- (meq)[a]	*I^- (meq)*	*Total*	*SCN^- (meq)*[a]	*I^- (meq)*	*Total*
0	0.570	0.887	0.004	0.891	0.872	0.005	0.877
1	—	0.187	0.715	0.902	—	—	—
2	0.006	0.051	0.848	0.899	0.032	0.864	0.896
3	—	0.018	0.885	0.903	—	—	—
4	0.006	0.012	0.891	0.903	0.009	0.879	0.887
5	—	0.009	0.887	0.896	—	—	—
6	—	0.009	0.890	0.899	0.008	0.876	0.884
		Average		0.899[b]			

[a] Co-titrated with 1% amine impurity in the Aliquat.
[b] Relative standard deviation 0.0049.

Halides not involved in the initial acidimetric titration can be determined after addition of mercury(II) acetate. While this compound is only slightly ionized in acetic acid[13] and has not direct effect on the acidimetric titration, it readily reacts with the halide ions according to eqn. (2), releasing an equivalent amount of strongly basic acetate ions. Perchloric acid used in the following titration corresponds to the amount of the quaternary ammonium ion present (eqn. 3).

The acidimetric determination of amines and quaternary ammonium ions in the Aliquat thiocyanate phase requires that the samples be metal-free. It was observed that metal thiocyanate complexes, such as $Co(SCN)_3^-$, are so stable in the organic phase that they are not decomposed by the perchloric acid titrant. This is in agreement with the great difference in the reported[14] stabilities of cobalt thiocyanato- or iodo-complexes in water and acetone, respectively. Preliminary results indicate that a direct acidimetric titration can be used to differentiate between the free and metal-bound thiocyanate in the Aliquat phase.

Stripping of metals

No problems were encountered when metals such as Co, Cu, Zn, and Fe, were stripped from the Aliquat thiocyanate phase. The ammonia stripping solution must contain an electrolyte, such as ammonium or sodium salts, to prevent emulsion formation. The rate of metal removal from the organic phase depends on the anion in the stripping solution and the stability of the metal–anion complex in the organic phase. Stripping is very effective in the presence of chloride or perchlorate, less so with iodide and incomplete with ammoniacal thiocyanate solution. Thus the metal-stripping and anion-loading processes can be combined when perchlorate or iodide are involved. To obtain a metal-free organic phase in the thiocyanate form, all metals must first be completely removed with the chloride stripping solution followed by re-loading of any lost thiocyanate. Usually, 3–4 equilibrations with the stripping solution (4.5 *M* NH_3) are needed to bring the metal content of Co or Cu down to 1–2 p.p.m.

Substitution of thiocyanate

The distribution ratios of anions between Aliquat and water decrease in the order $ClO_4^- > SCN^- > I^- \gg Cl^- \gg SO_4^{2-}$. This means that while only a fraction of the thiocyanate in the extractant can be exchanged by chloride or sulfate from the aqueous phase, it is readily replaced by perchlorate. Results in Table II show that two equilibrations with a 0.5 *M* perchlorate solution are sufficient to have all thiocyanate in the organic phase replaced by perchlorate. For a complete loading with iodide four contacts with a 1.5 *M* iodide solution are satisfactory.

Sources of error

Solubility of ammonia in toluene and in toluene-diluted Aliquat iodide. Ammonia remaining in the washed organic phase would seriously affect the amine titration. However, it was found that all ammonia which dissolves in the organic phase during the metal stripping can be readily washed out by two scrubbings with 2–3 volumes of water (Table III).

Loss of amine to the aqueous phase. Only amines with a sufficiently high molecular weight and, consequently, high distribution ratio in the organic–water

TABLE III

SOLUBILITY OF AMMONIA IN THE ORGANIC PHASE

($V_{org} : V_{aq} = 1:2$)

Contacted with	*NH_3 dissolved ($g\ l^{-1}$)*	
	Toluene	*Aliquat-1 (30%) diluted with toluene 1:5*
NH_3 (1+1)+0.5 *M* $(NH_4)_2SO_4$	0.197	0.334
1st water scrub	0.002	0.006
2nd water scrub	[a]	[a]

[a] Not detected.

TABLE IV

AMINE LOSS TO THE AQUEOUS PHASE

Sample	*Millimoles amine*	
	Organic phase	*Aqueous phase*
1	0.123	0.001
2	0.091	0.002
3	0.059	<0.0005

system can be readily determined by the present method. Evidence was obtained in analysis of several metal-loaded and stripped samples that no amine is lost from the sample solution to the aqueous phase during the analytical procedure (Table IV). For this purpose, the combined aqueous layers (*ca.* 500 ml) were filtered in order to separate the entrained droplets of the organic phase, and equilibrated with 15 ml of toluene which, in turn, was washed with 20 ml of water to remove the dissolved ammonia.

Effect of temperature. The coefficient of thermal expansion for glacial acetic acid is $1.1 \cdot 10^{-3}$, about five times greater than that for water. The molarity of the perchloric acid titrant should be corrected if the temperature at which it is used differs by 1°C or more from its standardization temperature by using

$$M_{T_1} = \frac{M_{T_0}}{1+0.0011\,(T_1 - T_0)}$$

where T_0 is the temperature at the time of standardization, T_1 that at the time of analysis, and M is the molarity at the temperature indicated by the subscript.

Effect of water. The presence of water should be avoided because it impairs the sharpness of the end-point, owing to flattening of the titration curve. Reportedly, up to 1% can be tolerated when titrating with 0.1 *M* perchloric acid[11]. Although the solubility of water in the Aliquat–toluene phase is well below this limit, the presence of water in the treated organic phase is controlled by the addition of anhydrous sodium sulfate.

Precision and accuracy

As in any titrimetric analysis, the precision obtainable with the present method largely depends on the sharpness of the end-point break, *i.e.* on either the indicator color change or the potential change. Since the basicity of all the titrated species is high enough, the visual end-point indication was used, although a better precision can be expected potentiometrically. The results obtained for total base during the stepwise loading of the organic phase with iodide (Table II) did not differ by more than 1.3% relative, and showed a relative standard deviation of 0.005. The percent recoveries of amine and R_4N^+ in mixtures (Table V) indicate an accuracy comparable to that of normal aqueous acid–base titrations. The Aliquat thiocyanate extractant was shown to contain 1% amine contaminant, presumably Alamine 336, which is in agreement with the manufacturer's (General Mills, Inc.) specifications for Aliquat 336. Reproducibility of the amine determination in the consecutive titration will be affected by the amine-to-quaternary-ion ratio since usually both are determined from a single sample. In samples with this ratio of 1:40, the amine results were reproducible within 3–5%, and the quaternary ion within 1–2%, all with visual end-point indication.

TABLE V

ANALYSIS OF MIXTURES BY THE RECOMMENDED PROCEDURE

Added (meq)		*Found*			
Amine	R_4N^+	*Amine*		R_4N^+	
		meq	*% Recovery*	*meq*	*% Recovery*
Alamine	*Aliquat-ClO_4*				
0.8098	0.8	0.8138[a]	100.5	0.000	—
Alamine	*Tetraheptylammonium iodide*				
0.3355	0.5888	0.3385	100.9	0.5881	99.8
0.3355	0.6861	0.3365	100.3	0.6844	99.7

[a] Including the amine impurity from Aliquat.

CONCLUSIONS

The acidimetric titration in non-aqueous medium proved to be useful as a reasonably fast and versatile method for the determination of amines and quaternary ammonium compounds in mixtures. It can be easily adapted to the analysis of the commercial quaternary ammonium salt extractants, such as Aliquat 336, to monitor their amine content. The choice of glacial acetic acid as the titration diluent makes it possible to determine an amine mixture as a group even when the basic strength of its constituents differs appreciably. With potentiometric indication, the method can be used for analysis of dark colored samples. The anion-exchange properties of the long-chain quaternary ammonium extractants are advantageously utilized and by working with the thiocyanate, perchlorate or iodide form, the scope of the method can be readily modified.

SUMMARY

The sequential determination of long-chain amines and quaternary ammonium ions by acidimetric titration in a non-aqueous medium is described. The method utilizes the ion-exchange properties of the extractants and the differences in the protonation of the selected anions such as ClO_4^-, I^- or SCN^- under the experimental conditions. Commercially available quaternary ammonium chlorides can be readily converted into these ionic forms. Both visual and potentiometric end-point indication is possible, the former giving a relative standard deviation of 0.005 meq. of the base present.

REFERENCES

1 I. D. Eubanks, *At. Energy Rev.*, 7 (1969) 49.
2 W. Müller, *Actinides Rev.*, 1 (1967) 71.
3 H. Green, *Talanta*, 20 (1973) 139.
4 W. E. Clifford, L. A. McClaine, J. H. B. George and C. E. O'Neill, *U.S. Patent 3, 194, 652*, July 13, 1965.
5 H. M. N. H. Irving and A. D. Damodaran, *Anal. Chim. Acta*, 50 (1970) 277.
6 R. Přibil and J. Adam, *Talanta*, 20 (1973) 49.
7 W. J. Harper, P. R. Elliker and W. K. Mosely, *Soap Sanit. Chemicals*, 24 (1948) 159.
8 A. Milun and F. Moyer, *Anal. Chem.*, 28 (1956) 1204.
9 A. Mukerjee and P. Mukerjee, *J. Appl. Chem.*, 12 (1962) 127.
10 L. D. Metcalfe, *Anal. Chem.*, 32 (1969) 70.
11 C. W. Pifer and E. G. Wollish, *Anal. Chem.*, 24 (1952) 300.
12 I. M. Kolthoff and A. Willman, *J. Amer. Chem. Soc.*, 56 (1934) 1007.
13 I. M. Kolthoff and A. Willman, *J. Amer. Chem. Soc.*, 56 (1934) 1014.
14 L.-G. Sillén and A. E. Martell, *Stability Constants, Special Publication Nos. 17 and 25*, Th Chemical Society, London, 1964 and 1971.

Analytica Chimica Acta, 74 (1975) 147–153

NUMERICAL EVALUATION OF COMPLEX STABILITY CONSTANTS FROM POLAROGRAPHIC DATA FOR QUASI-REVERSIBLE PROCESSES

B. GRABARIĆ, M. TKALČEC, I. PILJAC and I. FILIPOVIĆ

Laboratory of Inorganic Chemistry, Faculty of Technology, and Institute for Inorganic and Analytical Chemistry, University of Zagreb, Croatia (Yugoslavia)

VL. SIMEON

Institute for Medical Research and Occupational Health, Yugoslav Academy of Sciences and Arts, 41000 Zagreb, Croatia (Yugoslavia)

(Received 10th June 1974)

In a previous paper[1], an improved technique for the determination of complex stability constants from polarographic data based on the method of DeFord and Hume[2] was described. This method was used to determine stability constants of cadmium(II) and lead(II) complexes with 2-, 3-, and 4-hydroxybutyrates[3], where the cathodic reduction of cadmium(II) and lead(II) is polarographically reversible. In the present work, essentially the same technique has been applied for determining the stability constants of copper(II)–butyrate complexes; in this system the cathodic reduction of copper(II) is moderately quasi-reversible. The measuring system has been improved by utilizing operational amplifiers.

EXPERIMENTAL

Instrumentation

Polarograms were recorded by means of a controlled-potential polarographic instrument with operational amplifiers. Its potentiostat is similar in principle to that described by Kelley *et al.*[4,5], for which a detailed circuit analysis was made by Bezman and McKinney[6]. In order to reduce the *iR* drop through the solution between the working and the reference electrode, a three-electrode technique was employed.

The circuit diagram is shown in Fig. 1. The polarographic equipment consists of a power supply (Hewlett Packard, model HP 60155C) and potentiostatic circuit for the control of the potential in the proximity of the working electrode. This potential can be varied in discrete steps by means of a 1 kΩ (ten turn) precision potentiometer. The other part of the instrument is the current-measuring circuit. The current (which oscillates owing to the growth of the mercury drop) was passed through a low-pass filter (LPF) and a relay to the analogue memory. The relay was actuated by a drop-life timer (Radiometer, model DLT 1) just before the end of the drop life. Both the potential and the current were monitored by a digital voltmeter, (DVM) (Hewlett Packard, model HP 3480 A) with a resolution of 0.1 mV. The potential measurements were reproducible within 0.3 mV and the current measurements within less than 1% (the cell included). The polarographic cell has been described previously[1].

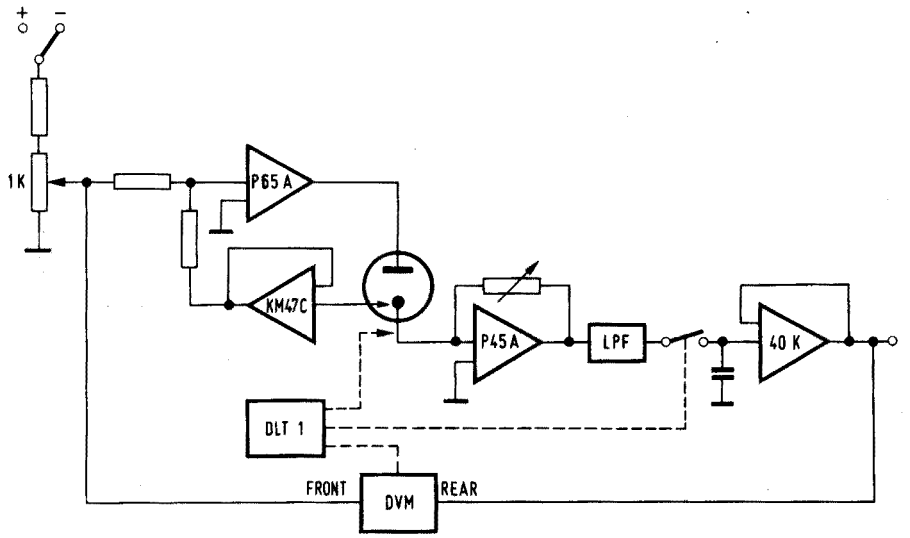

Fig. 1. The polarographic apparatus diagram.

Experimental conditions

All the chemicals used were of analytical-reagent grade. Copper(II) perchlorate was prepared from copper(II) oxide and perchloric acid. Sodium perchlorate, solutions of which were used as supporting electrolyte, was recrystallized three times. The measurements were made with buffer solutions having constant concentrations of butyric acid (HBut, 0.01 mole dm^{-3}) and copper(II) (0.4 mole dm^{-3}) and a constant ionic strength (2 mole dm^{-3}, adjusted with $NaClO_4$); the temperature was maintained at (298.2±0.2)°K. Total ligand concentration was varied up to *ca.* 1 mole dm^{-3}. The capillary constant ($m^{\frac{2}{3}}t^{\frac{1}{6}}$), measured in open circuit in a 0.1-mole dm^{-3} KCl solution for a mercury column height of 30 cm, was 1.79 $mg^{\frac{2}{3}}\,s^{-\frac{1}{2}}$. The drop time was kept at 3.4 s by means of the drop-life timer.

Calculations

According to DeFord and Hume[2] the cumulative stability constants β_n are calculated from the experimentally obtainable function

$$F_0 = \exp\left\{\frac{zF}{RT}(E^s_{\frac{1}{2}} - E^c_{\frac{1}{2}}) + \ln\frac{I^s_d}{I^c_d}\right\} \tag{1}$$

$$F_0 = 1 + \sum_n \beta_n [L]^n \tag{2}$$

This function is usually determined by recording the polarographic waves of a series of solutions with a constant metal concentration and ionic strength but a variable total ligand concentration; in all cases, $c_L \gg c_M$, so that $[L] \approx c_L$. The values of $E^c_{\frac{1}{2}}$ and i^c_d are obtained from the polarographic curves either graphically or numerically. The corresponding data for simple aquo ions, $E^s_{\frac{1}{2}}$ and i^s_d, are either measured directly, from the polarogram of the solution containing no ligand (but otherwise identical to those described above), or by extrapolating the functions $E^c_{\frac{1}{2}}$ *vs.* [L] and i^c_d *vs.* [L]

to [L] = 0. In the case of a partly reversible electrode process, the magnitude of $E^{s}_{\frac{1}{2}}$ as well as i^{s}_{d} can be estimated by a numerical method proposed by Momoki and Ogawa[7].

The procedures outlined above can be, at least in principle, applied to quasi-reversible electrode processes provided that the reversible half-wave potentials are determined. According to Matsuda *et al.*[8–10], it is possible to determine the reversible $E_{\frac{1}{2}}$ value from the polarographic wave of a quasi-reversible process by drawing the tangent to the log $i/(i_d - i)$ *vs.* E curve in its lower, positive enough part where the electrode process is still diffusion-controlled. A similar approach was employed in the present work but the polarographic waves of quasi-reversible electrode processes were processed numerically rather than graphically.

In the previous work[1], the $E_{\frac{1}{2}}$ and i_d values were computed simultaneously, by using the Gauss–Newton least-squares treatment as proposed by Vouk *et al.*[11], in order to avoid any subjective smoothing of the polarographic data. However, when applied to the polarographic waves of quasi-reversible processes, this method gave slightly different values for $E_{\frac{1}{2}}$ and i_d than would be expected on the grounds of graphical estimates. This is exemplified by the data shown in Fig. 2 where the logarithmic forms of the polarograms of 0.4 mmole dm^{-3} copper(II) in perchloric acid solutions (1 and 10 mmole dm^{-3}) of constant ionic strength (2 mole dm^{-3}) are plotted. The data points were calculated first by evaluating i_d numerically and then

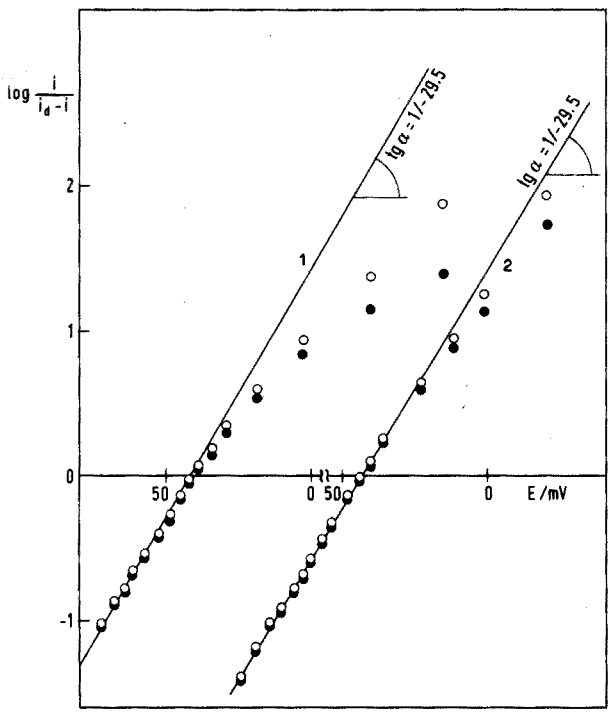

Fig. 2. The influence of the method of computing i_d upon the logarithmic form of the polarographic curve. Copper(II), 0.4 mmole dm^{-3}; $I = 2$ ($NaClO_4$). (1) 0.01 mole dm^{-3} $HClO_4$; (2) 0.001 mole dm^{-3} $HClO_4$. (○) With numerical i_d; (●) with graphical i_d.

graphically (circles and dots in Fig. 2, respectively). For low values of $\log i/(i_d - i)$, the data points are satisfactorily fitted by the line of theoretical slope, whereas at higher values the data begin to deviate more and more both from the line and among themselves. The deviation from the theoretical line is easily understood if the quasi-reversibility of the electrode process is kept in mind. The discrepancies among circles and dots can be, at least partly, explained by the non-orthogonality of the numerical method used: in the method proposed by Vouk *et al.*[11], the errors in any one parameter to be refined may cause considerable errors in the other (this can be verified by inspecting the correlation matrix), especially if the model applied (in this case a perfectly reversible electrode reaction) is not completely physically adequate. Besides, the information on i_d contained in the first ten or so points of a polarographic curve ($E > E_{\frac{1}{2}}$) can hardly be very abundant. Therefore it seems more correct to use a graphical estimate of i_d for the regression analysis of the polarographic wave. Needless to say, in such an analysis only that part of the wave is taken into account which is still diffusion-controlled.

RESULTS AND DISCUSSION

The linearized polarograms of copper(II) in the presence of 1 or 10 mmole dm^{-3} perchloric acid or 10 mmole dm^{-3} butyric acid as well as in pure supporting electrolyte (2 mole dm^{-3} $NaClO_4$) are shown in Fig. 3. It can be observed that with increasing acidity, the polarographic waves tend to be less reversible. The same was observed by Kolthoff and Okinaka[12] for copper(II) reduction in perchlorate medium of lower ionic strength (0.1 mole dm^{-3}), and by Hawkridge and Bauer[13] who investigated the kinetics of copper(II) reduction in lithium nitrate medium by a.c. polarography. Both groups explain the decreasing irreversibility by assuming the

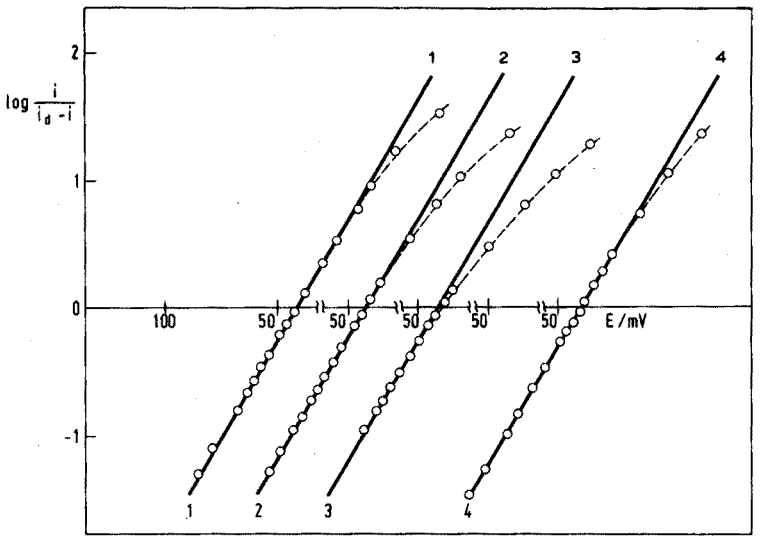

Fig. 3. Linearized polarograms of copper(II) in perchlorate media with varying acid concentration. 0.4 mmole dm^{-3} $Cu(ClO_4)_2$; $I = 2$ ($NaClO_4$). (1) pH 6; (2) 0.001 mole dm^{-3} $HClO_4$; (3) 0.01 mole dm^{-3} $HClO_4$; (4) 0.01 mole dm^{-3} butyric acid.

formation of $Cu(OH)(H_2O)_5^+$ species at higher pH values. A partial or complete dissociation of this species is believed to be faster than is the case with $Cu(H_2O)_6^{2+}$ species.

The $E_{\frac{1}{2}}$ and i_d values for copper(II) reduction in various media evaluated by alternative methods are presented in Table I. As explained in the preceding section, those $E_{\frac{1}{2}}$ values computed with graphically estimated i_d values were considered as more reliable. Any of the $E_{\frac{1}{2}}^c$ values quoted (except those measured in the presence of butyric acid) could be, in principle, selected as a final one. However, the polarogram recorded in the presence of 1 mmole dm^{-3} perchloric acid is characterized by the most positive $E_{\frac{1}{2}}$ value and the highest i_d value. These values were accepted as most reliable, because the presence of a higher concentration of acid influences the kinetics of electrode reaction. The finally adopted values are $E_{\frac{1}{2}}^c = (42.5 \pm 0.1)$ mV and $i_d^c = (4.70 \pm 0.04)$ μA.

TABLE I

HALF-WAVE POTENTIALS AND DIFFUSION CURRENTS OF COPPER(II) IN DIFFERENT MEDIA AT 298.15°K

($c_{Cu} = 0.4$ mmole dm^{-3}, $I = 2$ mole dm^{-3} ($NaClO_4$))

Acid added	$-s$ *(mV)*[a]	$E_{\frac{1}{2}}^{num.}$ *(mV)*	$E_{\frac{1}{2}}^{gr.}$ *(mV)*	$i_d^{num.}$ *(μA)*	$i_d^{gr.}$ *(μA)*
	30.2±0.1	41.6±0.1	42	3.92±0.01	4.20
$HClO_4$, 1 mmole dm^{-3}	29.6±0.1	42.5±0.1	43	4.59±0.06	4.70
$HClO_4$, 10 mmole dm^{-3}	31.0±0.1	40.5±0.1	41	3.71±0.04	4.58
HBut, 10 mmole dm^{-3}	30.6±0.1	39.3±0.1	40	4.01±0.06	4.48

[a] Estimate of the Nernst slope, 2.3 $RT/2F$.

The values of $E_{\frac{1}{2}}^c$ and i_d^c obtained by polarographing a series of solutions containing a constant concentration of copper(II) and a varying amount ($0.03 \leqslant c_L$/mmole $dm^{-3} \leqslant 1$) of ligand, are shown in Fig. 4, together with the computed estimates of the Nernst slope ($s = 2.3\ RT/2F$). The concentration of butyric acid was maintained at 10 mmole dm^{-3}, in order to prevent the formation of hydroxo complexes. According to Filipović and Piljac[14], higher concentrations of butyric acid should be avoided, because, the presence of a higher amount would make $E_{\frac{1}{2}}$ more positive through its influence on the viscosity of the solution and on the activity coefficients of the species present.

When the Leden extrapolation was used, it was found that four successive ML_n complexes are formed in the copper(II)–butyrate system, and their approximate stability constants were estimated. These values were then refined as described previously[1]. The computed refined values are quoted in Table II, together with the respective 95% confidence intervals. The same system has been examined by spectrophotometric and potentiometric methods under identical experimental conditions[15,16] and the values obtained (also quoted in Table II) are in very good agreement with those determined in the present work. Therefore, it can be concluded that correct values of complex stability constants can be obtained by polarography, even when the electrode reaction is not perfectly reversible, provided that adequate experimental and computation techniques are applied.

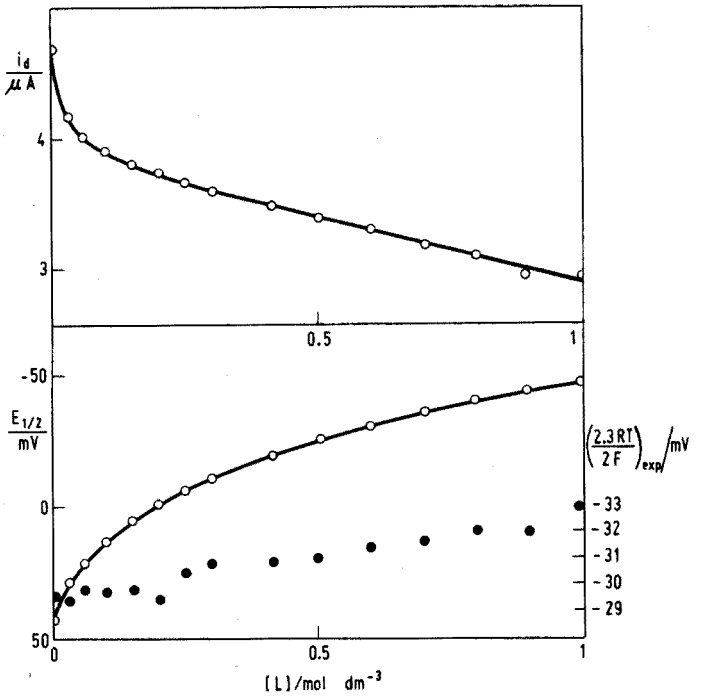

Fig. 4. The dependence of $E_{\frac{1}{2}}$ and i_d for copper(II) polarographic reduction on butyrate concentration.

TABLE II

STABILITY CONSTANTS OF COPPER(II) BUTYRATE COMPLEXES AT 298.15°K

($I = 2$ mole dm^{-3} ($NaClO_4$)[a])

Method	*Polarography*		*Potentiometry*[16] *Num.*	*Spectrophotometry*[15] *Num.*
	Num.	*Graph.*		
1 g β_1°	1.83±0.03	1.85	1.85±0.01	1.89±0.02
1 g β_2°	2.54±0.09	2.53	2.49±0.01	2.76±0.08
1 g β_3°	2.93±0.12	2.94		
1 g β_4°	2.83±0.13	2.82		

[a] $c^0 = 1$ mole dm^{-3}, $y^0 = 1$; after the ± sign, 95% confidence intervals are quoted.

SUMMARY

Stability constants of copper(II) butyrate complexes were determined by polarography. Numerical treatment of polarographic data for quasi-reversible electrode processes was developed and yielded good estimates of reversible $E_{\frac{1}{2}}$ values. An improved three-electrode polarographic apparatus was constructed based on operational amplifiers.

REFERENCES

1 I. Piljac, B. Grabarić and I. Filipović, *J. Electroanal. Chem.*, 42 (1973) 433.
2 D. D. DeFord and D. N. Hume, *J. Amer. Chem. Soc.*, 73 (1951) 5321.
3 S. Nushi, I. Piljac, B. Grabarić and I. Filipović, *Croat. Chem. Acta*, 45 (1973) 453.
4 M. T. Kelley, D. J. Fisher and H. C. Jones, *Anal. Chem.*, 31 (1959) 1475.
5 M. T. Kelley, D. J. Fisher and H. C. Jones, *Anal. Chem.*, 32 (1960) 1262.
6 R. Bezmen and P. S. McKinney, *Anal. Chem.*, 41 (1969) 1560.
7 K. Momoki and H. Ogawa, *Anal. Chem.*, 43 (1971) 1664.
8 H. Matsuda, *Z. Elektrochem.*, 61 (1957) 487; 62 (1958) 977.
9 H. Matsuda and Y. Ayabe, *Z. Elektrochem.*, 63 (1959) 1164.
10 H. Matsuda, Y. Ayabe and K. Adachi, *Z. Elektrochem.*, 67 (1963) 593.
11 V. B. Vouk, P. K. Karmalkar and O. A. Weber, *Arh. Kem.*, 27 (1955) 9.
12 I. M. Kolthoff and Y. Okinaka, *J. Amer. Chem. Soc.*, 81 (1959) 2296.
13 F. M. Hawkridge and H. H. Bauer, *Anal. Chem.*, 44 (1972) 364.
14 I. Filipović and I. Piljac, *Croat. Chem. Acta*, 36 (1964) 181.
15 B. Grabarić, B. Mayer, I. Piljac and I. Filipović, *J. Inorg. Nucl. Chem.*, in press.
16 B. Grabarić, B. Mayer, I. Piljac and I. Filipović, submitted for publication to *Electrochim. Acta.*

Analytica Chimica Acta, 74 (1975) 155–161

ÉTUDE D'UNE ÉLECTRODE À MEMBRANE LIQUIDE SÉLECTIVE DES IONS IODURES EN MILIEU NITRATES ALCALINS FONDUS À 160°C

A. ROUCHOUSE, J. MESPLEDE et M. PORTHAULT

Laboratoire de Chimie Analytique III, Université Claude Bernard–Lyon I, 43 Bd du 11 Novembre 1918, 69621, Villeurbanne (France)

(Reçu le 24 Juillet 1974)

De nombreux groupements organophiles[1] sont utilisés comme échangeurs d'ions dans les électrodes à membrane liquide. Le mécanisme de réponse de l'électrode est basé sur l'extraction plus ou moins sélective d'un cation ou d'un anion selon la nature du groupement utilisé. L'emploi d'agents organophosphorés neutres en solution dans des polyphényles a déjà été utilisé pour la réalisation d'électrodes sélectives des ions cobalt(II) en milieu nitrates fondus à 160°C[2].

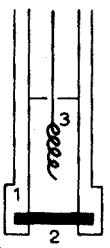

Fig. 1. Schéma d'une électrode à membrane liquide. 1, Corps en téflon; 2, membrane; 3, Ag/Ag(I) dans (Li–K)NO_3.

Nous proposons dans le présent travail l'étude d'une électrode à membrane liquide du type ci-dessus (Fig. 1). Le groupement organophile échangeur d'anions est le nitrate de tétraoctylphosphonium $(C_8H_{17})_4P^+NO_3^-$ (TOPN). À partir de la réponse de l'électrode aux ions iodures il nous est paru intéressant d'étudier l'interférence des ions Br^- et Cl^-, l'effet de la température et l'influence de la concentration en TOPN dans les polyphényles sur l'électrode.

PARTIE EXPÉRIMENTALE

Toutes les membranes utilisées ont été fabriquées suivant le même processus. La membrane est constituée par un mélange de graphite, de téflon (Soreflon 14 GA fourni par la société Ugine Kuhlmann) et d'une solution *ca.* 1 *M* de TOPN dans un binaire de méta et d'orthoterphényles P.F. = 80°C, solide à la température ambiante.

L'ensemble est soumis à une pression de 5t cm^{-2}. Ces membranes se présentent sous la forme de cylindres aplatis de diamètre 1 cm et d'épaisseur

1 mm. A la température de travail, les polyphényles sont liquides et on peut donc considérer que nous avons une membrane liquide à 160°C.

L'eutectique de nitrates fondus (Li–K)NO_3 (0,38 mole $LiNO_3$ pour 0,62 mole de KNO_3) est préparé et purifié suivant une méthode déjà décrite[4].

Le nitrate de tétra-n-octylphosphonium a été synthétisé suivant une méthode déjà décrite[5]. Son point de fusion est voisin de 65°C. L'électrode de référence est constituée par un fil d'argent plongeant dans une solution 10^{-2} molale de nitrate d'argent dans (Li–K)NO_3, contenu dans un tube de pyrex. La cellule de mesure peut être représentée de la manière suivante:

$$\underset{(\text{Li–K})NO_3}{Ag/AgNO_3\ 10^{-2}\text{ molale dans}} \parallel \underset{\text{membrane de verre}}{KX \text{ dans } (\text{Li–K})NO_3} \parallel \underset{\text{membrane liquide}}{AgNO_3\ 10^{-2}\text{ molale dans } (\text{Li–K})NO_3}/Ag$$

$X^- = Cl^-, Br^-, I^-$

Les f.e.m. sont mesurées avec un ionomètre digital Orion modèle 801 permettant des lectures à $\pm 0{,}1$ mV. Les expériences sont effectuées dans un four thermostaté à $\pm 0{,}5$°C pour la zone de température dans laquelle nous travaillons. Dans cette étude les lectures de potentiel sont faites environ toutes les 45 min, pour permettre la stabilisation des électrodes et être sûr d'atteindre l'équilibre.

RÉSULTATS ET DISCUSSION

Réponse de l'électrode aux ions Cl^-, Br^-, I^- à 160°C—Interférence

Conformément à nos résultats sur l'extraction des halogénures par le TOPN[4] l'électrode n'a présenté aucune réponse vis-à-vis des ions chlorures et bromures; par contre nous avons observé une variation linéaire des potentiels pris par l'électrode en fonction du logarithme de la concentration en ions iodures dans le domaine 10^{-3}–$5 \cdot 10^{-2}$ *m* avec une pente de 85 mV/pI^- proche de la pente théorique de 86 mV (Figs. 2 et 3). Ces deux figures montrent l'importance sur la reproductibilité du potentiel de l'électrode d'un certain nombre de paramètres comme l'état de l'eutectique, l'état de la solution de nitrate d'argent dans l'eutectique, la température, le temps laissé pour atteindre l'équilibre et le préconditionnement des électrodes. Lors d'essais réalisés sur des solutions séparées ces paramètres influent beaucoup plus, ce qui explique la moins bonne reproductibilité de réponse dans ce cas là.

La réaction d'échange d'ions qui a lieu au niveau de l'électrode s'écrit:

$$\overline{TNO_3} + X^- \rightleftarrows \overline{TX} + NO_3^- \qquad (1)$$

Les termes surlignés représentant les espèces en phase organique. Le potentiel pris par l'électrode est:

$$E = E_0 - 0{,}086 \log(a_{X^-} + K^{pot}_{XNO_3}\, a_{NO_3}) \qquad (2)$$

Dans cette expression $K^{pot}_{XNO_3}$ est la constante de sélectivité de l'électrode dont la valeur montre à quel point les ions NO_3^- interfèrent sur la réponse de l'électrode. Cette constante est inversement proportionnelle[4] à la constante d'extraction des différents halogénures K_{NO_3X}. Dans le cas des ions iodures $K^{pot}_{INO_3}$ doit être assez faible pour que le terme $K^{pot}_{INO_3}\, a_{NO_3}$ soit négligeable devant a_{I^-}.

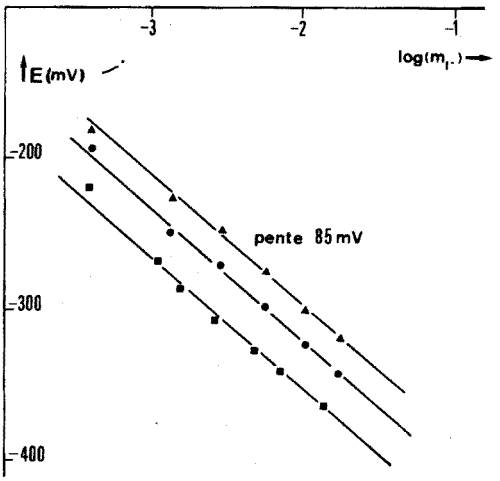

Fig. 2. Courbes de calibrage d'électrodes à membrane liquide à base de TOPN à 160°C (trois bains différents).

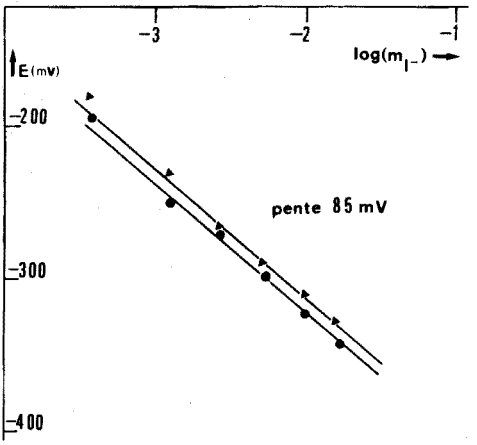

Fig. 3. Courbes de calibrage d'électrodes à base de TOPN à 160°C (deux membranes plongeant dans le même bain).

En ce qui concerne les ions chlorures et bromures on a $K_{NO_3Cl} < K_{NO_3Br} < K_{NO_3I}$ et le phénomène inverse se produit: $K^{pot}_{XNO_3} a_{NO_3}$ n'est plus négligeable, c'est pourquoi l'électrode ne répond pas aux ions chlorures et bromures mais garde un potentiel constant quelle que soit la molalité de l'eutectique en ions bromures et chlorures. Nous avons alors étudié l'interférence possible due aux ions chlorures et bromures sur la réponse de l'électrode. Pour cela à des solutions contenant une concentration bien déterminée soit en Cl^-, soit en Br^- nous avons suivi l'évolution du potentiel pris par l'électrode lors d'additions d'ions iodures dans le bain fondu. Les résultats sont reportés sur la Fig. 4. Les ions bromures et chlorures n'interfèrent pratiquement pas. A partir de ces courbes nous avons évalué les constantes de sélectivité K^{pot}_{ICl} et K^{pot}_{IBr} par la méthode des solutions mélangées[5]. Nous avons ainsi trouvé:

$$K^{pot}_{IBr} = 7{,}3 \cdot 10^{-2} \quad \text{et} \quad K^{pot}_{ICl} = 2{,}4 \cdot 10^{-3}$$

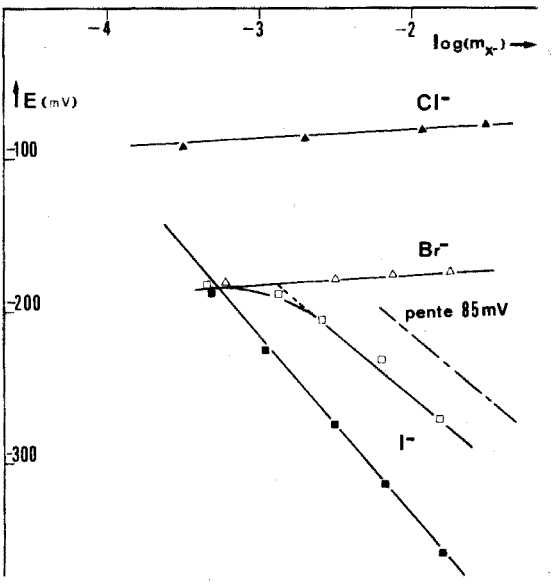

Fig. 4. Courbes de calibrage de l'électrode à base de TOPN—interférence des ions bromures et chlorures.

Réponse de l'électrode en fonction de la température

L'influence de la température sur la réponse de l'électrode aux ions iodures est donnée par la Fig. 5, les températures étant 140°C, 160°C, 180°C et 200°C.

De l'analyse de ces courbes il ressort que l'électrode est encore utilisable en milieu fondu jusqu'à 180°C. Au-dessus de cette température aucune réponse n'a été observée. Ce phénomène peut s'expliquer par le début de dégradation du TOPN vers ces températures, ce qui a été observé par Tan et Irvine[6]. D'autre

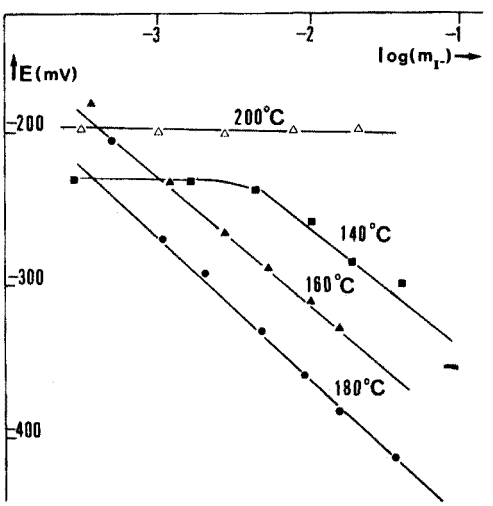

Fig. 5. Étude de l'influence de la température sur la réponse de l'électrode à base de TOPN—pentes obtenues: 140°C 79 mV/pI$^-$; 160° 86 mV/pI$^-$; 180°C 92 mV/pI$^-$.

part on peut penser que, même si le TOPN était très stable à 200°C, on risquerait de ne constater aucune variation de potentiel du fait de la conception de ces membranes. En effet elles demeurent assez fragiles même à 160°C, et vers des températures de plus en plus élevées elles ne doivent plus posséder de bonnes propriétés mécaniques et ainsi ne pas demeurer assez résistantes.

Aux autres températures les pentes des droites restent en bon accord avec les valeurs théoriques. A 180°C nous augmentons le domaine de linéarité puisque la solubilité de l'iodure de potassium que l'on ajoute est plus forte. A 140°C le domaine d'utilisation de cette électrode est assez restreint: l'électrode ne répond qu'à partir d'une certaine activité en ions iodures ($5 \cdot 10^{-3}$ *m*), et vers les plus fortes concentrations nous sommes vite limités par la solubilité de l'iodure de potassium.

Influence de la concentration en TOPN dans la membrane

L'influence de ce paramètre (concentration en agent organique actif) a déjà été étudiée[7] à l'aide d'une électrode à membrane liquide à 25°C. Dans notre cas elle se traduit par les courbes de la Fig. 6 se rapportant à une variation de

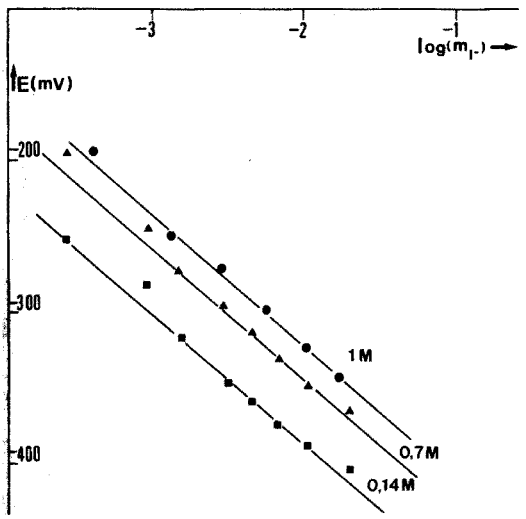

Fig. 6. Étude de l'influence de la concentration en TOPN dans la membrane sur la réponse de l'électrode.

concentration en TOPN dans la membrane de 0,14 à 1 *M*. Quelle que soit la concentration en agent extractant l'électrode répond linéairement à l'accroissement de l'activité en ions iodures avec des pentes voisines de la valeur théorique. Le mécanisme de réponse reste donc le même. La seule modification que l'on enregistre est le décalage systématique des potentiels de réponse vers les valeurs plus négatives lorsque la concentration en TOPN diminue. Nous observons ainsi une translation des droites de réponse de 65 mV quand nous passons de (TOPN)=1 *M* à (TOPN)=0,14 *M* qui peut être attribué à la variation du potentiel standard E_0 de l'électrode.

La théorie de Nicolsky[8] conduit pour le potentiel d'interface membrane–solution à l'expression:

$$E = \text{constante} - RT/F\ (\log a_i + K_{ij}/C_o) \quad (3)$$

Dans le cas présent $i = I^-$, $j = NO_3^-$, et $C_o = (TOPN)$ terme qui est constant pour une membrane donnée. Dans l'expression du potentiel final de la membrane, E_0 est de la forme:

$$E_0 = \text{constante} + RT/F \log C_o \quad (4)$$

Le terme $RT/F \log C_o$ traduit la contributon de la concentration en TOPN à la valeur E_0 et de ce fait à la valeur des potentiels mesurés.

Pour des concentrations en TOPN allant de 0,14 à 1 M son ordre de grandeur est de 0,086 log 1/0,14 donc proche de 75 mV en théorie. Dans notre cas nous trouvons bien un décalage de cet ordre. D'autre part d'après l'expression ci-dessus (3), C_o agit dans le sens inverse de a_i. L'augmentation de C_o doit conduire à des valeurs de E mesurées moins négatives. C'est encore ce que nous observons.

CONCLUSION

A partir des résultats obtenus sur l'extraction d'ions halogénures par le TOPN nous avons pu réaliser une électrode à membrane liquide sélective des ions iodures en milieu $LiNO_3$–KNO_3. L'étude de ses différents paramètres s'est montrée particulièrement intéressante du point de vue théorique. D'une part la sélectivité de l'électrode a confirmé le bon pouvoir extractant du nitrate de tétraoctylphosphonium vis à vis des ions iodures. D'autre part les résultats obtenus confirment le mode de fonctionnement de cette électrode. Le comportement d'électrodes de ce type dans les milieux fondus demeure tout de même assez complexe et n'autorise iusqu'à présent que peu d'applications pratiques.

RÉSUMÉ

Une électrode à membrane liquide, basée sur le principe de l'extraction d'ions halogénures à partir de l'eutectique (Li–K)NO_3 à 160°C par le nitrate de tétraoctylphosphonium (TOPN) présente une réponse linéaire et sélective vis à vis des ions iodures. Les différents paramètres pouvant influer sur le comportement de l'électrode (interférence de Br^- et Cl^-, température, concentration en TOPN dans la membrane) one été successivement examinés. La réponse de l'électrode a été interprétée par un simple équilibre d'échange d'anions dans la phase organique. Les ions Br^- et Cl^- n'interfèrent pas, ce qui est dû probablement aux faibles constantes de sélectivité K^{pot}_{IBr} et K^{pot}_{IC1} de l'électrode. En température nous sommes limités vers 180°C par la stabilité de l'agent extractant et la solidité de la membrane. La variation de la concentration de l'agent extractant (TOPN) en phase organique entraîne un décalage des potentiels mais n'affecte pas la linéarité de réponse de l'électrode.

SUMMARY

A liquid-exchanger membrane electrode based on extraction of halides from

a $LiNO_3$–KNO_3 eutectic at 160°C by tetraoctylphosphonium nitrate (TOPN) provides a linear selective response to iodide ions. The parameters affecting the electrode behaviour (interference of other halides, temperature, TOPN concentration) have been studied. The response of the electrode is interpreted as a simple ion-exchange equilibrium in the organic phase. Bromide and chloride do not interfere. The upper temperature limit is 180°C, because of the instability of the extraction agent and the membrane. Variation in the TOPN concentration in the organic phase causes a potential shift, but does not affect the linearity of the response.

BIBLIOGRAPHIE

1 J. W. Ross, dans R. A. Durst (Éd.), *Ion Selective Electrodes*, N.B.S. Spécial Publication No. 314, 1969, pp. 70, 71.
2 J. Mesplede et M. Porthault, *I.U.P.A.C., Cardiff*, Paper No. 37, 9 avril 1973.
3 A. Rouchouse, J. Mesplede et M. Porthault, *Bull. Soc. Chim. Fr.*, sous presse.
4 J. Mesplede et M. Porthault, *J. Inorg. Nucl. Chem.*, 33 (1971) 4275.
5 G. J. Moody et J. D. R. Thomas, dans Merrow (Ed.), *Selective Ion Sensitive Electrodes*, Merrow Technical Library, 1971.
6 Z. C. H. Tan et J. W. Irvine, *Inorg. Chem.*, 11 (1972) 1701.
7 P. R. Danesi, G. Scibona et B. Scuppa, *Anal. Chem.*, 43 (1971) 1892.
8 B. P. Nicolsky, *Acta Physicochim. U.S.S.R.*, 7 (1937) 597.

Analytica Chimica Acta, 74 (1975) 163–175

COMPARISON OF FUNDAMENTAL AND SECOND-HARMONIC A.C., AND NORMAL, DERIVATIVE AND DIFFERENTIAL PULSE LINEAR-SWEEP AND STRIPPING VOLTAMMETRIC METHODS

A. M. BOND

Department of Inorganic Chemistry, University of Melbourne, Parkville 3052, Victoria (Australia)

(1st Received 1st March 1974; In revised form, 6th June 1974)

As an alternative to d.c. polarography, the technique of linear-sweep voltammetry at stationary electrodes has been used widely[1–6]. With the widespread upsurge of interest in environmental and pollution problems, the technique of stripping analysis or inverse voltammetry has attracted considerable attention because of its inherent sensitivity, particularly for determining heavy metal pollutants such as lead, cadmium, etc.[7,8]. Most of the papers in this field still incorporate the use of d.c. linear-sweep potential scans in the stripping process.

However, certain aspects of the nature of the current–voltage curve in d.c. linear-sweep or stripping techniques are not very convenient. Derivative techniques have been employed to minimize some of the problems[9–13], but considerable limitations still remain.

Somewhat surprisingly perhaps, practical endeavours to move to linear-sweep or inverse a.c. voltammetry at stationary electrodes or at the dropping mercury electrode when the scan is synchronized to the drop time, have been rather restricted, despite the excellent survey of theory and experiment presented with respect to the fundamental harmonic by Underkofler and Shain[14] almost ten years ago, and the literature on practical a.c. voltammetry is rather sparse[14–26]. Similar observations apply to applications of pulse voltammetry at stationary electrodes where obviously worthwhile advantages have been pointed out for some time[27–29], but practical applications are only now starting to appear, particularly in the inverse or stripping mode[29–33]. In this paper, the methods of fundamental and second-harmonic a.c. voltammetry with and without phase-selective detection, and normal, derivative and differential pulse methods are compared, and the situations under which one would use an a.c. method in preference to a pulse method or *vice versa* are considered.

EXPERIMENTAL

Instrumentation and electrodes

Total alternating current voltammograms were recorded with Metrohm AC Modulator E393 used in conjunction with Metrohm Polarecord E261. An alternating potential of 10 mV r.m.s. at 50 Hz and a scan rate of 1 V min^{-1} were used. The conversion of this system to a three-electrode system is described elsewhere[34].

Phase-selective fundamental and second-harmonic a.c. voltammograms were recorded with PAR Electrochemistry System Model 170. Second-harmonic detection was achieved by electronic multiplication of the a.c. reference signal[35]. The alternating potential used was 1, 5 or 10 mV peak-to-peak at frequencies between 10 and 1,100 Hz. Scan rates of potential up to 200 mV s^{-1} were used and a 3-electrode system was employed. Normal, derivative and differential pulse voltammograms were also recorded with the PAR Electrochemistry System. The potential was applied for about 45 ms at 0.05, 0.1, 0.5, 1.0, 20 or 5.0-s intervals and a current sampling period of 5 ms at the end of the pulse period was used.

For the linear-sweep work at a dropping mercury electrode (DME), synchronization of the drop time and initiation of the potential scan were achieved with PAR Linear-Sweep Accessory, Model 174/51. Details of the use of this accessory in a.c. and other formats will be reported elsewhere[36].

In aqueous media, Ag/AgCl (5 *M* or 1 *M* NaCl) or SCE reference electrodes were used. Reference electrodes and other details of the non-aqueous work are reported in the Tables. Hanging mercury drop electrodes (HMDE) (Metrohm BM-503), platinum, glassy carbon (Tokai), wax-impregnated graphite (PAR) and dropping mercury electrodes were used as working electrodes in both aqueous and non-aqueous media.

Chemicals

All materials used were of reagent-grade purity. Compounds used were prepared according to methods described in the literature.

RESULTS AND DISCUSSION

Figure 1a shows an a.c. polarogram of a mixture of several elements. Figure 1b shows the inverse linear-sweep a.c. voltammogram at a hanging mercury drop electrode of an equivalent solution diluted 100-fold. Figure 2 shows the inverse linear-sweep d.c. voltammogram of the same solution as used for Fig. 1b. Figure 3 shows phase-selective second-harmonic and normal derivative and differential pulse voltammograms of 10^{-4} *M* cadmium solution in 1 *M* hydrochloric acid.

These diagrams clearly demonstrate the advantages inherent in the linear-sweep a.c. and pulse methods over their d.c. counterparts with respect to the nature of the readout. It can also be noted from these Figures that actual measurement of the parameters of interest, except for normal pulse voltammetry, is facilitated by the nature of the almost symmetrical current–potential curve. The peak height, I_p, (or peak-to-peak height in second-harmonic voltammetry) which is proportional to concentration, can be measured directly off the graph for each electrode process, as can the peak potential, E_p. In the d.c. case, the current does not return to zero at potentials beyond the peak current, and difficult, if not arbitrary, procedures for measuring peak currents must frequently be employed.

The reversible theory for the various voltammetric methods has been described in the literature[14,26–28]. Probably the result providing the greatest simplification and of most relevance to the analytical chemist is that equations

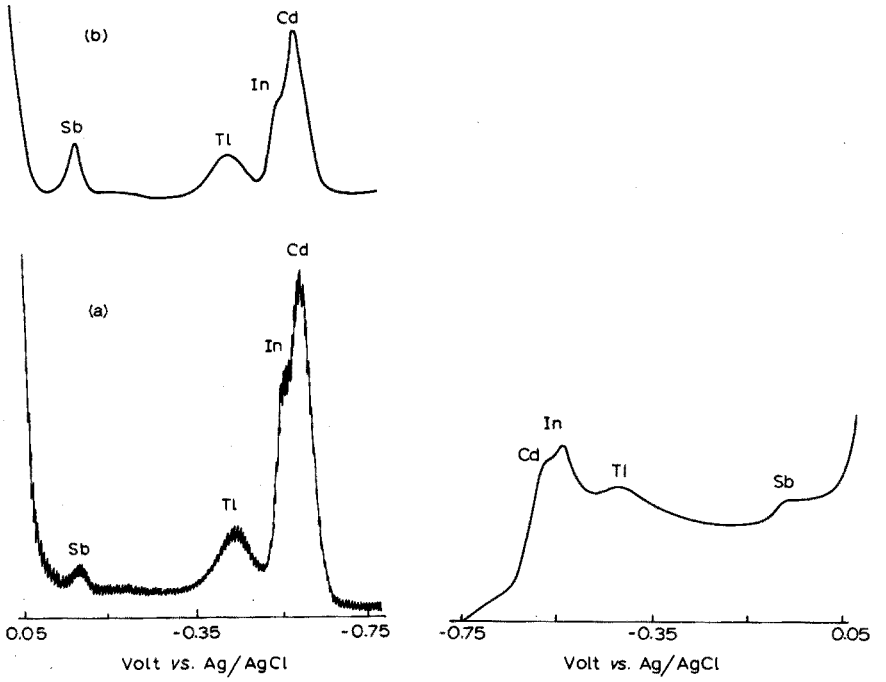

Fig. 1. Comparison of a.c. polarograms and inverse a.c. voltammograms for multicomponent systems in 1 *M* HCl. (a) Total a.c. polarogram recorded at DME with controlled drop time of 0.24 s. $\Delta E = 10$ mV, r.m.s. Frequency = 50 Hz. $[Cd(II)] \simeq 1.5 \cdot 10^{-4}$ *M*; $[In(III)] \simeq 5 \cdot 10^{-5}$ *M*; $[Tl(I)] \simeq 1 \cdot 10^{-4}$ *M*; $[Sb(III)] \simeq 5 \cdot 10^{-6}$ *M*. (b) Inverse a.c. voltammogram recorded at HMDE. $\Delta E = 10$ mV, r.m.s. Frequency = 50 Hz, Electrolysis time 3 min at −0.75 V *vs.* Ag/AgCl. Scan rate = 1 V min^{-1}. Solution in (a) diluted 100-fold.

Fig. 2. Inverse d.c. voltammogram for multicomponent systems as recorded at a HMDE. Same solution and conditions as Fig. 1(b) except d.c. recorded.

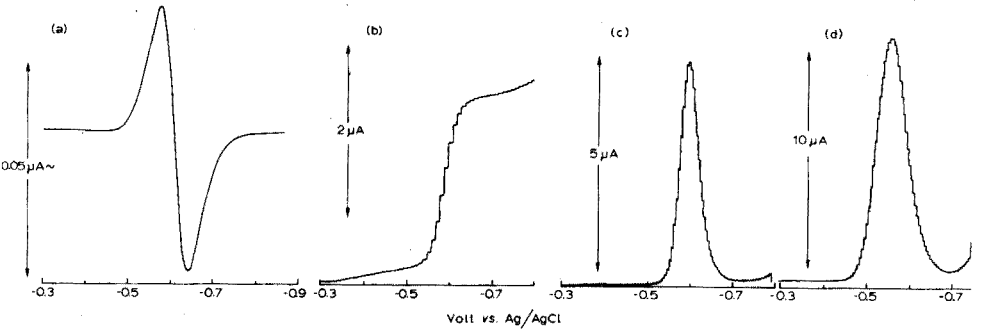

Fig. 3. Phase-selective second-harmonic a.c. and pulse voltammograms of $1 \cdot 10^{-4}$ *M* Cd(II) in 1 *M* HCl at HMDE. (a) Phase-selective second-harmonic voltammogram: in-phase component, amplitude = 10 mV p–p at 400 Hz. Scan rate = 20 mV s^{-1}. (b) Normal pulse voltammogram. Duration between pulses = 0.5 s. Scan rate = 20 mV s^{-1}. (c) "Derivative" pulse voltammogram. Duration between pulses = 0.5 s. Scan rate = 10 mV s^{-1}. (d) Differential pulse voltammogram. Pulse amplitude = 50 mV. Scan rate = 10 mV s^{-1}.

and data describing the current–potential curve are analogous to those derived for polarography. This is because, for a reversible electrode process, it is the frequency domain of the a.c. experiment and the pulse duration of the pulse experiment which basically govern the time scale of the experiment at a DME rather than the drop time. At a stationary electrode the frequency or pulse duration still determines the time scale of the voltammetric experiment under suitable conditions. However, in extrapolating from d.c. polarography to d.c. voltammetry, the parameter governing the time scale changes from drop time to scan rate, and the two d.c. techniques are therefore substantially different. The above, of course, does not refer to situations where the electrode process is governed by kinetic phenomena.

Soluble oxidized and reduced forms

The equation for a reversible fundamental harmonic a.c. electrode polarographic wave is given by the expression[37–39]

$$E_{dc} = E_p + \frac{2RT}{nF} \ln \left\{ \left(\frac{I_p}{I} \right)^{\frac{1}{2}} \pm \left(\frac{I_p - I}{I} \right)^{\frac{1}{2}} \right\} \tag{1}$$

provided that the amplitude of the alternating potential is $\leqslant 8/n$ mV, where E_{dc} = d.c. potential, E_p = peak or summit potential, which is equivalent to the d.c. $E^r_{\frac{1}{2}}$ value, I = alternating current at potential E, and I_p = peak or maximum value of the alternating current.

This equation can be rearranged in a format, which is most suitable for computation of data[38]

$$\frac{I}{I_p} = 4 \frac{\exp[(nF/RT)(E - E_p)]}{[1 + \exp(nF/RT)(E - E_p)]^2} \tag{2}$$

This equation can also readily be derived from eqn. (10) given by Underkofler and Shain[14]. An equivalent type of equation is also available for the second-harmonic experiment[38].

The equation for a derivative pulse polarogram or small amplitude differential pulse polarogram is also given by eqns. (1) or (2). The normal pulse polarogram can be described by the equation

$$E = E_{\frac{1}{2}} + \frac{RT}{nF} \ln \frac{i_l - i}{i} \tag{3}$$

where i_l is the limiting current and i the current at potential E. Extensive studies in acetone of the reversible electrode process

$$Cp_2V(IV)L + e \rightleftharpoons Cp_2V(III)L$$

(where Cp is cyclopentadienyl, and L is dibutylxanthate) verified the validity of using eqns. (1), (2) and (3). Figure 4 shows the fundamental harmonic linear-sweep a.c. curves recorded at mercury, platinum and glassy carbon electrodes. Theoretical data points are included for comparison purposes. The exact shape of the current–voltage curve was shown to be slightly influenced by the geometry of the electrode, presumably reflecting the influence of non-linear diffusion[37]. Calculations of $E^r_{\frac{1}{2}}$ at the various electrodes and by different techniques also confirm the theory. Results are tabulated in Table I.

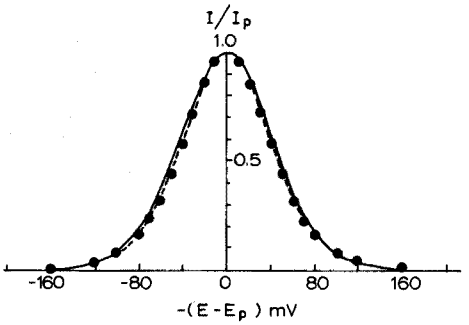

Fig. 4. Theory *versus* experiment correlation for equation describing reversible a.c. electrode process. All curves normalized. $\Delta E = 5$ mV p–p. Frequency = 225 Hz. Scan rate = 50 mV s^{-1}. (●) Theory, a.c. polarogram at DME, a.c. voltammogram at HMDE. (——) Pt wire electrode and (-----) planar glassy carbon electrode for electrode process. $[Cp_2V(IV)L]^+ \rightleftharpoons Cp_2V(III)L$ in acetone (0.1 *M* Et_4NClO_4).

LE I

MINATION OF THEORY FOR A REVERSIBLE ELECTRODE PROCESS

V(IV)L + $e \rightleftharpoons Cp_2V(III)L$, where both the oxidized and reduced forms are soluble. Concentration $Cp_2V(IV)L$ = *M*[a])

trode	$-E_{\frac{1}{4}}^{r}(V)$ *vs. Ag/AgCl*					
	D.c.	*A.c. (harmonic)*[b]		*Pulse*		
		Fundamental	*Second*	*Normal*	*Derivative*	*Differential*[c]
E (polarography)[d]	0.288	0.288	0.288	0.289	0.289	0.290
E (linear sweep)[e]	—	0.290	0.288	—	—	—
DE	—	0.288	0.289	0.290	0.289	0.291
ire	—	0.291	0.290	0.289	0.291	0.292
sy carbon	—	0.292	0.290	0.291	0.291	0.293
hite	—	0.290	0.290	0.291	0.291	0.293

= cyclopentadienyl, L = butylxanthate, solvent = acetone (0.1 *M* Et_4NClO_4), $T = 20°C$, reference electrode = Ag/AgCl
etone, 0.1 *M* LiCl).
ernating potential = 10 mV p–p at 100 Hz.
ıplitude = 5 mV.
op time = 2 s.
ın rate 100 mV s^{-1}, commenced 2 s after drop initially formed.

Amalgam formation and inverse voltammetry

In Figs. 1–3, several systems where the electrode process involves amalgam formation are presented. The electrode process is $M(X) + Xe \rightleftharpoons M(amalgam)$, and a hanging mercury drop electrode was used. With these systems, and those listed in Table II, slight departures from eqns. (1)–(3) were evident. For example, with lead and cadmium, the half-width in the fundamental harmonic stripping a.c. method, was (50 ± 2) mV, in 0.5 *M* KNO_3, compared with a theoretical value of $90/n$ or 45 mV at 25°C. Results with different systems with $n = 1$, 2 or 3 showed that where amalgam formation is involved the half-width is experimentally given by

the expression $(100 \pm 8)/n$ mV. With the HMDE used in this work scan rate dependence on half-width was indicated, particularly in the stripping mode. However, the half-width still provides a simply measured quantitatively useful parameter to characterize a particular electrode process. Figure 3 clearly shows the non-equivalence of the positive and negative peaks in the second-harmonic experiment. The influence of amalgam formation in voltammetry has been described in the literature[40-42] and differences to the previously described case where no amalgam formation occurs are not unexpected.

Limits of detection and calibration curves

For the series of electrode processes cited in Table II, linear calibration curves of peak height or limiting current (for normal pulse) *versus* concentration were found over at least the range 10^{-3}–10^{-6} *M*. Figure 5 shows the results for

TABLE II

ELECTRODE PROCESSES USED AT A HANGING MERCURY DROP ELECTRODE TO STUDY AMALGAM FORMATION AND TO EVALUATE OTHER ASPECTS OF A.C. AND PULSE VOLTAMMETRY AT STATIONARY ELECTRODES

Electrode process	*Medium*
Pb(II)+2 $e \rightleftharpoons$ Pb(amalgam)	1 *M* HCl, 0.5 *M* KNO_3, 1 *M* $NaClO_4$
Cd(II)+2 $e \rightleftharpoons$ Cd(amalgam)	1 *M* HCl, 0.5 *M* KNO_3, 1 *M* $NaClO_4$
Tl(I)+$e \rightleftharpoons$ Tl(amalgam)	1 *M* HCl, 1 *M* $NaClO_4$
Bi(III)+3 $e \rightleftharpoons$ Bi(amalgam)	1 *M* HCl
Sb(III)+3 $e \rightleftharpoons$ Sb(amalgam)	1 *M* HCl
In(III)+3 $e \rightleftharpoons$ In(amalgam)	1 *M* HCl
Sn(II)+2 $e \rightleftharpoons$ Sn(amalgam)	5 *M* HCl
Cu(I)+$e \rightleftharpoons$ Cu(amalgam)	1 *M* HCl
Cu(II)+2 $e \rightleftharpoons$ Cu(amalgam)	1 *M* $NaNO_3$

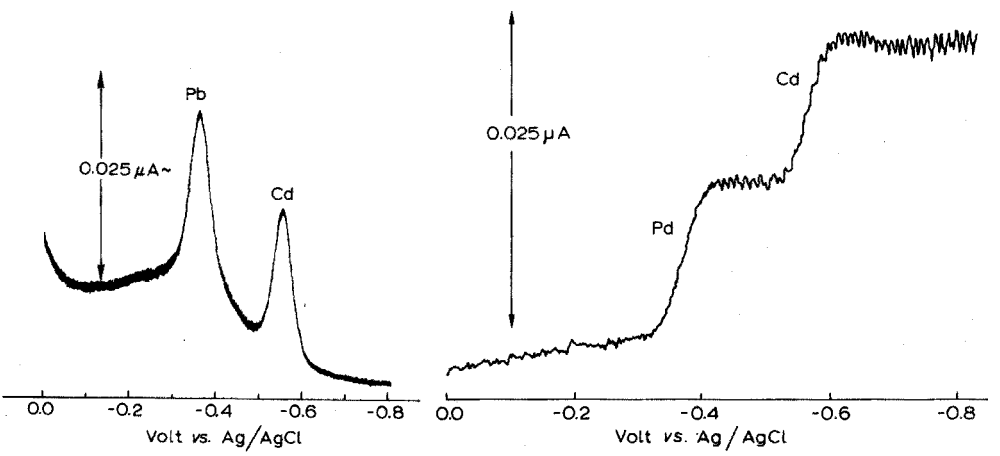

Fig. 5. Comparison of phase-selective fundamental harmonic a.c. and normal pulse voltammograms for 10^{-6} *M* Pb(II) and 10^{-6} *M* Cd(II) solution in 0.5 *M* KNO_3. (a) Fundamental harmonic a.c. Amplitude = 10 mV, p–p at 80 Hz. (b) Normal pulse. Duration between pulses = 5 s.

TABLE III

LIMITS OF DETECTION FOUND AT A HMDE FOR LEAD(II) AND CADMIUM(II) IN 0.5 *M* KNO_3

(For the inverse or stripping work a 6-min electrolysis was used with 5-min stirring and 1 min without stirring.)

Technique	*Limit of detection*				*Comments*
	Linear-sweep		*Inverse (stripping)*		
	Pb(II) (M)	*Cd(II) (M)*	*Pb(II) (M)*	*Cd(II) (M)*	
D.c.	$1 \cdot 10^{-6}$	$1 \cdot 10^{-6}$	$2 \cdot 10^{-8}$	$2 \cdot 10^{-8}$	
Normal pulse	$2 \cdot 10^{-7}$	$2 \cdot 10^{-7}$	$5 \cdot 10^{-9}$	$5 \cdot 10^{-9}$	Non-linear baseline at low concentration in stripping work restricted limit of detection
"Derivative" pulse	$8 \cdot 10^{-7}$	$8 \cdot 10^{-7}$	$4 \cdot 10^{-8}$	$4 \cdot 10^{-8}$	Signal processing involving taking a difference introduces more noise into signal, thereby limiting sensitivity. Sloping baseline as in normal pulse stripping also limited sensitivity
Differential pulse	$1 \cdot 10^{-7}$	$1 \cdot 10^{-7}$	$1 \cdot 10^{-9}$	$1 \cdot 10^{-9}$	Amplitude, 50 mV
Fundamental harmonic (total)	$5 \cdot 10^{-5}$	$5 \cdot 10^{-5}$	$1 \cdot 10^{-8}$	$1 \cdot 10^{-8}$	A.c. 10 mV at 50 Hz
Fundamental harmonic	$2 \cdot 10^{-7}$	$2 \cdot 10^{-7}$	$2 \cdot 10^{-9}$	$2 \cdot 10^{-9}$	In-phase component, 10 mV p–p, 80 Hz
Second harmonic	$3 \cdot 10^{-7}$	$3 \cdot 10^{-7}$	$2 \cdot 10^{-9}$	$2 \cdot 10^{-9}$	In-phase component, 10 mV p–p at 400 Hz. Magnitude of current small, and noise limited sensitivity. Larger amplitude of alternating potential should improve detection limit

a 10^{-6} *M* solution of cadmium and lead with phase-selective fundamental harmonic and pulse techniques. The presence of these two elements was barely detectable with d.c. linear-sweep voltammetry at this concentration. The limit of detection in general was found to be in the $5 \cdot 10^{-7}$–10^{-7} *M* region when phase-selective detection was used in a.c. experiments and with normal or differential pulse experiments, and indeed similar to the limit of detection found with polarography, as would be expected from theoretical predictions. Limits of detection for the determination of lead and cadmium in 0.5 *M* potassium nitrate are given in Table III.

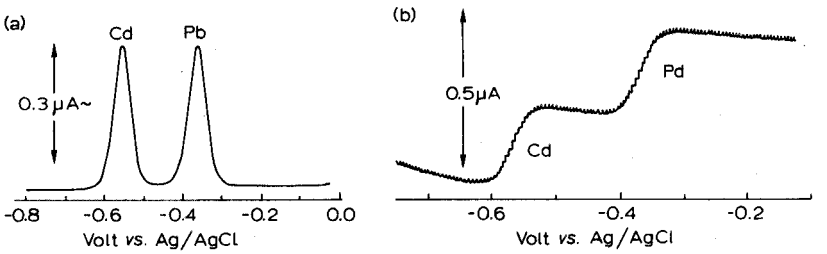

Fig. 6. Comparison of phase-selective fundamental harmonic a.c. and pulse stripping voltammograms for 10^{-6} *M* Pb(II) and 10^{-6} *M* Cd(II) in 0.5 *M* KNO_3. Electrolysis time = 6 min, with stirring for first 5 min. (a) Fundamental harmonic a.c. Amplitude = 10 mV, p–p at 80 Hz. (b) Normal pulse. Duration between pulses = 0.5 s.

Figure 6 shows the same solutions as in Fig. 5, but examined by the inverse or stripping mode. The peaks are obviously extremely well defined at this level. With a 6-min electrolysis period, and the elements listed in Table II, detection limits of 10^{-8}–10^{-9} *M* were observed. Table III gives detailed data for lead and cadmium in 0.5 *M* KNO_3. Provided that the electrode process was reversible, this represented improvement of at least an order of magnitude over d.c. stripping analysis. Linear calibration curves were obtained on all solutions examined. Thus the method of standard additions frequently employed in d.c. anodic stripping voltammetry is also valid for these techniques.

Resolution

Apart from the obvious advantages listed above with respect to limit of detection, the greatest asset of many of the a.c. and pulse techniques compared with d.c. voltammetry is found in the area of resolution. With the exception of normal pulse voltammetry, electrode processes occurring at more negative potentials than another electrode process can be treated independently (provided that there is no actual overlap of the two waves or chemical interference), and measurement of the more negative process is greatly facilitated. By contrast, the reproducibility and precision of measurement in the d.c. linear-sweep mode drops off sharply if the presence of a more positive electrode process has to be considered. Analogous considerations also apply to comparisons made with anodic stripping voltammetry.

The use of an approach described previously[43,44] for a.c. polarography enables resolution to be defined as being the tolerable concentration ratio of a neighbouring electrode process, such that the peak height of the electrode process being

TABLE IV

COMPARISON OF RESOLUTION IN LINEAR-SWEEP VOLTAMMETRY[a,b]

Technique	*More negative process overlaps more positive* $(\Delta E_{\frac{1}{4}})n$ *(mV)*	*More positive process overlaps more negative* $(\Delta E_{\frac{1}{4}})n$ *(mV)*
D.c. linear-sweep	168	1840[c], 1780[d]
First derivative d.c. linear-sweep	148	857[c], 837[d]
Second derivative d.c. linear-sweep	188, 143[e]	275
D.c. polarography or normal pulse voltammetry	236	—
Fundamental harmonic a.c., derivative pulse, differential pulse (small amplitude) voltammetry	154	154
Second harmonic a.c. voltammetry	144[e]	144[e]

[a] D.c. data are taken from ref. 45 which should be consulted for further details.
[b] Both electrode processes are reduction and $n_1 = n_2 = n$ in the example given. Equal concentrations of both species are present. $\Delta E_{\frac{1}{4}}$ is the minimum separation of $E_{\frac{1}{4}}$ or E_p required for 1% overlap in the two component system.
[c] Planar diffusion.
[d] Spherical diffusion.
[e] First peak used for analysis.

measured is unaltered by less than 1% by the presence of another depolarizer. Table IV defines resolution, within the above definition.

Comparison of a.c. and pulse techniques

The use of linear-sweep techniques at a dropping mercury electrode when the scan is synchronized to the electrode is highly attractive from time-saving and other points of view[1,2,5]. However, this method requires fast scan rates of potential so that the potential sweep is completed with little growth of the mercury drop. Phase-selective a.c. methods can be used very simply at fast scan rates, whilst maintaining the discrimination against charging current. Indeed, for the second-harmonic a.c. version there is virtually no charging current contribution, and this method is particularly favourable for linear-sweep techniques at a DME, as sloping base-lines arising from drop growth are non-existent[36]. Pulse methods require current-sampling at particular points in time rather than continuous monitoring of current. Furthermore, the mode of discrimination against charging current in normal pulse polarography is not favoured by the use of fast scan rates. The performance and ease of undertaking the experiment therefore recommend the use of a.c. methods in preference to pulse methods when linear-sweep voltammetry at a DME is being considered.

In the general context, where the use of high scan rates and time saving are not required, other considerations become of paramount importance. For the determination of a reversible electrode process such as that of cadmium or lead in 0.5 *M* KNO_3 considered previously (see Table III), the limits of detection and reproducibility with phase-selective a.c., normal pulse and differential pulse methods leave little to choose between them. Further, all give linear calibration curves over wide concentration ranges. The resolution of the normal pulse method counts

against this technique in multi-component analysis. In general, the sigmoidal rather than peak-shaped curve of the readout of this technique places it at a disadvantage. However, under conditions where adsorption or other surface phenomena cause analytically undesirable complications in the current–voltage curve[27,33,46], the normal pulse method can prove most advantageous. The potential in normal pulse voltammetry is held at a value where no redox reaction occurs, except for the short duration of the application of the pulse; this prevents accumulation of electrode reaction products, including potentially adsorbing materials, during the course of recording the current–potential curve. In many respects, the normal pulse technique simulates the advantageous conditions operative at a DME in that a periodic renewal of the electrode surface condition occurs.

The major reason for choosing either an a.c. or pulse method, however, will usually be decided by the considerable difference between their behaviours towards the reversibility of the electrode process. A.c. methods, particularly the second-harmonic version, are remarkably sensitive to departures from reversibility. Thus, the determination of a particular species giving rise to a reversible electrode process, in the presence of a complex mixture, is much more likely to be possible by a.c. techniques. However, to counterbalance this, many more of the entities in the complex mixture are likely to be determinable at the trace level by pulse voltammetry, if the required resolution can be achieved. The complementary rather than competitive nature of the two electroanalytical methods is therefore seen.

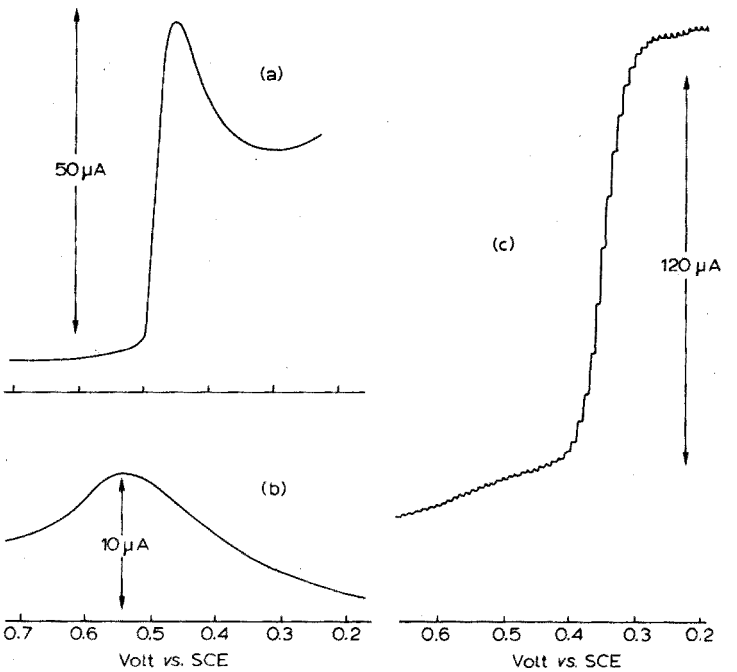

Fig. 7. Linear-sweep d.c., a.c. and pulse voltammograms of the $Hg(II) \overset{2e}{\rightleftharpoons} Hg(0)$ electrode process at th glassy carbon electrode in 50% HF. $[Hg(II)] = 5 \cdot 10^{-3}$ *M*. Temperature = 13.8°C. Details available i reference 33.

All the previous Figures shown have involved reversible electrode processes. Figure 7 shows a comparison of d.c., a.c. and pulse voltammograms for the $Hg(II) + 2e \overset{2e}{\rightleftharpoons} Hg(0)$ electrode process at a glassy carbon electrode in 50% hydrofluoric acid[33]. For this irreversible complex process involving deposition of mercury metal, the superiority of the pulse method is most apparent. Generally, when deposition of a product or film onto an electrode occurs, normal pulse voltammetry is the preferred technique.

Practical examples of HMDE and thin-film stripping techniques

A series of comparative stripping studies, with all the electroanalytical methods described in this paper, based on both thin-film mercury electrodes and HMDE's has recently been undertaken in this department[47]. Brief mention of the results of one such study illustrates the complementary nature of the various approaches.

Zinc sulphate electrolyte is used for the electrolytic production of zinc and the presence of trace impurities can have considerable influence on the efficiency of the industrial process. Samples consisted of an almost saturated solution of zinc sulphate (pH 1) and Cd, Tl, Cu and Sb were to be determined. Samples spiked with known concentrations were also provided and the concentration range to be covered was approximately $5 \cdot 10^{-8}$–10^{-5} *M*. Thus, sensitivity was not a limiting factor with any of the methods. Cd, Cu and Tl could in principle be determined directly in the electrolyte. At the HMDE, cadmium could equally well be determined by a.c. or differential pulse methods. For copper, a sloping baseline was found in the a.c. methods, but not with the differential pulse method, which mitigated against the former approach. For thallium, the resolution from cadmium was superior with a.c. methods, and this provided the preferred approach. Even then, resolution was restricted to favourable concentration ratios and addition of EDTA was frequently required to separate the waves. For antimony, the electrolyte was diluted (1:1) with concentrated hydrochloric acid. Excellent pulse or a.c. stripping waves were obtained, and either method could be used.

Thin-film studies were also undertaken at wax-impregnated and glassy carbon electrodes using both *in situ* mercury deposition[48] and pre-formed electrodeposited mercury films. The theory for stripping voltammetry at thin-film electrodes is entirely different from the HMDE case and previous conclusions are no longer valid. The d.c. method itself gave a peak-shaped curve and extremely high sensitivity. Contrary to stripping studies at the HMDE, little or no advantage was found in using non-d.c. methods. However, in the zinc sulphate electrolyte at the higher concentrations, non-linear calibration curves and intermetallic interferences were observed. Furthermore, antimony could not be satisfactorily determined. The electrode process used is $Sb(III) \rightleftharpoons Sb(amalgam)$; antimony exists predominantly in the pentavalent oxidation state in the electrolyte and apparently the reduction to the trivalent state does not proceed readily at thin-film electrodes. Thus, despite the inherently higher sensitivity and greater resolution of thin-film techniques, the HMDE was preferred in the above-mentioned example. Generally, the HMDE seems to have wider applicability, but the two methods are by no means equivalent and in a given situation both might need to be examined.

SUMMARY

Linear-sweep and stripping a.c. and pulse voltammetric methods have been compared for a variety of electrodes and electrode processes. Each of the linear-sweep techniques is readily used systematically because, in contrast to d.c. linear-sweep voltammetry, the theory for reversible electrode processes is basically analogous to that for polarography at a dropping mercury electrode. In stripping analysis, some departures are found at a hanging mercury drop electrode because of spherical diffusion effects. For reversible electrode processes, the limits of detection for a.c. and pulse methods are comparable. However, a.c. methods offer advantages over pulse methods in discriminating against irreversible electrode processes and permit the ready use of faster scan rates. Pulse methods are more sensitive for irreversible electrode process. Normal pulse polarography is particularly favourable in minimizing undesirable phenomena arising from adsorption or deposition of material on electrodes.

REFERENCES

1 J. Heyrovsky and J. Kuta, *Principles of Polarography*, Academic Press, New York, 1966.
2 H. Schmidt and M. Von Stackelberg, *Modern Polarographic Methods*, Academic Press, New York, 1963.
3 H. M. Davis and J. E. Seaborn, *Electron. Eng.*, 26 (1953) 314.
4 H. M. Davis and J. E. Seaborn in I. S. Longmuir (Ed.), *Advances in Polarography*, Pergamon, Oxford, 1966, p. 239.
5 P. Delahay, *New Instrumental Methods in Electrochemistry*, Interscience, New York, 1954.
6 L. Meites, *Polarographic Techniques*, Interscience, New York, 2nd edn., 1965.
7 E. Barendrecht in A. J. Bard (Ed.), *Electroanalytical Chemistry*, Vol. 2, Dekker, New York, 1967, pp. 53–109.
8 I. Sinko and L. Kosta, *Int. J. Environ. Anal. Chem.*, 2 (1972) 167.
9 S. P. Perone and T. R. Mueller, *Anal. Chem.*, 37 (1965) 2.
10 F. B. Stephens and J. E. Harrar, *Chem. Instrum.*, 1 (1968) 169.
11 S. P. Perone, J. E. Harrar, F. B. Stephens and R. E. Anderson, *Anal. Chem.*, 40 (1968) 899.
12 S. P. Perone, D. O. Jones and W. F. Gutnecht, *Anal. Chem.*, 41 (1969) 1154.
13 W. F. Gutnecht and S. P. Perone, *Anal. Chem.*, 42 (1970) 906.
14 W. L. Underkofler and I. Shain, *Anal. Chem.*, 37 (1965) 218.
15 A. L. Juliard, *J. Electroanal. Chem. Interfacial Electrochem.*, 1 (1959) 101; A. L. Juliard, *Nature (London)*, 183 (1959) 1040; D. N. Walker, R. N. Adams and A. L. Juliard, *Anal. Chem.*, 32 (1960) 1526.
16 D. E. Smith and W. H. Reinmuth, *Anal. Chem.*, 32 (1960) 1892.
17 D. E. Smith, *CRC Crit. Rev. Anal. Chem.*, 2 (1971) 247 and references therein.
18 A. M. Bond, *Anal. Chem.*, 42 (1970) 1165.
19 A. M. Bond, T. A. O'Donnell and R. J. Taylor, *Anal. Chem.*, 44 (1972) 464.
20 A. M. Bond and D. R. Canterford, *Anal. Chem.*, 44 (1972) 721.
21 M. Stulikova and F. Vydra, *J. Electroanal. Chem. Interfacial Electrochem.*, 42 (1973) 127.
22 T. Rohahn, *Anal. Chim. Acta*, 62 (1972) 438.
23 C. I. Mooring, *Leybold Polarogr. Ber.*, 6 (1958) 63.
24 R. Neeb, *Z. Anal. Chem.*, 186 (1962) 53.
25 R. D. Jee, *Z. Anal. Chem.*, 264 (1973) 143; B. Fleet, R. D. Jee and C. J. Little, *J. Electroanal. Chem. Interfacial Electrochem.*, 43 (1973) 349.
26 H. Blutstein and A. M. Bond, *Anal. Chem.*, 46 (1974) 1063.
27 K. B. Oldham and E. P. Parry, *Anal. Chem.*, 38 (1966) 867.
28 H. E. Keller and R. A. Osteryoung, *Anal. Chem.*, 43 (1971) 342.
29 G. D. Christian, *J. Electroanal. Chem. Interfacial Electrochem.*, 22 (1969) 333; 23 (1969) 1 and references therein.

30 J. B. Flato, *Anal. Chem.*, 44 (1972) 75A.
31 H. Siegerman and G. O'Dom, *Amer. Lab.*, 4 (1972) 59.
32 T. R. Copeland, J. H. Christie, R. A. Osteryoung and R. K. Skogerbo, *Anal. Chem.*, 45 (1973) 2171; J. H. Christie and R. A. Osteryoung, *Anal. Chem.*, 46 (1974) 351.
33 A. M. Bond, T. A. O'Donnell and R. J. Taylor, *Anal. Chem.*, 46 (1974) 1063.
34 A. M. Bond and J. R. Thackeray, *Chem. Instrum.*, 4 (1972) 299.
35 H. Blutstein, A. M. Bond and A. Norris, *Anal. Chem.*, in press.
36 H. Blutstein and A. M. Bond, *Anal. Chem.*, in press.
37 D. E. Smith in A. J. Bard (Ed.), *Electroanalytical Chemistry, Vol.* 1, Dekker, New York, 1966, ch. 1.
38 A. M. Bond, *J. Electroanal. Chem. Interfacial Electrochem.*, 35 (1972) 343.
39 A. M. Bond, *Anal. Chem.*, 44 (1972) 315.
40 W. Stevens and I. Shain, *Anal. Chem.*, 38 (1966) 865.
41 J. R. Delmastro and D. E. Smith, *Anal. Chem.*, 38 (1966) 169.
42 F. H. Beyerlein and R. S. Nicholson, *Anal. Chem.*, 44 (1972) 1647.
43 A. M. Bond and J. H. Canterford, *Anal. Chem.*, 44 (1972) 732.
44 A. M. Bond, *Rev. Anal. Chem.*, 2 (1974) 129.
45 T. R. Mueller, *Chem. Instrum.*, 1 (1968) 113.
46 W. O'Deen and R. A. Osteryoung, *Anal. Chem.*, 43 (1971) 1879.
47 H. Blutstein, A. M. Bond and E. Freemantle, Department of Inorganic Chemistry, University of Melbourne, 1972–74.
48 T. M. Florence, *J. Electroanal. Chem. Interfacial Electrochem.*, 27 (1970) 273; 35 (1972) 237.

Analytica Chimica Acta, 74 (1975) 177–187

POINTWISE VARIANCE ANALYSIS: A TECHNIQUE FOR GUIDING DATA ACQUISITION

LOUIS MEITES

Department of Chemistry, Clarkson College of Technology, Potsdam, New York 13676 (U.S.A.)

(Received 17th June 1974)

Several authors have developed data-handling techniques by which the values of a number of different parameters can be deduced from the data obtained in a single experiment. Occasionally all of the parameters are of more or less equal interest, but more often some are much more important than others. From the concentration–time data obtained in the kinetic analysis of a mixture of two reacting species, it is possible to deduce the values of four parameters: the initial concentration of each reactant and the rate constant for its reaction. Of these, the two concentrations are of much greater interest than the two rate constants, and it would therefore be advantageous to maximize the certainties with which the concentrations can be calculated even if this entailed some loss of certainty regarding the rate constants. Similarly, data showing how the current flowing through a polarographic cell varies with the applied e.m.f. on the rising part of a wave can be used to evaluate three parameters, of which the half-wave potential and log-plot slope are usually of much more interest than the cell resistance.

There are some situations in which it is clear that there is one portion of the experimental curve where the data should be concentrated so as to maximize the certainties obtained in evaluating the parameters that are of most interest, and in which it is easy to decide where that portion is. Current–time data for a controlled-potential electrolysis in which the current decays exponentially toward zero may be used to compute the initial current and the mass-transfer constant; if the latter is of little interest the data should certainly be more numerous during the first half of the electrolysis than during the second.

Often, however, it may be unclear where the most useful portions of the curve are, or even if there are any. For the kinetic analysis mentioned above, it may seem apparent that increasing the fraction of the data that lie on the first portion of the curve will provide greater accuracy in both the concentration and the rate constant of the reactant that is the more rapidly consumed, while increasing the fraction of the data taken during the later stages of the reaction, when most of the more rapidly reacting substance has already been consumed, will provide greater accuracy in both the concentration and the rate constant of the reactant that is the more slowly consumed. If these things were true, they would have several consequences. There would be no way in which data-acquisition could be programmed so as to maximize the accuracies of the concentrations while sacrificing some accuracy in the rate constants. If the two concentrations were of about equal interest, approximately equal numbers of points should be taken in the two portions

of the curve in which the faster and slower reactions predominate. Finally, the reliabilities of both the concentration and the rate constant of either reactant could be increased by taking a larger fraction of the data in the portion of the curve where its reaction predominates, although this would be accompanied by a corresponding deterioration in the reliabilities of the parameters that characterize the other reactant.

This paper describes a way of identifying the portion, or portions, of any experimental curve in which the data have the greatest influence on the value of any desired parameter. Once this is known, either of two courses can be adopted. From any total number of data points, most of those outside the most influential portions can be discarded, with the result that much computational time can be saved with little adverse effect on the value of interest. Alternatively, the data-acquisition schedule may be designed to emphasize the most influential portions while acquiring the same number of data, with the result that the reliability of the value of interest can be improved without increasing the computational time required.

The technique is called "pointwise variance analysis" to suggest both its similarity to and its differences from Fisher's well-known analysis of variance[1]. Very similar computations have been made recently by Isbell *et al.*[2], but with an *a posteriori* emphasis rather than the *a priori* one stressed here.

THEORY

It is assumed that the experimental data represent the variation of some dependent variable y with some independent one x and that the functional relationship between y and x is known:

$$y = f(x, V_1, V_2, \ldots, V_j)$$

where V_i denotes the ith one of a total of j numerical parameters involved. The least-squares "best" values of these parameters may be calculated by multiparametric curve-fitting[3] or any other technique of non-linear regression[4–7], or by linear regression if that is applicable.

The reliabilities of the resulting values may be assessed by computing their variances from the familiar equation

$$\sigma_{V_i}^2 = \sum_{m=1}^{n} \left(\frac{\partial V_i}{\partial y_m}\right)^2 \sigma_{y_m}^2 \qquad (1)$$

where n is the number of experimental points obtained. The partial derivative implies that the mth value of y is changed slightly from the experimental value, denoted henceforth by y_m^0, to an arbitrary new value y_m'; that the minimum on the new error surface produced by this change is located by finding the new values $V_1', V_2', \ldots$ of all the parameters that yield the best fit; and that the differences $V_i' - V_i^0$ between these values and the ones that gave the best fit to the unaltered data are compared with the change $y_m' - y_m^0$ applied.

The technique proposed here deals with the individual values of the product $(\partial V_i/\partial y_m)^2 \sigma_{y_m}^2$ for the different parameters and successive data points, or, more properly, with the finite-difference approximations $e_{i,m}$ defined by

$$e_{i.m} = \left(\frac{V_i' - V_i^0}{y_m' - y_m^0}\right)^2 \sigma^2_{y_m^0} \tag{2}$$

In the performance of the original fit to obtain the values of V_i^0, either the absolute or the relative errors in the y_m^0 may have been considered to be randomly distributed. Though the grounds for this decision will not be discussed again here, it must be noted that the first assumption yields a value of $\sigma_{y_m^0}$, while the second yields a value of $\sigma_{y_m^0}/y_m^0$, that is independent of y_m^0. If the successive values of y_m' are obtained through the relation

$$y_m' = (1 \pm c) y_m^0 \tag{3}$$

where c is some small constant, we have

$$e_{i.m} = \left(\frac{V_i' - V_i^0}{c y_m^0}\right)^2 \sigma^2_{y_m^0} \tag{4a}$$

in the first case and

$$e_{i.m} = \left(\frac{V_i' - V_i^0}{c}\right)^2 \left(\frac{\sigma_{y_m^0}}{y_m^0}\right)^2 \tag{4b}$$

in the second. In either case the value of the term involving the standard error of y_m^0 is readily available from the result of the fit to the original data. An essential requirement is that the value of c be large enough to alter the value of each parameter at every point by an amount that is large in comparison with the round-off errors in the computations. Values between 0.01 and 0.2 were used in the computations reported below; as a general guide the choice $c = 0.05j$ is suggested.

For convenience, the values of $e_{i.m}$ for each parameter may be normalized by division by the largest of them, denoted by $(e_{i.m})_{\max.}$. These normalizing values will in general be widely different for the different parameters, but this is of no importance for the present purpose and attention need be paid only to the normalized values $E_{i.m}$ defined for each parameter by

$$E_{i.m} = e_{i.m}/(e_{i.m})_{\max.} \tag{5}$$

or, for some purposes, to the normalized sum E_m of these values for all of the parameters at the successive data points:

$$E_m = \frac{1}{j} \sum_{i=1}^{j} E_{i.m} \tag{6}$$

What is proposed is that the accuracy, reliability, and efficiency of evaluating the ith parameter are maximized by clustering the data most thickly in the region or regions where $e_{i.m}$ and $E_{i.m}$ are largest or, if no one parameter is of special interest, that the data should be most thickly clustered in the region or regions where E_m is largest. As $e_{i.m}$ and $E_{i.m}$ have the form of weighting factors, the procedure is equivalent to choosing the data in such a way as to emphasize those regions that have the greatest intrinsic weight in the computation of the desired parameter or parameters.

It is best to generate and analyze a set of synthetic data that obey the theoretical relationship to which the experimental data will be fitted. A plot of E_m

against the independent variable for these synthetic data will show maxima in the regions of greatest overall weight; similar plots of $E_{i,m}$ will show maxima in the regions that are most influential in determining the individual parameters. We shall call such plots "pointwise-variance-analysis plots." They may be obtained from experimental data rather than synthetic ones, but if they are they usually show small irregularities and distortions. These small perturbations are due to the random errors of measurement and are illustrated by Fig. 5 below. Although they are unlikely to complicate the interpretation, and although the general features of pointwise-variance-analysis plots constructed from synthetic data can always be perceived on the corresponding plots obtained from experimental ones, the use of synthetic data seems slightly but definitely advantageous.

COMPUTATIONS

All of the computations were performed on a PDP8/I computer (Digital Equipment Corp., Maynard, Massachusetts) operated in an early version of the manufacturer's EDUSystem-25 BASIC and in a multi-user configuration that made 4096 words of core memory available for this work.

The program* was developed from a multiparametric curve-fitting program used for many other purposes in this laboratory. It provides for the incrementation of each value of y in turn, printout and storage of the successive values of $e_{i,m}$, computation and printout of the standard errors of the parameters, and finally the computation and printout of the values of $E_{i,m}$ for each parameter and of the overall values of E_m.

RESULTS AND DISCUSSION

Polarographic wave analysis

Most polarographic waves obey the equation

$$i = i_d/\{1+\exp[(E-E_{\frac{1}{2}})/S]\} \tag{7}$$

where i is the current measured at the applied potential E, i_d is the diffusion or limiting current measured on the plateau, $E_{\frac{1}{2}}$ is the half-wave potential, and S is the absolute value of the slope of a natural-log plot, which is a plot of E against $\ln[i/(i_d-i)]$. If a wave is sufficiently well defined to make direct measurement of i_d possible, there are two parameters to be evaluated: $E_{\frac{1}{2}}$ and S.

To guide such analyses, synthetic current–potential data were generated and analyzed for a hypothetical wave having $E_{\frac{1}{2}} = -0.6$ V and $S = 12.84$ mV, of which the latter is the theoretical value for a reversible two-electron wave at 25°C. Thirteen points were taken at 10-mV intervals from -0.54 to -0.66 V, a range over which i/i_d varies from 0.01 to 0.99.

Figure 1 shows the resulting pointwise-variance-analysis plot. The ordinate

* Listings, in BASIC, of the program VARPAR, and the parent program CFT3, together with listings in POLYBASIC and FORTRAN-IV of CFT3 and approximately 160 pages of documentation, explanation, and discussion of their operation and use, may be obtained by remitting $10.00, to cover the cost of duplication and postage, to the Computing Laboratory of the Department of Chemistry, Clarkson College of Technology, Potsdam, N.Y. 13676.

axis extends over only two decades because points having relative weights below 0.01 are not important enough to deserve consideration. The plot for $E_{\frac{1}{2}}$ is a smooth curve, concave downward everywhere and having a maximum at the half-wave potential itself. The plot for S has one maximum at a point where i/i_d is approximately 0.18 and another at a point where i/i_d is approximately 0.82, but has a minimum at the half-wave potential. These facts are readily understood by imagining that the same parameters are to be evaluated from the same data by means of a conventional log plot. An error in the measured current at the half-wave potential will shift that plot with respect to the potential axis but will not affect its slope when, as here, the points are symmetrically distributed around the half-wave potential. An error in the measured current at any other potential will affect the values of both $E_{\frac{1}{2}}$ and S, but as that potential moves farther away from the half-wave potential, the effect on $E_{\frac{1}{2}}$ will decrease while that on S increases. This continues until either i or $i_d - i$ becomes so small that the error of measurement renders it too uncertain to merit giving serious consideration to a deviant point.

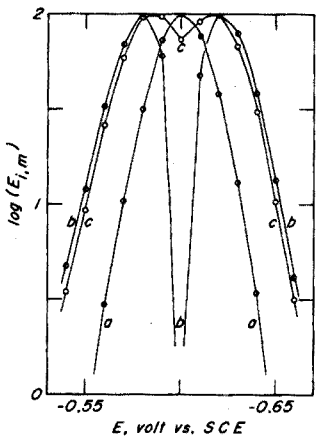

Fig. 1. Pointwise-variance-analysis plot showing the relative weights $E_{i,m}$ of the individual points in computing (a) $E_{\frac{1}{2}}$ and (b) S from synthetic current–potential data for a polarogram with $E_{\frac{1}{2}} = -0.60$ V and $S = 12.84$ mV. Curve (c) represents the overall relative weights E_m.

These considerations have been described in some detail because this simple situation is one in which it is easy to understand and interpret the results of the computations. With more complex relationships involving more parameters the interrelationships become more intricate, the plots more complex, and prediction and interpretation much more difficult.

The results show that only points close to the half-wave potential are worth measuring if $E_{\frac{1}{2}}$ is of most interest, but that the points should be clustered around those for which i/i_d is 0.18 and 0.82 if S is of most interest, while if the aim is to secure the most reliable values of both parameters the points should be nearly evenly spaced over the range $0.1 \leqslant i/i_d \leqslant 0.9$. Over this range the overall weight E_m is always above 0.6 and its variation is small, but points outside it cannot contribute significantly to the final results unless they are included in numbers too large to be worth while in view of the increase of computation time involved.

Polarographic wave analysis for high-resistance cells

When the resistance of the cell is high or when, as in the polarograms analyzed below, a resistance is connected in series with the cell, polarographic waves are deformed by iR drops. They are then described by eqn. (7) and

$$E = V + (-i)R \tag{8}$$

where $(-i)$ is the cathodic current (μA), R is the total series resistance (MΩ), and V is the applied e.m.f. Values of $E_{\frac{1}{4}}$, S, and R may be obtained by solving eqns. (7) and (8) simultaneously to evaluate $-i$ at each point for the values currently assumed, adjusting those values in successive cycles so as to optimize the fit.[8]

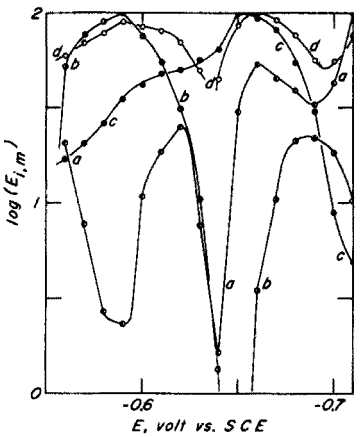

Fig. 2. Pointwise-variance-analysis plot showing the relative weights $E_{i,m}$ of the individual points in computing (a) $E_{\frac{1}{4}}$, (b) S and (c) R from synthetic current–potential data for a polarogram with $E_{\frac{1}{4}} = -0.60$ V, $S = 12.84$ mV, and $R = 0.05$ MΩ. Curve (d) represents the overall relative weights E_m.

As polarograms of cadmium(II) in 0.1 M potassium nitrate, which had been recorded with various known high resistances in series with the cell, were available for analysis, the pointwise-variance-analysis plot shown in Fig. 2 was constructed for synthetic data identical with those for Fig. 1, save for the superimposition of iR drops up to 50 mV computed for an assumed resistance of 0.05 MΩ. The relative weight of a point in determining the resistance is appreciable even if that point is near the foot of the wave; it increases slowly as the applied e.m.f. increases until, after passing through a maximum near the three-quarter-wave potential, it decreases sharply as the plateau is approached. The curve for the log-plot slope resembles that in Fig. 1 but is distorted by the presence of the cell resistance: its peaks are a little farther apart (at $i/i_d = 0.17$ and 0.92), and the one near the plateau is diminished in importance by the fact that errors in that region can alter the estimate of R as well as that of S. The curve for the half-wave potential is affected even more: whereas in Fig. 1 an error in the current at the half-wave potential exerted great influence on $E_{\frac{1}{4}}$ because it could not alter the estimate of S, here the same error can affect both $E_{\frac{1}{4}}$ and R, and the region of greatest importance to $E_{\frac{1}{4}}$ is therefore displaced toward the plateau. This has the unexpected result that data in the vicinity of the half-wave applied e.m.f. have almost no effect on $E_{\frac{1}{4}}$, which is exactly the opposite

TABLE I

RESULTS OF TYPICAL FITS TO POLAROGRAPHIC DATA

Number of points employed	*S (mV)*		*$E_{\frac{1}{2}}$ vs. SCE (V)*		*R (megohms)*	
	Value	*Relative standard error (%)*	*Value*	*Standard error (mV)*	*Value*	*Relative standard error (%)*
11 (Covering entire wave)	13.08	0.96	−0.5780	0.086	0.05020	0.43
11 (Emphasizing regions of greatest weight)	13.06	0.86	−0.5780	0.022	0.05029	0.05
5 (Emphasizing regions of greatest weight)	12.87	1.16	−0.5781	0.064	0.05064	0.34

of what reasoning by analogy with the situation of Fig. 1 would suggest. The overall weight passes through a minimum around the half-wave applied e.m.f. that is both deeper and broader than the similar minimum in Fig. 1, so that, if no one parameter is of especial interest, the overall efficiency of experimentation and computation can be maximized by concentrating on the regions around $i/i_d = 0.17$ and 0.77. Though the exact shapes and positions of all these curves are of course dependent on the value of R, the locations of the regions of greatest weight are relatively insensitive to R. From Fig. 1, for example, they are at $i/i_d = 0.24$ and 0.76 for $R = 0$. On the basis of these results it should be easy to approach the theoretical optimal efficiency very closely over a wide range of experimental conditions.

Table I illustrates the practical application of these ideas. The first line shows the values and standard errors of S, $E_{\frac{1}{2}}$, and R obtained from 11 points evenly spaced along the abscissa of a typical polarogram. The second line gives the results of a similar fit to a different group of 11 points from the same polarogram: 5 closely spaced around $i/i_d = 1/6$, and 6 others closely spaced around $i/i_d = 3/4$. As Fig. 2 showed, these are the regions of greatest weight. The standard errors of these two fits differed by less than 2%, showing that the second group of points was not accidentally superior to the first. Emphasizing the regions of greatest weight had little effect on the values of S, $E_{\frac{1}{2}}$, and R in this case (with other polarograms the differences were occasionally larger), but all three of the standard errors decreased and two of the three decreases are dramatic. The last line shows that results whose quality would be hard to fault can be obtained with as few as 5 points (which were not specially selected for this example) if these are concentrated in the regions of greatest weight: this should not be construed as advocacy of fits in which the number of parameters exceeds the number of degrees of freedom.

Kinetic analysis of a mixture of two reactants

The pointwise-variance-analysis plot shown in Fig. 3 describes the kinetic

analysis of a mixture of the reactants A and B reacting with the common reagent R under pseudo-first-order conditions to yield the respective products P_A and P_B; it is assumed that these products are indistinguishable by the method employed and hence that the measured signal S is proportional to the sum of their concentrations. By these assumptions the time dependence of S is given by

$$S = cC_A^0(1-e^{-k_A t}) + cC_B^0(1-e^{-k_B t}) \tag{9}$$

where k_A and k_B are the pseudo-first-order rate constants, C_A^0 and C_B^0 are the initial concentrations, and c is a constant of proportionality. There are four parameters: cC_A^0 and cC_B^0, from which the initial concentrations can be calculated if c is evaluated separately, and the two rate constants.

The overall weight and the weights in determining cC_A^0 and cC_B^0 vary almost identically. In large part, this is because cC_A^0 and cC_B^0 are not really independent: unless the measurements are terminated long before the slower reaction is complete, the sum of these two quantities is constrained within very narrow limits. These curves show three peaks, whose locations are most conveniently described by referring to the more familiar plot in Fig. 4, which is drawn for the same synthetic data as Fig. 3. The most important region, 3, is that around the time when the concentration, and hence the rate of reaction, of the more rapidly reacting starting material just becomes indetectable. An only slightly less important region, 2, is centered around the time when the rates of reaction of the two starting materials are equal. Finally, there is a very minor peak, 1, which occurs soon after the start of the reaction, in the region where the rate of the faster reaction predominates but after enough of the products have accumulated to decrease the random errors of measurement to a small fraction of the value of S. It may be mentioned that all these calculations were performed by assuming the absolute errors in the dependent

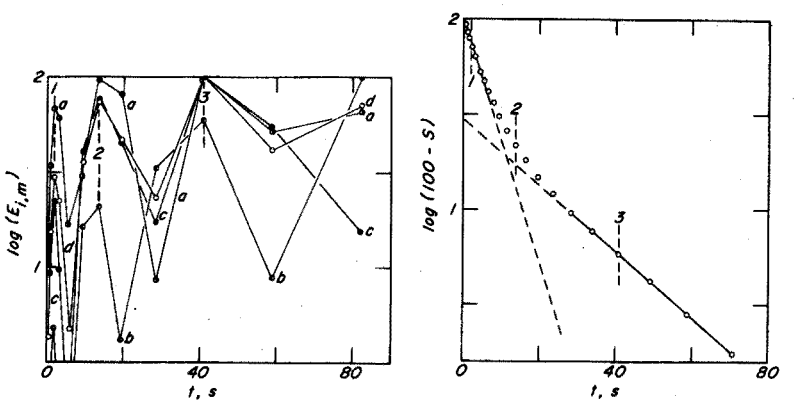

Fig. 3. Pointwise-variance-analysis plot showing the relative weights $E_{i,m}$ of the individual points in computing (a) k_A, (b) k_B, and (c) cC_A^0 or cC_B^0 (for which the individual curves are indistinguishable on this scale) from synthetic data for a kinetic analysis with $cC_A^0 = 70$, $k_A = 0.2\ s^{-1}$, $cC_B^0 = 30$, and $k_B = 0.04\ s^{-1}$. Curve (d) represents the overall relative weights E_m. The numbers on the plot identify the successive peaks for comparison with Fig. 4.

Fig. 4. Plot of log $(100 - S)$ against time for the data of Fig. 3, showing the times that correspond to the successive peaks in Fig. 3.

variable to be randomly distributed, as is appropriate if the measurements are made from a recorded curve or with *A/D* conversion; very different results would be obtained by assuming the relative errors to be randomly distributed (and to be independent of the measured values), but there are few circumstances under which this would be realistic.

Although the weights vary similarly for cC_A^0 and cC_B^0, they do not do so for k_A and k_B, and Fig. 3 shows that it is possible to gather the data so as to optimize the evaluation of either k at the cost of some loss of certainty regarding the other. If the value of k that is of more interest is the larger one, the data should be concentrated in regions 1 and 2; if it is the smaller one, they should be concentrated in region 3 and toward the very end of the reaction.

These conclusions were confirmed by various calculations, based on the experimental data of de Oliveira and Meites[9], which were analogous to those in Table I and gave generally similar results. Data concentrated in the regions of greatest weight gave values of the parameters that were nearly equal to, but had much smaller variances than, equally numerous data equally spaced along either the *S*- or the time-axis, while six or seven points concentrated in the regions of greatest weight yielded variances comparable with those obtained from 20 that were equally spaced.

Potentiometric titration of a weak base with a strong acid

Barry, Meites, and Campbell[10] showed that data obtained in titrations of acetate with hydrochloric acid could be used to evaluate four parameters: the concentrations of both acetate (C_b^0) and acid (C_a), the conditional dissociation constant K_a of acetic acid in the titration medium employed, and the apparent molarity activity coefficient y_{H^+} of hydrogen ion in that medium. This is done by performing fits to the equations

$$[H^+]^2 + \left(\frac{V_b^0 C_b^0 - V_a C_a}{V_b^0 + V_a} + K_a\right)[H^+] - \frac{V_a C_a K_a}{V_b^0 + V_a} = 0 \qquad (10a)$$

$$pH = -\log(y_{H^+}[H^+]) \qquad (10b)$$

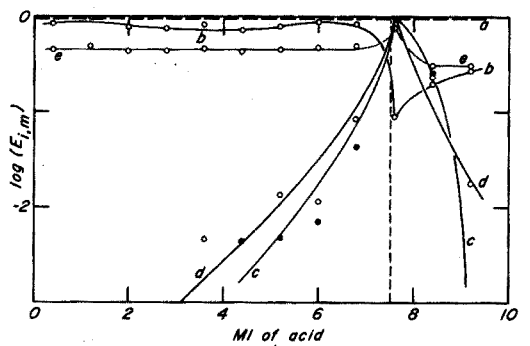

Fig. 5. Pointwise-variance-analysis plot showing the relative weights $E_{i,m}$ of the individual points in computing (a) y_{H^+}, (b) K_a, (c) C_a, and (d) C_b^0 from the data obtained in a potentiometric titration of 80 cm^3 of 0.099 *M* ($=C_b^0$) potassium acetate with 1.06 *M* ($=C_a$) hydrochloric acid under the conditions given previously[10]. Curve (e) represents the overall relative weights E_m. The vertical dashed line represents the equivalence point.

Figure 5 shows the pointwise-variance-analysis plot obtained from the data of a typical titration. Except for minor fluctuations attributable to the random errors of measurement, the points contribute equally to the variance of y_{H^+} throughout the titration, and almost equally to that of K_a up to the equivalence point but to a much smaller extent thereafter. For both concentrations the weights are significant only in a very narrow range around the equivalence point, again largely because of interaction between the values of C_b^0 and C_a and the fact that the volume of acid required to reach the equivalence point is governed by the ratio of these values. This suggests that the reliability of a titration performed in this way might be maximized by following one titration in which the points were evenly spaced along the volume axis with a second in which they were dense around the equivalence point located by a preliminary fit to the results of the first. This procedure would probably be advantageous in titrations of bases so weak or so dilute that the titration curve had no inflection point.

Assessment of the required precision of measurement

Another consideration that is important in the design of an experiment is the relation between the standard error of the value of a parameter that is to be calculated from the data and the standard error of the individual measurements. These quantities are σ_{V_i} and σ_{y_m}, respectively, in eqn. (1). Of course they are proportional, but there are two dangers that may arise if their ratio is unknown: either time may be wasted in performing experiments in which σ_{y_m} is not small enough to yield an acceptably precise result, or the experiment may be overdesigned and time may be wasted in obtaining data far more precise than are required. Values of such ratios are obtained by the computations described above, and a few typical ones are cited herewith.

In evaluating the half-wave potential and log-plot slope for a polarogram from data like those described above, $\sigma_{E_{\frac{1}{4}}}/\sigma_{i_m}=0.024$ and $\sigma_s/\sigma_{i_m}=0.022$. The form of eqn. (7) is such that the calculations are based on values of i/i_d; if the standard error of measuring each current i is equal to 0.01 i_d, which is not unrealistic in polarographic practice, the standard error of $E_{\frac{1}{4}}$ will be 0.24 mV and that of S will be 0.22 mV. The first of these has only an absolute significance; the second is equivalent to about 2% of the theoretical value, 12.8 mV, for a reversible two-electron process. If standard errors of, say, 1 mV in $E_{\frac{1}{4}}$ and $\pm 10\%$ of the theoretical value of S were acceptable, it would suffice to achieve a standard error of 0.04 i_d in the individual measurements of current.

Similarly, for the acid–base titration described above, $(1/C_b)(\sigma_{C_b}/\sigma_{pH})=5.2\%$, $(1/C_a)(\sigma_{C_a}/\sigma_{pH})=5.4\%$, $(1/K_a)(\sigma_{K_a}/\sigma_{pH})=82\%$, and $(1/y_{H^+})(\sigma_{y_{H^+}}/\sigma_{pH})=66\%$. These figures mean, for example, that to attain a relative standard error of about $\pm 0.02\%$ in the concentration of either the acid or the base, it is only necessary to measure the pH values with a standard error of about 0.004 pH unit, but that the same standard error of measurement will give values of K_a and y_{H^+} having relative standard errors of about 0.33% and 0.26%, respectively.

The results of such calculations will naturally depend on the number of points taken and on their distribution, but once a data-acquisition schedule has been devised, they should help the experimenter to decide what precision his measurements must have to ensure his satisfaction with the results.

This work was supported in part by the National Science Foundation (GP-10325) and by the Institute of General Medical Sciences, National Institutes of Health (GM-16561). Thanks are expressed to the National Science Foundation and the Eastman Kodak Company that made possible the purchase and maintenance of the computer system employed.

SUMMARY

In any experiment in which the variation of a dependent variable with an independent one is examined so that one or more parameters can be evaluated, the different points exert different degrees of influence on the values of the parameters. Pointwise variance analysis deals with the contributions of individual data points to the variance of each parameter and with the dependences of these contributions on the value of the independent variable. It shows where the data should be concentrated to maximize the certainties with which the parameters of greatest interest can be obtained, or to minimize the amount of data that must be analyzed to provide given levels of certainty. Four examples—two from polarography, one from kinetic analysis, and one from potentiometric acid–base titrimetry—are given.

REFERENCES

1 R. A. Fisher, *Statistical Methods for Research Workers*, Oliver and Boyd, Edinburgh, 7th edn., 1938.
2 A. F. Isbell, Jr., R. L. Pecsok, R. H. Davies and J. H. Purnell, *Anal. Chem.*, 45 (1973) 2363.
3 T. Meites and L. Meites, *Talanta*, 19 (1972) 1131.
4 M. H. Lietzke, *ORNL-3259*, Oak Ridge National Laboratory, 1962.
5 D. W. Marquardt, *J. Soc. Ind. Appl. Math.*, 11 (1963) 431.
6 C. Daniel and F. S. Wood, *Fitting Equations to Data*, Interscience, New York, 1971.
7 Y. Bard, *Nonlinear Parameter Estimation*, Academic Press, New York, 1974.
8 L. Meites and L. Lampugnani, *Anal. Chem.*, 45 (1973) 1317.
9 V. A. de Oliveira and L. Meites, *Anal. Chim. Acta*, 70 (1974) 383.
10 D. M. Barry, L. Meites and B. H. Campbell, *Anal. Chim. Acta*, 69 (1974) 143.

Analytica Chimica Acta, 74 (1975) 189–191

SHORT COMMUNICATION

The rate of loss of selenium from aqueous solution stored in various containers

A. D. SHENDRIKAR and P. W. WEST

Environmental Sciences Institute, Coates Chemical Laboratories, Louisiana State University, Baton Rouge, La. 70803 (U.S.A.)

(Received 3rd January, 1974)

In a previous paper[1], the adsorptive losses of chromium on the walls of Pyrex, flint and polyethylene beakers were reported. These materials were chosen for investigation because they were representative of the vessels usually used for storing and shipping water samples. The study of metal losses in dilute solutions has been extended to investigate the adsorption pattern of selenium. The findings obtained are presented in this communication.

Experimental

Apparatus and materials. The details of the scintillation counter, counting procedure, etc. were given previously[1].

Selenium tracer (selenium-75) was obtained from New England Nuclear, Boston, Mass. in the form of selenous acid. Appropriate volumes of the selenium stock solution were taken to provide a convenient activity in the test beakers (at least 2000 c.p.m. per ml).

Selenium carrier solution was prepared by weighing 0.5 mg of metal and dissolving in a few drops (minimum required) of concentrated nitric acid. The resulting solution was boiled gently to expel oxides of nitrogen, cooled and made up to 100 ml in a volumetric flask. Working solutions (100 p.p.m.) were prepared by appropriate dilution of the selenium stock solution.

New Pyrex, flint and polyethylene beakers were cleaned before use[1].

Results and discussion

Pyrex (No. 14000). This was selected for the study as representative of the borosilicate glasses. The adsorption characteristics of 1 p.p.m. selenium solutions held in Pyrex beakers at various hydrogen ion concentrations are shown in Fig. 1. Portions (100 ml) of spiked solutions were stored in the beakers at pH 7.00, 3.80 and in nitric acid (5.0 ml of concentrated nitric acid per liter of solution). The selenium solutions containing nitric acid exhibited quite favorable stability in this medium, as losses of only 1% or less were observed even at the end of 15 days. The adsorption losses of selenium in nitric acid were studied mainly to verify the reports[2] and recommendation of the Environmental Protection Agency[3]. Selenium solutions at pH 7.00 show greater percentage losses than solutions held in Pyrex

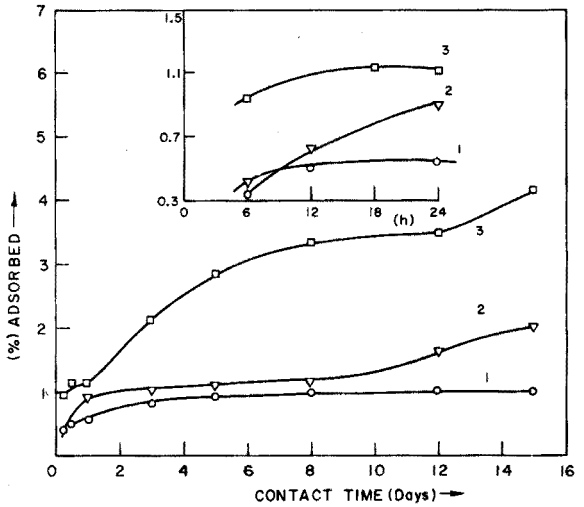

Fig. 1. Adsorption of selenium on pyrex beakers at various hydrogen ion concentrations. (1) HNO_3, (2) pH 3.80, (3) pH 7.00. The inset shows the curves 1, 2 and 3 drawn to a larger scale at lower contact times and percent adsorption. Temp. 23±2 °C.

beakers at pH 3.80. The latter pH shows a steady state of loss (1.5%) for a period of eight days and a maximum 2% for the 15-day period.

Flint glass. Before plastic became popular, flint glass was a common material for sample bottles and even today is recommended in many procedures for reagent and sample storage. Figure 2 summarizes the adsorption characteristics of selenium solution on the walls of such containers. Greatest stability was obtained in the presence of nitric acid, and the greatest losses were from solutions of pH 7.00. In general, flint glass beakers exhibited an induction period for adsorption of about 3 days.

Polyethylene. Polyethylene is probably now the most extensively used material

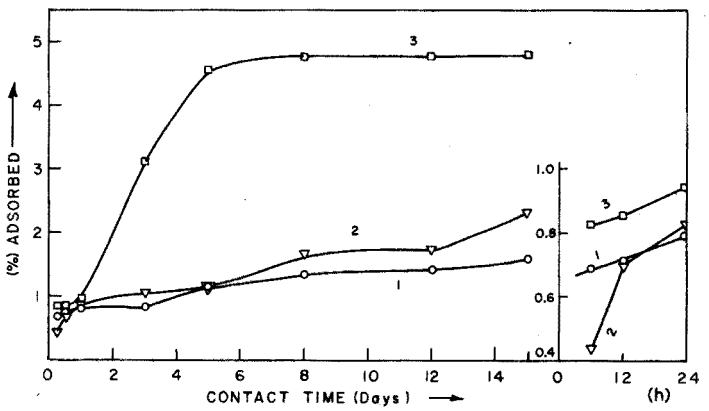

Fig. 2. Adsorption of selenium on flint glass at various hydrogen ion concentrations. pH conditions for curves 1–3 are as in Fig. 1. The inset shows the curves 1, 2 and 3 drawn to a larger scale at lower contact times and percent adsorption. Temp. 23±2°C.

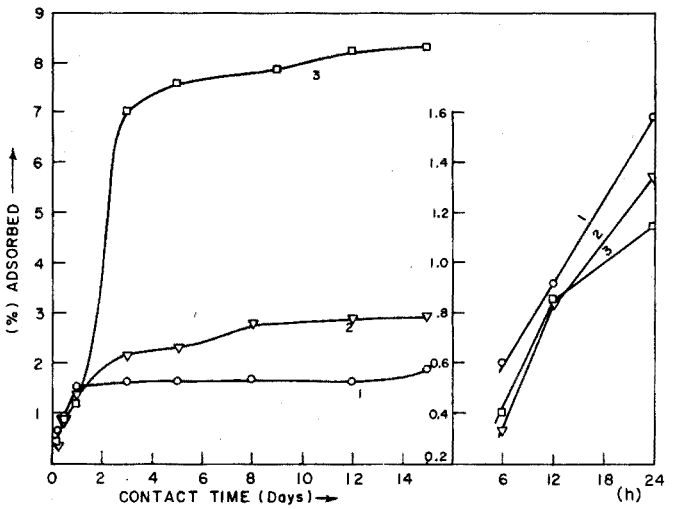

Fig. 3. Adsorption of selenium on polyethylene beakers at various hydrogen ion concentrations. pH conditions for curves 1–3 are as in Fig. 1. The inset shows curves 1, 2 and 3 drawn to a larger scale at lower contact times and percent adsorption. Temp. 23±2 °C.

for sample and reagent storage in water quality and control laboratories. Figure 3 shows the stability of selenium solutions stored in such containers at various hydrogen ion concentrations. Losses of more than 8% occurred within 15 days, and thus were higher than the losses observed for Pyrex and flint glass.

Autoradiography of the beakers holding solutions was performed to determine the distribution of adsorbed selenium by following a procedure described earlier[1]. The autoradiography of the Pyrex, flint and polyethylene beakers holding selenium solutions at pH 7.00, 3.80 and nitric acid showed a pattern of distribution similar to that observed by West *et al.*[4] in their silver work. In general, the selenium activity was found to be concentrated at the center bottom portion of the beaker and to a lesser extent, but in a random fashion, on the side walls of the beakers.

This work was supported by the National Science Foundation RANN Program, Grant GI-35114X.

REFERENCES

1 A. D. Shendrikar and P. W. West, *Anal. Chim. Acta.*, 72 (1974) 91.
2 *Standard Methods For the Examination of Water and Wastewater*, 13th ed., 1971, APHA. AWWA. WPCF.
3 *Methods For Chemical Analysis of Water and Wastes*, Environmental Protection Agency, National Environmental Research Center, Analytical Quality Control Laboratory, Cincinnati, Ohio, 45268.
4 F. K. West, P. W. West and F. A. Iddings, *Anal. Chim. Acta*, 37 (1967) 112.

Analytica Chimica Acta, 74 (1975) 192–196

SHORT COMMUNICATION

Intramolecular field effects on the adsorption and fluorescence spectra of N-(1-naphthyl)ethylenediamine

ROY J. STURGEON and STEPHEN G. SCHULMAN
College of Pharmacy, University of Florida, Gainesville, Florida 32610 (U.S.A.)
(Received 3rd June 1974)

N-(1-naphthyl)ethylenediamine (Bratton–Marshall reagent) has been employed in the colorimetric analysis of arylamine type drugs[1,2]. It has been found here that while the Bratton–Marshall reagent fluoresces intensely in various solvents, its colored diazo derivatives with arylamines such as sulfanilamide, do not. Greater analytical sensitivity is to be had for arylamines by reacting the diazotized arylamine with a slight excess of the Bratton–Marshall reagent and then determining the excess reagent fluorimetrically. The arylamine concentration is then related to the difference in fluorescence intensity between the total reagent added and the unreacted reagent. Because the reagent contains two functional groups, it was deemed desirable to study the pH dependence of its electronic spectra, in order to determine the spectroscopic properties of its various prototropic forms and thereby to establish the optimum pH conditions for fluorimetric analysis.

Experimental

N-(1-naphthyl)ethylenediamine dihydrochloride (Matheson, Coleman and Bell, Inc.) was recrystallized twice from ethanol. The free base was prepared by neutralization of the dihydrochloride with ethylamine followed by removal of the excess of ethylamine by flash evaporation. Reagent-grade sulfuric acid, sodium hydroxide, acetonitrile, dioxane and cyclohexane (Mallinckrodt Chemical Works) were used. Benzene-free ethanol was also employed as a solvent. Sulfuric acid solutions were prepared by dilution with distilled deionized water. The corrected Hammett acidity scale of Jorgenson and Hartter[3] was employed to calibrate the sulfuric acid solutions. Solutions in the pH region 1–3 were prepared by dilution of sulfuric acid. Acetate, phosphate and borate buffers were employed to prepare solutions of pH 4–10. Dilute sodium hydroxide solutions were employed for solutions of pH 11–14.

A 100-μl aliquot of an aqueous $1 \cdot 10^{-3}$ *M* stock solution of Bratton–Marshall reagent was delivered to a 10.00-ml volumetric flask, which was then filled to capacity with buffer or acid solution and mixed by inversion, to prepare each aqueous solution for spectroscopic measurement. For spectroscopic studies of nonaqueous solutions, the free base or monohydrochloride was dissolved directly

in the appropriate solvent and diluted to $1 \cdot 10^{-5}$ *M* in the Bratton–Marshall reagent. Each solution was prepared immediately before spectral measurement in order to minimize decomposition errors.

Fluorescence spectra were taken on a Perkin-Elmer MPF-2A fluorescence spectrophotometer whose monochromators were calibrated against the xenon line emission spectrum and whose output was corrected for wavelength variable response of lamp, monochromators and phototube by means of a rhodamine-B quantum counter. Absorption spectra were taken on a Beckman DB-GT spectrophotometer. pH measurements were made on an Orion model 801 digital pH meter employing a Corning combination pH electrode.

Results and discussion

The long wavelength absorption and fluorescence maxima of N-(1-naphthyl)-ethylenediamine in various solvents and at different pH, in water, are presented in Table I. The pK_a values of the Bratton–Marshall reagent in aqueous media, correspond to the ionization scheme shown below.

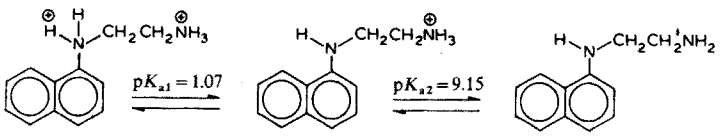

(1)

pK_{a_1} was determined absorptiometrically. However, the absorption spectrum did not change sufficiently in the conversion of the singly charged to the neutral species, to be of analytical value, hence pK_{a_2} was determined by potentiometric titration.

TABLE I

ELECTRONIC ABSORPTION ($\lambda_{1_{L_b}}$ AND $\lambda_{1_{L_a}}$) AND FLUORESCENCE (λ_f) MAXIMA OF THE DOUBLY CHARGED CATION, SINGLY CHARGED CATION AND NEUTRAL SPECIES DERIVED FROM N-(1-NAPHTHYL)ETHYLENEDIAMINE IN VARIOUS SOLVENTS

	$\lambda_{1_{L_b}}$ (nm)	$\lambda_{1_{L_a}}$ (nm)	λ_f (nm)
Doubly charged cation			
H_2SO_4 ($H_0 = -5.8$)	317	281	332
Singly charged cation			
Water (pH = 3.2)	[a]	323	427
Ethanol	[a]	326	402
Acetonitrile	[a]	328	402
Dioxane	[a]	334	396
Cyclohexane	[a]	334	372
Neutral species			
Water (pH = 11.5)	[a]	325	443
Ethanol	[a]	329	412
Acetonitrile	[a]	334	418
Dioxane	[a]	335	403
Cyclohexane	[a]	335	387

[a] The 1_{L_b} band in these species is buried under the much more intense 1_{L_a} band.

In the pH region near 1 (pK_{a_1}), the naphthylamine-like fluorescence of the singly charged cation was quenched with decreasing pH, being completely quenched at H_0-2. However, the fluorescence of the doubly charged cation did not rise to a maximum until a Hammett acidity of -5.5 was attained. In more concentrated sulfuric acid the fluorescence of the dication was quenched. This fluorimetric titration behavior is similar to that of 1-naphthylamine[4] and is therefore attributed to two-step protonation of the monocation in the lowest excited singlet state, hydrogen-bonding with H_3O^+ at the arylamino group preceding actual protonation of the latter.

At about pH 9 (pK_{a_2}), the blue fluorescence of the monocation shifts by about 800 cm^{-1} to lower frequency with increasing pH. This is attributed to the ground-state dissociation of the monocation which is also accompanied by a small shift of the long-wavelength absorption band (the transversely polarized $^1L_a \leftarrow {}^1A$ transition) on dissociation. The shifting of the absorption and fluorescence spectra to longer wavelengths upon dissociation of the aliphatic ammonium group is apparently related to the loss of positive charge from that group. This could be due either to the electrostatic field effect (inductive effect) of the ammonium group relative to that of the free amino group, or to the existence of an intramolecular hydrogen bond between a proton of the alkylammonium group and the lone pair of the arylamino group of the monocation which is not present in the neutral species:

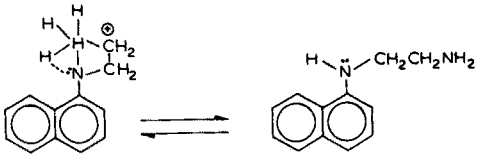

(2)

In either case, the attractive influence of the ammonium group upon the lone pair of the arylamino group in the monocation would stabilize the ground state relative to the excited state, because of the greater degree of residence of the lone pair on the arylamino group in the ground state, thereby raising the energy of the intramolecular charge-transfer absorption ($^1L_a \leftarrow {}^1A$) and fluorescent ($^1L_a \rightarrow {}^1A$) transitions relative to those in the neutral species. It is the same physical phenomenon (positive polarization of the arylamine lone pair) which results in shifting of the long wavelength intramolecular charge transfer ($\pi \rightarrow \pi^*$) absorption bands of arylamines to shorter wavelengths on going from aprotic to protic solvents even though the latter are usually more polar than the former[4]. Obviously, the hydrogen bonding of the arylamine lone-pair, in the ground state, by the solvent, has a greater effect upon the absorption spectrum than the dipolar stabilization of the Franck–Condon excited state. However, the fluorescences of arylamines invariably shift to longer wavelengths with increasing solvent polarity regardless of the hydrogen-bonding capacity of the solvent. This is the result of the reorganization of the solvent cage in the excited state, after excitation, which, as a result of the reduced electron density at the arylamino group, in the excited state, does not entail appreciable hydrogen bonding at the amino group. Thus the dipolar stabilization of the thermally equilibrated excited state and the absence of a hydrogen-bonding solvent configuration in the Franck–Condon ground state

result in decreasing energy or increasing wavelength of fluorescence with increasing solvent dielectric strength. The degree of solvent shifting of the fluorescence spectra is greater than that of the absorption spectra of arylamines, largely because the hydrogen-bonding and dipolar solvent effects upon the absorption spectra are antagonistic while only the dipolar effect is manifested in the fluorescence spectra[5].

The data of Table I show that although the monocation and neutral species derived from N-(1-naphthyl)ethylenediamine absorb and fluoresce, respectively, at different wavelengths in each solvent, the blue shift of the absorption spectrum with increasing solvent hydrogen-bond donor strength, and the red shift of the fluorescence spectrum with increasing solvent polarity, are comparable in magnitude in each species. For example, on going from cyclohexane to water there is a blue shift of 1000 cm^{-1} and of 1100 cm^{-1} in the absorption spectrum of the neutral species and of the monocation, respectively, while the fluorescences of the neutral species and of the monocation red-shift by 3200 cm^{-1} and 3500 cm^{-1}, respectively. These results suggest that the alkylammonium group of the monocation exerts its influence predominantly by an electrostatic field effect rather than by hydrogen bonding, in both ground and excited states. If the opposite were true, the existence of a hydrogen bond between the alkylammonium group and the lone-pair of the arylamino group should inhibit hydrogen bonding with protic solvents, such as water, and the absorption spectrum of the monocation should show predominantly or entirely the effects of dipolar stabilization of the excited state in the polar protic solvents. Thus on going from, say, cyclohexane to water, either a much diminished blue shift (relative to the neutral species) or a red shift should be observed in the absorption spectrum. The occurrence of an intramolecular hydrogen bond in the excited monocation would be expected to stabilize the Franck–Condon ground state relative to the thermally equilibrated excited state, and result in a much smaller red-shift of the fluorescence spectrum than in the neutral species, on going from cyclohexane to water. This was not observed. However, because of the loss of hydrogen bonding with the solvent in the excited state solvent cage, even if an intramolecular hydrogen bond existed in the ground state of the monocation, it should have been destroyed in configurational relaxation following the charge-transfer absorption process. Consequently, it is concluded that the shift of the absorption and fluorescence spectra of N-(1-naphthyl)ethylenediamine to longer wavelengths, on dissociation of the monocation, results from the reduction of the positive field effect of the alkylammonium group which stabilizes the ground state relative to the Franck–Condon excited state in the monocation to a greater degree than does the uncharged alkylamino group in the neutral molecule. The stabilization of the ground state of the monocation also accounts for the lower value of pK_{a_1} relative to that of 1-naphthylamine[6] while the electron-withdrawing influence of the naphthyl group results in pK_{a_2} being lower than that of ethylenediamine[7].

Above pH 9 the fluorescence of the neutral species is quenched. This quenching of arylamine fluorescence by hydroxide is a fairly general phenomenon[8,9] and is attributed to abstraction of a proton from the arylamino group, in the lowest excited singlet state. Since the quenching of N-(1-naphthyl)ethylenediamine fluorescence in basic solution is not accompanied by changes in the absorption spectrum, presumably excited-state proton abstraction is involved here as well:

(3)

In the light of these experiments it appears that the optimum region in which to observe stable, intense fluorescence from N-(1-naphthyl)ethylenediamine, for analytical purposes, is pH 2–8.

Conclusion

N-(1-naphthyl)ethylenediamine can be employed in the quenchofluorimetric analysis of arylamines. The optimum pH range for fluorimetric measurement of the unreacted reagent is 2–8 and corresponds to the singly charged cation. Protonation of the monocation to yield the dication gives similar spectral changes to those observed in the protonation of 1-naphthylamine. Dissociation of the monocation, from the alkylamino group results in small spectral shifts, which are shown by solvent perturbation studies to be due to electrostatic field effects rather than to intramolecular hydrogen bonding in the monocation.

REFERENCES

1 A. C. Bratton, E. K. Marshall, D. Babbitt and A. R. Hendrickson, *J. Biol. Chem.*, 128 (1939) 537.
2 K. A. Connors, *Amer. J. Pharm. Educ.*, 29 (1965) 29.
3 M. J. Jorgenson and D. R. Hartter, *J. Amer. Chem. Soc.*, 85 (1963) 878.
4 S. G. Schulman and P. Liedke, *Z. Physik. Chem. (Frankfurt am Main)*, 84 (1973) 317.
5 S. G. Schulman, *Fluorescence News*, 6 (4) (1972) 1.
6 N. F. Hall and M. R. Sprinkle, *J. Amer. Chem. Soc.*, 54 (1932) 3469.
7 C. J. Nyman, D. K. Roe and D. B. Masson, *J. Amer. Chem. Soc.*, 77 (1955) 4191.
8 H. Boaz and G. K. Rollfson, *J. Amer. Chem. Soc.*, 72 (1950) 3435.
9 S. G. Schulman, A. C. Capomacchia and M. S. Rietta, *Anal. Chim. Acta*, 56 (1971) 91.

Analytica Chimica Acta, 74 (1975) 197–199

SHORT COMMUNICATION

Extraction–spectrophotometric determination of palladium with potassium benzyl xanthate

PRAPHULLA K. PARIA and SANTOSH K. MAJUMDAR
Department of Chemistry, North Bengal University, Darjeeling (India)
(Received 17th May 1974)

Xanthates have been used as extractants for various metals[1,2], the two most important being potassium ethyl xanthate and potassium benzyl xanthate. The ethyl xanthate has been used for the extraction of Pb(II), Cu(II), Co(II), Ni(II), Bi(III), etc.[1–3].

The present communication describes a method in which the palladium(II) complex with potassium benzyl xanthate is extracted into chloroform, and the resulting bright yellow complex is measured spectrophotometrically; palladium(II) can be quickly determined at the milligram level.

Experimental

Apparatus and reagents. A Carl Zeiss (Jena, Germany) spectrophotometer with 1-cm glass cells was used. The chemicals were either chemically pure or reagent-grade material unless otherwise mentioned.

Potassium benzyl xanthate was prepared in the laboratory[4]. Chloroform (E. Merck) was distilled before use. A stock solution of palladium(II) was prepared by dissolving 1 g of $PdCl_2$ (Johnson-Matthey) in 1 ml of concentrated hydrochloric acid and diluting to 250 ml with distilled water; this was standardized gravimetrically with dimethylglyoxime[5].

Buffer solutions of different pH were prepared by standard procedures: hydrochloric acid–potassium chloride (pH 1–2.5), potassium hydrogenphthalate–hydrochloric acid (pH 3–4), potassium hydrogenphthalate–sodium hydroxide (pH 4.5–5.5), potassium dihydrogenphosphate–sodium hydroxide (pH 6–8).

General procedure. Treat an aliquot of palladium chloride solution containing 1–4.7 mg of palladium(II) with 15 ml of buffer solution (pH 2) in a 250 ml separating funnel. Shake for 10 min with 10 ml of 1% (w/v) benzyl xanthate in chloroform. Allow the layers to settle for about 3 min. Transfer the chloroform extract to a flask, and dilute to exactly 25 ml with chloroform. Measure the absorbance at 460 nm against a reagent blank. Prepare a calibration curve in the same way.

Results and discussion

The absorbance spectrum of the palladium(II)–benzyl xanthate complex

extracted as above and measured against a reagent blank (Fig. 1) shows strong absorbance at 400 nm which falls steadily to 440 nm and then shows a maximum at 460 nm. The reagent itself shows insignificant absorbance above 440 nm. The colour of the complex is very stable, even after several days.

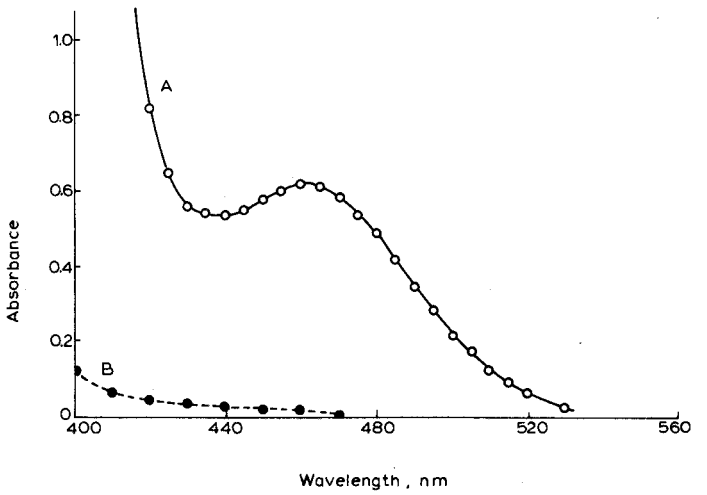

Fig. 1. (a) Absorption spectrum of palladium(II)–benzyl xanthate complex in chloroform against reagent blank. (b) Reagent blank against chloroform.

The solvent extraction behaviour of the palladium(II)–benzyl xanthate system was studied over the pH range 1.0–7.0; palladium(II) was quantitatively extracted over this whole range. At higher acidities a brownish suspension was formed at the interface and hampered the extraction. Above pH 7.0, palladium(II) formed an insoluble suspension.

The absorbances of different amounts of palladium extracted at pH 2.0 were noted against a reagent blank at 460 nm. Beer's law was obeyed over the concentration range 0.95–4.73 mg of palladium(II).

Diverse ions were examined for interference on the determination of 2.36 mg of palladium(II) at pH 2.0. Palladium(II) could safely be determined in the presence of chromium(III), manganese(II), zirconium(IV), uranium(VI), zinc(II), thorium(IV), calcium(II), barium(II), lithium(I), magnesium(II), strontium(II), beryllium(II), aluminium(III) and lanthanum(III), in weight ratios of 1:25. Interferences from iron(III) and lead(II) could be overcome by performing the extraction in the presence of ammonium hydrogenfluoride and sodium acetate, respectively. Nickel(II), cobalt(II) and cerium(III) were masked with EDTA to remove their interferences. Mercury(II) and cadmium(II) interfered by forming a white turbidity in the chloroform layer at ratios of 1:25. Bismuth(III) and copper(II) interfered owing to their characteristic colours.

Among the platinum metals, rhodium(III), ruthenium(III) and platinum(IV) did not interfere in ratios of 1:2 (Table I). The interference of osmium(VIII) was easily eliminated by a preliminary extraction with hexamethylenetetramine into chloroform in the presence of EDTA; palladium(II) is retained in the aqueous

TABLE I

EFFECT OF PLATINUM METALS

(Taken, 2.36 mg of palladium(II))

Foreign ion	*Amount added (mg)*	*Added as*	*Absorbance at 460 mμ*
None	—	—	0.162±0.003
Rh(III)	5	$RhCl_3 \cdot 3\ H_2O$	0.167
Ru(III)	5	$RuCl_3 \cdot 3\ H_2O$	0.164
Os(VIII)	6	OsO_4	0.170
Pt(IV)	4	$H_2PtCl_6 \cdot 6\ H_2O$	0.161

phase, while osmium is extracted, and palladium(II) may then be extracted as usual with xanthate in chloroform.

Anions like citrate, tartrate, fluoride, oxalate, tungstate, phosphate, borate, sulphate, bromide, iodide, EDTA, thiocyanate, thiosulphate did not interfere in weight ratios of 1:50. Vanadate and molybdate interfered by completely preventing colour formation.

In six runs with 2.36 mg of palladium(II), the absorbance found was 0.162±0.003. The relative standard deviation was ±1.4%. Thus the proposed method is fairly precise and reproducible. The process is rapid and simple. The total time for each run is only 20–25 min.

The authors thank the University Grant Commission, India, for awarding a fellowship to one of them (P.K.P.), and Prof. H. N. Khastgir for laboratory facilities.

REFERENCES

1 T. W. Steele *et al.*, *Talanta*, 16 (1969) 1129.
2 A. K. De, S. M. Khopkar and R. A. Chalmers, *Solvent Extraction of Metals*, V.N.R. Company.
3 S. Mukherjee, *Proc. 60th Sess. Indian Sci. Congress, Part III*, 1.2.11 (1973) 69.
4 A. I. Vogel, *Textbook of Practical Organic Chemistry*, Longmans, London, 1960.
5 A. I. Vogel, *Textbook of Quantitative Inorganic Analysis*, Longmans, London, 1960.

Analytica Chimica Acta, 74 (1975) 200–204

SHORT COMMUNICATION

The reaction of gold and dithizone

Part II*. The formation of tribromo- and trichlorodehydrodithizonegold(III)

J. J. COX and D. M. SERVANT
Department of Chemistry, The Polytechnic, Wolverhampton WV1 1LY (England)
(Received 24th May 1974)

The reaction between gold(III) in aqueous solution and dithizone (1,5-diphenyl-3-thiolformazan, H_2Dz) in chloroform was recently shewn[1] to be essentially oxidative, the mixture of organic products depending on the concentration in the aqueous phase of gold(III), of halide ion, of hydrogen ion, and on the duration and the vigour of extraction. The product absorbing at 420 nm, generated from aqueous gold(III) ($6 \cdot 10^{-3}$ *M*) and chloride (0.775 *M*) solution with dithizone in chloroform ($8.4 \cdot 10^{-5}$ *M*), was identified as bis-3,3′-(1,5-diphenylformazan)disulphide[2] and exhibited a highly characteristic reaction in spontaneously regenerating up to 50% of its dithizone. Absorbance near 420 nm was ascribed by earlier workers to a "gold dithizonate"; thus Fischer[3] concluded that gold(III) was first reduced to gold(I) and then formed a dithizonate with the residual dithizone. Erdey and Rady[4] also associated the extraction of gold with absorbance in this region, assigning the formula $Au(HDz)_3$, and several workers[5–7] associated the extraction of gold with yellow colours and with various stoicheiometries. This paper describes a more detailed study of the behaviour of bis-3,3′-(1,5-diphenylformazan)disulphide in this system.

Results

When the conditions in the eaction between aqueous gold(III) solution and dithizone in chloroform were adjusted to yield bis-3,3′-(1,5-diphenylformazan)disulphide, the disulphide reacted with residual gold(III), so that on prolonged extraction the absorbance at 420 nm fell, with a concomitant rise in absorbance at 240 and 320 nm. [The maximum of the band at 240 nm is probably at a lower wavelength but was obscured by the absorbance of chloroform (Fig. 1). Where bromide replaced chloride, the maxima were at 260 and 390 nm; in both cases a transient species absorbed at 275 nm, but could not be obtained separately.] A radiometric study shewed that the extraction of gold arose from this secondary reaction, and not from the formation of a species absorbing at 420 nm, as suggested earlier[4]. Thus in extracting aqueous gold(III) solution with dithizone in chloroform, when the ab-

* For Part I see ref. 1.

sorbance at 420 nm was that expected for complete transformation of dithizone to the disulphide[1,2], the molar ratio of the extracted gold to dithizone consumed was negligible (0.05:1). In the plot of absorbance at 420 nm *vs.* gold/dithizone ratio (Fig. 2) a least squares procedure for fitting the best straight line gave an intercept at the molar ratio *ca.* 1.15:1; fitting by eye would probably have given a figure much closer to 1.0. The deviation was probably due to increasing interference at the higher ratios from the absorbance of the product at 390 nm.

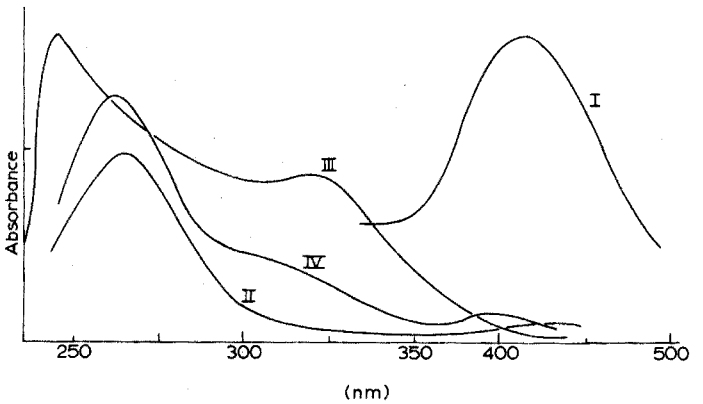

Fig. 1. Absorption spectra of relevant species (note change in scale between 350 and 400 nm), (I) Bis-3,3'-(1,5-diphenylformazan)disulphide ($4.2 \cdot 10^{-5}$ *M*). (II) Dehydrodithizone ($2.9 \cdot 10^{-5}$ *M*). (III) Trichloro-(dehydrodithizone)gold(III) (*ca.* 10^{-4} *M*). (IV) Tribromodehydrodithizonegold(III) ($3.27 \cdot 10^{-5}$ *M*).

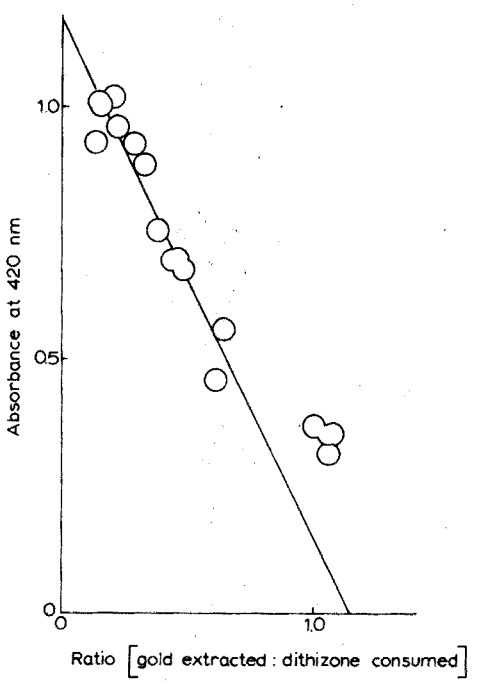

Fig. 2. Plot of absorbance at 420 nm *vs.* ratio of gold extracted to dithizone consumed.

The absorbances at 320 and 240 nm, and at 390 and 260 nm, could be interconverted by shaking the organic phase with gold(III) in an excess of aqueous potassium bromide or chloride, respectively, and they could be generated by extracting gold(III) in aqueous potassium chloride or bromide, respectively, with solutions of dehydrodithizone(I)[8,9] in chloroform.

Radiotracer studies with gold-198 (experimental) shewed that the molar ratio (extracted gold: dehydrodithizone consumed) was 1: 1, and studies with chlorine-36 shewed that for the species absorbing at 320 and 240 nm, the molar ratio for the extract (based on the initial dithizone) was chlorine:dehydrodithizone = 2.92 : 1.

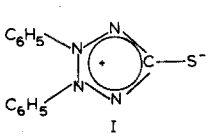

I

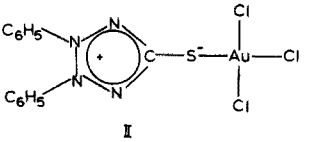

II

Discussion

From the results it is clear that bis-3,3'-(1,5-diphenylformazan)disulphide formed by the oxidation of dithizone with aqueous gold(III) disproportionates to dithizone and dehydrodithizone. The dithizone is then oxidized by more gold(III), and the dehydrodithizone reacts with the excess of gold(III) to form trichlorodehydrodithizonegold(III) which has the formula II. It is this species that causes extraction of gold(III) into chloroform with a fall in absorbance at 420 nm, not a rise. It is probably the extraction of gold in this form which has led to confusion over "gold dithizonate" in the past.

The complex is analogous to the ion bis(dehydrodithizone)mercury(II) obtained by Irving *et al.*[2], and it is assumed that coordination is though the sulphur atom, and square planar about the gold(III)[10].

The behaviour of dithizone with gold(III) under weakly acidic conditions may be summarised as follows.

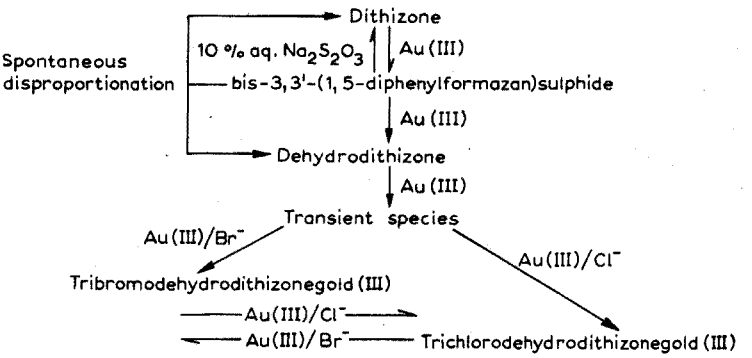

Experimental

Gold-198 was counted with a Panax scintillation counter (dead-time 400 μs) and a well-type crystal (NaI(Tl), 2 × 1.75 in.). Chlorine-36 was measured by evaporating solutions onto planchets and counting with an end-window Geiger–Müller tube. The concentration of dithizone in chloroform was determined spectrophotometrically from the absorbance at 605 nm[11], and that of gold(III) solutions as tetrabromoaurate(III)[12]. Ammonia and hydrochloric acid solutions were prepared

by isopiestic distillation[13]. Extractions were carried out as described previously[1].

Formation of bis-3,3'-(1,5-diphenylformazan)disulphide. The reaction was not entirely reproducible; insufficient shaking left unreacted dithizone, and excessive shaking led to further reaction, the absorbance at 420 nm falling. In some cases, the secondary reaction was so rapid that it was impossible to isolate an organic phase where the absorbance at 420 nm corresponded to the total conversion of the dithizone to dehydrodithizone. The addition of chloride, and specially bromide, to the aqueous phase stabilized the disulphade (Fig. 1).

The effect of prolonged extraction. Gold(III) ($1.25 \cdot 10^{-3}$ *M*) in aqueous potassium chloride (1 *M*, 4 cm^3) and dithizone ($9.6 \cdot 10^{-5}$ *M*) in chloroform (20 cm^3) were shaken together for successive periods of 10 s. Some of the organic phase was removed each time and the spectrum recorded until there was no change from one sample to the next (Fig. 1). The experiment was repeated with gold(III) ($3.7 \cdot 10^{-4}$ *M*) in aqueous potassium bromide (0.5 *M*, 10 cm^3) and dithizone ($5 \cdot 10^{-5}$ *M*) in chloroform (10 cm^3). (See Fig. 1)

TABLE I

EXTRACTION OF GOLD INTO THE ORGANIC PHASE BY FORMATION OF TRIBROMODEHYDRODITHIZONEGOLD(III)

Shaking time (min)	*Corrected count[a] rate (s^{-1})*	*Absorbance at 420 nm*	*Gold : dithizone ratio (organic phase)*
Solvent blank	10.8	—	0
0.25	24.0	1.00	0.158
0.50	21.9	0.93	0.133
0.50	22.9	1.01	0.145
0.50	29.3	0.96	0.221
1.0	28.3	1.02	0.209
2	34.9	0.93	0.288
2.5	37.3	0.89	0.317
3	42.6	0.76	0.380
4	49.7	0.70	0.465
5	51.7	0.68	0.489
6	47.5	0.70	0.439
10	63.8	0.56	0.643
15	62.6	0.46	0.619
20	99.0	0.30	1.054
20	99.0	0.31	1.054
30	102.3	0.35	1.093
45	99.4	0.35	1.059
60	94.5	0.37	1.000

[a] 10^3 c.p.s. corresponds to $1.195 \cdot 10^{-7}$ moles of gold in 2 cm^3.

The extraction of gold. Gold(III) ($4.82 \cdot 10^{-4}$ *M*), labelled with gold-198, in aqueous potassium bromide (1 *M*) was shaken mechanically in 1-cm^3 portions with dithizone ($5 \cdot 10^{-5}$ *M*) in chloroform in 4-cm^3 portions for the times stated in Table I. Each organic phase was separated as rapidly as possible, and washed with water. A portion (2 cm^3) was taken for the spectrum to be recorded and the absorbance at 420 nm measured, and the remainder was used to determine the gold content radiometrically.

Interconversion of trichlorodehydrodithizonegold(III) and tribromodehydrodithizonegold(III). Aqueous gold(III) ($5 \cdot 10^{-4}$ *M*, 10 cm^3) and dithizone in chloroform ($5 \cdot 10^{-5}$ *M*, 10 cm^3) were shaken for 6 h, the change from bis-3,3'-(1,5-diphenylformazan)disulphide to trichlorodehydrodithizonegold(III) being monitored by the spectrum of the organic phase. The aqueous phase was then changed to gold(III) ($5 \cdot 10^{-5}$ *M*) in aqueous potassium bromide (1*M*, 10 cm^3). After 10 min of shaking the spectrum of the oganic phase was that of tribromodehydrodithizonegold(III) (Fig. 1). The complementary experiment, starting from gold(III) ($5 \cdot 10^{-4}$ *M*) in potassium bromide (1 *M*, 10 cm^3), shewed that the conversion of tribromodehydrodithizonegold(III) into trichlorodehydrodithizonegold(III) also took place. Studies on the displacement of bromide with chloride-36 gave a molar ratio (dithizone consumed : chloride required for displacement) of 1 : 3.21.

The preparation of dehydrodithizone and its complexes with gold(III). Dithizone ($2.95 \cdot 10^{-5}$ *M*) in chloroform (20 cm^3) was shaken with aqueous ammoniacal (0.03 *M*) potassium hexacyanoferrate(III) (0.075 *M*, 4 cm^3) until the spectrum of the organic phase was constant[8,9]. Portions of this solution (5 cm^3) were shaken with gold(III) ($5 \cdot 10^{-5}$ *M*) in aqueous potassium chloride (1 *M*, 5 cm^3) or potassium bromide (1 *M*, 5 cm^3). The spectra of the organic extracts were identical with those obtained from dithizone via bis-3,3'-(1,5-diphenylformazan)disulphide.

The stoicheiometry of the dehydrodithizone complexes. Aqueous gold(III) ($1.19 \cdot 10^{-3}$ *M*), labelled with gold-198, was shaken with dehydrodithizone ($3.27 \cdot 10^{-5}$ *M*) in chloroform (5 cm^3) and (a) solid potassium chloride or (b) solid potassium bromide, until the spectrum of the organic phase shewed complete conversion into the complex in each case. The gold extracted was determined radiometrically; molar ratios (gold extracted : dehydrodithizone) of 1.005 : 1 were obtained for the chloro-complex (mean of 3 determinations) and 0.988 : 1 for the bromo-complex. Gold(III) ($1.7 \cdot 10^{-2}$ *M*) in aqueous potassium chloride ($2 \cdot 10^{-2}$ *M*, 1.5 cm^3) labelled with chloride-36 was extracted with dehydrodithizone ($3.75 \cdot 10^{-4}$ *M*) in chloroform (20 cm^3). Successive portions of the organic phase were centrifuged and their spectra and content of chloride-36 measured, giving a molar ratio dehydrodithizone : chloride of 1 : 2.92 at equilibrium.

REFERENCES

1 J. J. Cox and D. M. Servant, *Anal. Chim. Acta*, 66 (1973) 123.
2 H. M. Irving, A. M. Kiwan, D. C. Rupainwar and S. S. Sahota, *Anal. Chem. Acta*, 56 (1971) 205.
3 H. Fischer, *Angew. Chem.*, 47 (1934) 685; H. Fischer and W. Weigl, *Wiss. Veroeff. Siemens-Werken*, 14 (1935) 41.
4 L. Erdey and G. Rady, *Z. Anal. Chem.*, 135 (1952) 1.
5 D. A. Beardsley, G. B. Briscoe, J. Růžička and M. Williams, *Talanta*, 13 (1966) 328.
6 A. W. Titley, *Analyst (London)*, 87 (1962) 349.
7 M. Hranisavljevic-Jakovljevic, I. Pejkovic-Tadic and J. Miljkovic-Stojanovic, *Mikrochim. Acta*, (1965) 141.
8 J. W. Ogilvie and A. H. Corwin, *J. Amer. Chem. Soc.*, 83 (1961) 5023.
9 Y. Kushi and Q. Fernando, *J. Chem. Soc. D*, (1969) 2401.
10 F. A. Cotton and G. Wilkinson, *Advanced Inorganic Chemistry*, Interscience, London, 3rd edn., 1972, p. 1052.
11 S. S. Cooper and M. L. Sullivan, *Anal. Chem.*, 23 (1951) 613.
12 A. Chow and F. Beamish, *Talanta*, 10 (1963) 883.
13 H. M. Irving and J. J. Cox, *Analyst (London)*, 83 (1958) 526.

Analytica Chimica Acta, 74 (1975) 205–207

SHORT COMMUNICATION

Modification to the automatic alkaline carminic acid method for the determination of boric acid in water

P. S. BULL, J. V. EVANS and J. J. FOY

Chemical Technology Division, AAEC Research Establishment, Lucas Heights, N.S.W. (Australia)

(Received 12th June 1974)

Many nuclear reactors use boric acid dissolved in their coolant or moderator as a chemical neutron poison to control reactivity[1]. The range of interest for boron concentration depends on the type of reactor, but it can be 0–10 mg l^{-1} in the moderator and 10–2000 mg l^{-1} in the coolant. Demmitt[2] described an automatic procedure for such solutions based on an alkaline carminic acid method. The method dispensed with the concentrated sulphuric acid medium formerly recommended[3] because it posed problems for in-line monitoring applications. The automated alkaline carminic acid method has been used in a study[4] of the use of ion-exchange resins to control boric acid concentrations over the range 0–100 mg l^{-1}. Experience showed that metals present in the water, arising from corrosion of the construction materials of the water loop used, which were of similar levels of concentration to those normally found in reactor circuits, were sufficient to reduce the reproducibility of the method considerably.

When the method was calibrated with pure standard solutions, a sensitivity of 1% of full scale deflection (f.s.d.) was obtained with a reproducibility of 2% f.s.d.; these are the same as the values found by Demmitt. However, when boric acid solutions which had been circulated in a stainless steel loop were analysed, the reproducibility could become as bad as $\pm 10\%$ f.s.d. Spectrographic analysis showed that metal ion impurities were present, in particular lead and iron at concentrations up to 2 mg l^{-1}. The interference effect is probably due to precipitation of insoluble hydroxo compounds of these metals in the alkaline solution, which leads to significant light scattering in the flow cell. Since these precipitates travel more slowly than the solution through the autoanalyser tubing, interference is caused not only in the sample itself but also in the following reference blanks standards and samples. Passage of one contaminated sample was shown to interfere with the analysis of the following eight standard reference samples; this represented the time required to flush the precipitate from the tubing.

Interference by these low levels of metals meant that the method would not be satisfactory for use as an in-line analytical method for reactor water circuits. However, since the determination is made in alkaline conditions, it was thought that the use of the di-sodium salt of ethylenediaminetetraacetic acid (EDTA) as a sequestering agent should prevent interference. The masking effect of EDTA on lead iron and aluminium, in the analysis for boric acid, was therefore investigated.

Experimental

Two buffer solutions were prepared, one as described by Demmitt[2] (4 *M* NH_4Cl and 1 *M* NH_4OH) and the other identical but with the addition of 1 g l^{-1} of EDTA (di-sodium salt). Standard boric acid solutions were prepared containing 10, 20, 40, 50, 60, 80 and 100 mg l^{-1} of boron, and a calibration curve was obtained for each buffer with these standards.

Several 50 mg l^{-1} and 10 mg l^{-1} boron standards were also prepared and doped with various concentrations of lead nitrate, aluminium sulphate or iron(III) nitrate. Duplicate samples of these solutions were then analysed, and the extent of interference from the metal ions and the level masked by EDTA were determined. All solutions were prepared directly by dissolving analytical reagent-grade chemicals in distilled demineralized water. A 0.02% (w/v) carminic acid solution was prepared, stirred overnight and filtered to remove any residue. Distilled demineralized water was used as the reference blank. Analyses were carried out on a Technicon Auto-analyser; transmittance was measured at 575 nm in a triple-pass 50-mm light-path flow cell. For convenience, these analyses were done with 50 mg l^{-1} as f.s.d.

Results

The calibration curves were identical with both buffers; thus EDTA itself does not interfere. The EDTA reduced the interference from all three metals (Table I).

TABLE I

REDUCTION OF METAL ION INTERFERENCE BY EDTA

Metal ion	*Highest concentration masked by EDTA (1 g l^{-1}) (mg l^{-1})*	*Error caused by this metal concentration in absence of EDTA (mg l^{-1})*
Al^{3+}	0.1	−4
Fe^{3+}	1.0	−7
Pb^{2+}	20.0	−20

Above the concentrations quoted, the metals caused a significant deviation from the normal reproducibility of the method which, under the conditions used, was ±1 mg l^{-1}. Of the metals examined, the treatment was least successful with aluminium.

Conclusion

The automated alkaline carminic acid analysis is satisfactory for on-line determination of boric acid concentration in reactor circuits, or in similar applications. Interference from precipitation of the dissolved metal ions, picked up from corrosion of such circuits, may be prevented by the addition of the di-sodium salt of EDTA to the buffer solution. At the concentrations of these metals likely to be found in solution, 1 g l^{-1} of EDTA in the buffer is sufficient to mask any interference.

REFERENCES

1 P. Cohen, *Water Coolant Technology of Power Reactors*, Gordon and Breach, New York, 1969.
2 T. F. Demmitt, *Automation in Analytical Chemistry, Symposium*, Mediad Inc., New York, Sept. 1965, p. 204.
3 F. D. Snell and C. F. Snell, *Colorimetric Methods of Analysis*, Volume IIA, Heinemann, London, 1959.
4 P. S. Bull and J. V. Evans, to be published.

Analytica Chimica Acta, 74 (1975) 208–211

SHORT COMMUNICATION

Determination of calcium in cements by titration with EGTA

HALLDÓR ÁRMANNSSON* and HELGI F. MAGNÚSSON
Industrial Research and Development Institute, Keldnaholt, Reykjavík (Iceland)
(Received 22nd November 1973)

Calcium in cement is usually determined by precipitation with ammonium oxalate, after treatment with sulphuric and hydrofluoric acids to remove silica, and a precipitation treatment with ammonia solution to remove other interfering oxides[1]. As this procedure is lengthy and rather imprecise, a study of alternative methods was undertaken. The methods studied were atomic absorption spectrometry and complexiметric titrations with EDTA or EGTA (ethyleneglycol-bis(aminoethylether)-tetraacetic acid). The EGTA method proved superior, and is reported here. Schwarzenbach[2] has shown that EGTA forms a more stable complex with calcium than with magnesium; it is thought that the size of the metal ion is a major influence in determining the stability of EGTA complexes. Ringbom *et al.*[3] described an EGTA titration for the determination of calcium in the presence of magnesium, with zincon as an indirect indicator. The solution was buffered at pH 10, and care was taken that the ratio between the concentrations of the zinc-complex used (ZnX) and the calcium-complex (CaX) did not exceed 1:10.

Experimental

Apparatus. An Eel phototitrator connected to a Unigalvo galvanometer was used. Filter no. 607, with maximal absorption at 600 nm, gave the maximal difference between the blue and orange colours of zincon solutions.

Samples. Tests were made on five samples of standards from the National Bureau of Standards (Nos. 1011, 1013, 1014, 1015 and 1016), and eight samples of cement employed in the Icelandic building industry. (Nos. I–VI are Icelandic Portland samples with CaO content 60–62%, while VII and VIII are low alkali cements with CaO content 64–66%).

Conditions. The effect of different ZnX/CaX ratios was tested with solutions of zinc and calcium in distilled water, and in cement solutions containing different concentrations of zinc; there was an obvious interdependence in the distilled water solutions, but this was absent in the cement solutions.

The sharpness of the end-point depended on the amount of indicator. Because of difficulties in dissolution, the indicator was added in a relatively large volume.

Interferences. The most probable potential interfering ion was iron(III). It is

* Present address: Department of Oceanography, The University, Southampton (England).

known that moderate concentrations of iron(III) (7 mg l^{-1}) and aluminium(III) (5 mg l^{-1}) interfere with the colour of the zincon solution[4]. Culkin and Cox[5], who applied the method to sea water found that magnesium and strontium both caused slightly high results, in direct proportion to their concentrations. The effects of the additions of Si, Al, Fe, and Mg in different concentrations and different proportions to calcium were investigated (Table I). Mg, Si, and Fe, when present on their own, interfered only slightly (errors did not exceed $\pm 0.5\%$), but Fe and Si together caused low results and poor end-points. It was therefore decided to remove silicon and iron before the titration, by treatments with sulphuric–hydrofluoric acid, and ammonia solution[1]. Residues from the acid treatment and single and double precipitations with ammonia solution were dissolved and their calcium contents determined by atomic absorption spectrometry. The results (Table II) show that the residue from the hydrofluoric acid treatment must be combined with the bulk solution and that double precipitation with ammonia is necessary.

Standardization. The EGTA solution was originally standardized against a standard calcium solution, prepared by dissolving calcium carbonate in dilute nitric acid. The titres thus obtained were satisfactory for the analysis of N.B.S. cement

TABLE I

THE EFFECTS OF Si, Al, Fe AND Mg ON THE TITRATION OF CALCIUM WITH EGTA

(Solutions containing 11.70 mg of calcium(II) and the listed amounts of other ions were titrated.)

Solution (mg)/20 ml				*Ca found (mg)*	*% Deviation*
Si	*Al*	*Fe*	*Mg*		
3	0.6	0.6	0.6	11.33	−4.84
—	0.6	0.6	0.6	11.55	−1.92
3	—	0.6	0.6	11.22	−6.26
3	0.6	—	0.6	11.51	−2.52
3	0.6	0.6	—	11.31	−5.56
—	—	0.6	0.6	11.66	−0.50
—	0.6	—	0.6	11.67	−0.45
—	0.6	0.6	—	11.52	−2.37
3	—	—	0.6	11.61	−1.11

TABLE II

CaO IN RESIDUES FROM ACID TREATMENT AND PRECIPITATIONS WITH AMMONIA SOLUTION

Residue from	*No. of tests*	*% CaO*	
		Average	*Range*
H_2SO_4–HF treatment	7	0.49	0.13–0.86
Single precipitation with NH_4OH	7	0.38	0.04–0.74
Double precipitations with NH_4OH	7	0.02	0.00–0.09

standards. However, in view of the difficulties in obtaining high-purity calcium carbonate, it was considered advisable to carry out empirical standardizations. These tests on standard cements also showed that the MgO and SrO contents of the cement standards did not affect the results of the titration.

Reagents

EGTA (0.01 M). Dissolve 7.604 g of EGTA in 40 ml of 1 *M* sodium hydroxide in water and dilute to 2 l.

Buffer solution. Dissolve 50 g of borax, 7 g of ammonium chloride and 11.4 g of sodium hydroxide in water and dilute to 2 l.

Indicator solution. Dissolve 65 mg of zincon and 2.0 ml of 0.1 *M* sodium hydroxide in water and dilute to 100 ml.

Zn–EGTA solution (0.005 M). To 20 ml of 0.01 *M* zinc sulphate solution add 20 ml of buffer solution and 0.5 ml of indicator solution; titrate with EGTA (0.01 *M*). The ratio ($T/20$) between the titre (T) and the volume of the zinc(II) solution shows in which ratio the zinc(II) and EGTA solutions should be mixed to obtain exact equivalence.

Preparation of sample solutions. The solutions are prepared as for precipitations with ammonium oxalate[1]. Dissolve 0.5 g of sample in 15 ml of (1+2) hydrochloric acid, evaporate to dryness, add 20 ml of (1+1) hydrochloric acid to the residue, filter off the separated silicic acid, ignite it at 1100–1200°C and treat it, after cooling, with 0.5 ml of distilled water, 2 drops of (1+1) sulphuric acid and 10 ml of hydrofluoric acid (*ca.* 40%). Fuse the residue left after this treatment with 0.5 g of potassium pyrosulphate, dissolve the melt in water and add the resulting solution to the original filtrate, whose volume should now be *ca.* 200 ml. Add a 10–15 ml excess of hydrochloric acid, neutralize the solution to methyl red (add a few drops), with (1+1) ammonia solution, and add one drop in excess. Redissolve the precipitate in (1+3) hydrochloric acid, dilute the resulting solution to *ca.* 100 ml, and repeat the precipitation. Combine the filtrates and dilute to 500 ml with distilled water.

Titration. Add 20 ml of cement solution, 20 ml of buffer solution, 10 ml of Zn–EGTA solution and 0.5–1.0 ml of indicator solution to the titration vessel. Start the magnetic stirrer and set the galvanometer at 10. Titrate with 0.01 *M* EGTA solution until a colour change is detectable by eye. Then take galvanometer readings at 0.1–0.2-ml intervals until constant readings are obtained. Plot the readings and obtain the exact end-point by extrapolation.

TABLE III

COMPARISON OF STANDARD DEVIATION AND PRECISION VALUES FOR THREE METHODS OF DETERMINATION OF CALCIUM IN CEMENT

Method	*Standard deviation* (s_r) (%)	*Precision at the 95% level* ($x+2s_r$) (%)
Titrimetric with EGTA	0.10	0.35
Gravimetric	0.69	2.0
Atomic absorption spectrometry	2.14	6.4

Results and discussion

Precision. The standard deviation was derived from measurements on 8 replicate samples. Similar tests were performed using ammonium oxalate precipitation and atomic absorption spectrometry. The results (Table III) show that the present method compares advantageously.

Constituent sums. The total composition of six samples was determined. These were analyzed for calcium titrimetrically with EGTA and gravimetrically with ammonium oxalate. The results are shown in Table IV. The sums of all constituents fall within the limits of 99.50% and 100.75% in both cases, but the values are less scattered and lower on average for the titrimetric method.

ABLE IV

OMPARISONS OF TITRIMETRIC (EGTA) AND GRAVIMETRIC DETERMINATIONS OF CaO IN EMENTS

mple	*Gravimetric (% CaO)*	*Titrimetric (% CaO)*	*Difference (% CaO)*	*Difference as % of mean*	*Sum including gravimetric result (%)*	*Sum including titrimetric result (%)*
I	61.06	61.41	+0.35	0.57	99.78	100.13
'	60.90	60.69	−0.21	0.34	99.99	99.78
	61.67	60.90	−0.77	1.26	100.68	99.91
I	61.09	60.80	−0.29	0.48	99.81	99.52
II	64.76	64.16	−0.60	0.93	100.40	99.80
III	65.56	65.89	+0.33	0.50	99.50	99.83

REFERENCES

1 *ASTM Standards*, Part 4, 1958, Method C 114–58.
2 G. Schwarzenbach, *Die Komplexometrische Titration*, Ferdinand Enke Verlag, Stuttgart, 2nd edn., 1956.
3 A. Ringbom, G. P. Pensar and E. Wänninen, *Anal. Chim. Acta*, 19 (1958) 525.
4 *Standard Methods for the Examination of Water and Wastewater*, American Public Health Association, Inc., New York, 12th edn., 1965.
5 F. Culkin and R. A. Cox, *Deep Sea Res.*, 13 (1966) 789.

Analytical Chimica Acta, 74 (1975) 212–215

SHORT COMMUNICATION

Microdosage colorimétrique de l'anion cyanure dans le sodium

J. PELERIN et A. HATTERER
École Supérieure de Chimie de Mulhouse, 3, rue Alfred Werner, 68093 Mulhouse (France)
(Reçu le 24 juin 1974)

Dans le cadre de l'étude du mécanisme de transfert du carbone entre aciers par l'intermédiaire du sodium liquide, nous avons été amenés à doser divers composés carbonés dans le métal alcalin.

Pour les dosages des carbonates et du carbone libre, les modes opératoires décrits dans de nombreuses publications permettent d'opérer sans difficultés au niveau de 1 à 5 p.p.m. (en masse) environ. Par contre, le dosage du cyanure dans le sodium a été peu étudié et les méthodes employées jusqu'à présent restent peu sensibles. Ainsi Hobert et Bjork[1] déterminent la quantité de cyanure à 0,5 μg près par volumétrie. Fischer et Cafasso[2] ne disposent pas d'une méthode pouvant détecter moins de 7 p.p.m. Luner[3] et Veleckis *et al.*[4] utilisent une détermination colorimétrique proposée par Nusbaum et Skupeko[5] et dont la limite de détection est de 0,75 p.p.m. La méthode préconisée par Silverman[6] ne permet guère de doser moins de 1 p.p.m. La méthode que nous proposons a une sensibilité de l'ordre de 0,01 p.p.m.

Choix d'une méthode

L'anion cyanure est généralement dosé en colorimétrie par le réactif pyridine–pyrazolone (Epstein[7]). Cependant, nous lui avons préféré le réactif pyridine–acide barbiturique (méthode de Asmus et Garschagen[8], reprise par Weiner et Leiss[9]), dont la préparation est plus facile et la conservation meilleure, la sensibilité du dosage étant sensiblement identique.

Le cyanure est transformé par de la chloramine-T en chlorure de cyanuryle ClCN. Celui-ci réagit avec de la pyridine et de l'acide barbiturique pour former une polyméthine violette (réaction de Zincke–König[10,11]) dont l'absorbance est mesurée à 580 nm.

Après minéralisation du sodium, puis neutralisation de la solution aqueuse alcaline, avec de l'acide sulfurique, l'anion cyanure se trouve en présence d'ions Na^+ et SO_4^{2-}. Ces ions sont en concentrations trop grandes pour ne pas gêner le dosage direct du cyanure, dont la séparation est ainsi rendue indispensable. L'acide cyanhydrique étant un acide faible ($pK_A = 9{,}3$) et très volatil ($E_{760} = 25{,}7°C$), se déplace aisément par distillation en présence d'un acide fort (H_2SO_4).

Partie expérimentale

Appareillage. L'appareillage proposé permet de réaliser les différentes opérations suivantes:

minéralisation du sodium sous atmosphère contrôlée: dosage des acétylures, des sodium–alkyls et des hydrocarbures dissous;

acidification: dosage des carbonates sous forme CO_2;

distillation de l'acide cyanhydrique;

dosage du carbone libre libre par la voie humide selon Pepkowitz et Downer[1,2]. Les dosages autres que celui du cyanure et l'appareillage correspondant ne sont pas décrits en détail mais sont mentionnés, car ils s'intègrent dans notre travail de recherche.

Le ballon en quartz (Fig. 1) résiste aux chocs thermiques de la minéralisation. Sa forme cônique est imposée par la hauteur de barbotage d'hélium qui doit être importante, de façon à bien dégazer la solution (dosage des hydrocarbures et des carbonates).

Pour ces dosages, l'introduction de l'échantillon de sodium se fait sous argon purifié en boîte à gants, afin d'éviter tout contact avec l'anhydride carbonique atmosphérique. Le robinet trois voies (4) permet alors de purger la canalisation avant d'envoyer le gaz vecteur (hélium) dans le ballon.

Si l'appareillage n'est destiné qu'au dosage du cyanure, un ballon de forme sphérique parait préférable (meilleure résistance mécanique et surface d'évaporation plus importante); aucun gaz ne devant alors être recueilli dans l'azote liquide, l'hélium peut être avantageusement remplacé par de l'argon.

Appareil de mesure. Spectrophotomètre à double faisceau, à longueur d'onde réglable. L'appareil utilisé pour nos essais est un modèle Jean & Constant (Prolabo).

Réactifs. Tous les réactifs sont du type R.P. ou Suprapurs. La pyridine est du type pour spectroscopie.

Préparer l'antidote de HCN (chlorure ferreux et carbonate de sodium) avant de manipuler.

Chloramine-T. 1% dans de l'eau distillée (à refaire journellement).

Réactif pyridine–acide barbiturique. Placer dans un ballon jaugé de 50 ml, 3 g d'acide barbiturique, 15 ml de pyridine, 3 ml d'acide chlorhydrique concentré et compléter avec de l'eau distillée. Le réactif se conserve deux à trois semaines. Il se colore alors légèrement en jaune, ce qui n'affecte pas le dosage.

Étalonnage. Peser avec précision environ 110 mg de cyanure de potassium. Les placer dans un ballon jaugé de 1 l, ajouter 4–5 gouttes de solution aqueuse de soude caustique (1 *M* environ) et compléter avec de l'eau distillée. Diluer 20 fois (5 ml dans une fiole de 100 ml), puis encore 10 fois (10 ml dans 100 ml) en utilisant toujours de l'eau légèrement alcaline (pH 8–9). La dernière solution contient 0,100 μg C(CN) ml^{-1} pour une masse de cyanure initiale de 108,5 mg. Si cette solution est finalement utilisée avec une pipette de 1 ml, l'erreur relative due à la verrerie (classe A) est de 1,5%.

Tracé de la courbe d'étalonnage. Introduire 1, 2, 3, etc... ml de solution ci-dessus dans un ballon jaugé de 25 ml. Ajouter 5 ml de solution tampon pH 5,5 (phosphate), puis 1 ml de chloramine-T à 1%, fermer immédiatement le ballon et agiter. Après 1 min, 3 ml de réactif pyridine–acide barbiturique sont introduits, et le volume est complété par de l'eau distillée jusqu'à environ 1 cm sous le trait de jauge. Le remplissage exact se fait après 5 min en bain thermostaté.

A la huitième minute, l'absorbance est déterminée à 580 nm en plaçant dans

le faisceau de référence, une solution préparée comme précédemment, c'est-à-dire contenant tous les réactifs sauf le cyanure.

La loi de Lambert–Beer est bien vérifiée pour 0,1 à 0,9 μg C(CN). Avec notre spectrophotomètre, l'absorbance est de 1,00 pour 0,83 μg C.

Mode opératoire pour le dosage du cyanure dans le sodium. Peser environ 1 g de sodium à analyser. L'introduire dans le ballon en quartz. Laisser la sortie après le robinet (7) à l'air libre. Lubrifier les rodages à la graisse si l'appareillage n'est jamais utilisé pour le dosage du carbone libre, à l'acide phosphorique concentré dans le cas contraire. Faire plonger le ballon (1) dans un mélange d'eau et de glace. Purger 15 min avec un débit de gaz vecteur de 70 ml min^{-1}. Remplir l'ampoule (3) d'eau distillée. Minéraliser lentement le sodium (1 goutte/20 à 30 s). Utiliser environ 10 ml d'eau par g du sodium.

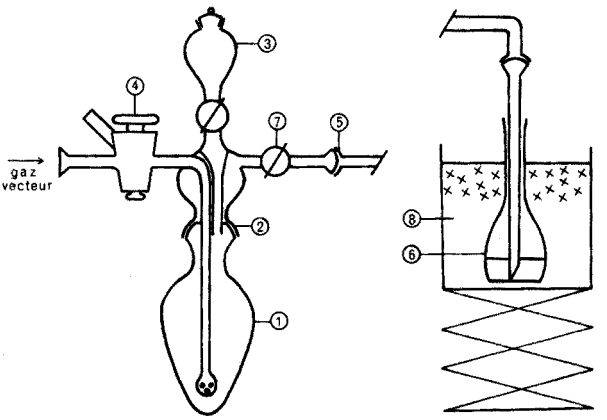

Fig. 1. L'appareillage. 1: Ballon en quartz; 2: rodage sphérique 29/15; 3: ampoule supérieure; 4: robinet 3 voies; 5: rodage sphérique 13/5; 6: fiole jaugée de 25 ml; 7: robinet de sortie; 8: eau + glace.

Compléter le montage de la Fig. 1. Introduire 5 à 7 ml d'eau dans la fiole de 25 ml et deux gouttes de solution aqueuse de soude caustique (1 *M*). Placer le mélange réfrigérant autour de la fiole. Règler le débit de gaz vecteur à 1 ou 2 bulles/s. Placer environ 6 ml d'acide sulfurique à 25% dans l'ampoule (3). Les introduire lentement dans le ballon. Remplacer sous le ballon la glace par un bain d'acide phosphorique concentré. Y plonger un thermomètre gradué au moins jusqu'à 150°C. Chauffer doucement. L'ébullition dans le ballon est régularisée par le barbotage de gaz vecteur. Conduire la distillation très lentement.

Lorsque environ la moitié du contenu du ballon est distillée, tout le cyanure se retrouve dans le ballon jaugé qui est alors retiré et réchauffé jusqu'à la température ambiante.

Le mode opératoire est alors poursuivi comme lors de l'étalonnage: tamponner à pH 5,5, ajouter la chloramine-T puis le réactif pyridine–acide barbiturique.

Efficacité de la distillation. Nous avons effectué plusieurs essais de recoupement avec des quantités connues de cyanure en solution aqueuse introduite dans le ballon par pipetage. L'erreur relative est de 2 à 3% par défaut, au niveau de

0 μg C (10 p.p.m. à partir de 1 g Na) et 5 à 10% par défaut, pour 0,5 μg 0,5 p.p.m.).

Conclusion

Cette méthode de dosage très sensible doit nous permettre de vérifier l'hypothèse du transfert du carbone entre aciers dans le sodium par l'intermédiaire du cyanure[13]. L'azote provenant des réactifs en présence (aciers–sodium–gaz de couverture) évolue entre les diverses phases dans un cycle permettant la solubilisation du carbone de l'acier ferritique avec formation de cyanure capable de carburer l'acier austénitique.

Les auteurs remercient Monsieur Oberlin (Electricité de France, les Renardières) pour l'aide qu'il bien voulu apporter à ce travail.

BIBLIOGRAPHIE

1 E. W. Hobart et R. D. Bjork, *Nucl. Appl. Technol.*, 1 (1965) 490.
2 A. K. Fischer et F. A. Cafasso, *American Nuclear Sciences Transactions ANS*, 14 (1971) 2, 624.
3 C. Luner, A. Cosgara et H. M. Feder, *Symp. Alkali Metal Coolants*, Vienne, 1966.
4 E. Veleckis, K. E. Anderson, F. A. Cafasso et H. M. Feder, *Argonne National Laboratory, ANL 7520, Part 1*, Nov. 1968, p. 295.
5 I. Nusbaum et I. Skupeko, *Metal Finish.*, 49 (1951) 61.
6 L. Silverman, *Determination of Impurities in Nuclear Grade Sodium Metal*, Pergamon, Oxford, 1971.
7 J. Epstein, *Anal. Chem.*, 19 (1947) 4, 272.
8 E. Asmus et H. Garschagen, *Fresenius' Z. Anal. Chem.*, 138 (1953) 44.
9 R. Weiner et C. Leiss, *Metalloberflache*, 25 (5) (1971) 185.
10 T. Zincke, *Justus Leibigs Ann. Chem.*, 333 (1904) 340.
11 W. König, *J. Prakt. Chem.*, 69 (1904) 105.
12 L. P. Pepkowitz et R. J. Downer, *Anal. Chem.*, 28 (1953) 520.
13 A. Hatterer *et al., Vè Congrès de Corrosion—Thème B, Paris, 26 septembre 1973.*

Analytica Chimica Acta, 74 (1975) 216–219

SHORT COMMUNICATION

Analysis of paints for lead by atomic absorption spectrometry

WALTER HOLAK
Food and Drug Administration, 850 Third Avenue, Brooklyn, New York 11232 (U.S.A.)
(Received 18th April 1974)

In the determination of heavy metals in paints by conventional atomic absorption spectrometry, the metals in the paint must first be solubilized through a dry ash or acid digestion procedure[1,2]. Scott[3] has described the analysis by four laboratories of 98 paints and related products which were performed to comply with the FDA Commissioner's request for information on heavy metals in paints. Atomic absorption spectrometry was the means of measurement used in each case; the sample treatment generally consisted of dry ashing at about 500°C and the digestions were carried out with acids (HNO_3, $HClO_4$, H_2SO_4) in open vessels. The drawbacks to these sample treatments include the volatility losses of some elements and the cumbersome and time-consuming nature of the procedures.

This communication describes a somewhat different approach to the analysis of paints for lead (which may be applicable to other metals) by atomic absorption, which overcomes some of these drawbacks. First, a rapid qualitative test is performed by means of a nichrome wire sampling step. If the result is positive for lead, the lead is determined as follows: the lead in the paint is solubilized by a closed system nitric acid digestion followed by the standard flame atomic absorption spectrometry or the "sampling boat" technique for low lead levels.

Experimental

Instruments and apparatus. All measurements were made on a Perkin–Elmer Model 403 atomic absorption spectrophotometer equipped with the microsampling and background correction accessories. The 283.3-nm line from a lead hollow-cathode lamp was used. The flame was air–acetylene. Absorption signals were traced on a Hitachi 165 recorder and/or obtained from the instrument digital output indicator operated in the "concentration" mode. Samples were digested in a closed system Teflon vessel[4].

Reagents. All reagents used were analytical-reagent grade. Lead standard solutions were prepared from lead nitrate.

Qualitative test for lead. Bend a length of size 26 nichrome wire so as to form a loop (*ca.* 7 mm diameter) that will serve as the sampling device. Dip the loop of the wire into the paint to deposit *ca.* 0.3 mg of paint. If the test object is a painted surface, place a drop of a suitable solvent (acetone, methylene chloride, methyl isobutyl ketone, etc.) on the painted surface. Dip the loop of the wire

into the solvent and rub on the paint film. As the solvent softens the paint and evaporates, a small amount (*ca.* 0.3 mg) of the paint will adhere to the wire. Connect the wire to the microsampling slide in place of the Delves sampling cup holder. While the instrument is operating and the recorder tracing, push the loop of the wire with the sample into the flame below the light beam of the hollow-cathode lamp. When the recorder pen returns to the base line, pull the nichrome wire out of the flame.

Quantitative analysis for lead. Spread thinly *ca.* 0.3 g of paint on a glass slide and place in an oven at 120°C to dry for 2 h. Scrape off with a razor blade about 0.1 g of the dried paint film and weigh accurately into the Teflon vessel. (Omit the drying in the case of painted objects). Add 3.0 ml of concentrated nitric acid, close the vessel and place into an oven for at least 1 h at 150°C. Allow the vessel and the contents to come to room temperature, transfer the solution and any precipitate that is present with the aid of distilled water to a 25-ml volumetric flask, dilute to volume and mix. Allow any precipitate to settle or filter the solution.

For lead levels greater than 1 μg ml^{-1}, determine lead by conventional atomic absorption spectrometry. Prepare lead standards in 12% nitric acid. The lower limit is about 1 μg Pb ml^{-1} in solution or 0.025% in the sample based on a 0.1-g sample diluted to 25 ml.

For lead levels less than 1 μg ml^{-1}, determine lead by the "sampling boat" technique. Add 5 drops of ammonia water to the boat or enough to maintain the solution at an alkaline pH after the sample is added (ammonia is added to prevent the oxidation of the tantalum boat by nitric acid). Add 0.1–0.3 ml of the sample solution by means of an Eppendorf pipet. Push the boat close to the flame to evaporate the solvent. While the recorder is tracing, depress the instrument "100 AVERAGE" pushbutton and immediately after the "UPDATE" indicator light goes off, and the instrument is zeroed, push the boat into the flame. When the recorder pen returns to the base line, pull the boat out of the flame and note the displayed digital signal. Repeat the procedure for the sample with aliquots of lead standard. Determine the sample lead content from the standard additions plot.

Results and discussion

The purpose of the qualitative test is to screen a large number of samples rapidly for lead. Those samples which contain no lead will, of course, not require additional analysis, thus saving a considerable amount of time and effort. This test can easily be made flexible with respect to the detection limit; other lead wavelengths may be used, *e.g.* the 261.4-nm line.

In Table I are shown the results of the determination of lead in 14 paint samples, which were 7 sets of duplicates, a fact not known to the analysts. These samples were treated by the generally used nitric acid reflux digestion (2 h) for comparison in addition to the proposed method. The agreement among the results is good, considering the nature of the samples. The theoretical values, where known, are also given.

A comment may be in order concerning the closed system sample digestion. Although, in this work lead was the metal sought, the technique should be

TABLE I

COMPARATIVE ANALYTICAL RESULTS FOR THE DETERMINATION OF LEAD IN PAINTS

Sample no.[a]	*Per cent lead*		
	Theoretical	*Open vessel wet digestion*	*Closed system digestion*
2	0.096	0.090	0.093
5		0.092	0.102
4	0.091	0.087	0.094
9		0.084	0.090
6	0	0	0
10		0	0
12	—	0.308	0.302
13		0.312	0.297
8	—	0.321	0.319
11		0.309	0.315
3	0.108	0.106	0.099
7		0.103	0.099
1	—	0.025	0.025[b]
14		0.020	0.029

[a] Samples 2,5; 4,9; 6,10 were latex paints; samples 12,13; 8,11; 3,7; 1,14 were alkyd paints.
[b] Determined using the "sampling boat" technique.

especially valuable for metals which are volatile at low temperatures and can be lost by the usual digestion. For example, mercury can easily be determined in paints by the proposed method followed by flameless atomic absorption spectrometry[5]. In addition, the closed system digestion is more efficient than the digestion in open vessels because pressure is developed in the former. Finally, since the closed system digestion requires no attention by the analyst it is more convenient than the open vessel digestions.

The "sampling boat" technique was found useful for low levels of lead in paints and can probably be applied to other metals, *e.g.* cadmium. The signal measurement technique described provides an output which is proportional to the area under the peak and was found to be more reproducible than measuring peak heights.

Conclusion

Procedures for the analysis of lead in paints by atomic absorption spectrometry are presented. A rapid qualitative wire sampling test is used for screening. A closed system digestion in a Teflon vessel followed by conventional atomic absorption or the "sampling boat" technique is used for determination. These techniques were found to save time and overcome some of the drwabacks of other generally used atomic absorption methods.

The author is grateful to Dr. Thomas Medwick, Science Advisor, Food and Drug Administration, New York District, and Professor of Pharmaceutical Chemistry, College of Pharmacy, Rutgers University, for his invaluable assistance

in the preparation of this manuscript, and to Warren Porter, Consumer Product Safety Commission, Washington, D.C. for supplying the samples and information.

REFERENCES

1 B. Searle, Wing Chan, Curt Jensen and B. Davidow, *At. Absorption Newslett.*, 8 (6) (1969) 126.
2 J. H. Barker, W. B. Chapman and A. J. Harrison, *J. Ass. Pub. Anal.*, 2 (4) (1964) 89.
3 R. W. Scott, *166th ACS National Meeting, Chicago, Illinois, Aug. 26–31, 1973.*
4 B. Bernas, *Anal. Chem.*, 40 (1968) 1682.
5 R. K. Munns and D. C. Holland, *J. Ass. Offic. Anal. Chem.*, 54 (1971) 202.

Analytica Chimica Acta, 74 (1975) 220–222

SHORT COMMUNICATION

Calculation of the stability constants of complexes with respect to Simms' conception of dissociation of polyvalent acids

J. KLAS

Department of Inorganic Chemistry, Slovak Technical University, Bratislava 880 37 (Czechoslovakia)

(Received 17th June 1974)

This communication presents a general, accurate and relatively simple mathematical method for the determination of the stability constants of complexes by means of the average ligand number of a system of complexes ML_i $(i=1, 2, \ldots, N)$.

In a system of complexes ML, ML_2, ..., ML_N, the average ligand number $(\bar{n})$ may be expressed by the relationship[1]

$$\bar{n} = \frac{\beta_1[L]+2\beta_2[L]^2+\ldots+N\beta_N[L]^N}{1+\beta_1[L]+\beta_2[L]^2+\ldots+\beta_N[L]^N} \quad (1)$$

where β_i is the overall stability constant of the i^{th} complex, and [L] is the equilibrium concentration of the free ligand.

This function can be transformed in accordance with Simms' concept[2,3] of the dissociation of polyvalent acids

$$\bar{n} = \frac{G_1}{G_1+[L]^{-1}} + \frac{G_2}{G_2+[L]^{-1}} + \ldots + \frac{G_i}{G_i+[L]^{-1}} + \ldots + \frac{G_N}{G_N+[L]^{-1}} \quad (2)$$

which is equivalent to eqn. (1) if the β constants are related to the G constants in the following way:

$$\beta_1 = \sum_i G_i,\ \beta_2 = \sum_{i<j} G_iG_j,\ \beta_3 = \sum_{i<j<k} G_iG_jG_k, \ldots, \beta_N = G_1G_2\ldots G_N \quad (3)$$

where the indices i, j, k are integers 1, 2, 3, ... N.

When $[L]^{-1} = G_i$ in accordance with eqn. (2), then $\bar{n} = \bar{n}_i$ and

$$\bar{n}_i = \frac{G_1}{G_1+G_i} + \frac{G_2}{G_2+G_i} + \ldots + \frac{1}{2} + \ldots + \frac{G_N}{G_N+G_i} \quad (4)$$

Equation (4) expresses a suitable relationship between the $(G_1, G_2, \ldots G_N)$ constants and the corresponding values of the average ligand number $(\bar{n}_1, \bar{n}_2, \ldots \bar{n}_N)$. The relationship mentioned above can be used for the calculation of overall stability constants according to eqn. (3).

Particular examples

(A) If the G constants form a decreasing series $G_1 > \ldots > G_{i-1} \gg G_i \gg G_{i+1} > \ldots > G_N$, then according to eqn. (4), one can obtain

$$\bar{n}_i^{(A)} = i - \tfrac{1}{2} \tag{5}$$

(B) If the G constants form an increasing series $G_1 < \ldots < G_{i-1} \ll G_i \ll G_{i+1} < \ldots < G_N$, then according to eqn. (4) one can obtain

$$\bar{n}_i^{(B)} = N - i + \tfrac{1}{2} \tag{6}$$

In case (A), the average ligand number forms an increasing series of half-integer values $\bar{n} = (\frac{1}{2}, \frac{3}{2}, \ldots N - \frac{3}{2}, N - \frac{1}{2})$. In case (B), the average ligand number forms a decreasing series of the same values of $\bar{n} = (N - \frac{1}{2}, N - \frac{3}{2}, \ldots \frac{3}{2}, \frac{1}{2})$ and $\bar{n}_i^{(A)} + \bar{n}_i^{(B)} = N$. The overall stability constants of complexes by eqn. (3) do not depend on the sequence of G constants, but only on their values. Hence, it can be seen that the distinction between the cases (A) and (B) is not intrinsic and from a mathematical point of view the cases above are equal to each other.

(C) If all the G values are identical ($G_1 = G_2 = \ldots = G_N$), then according to eqn. (4), we have:

$$\bar{n}_i^{(C)} = N/2 \tag{7}$$

for each integer i.

In this special case the overall stability constants of complexes, eqn. (3), may be expressed by the equations:

$$\begin{aligned}
&\beta_1 = NG \\
&\ldots \\
&\beta_{i-1} = \frac{N!}{(N-i+1)!(i-1)!} G^{i-1} \\
&\beta_i \quad = \frac{N!}{(N-i)!\, i!} G^i \\
&\beta_{i+1} = \frac{N!}{(N-i-1)!(i+1)!} G^{i+1} \\
&\ldots \\
&\beta_N = G^N
\end{aligned} \tag{8}$$

Since $\beta_i = \prod_{j=1}^{i} K_j$, in which K_j is the stepwise stability constant, it may be expressed in terms of eqn. (8):

$$K_i = \frac{\beta_i}{\beta_{i-1}} = \frac{N-i+1}{i} G \tag{9}$$

and

$$K_{i+1} = \frac{\beta_{i+1}}{\beta_i} = \frac{N-i}{i+1} G \tag{10}$$

According to eqn. (9), the G constant

$$G = iK_i/(N-i+1) \tag{11}$$

expresses the intrinsic association constant of the complex[4]. This constant does

not depend on the index i, when statistical factors are the only cause of the formation of the complexes[1].

In the statistical mechanism of complexes, eqns. (9) and (10) provide the well known relationship[1,5]:

$$\frac{K_i}{K_{i+1}} = \frac{(N-i+1)(i+1)}{i(N-i)} \tag{12}$$

Note that if the conditions of case (A) are fulfilled, the relationship $K_i = G_i$ can be obtained. When these conditions hold for each of $i = 1, 2, 3, \ldots N$, then the determination of K_i constants according to Bjerrum's method is identical with the determination of G_i constants.

Evaluation of stability constants

For the correct evaluation of the stability constants of complexes on the basis of the experimental findings of the average ligand number $\bar{n} = (c_L - [L])/c_M$ (where c_L and c_M are the total concentration of a ligand and a metal), it is necessary to know the number and the type of the complexes[6]. Calculation of the stability constants according to eqns. (2)–(4) and the known (experimentally obtained) function $\bar{n} = f([L])$ may be begun by means of the set half-integer $\bar{n} = (\frac{1}{2}, \frac{3}{2}, \ldots, N-\frac{1}{2})$. The approximate values of the constants $G = (G_1^{(0)} = (1/[L])_{\frac{1}{2}}, G_2^{(0)} = (1/[L])_{\frac{3}{2}}, \ldots, G_N^{(0)} = (1/[L])_{N-\frac{1}{2}})$ correspond to the curve $\bar{n} = f([L])$ (or $[L]^{-1} = \varphi(\bar{n})$). By means of the values G_i obtained in this way and with eqn. (4), one may calculate a new set of average ligand numbers $\bar{n}_i$ with a corresponding more exact set of $G_i^{(1)}$ values (or $G_{N-i+1}^{(1)}$ values; the indices i or $N-i+1$ are not important) according to the above curve $\bar{n} = f([L])$, etc. This procedure is finished when each of the values $\bar{n}_i$ and G_i do not change significantly; continuing divergence, or oscillation of the values $\bar{n}_i$ and G_i, may be the result of the number and/or of the type of the complexes in the system or the function $\bar{n} = f([L])$ not being correctly determined.

Finally, the G values obtained as above may be used to calculate the overall stability constants according to eqn. (3).

This method for the calculation of the stability constants is quite general and may be used for systems containing an arbitrary, known number of mononuclear complexes. The method above is simple in comparison with other similar ones[5].

REFERENCES

1 J. Bjerrum, *Metal Ammine Formation in Aqueous Solutions*, Haase, Copenhagen, 1941.
2 H. S. Simms, *J. Amer. Chem. Soc.*, 48 (1926) 1239.
3 J. Klas, *Anal. Chim. Acta*, 41 (1968) 549.
4 J. Edsall, G. Felsenfeld, D. S. Goodman and F. R. N. Gurd, *J. Amer. Chem. Soc.*, 76 (1954) 3054.
5 B. Sen, *Anal. Chim. Acta*, 27 (1962) 515.
6 Y. Wormser, *Bull. Soc. Chim. Fr.*, (1954) 387.

Analytica Chimica Acta, 74 (1975) 223–224

ANNOUNCEMENT

The Pittsburgh Conference on Analytical Chemistry and Applied Spectroscopy

1975 – The 2nd 25 – 1999

The Twenty-sixth Pittsburgh Conference on Analytical Chemistry and Applied Spectroscopy will be held at the Cleveland Convention Center, Cleveland, Ohio, USA, March 3–7, 1975. Many aspects of the general fields of Analytical Chemistry and Spectroscopy will be represented. In addition to the general sessions, symposia are being arranged on the following specific topics:

1. Coblentz Society award symposium.
2. Spectroscopy awards symposium.
3. Symposium on surface chemistry (ASTM E-2).
4. Panel forum and discussion–computer laboratory systems (ASTM E-31).
5. The impact of tunable lasers on spectroscopy and chemistry.
6. Supplemental fuels from coal: New analytical needs.
7. Liquid chromatography–Today and Tomorrow; A symposium, panel discussion, and open forum.
8. Field sampling and analysis of atmospheric contaminants.
9. The role of standards in accurate measurements.
10. Polymer analysis.
11. The science of toxicology.

As in the past, the Conference will be the site of the Exposition of Modern Laboratory Equipment. In 1975, with an anticipated international participation of about 280 companies, the Exposition will again be the premier exhibit of analytical and scientific instrumentation and related products. Anyone desiring reservation of exhibition space or wishing information regarding the Exposition should address their inquiries to:

Mr. S. David Cifrulak
Calgon Corporation
Pittsburgh Activated Carbon
P.O. Box 1346
Pittsburgh, Pennsylvania 15230 U.S.A.

EUCHEM Conference No. 67 "Electrochemistry and Solid State Chemistry with Special Regard to Application in Batteries", April 1975

The EUCHEM Conference No. 67 "Electrochemistry and Solid State Chemistry with special regard to application in batteries" will take place from 13–17 April, 1975, at Schloss Elmau near Mittenwald (BRD). Chairman will be Prof. K.-J. Euler, Kassel (BRD). Co-Chairmen will be Profs. J. P. Brenet, Strasbourg (France), M. Gross, Strasbourg (France), H. Rickert, Dortmund (BRD), and H. Seifert, Kassel

(BRD). Gesellschaft Deutscher Chemiker will organize the Conference.

The provisional program as well as the preliminary registration forms may be obtained from Dr. W. Fritsche, Gesellschaft Deutscher Chemiker, D-6000 Frankfurt/M 90, Post Office Box 90 04 40.

Fourth Thermal Analysis School. Salford, England. April, 1975

The 4th Thermal Analysis School held under the auspices of the Thermal Methods Group of the Analytical Division of the Chemical Society will be held at Salford University from 7th–11th April 1975. Topics covered will include Thermometric and Enthalpimetric Methods introduced by Dr. L. S. Bark, Thermogravimetry (Dr. D. Dollimore), Surface Area and Texture of Powdered Materials subjected to Heat Treatment (Dr. D. Dollimore), Differential Thermal Analysis (Dr. F. W. Wilburn), Differential Scanning Calorimetry (Mr. K. E. J. Barrett), Thermo-mechanical Methods (Dr. A. Dyer), Gas Analysis Methods in Thermal Analysis (Dr. G. R. Heal), Applications of Thermal Analysis in Organic Chemistry (Mr. R. E. Waller), Applications of Thermal Analysis in Inorganic Chemistry (Mr. C. J. Keattch), and Applications of Thermal Analysis in Physical Chemistry (Dr. J. H. Sharp). There will be ample time for practical work and it is hoped that new equipment available for thermal analysis will be demonstrated by the instrument manufacturers. Accommodation will be provided in the University Halls of Residence. The School will be concluded by a Thermal Analysis Talk-In with a Questions and Answers Session on an informal basis. The cost will be in the region of £65. People interested should write directly to Dr. D. Dollimore, Reader in Physical Chemistry, University of Salford, Salford M5 4WT. Early provisional booking is recommended as the total capacity for the school is limited to 30.

International Symposium on Microchemical Techniques, 1977

Davos, Switzerland, 22–27 May 1977

This International Symposium continues the successful series of similar meetings in Graz, Birmingham and at The Pennsylvania State University. The organizing committee plans to include in the scientific program the application of microchemical techniques to all disciplines, including trace analysis, environmental studies, clinical and biochemical applications, and special problem areas. Suggestions for program topics are welcomed.

Program details and travel arrangements will be announced at a later date. For any immediate information please contact:

Dr. Wolfgang Merz
BASF Aktiengesellschaft
Untersuchungslaboratorium, WHU
D 6700 Ludwigshafen/Rhein
Federal Republic of Germany

(Continued from page 4 of cover)

CONTENTS

(Continued on inside page of cover)